ABSTRACT

SKUTNIK, STEVEN EUGENE. A Methodology for Enhancing Nuclear Fuel Cycle Proliferation Resistance Assessment. (Under the direction of Man-Sung Yim.)

The comparative evaluation of nuclear fuel cycle proliferation resistance (PR) is of a significant interest to the policymaking community, particularly in light of a recognized need to develop a more sustainable nuclear waste management strategy.

While robust probabilistic risk assessment (PRA)-based methods for PR evaluation have been developed by experts at the national laboratories, such methods are generally resource-intensive and often rely upon sensitive, non-public data to perform their analyses. In as much, there remains a strong need for open-source alternative PR models which can be used by the academic and policymaking communities, particularly for such tasks as scoping analysis of novel fuel cycles.

An alternative to PRA has been in attribute-based models, such as attribute analysis (AA) and multi-attribute utility analysis (MAUA), which characterize PR through the use of multiple independent "barriers" to a proliferation attempt. Using one such method developed at NC State (the Fuzzy Logic Barrier model) as a demonstration platform, this study describes a methodology for enhancing PR evaluation using such models. These enhancements include the exploration of system PR dynamics via direct coupling with nuclear materials characterization analysis (via nuclear fuel depletion codes such as SCALE) and methods to reduce the inherent subjectivity of attribute weighting. In addition, improvements to the Fuzzy Logic Barrier model are presented which are designed to draw upon verified physical data for barrier performance evaluation as much as possible.

A wide variety of nuclear fuel cycle configurations were evaluated using this methodology. These fuel cycles fall into three categories: "open cycles" with no actinide recycling, "modified open cycles" which consist of limited actinide recycling (e.g., separating plutonium for single-recycle in mixed-oxide fuels), and "fully closed" cycles consisting of the recovery of all transuranic materials in spent nuclear fuel for use in fast-spectrum reactors. The characteristics of system PR were explored for each of these fuel cycle classes, including the dynamics of system PR in response to the fuel cycle parameters identified above. The dynamics of system PR showed the strongest response for parameters which show a sustained "cascade" throughout the fuel cycle, such as uranium fuel burnup (impacting the plutonium composition) in partially-closed and full-closed fuel cycles, affected also by the choice of

actinide recovery strategy.

The technique of Adversary Pathway Analysis (APA) is also developed in this study as an additional means of enhancing AA/MAUA methods for fuel cycle PR analysis. APA involves the characterization of fuel cycle PR as a function of assumed adversary capabilities and final target material. This technique can be used to refine PR evaluation carried out in AA/MAUA methods by providing an analysis of the convergent pathways evaluated in PRA-based techniques, thus providing a "bridge" between the methodologies.

Finally, an evaluation was made as to the effect of simplifications in the nuclear fuel depletion calculation as well as cross-section uncertainty effects upon the material attractiveness calculation used for PR analysis. Based upon a comparative evaluation of material attractiveness based on data obtained from ORIGEN-S, a more sophisticated lattice physics model calculated in TRITON, and experimental data, characterization of material attractiveness was carried out as function of fuel burnup for mixtures consisting both of pure plutonium and transuranic materials. While reactor simplifications such as homogeneous core enrichments impact factors such as the total plutonium produced, such simplifications do not adversely affect material attractiveness evaluations compared to higher-fidelity lattice physics calculations and experimental data. Other simplifying assumptions such as a uniform irradiation power history (e.g., compared to the actual non-uniform power history) do not produce unreasonable differences in evaluated material attractiveness and thus may be used for PR evaluation purposes.

A Methodology for Enhancing Nuclear Fuel Cycle Proliferation Resistance Assessment

by
Steven Eugene Skutnik

A dissertation submitted to the Graduate Faculty of
North Carolina State University
in partial fulfillment of the
requirements for the Degree of
Doctor of Philosophy

Nuclear Engineering

Raleigh, North Carolina

2011

APPROVED BY:

David McNelis	Paul J. Turinsky
Peter Bloomfield	Paul Huffman

Man-Sung Yim
Chair of Advisory Committee

DEDICATION

To each of those whose encouragement and faith in me has brought me to this point;
I thank all of you.

BIOGRAPHY

Steve Skutnik was born in Omaha, Nebraska on June 24th, 1980 to Eugene and Rita Skutnik, the older of two children. He earned his bachelors of science in Physics at Iowa State University in 2002. In 2005, he obtained his masters of science in Nuclear Physics at Iowa State, working under the direction of Dr. John Lajoie, where his research involved the prediction of radiation-induced data errors in programmable logic devices for use in nuclear physics experiments. In 2005, he was awarded a teaching excellence award by the Graduate College at Iowa State University.

From 2005 to 2007, he worked as a science educator at the Adler Planetarium in Chicago. In 2007, he came to North Carolina State University to pursue his PhD in Nuclear Engineering under the direction of Dr. Man-Sung Yim. In 2009, he helped to found the Institute of Nuclear Materials Management Triangle-Area Universities student chapter, for which he served as president for two years. In 2010, he was awarded a Nuclear Nonproliferation and International Safeguards fellowship from the National Nuclear Security Administration.

He married his wife Anne Greenwood on October 2nd, 2010.

ACKNOWLEDGEMENTS

There are a number of people who I wish to thank individually for their contributions to this work.

First, I wish to thank my advisor, Dr. Man-Sung Yim, who has provided me with encouragement, guidance, and support throughout this process. I am sincerely grateful for the mentorship on both a personal and professional level he has provided me throughout the research process; however, I am most deeply obliged by the fact that he chose to take me on as his student. I also wish to thank my committee member Dr. David McNelis, who has provided thoughtful guidance and support from the beginning of this endeavor.

I would be of course remiss if I did not also express my deepest gratitude for the love, support, and extreme patience of my wife Anne, without whom this would not have been possible. I wish to similarly thank my parents, who have always supported my academic endeavors; likewise my sister Julie, who provided much commiseration and moral support.

I also wish to thank Ian Gauld of Oak Ridge National Laboratory for his invaluable assistance in developing the OASIS module for SCALE (which has been an essential component of this work) as well as his gracious assistance with other SCALE-related matters, including his helpful advice and for providing fast spectrum cross-section libraries for use with ORIGEN.

I also wish to acknowledge Dr. Jun Li, who provided much early assistance in understanding the theory behind the Fuzzy Logic Barrier model, for which I am quite indebted.

Likewise, I would like to thank my committee member Dr. Paul Turinsky for his challenging questions which prompted much of the study into the effect of factors such as simplifying assumptions and uncertainties in reactor calculations used for this work. Though I may have dreaded his most difficult questions at the time, they helped me to discover new insights about this work which have greatly contributed to its quality. I also wish to express my gratitude toward my committee members Dr. Paul Huffman and Dr. Peter Bloomfield for their guidance and perspective in making this research as thorough and complete as possible.

Finally, part of this research was performed under appointment to the U.S. Department of Energy Nuclear Nonproliferation International Safeguards Graduate Fellowship Program sponsored by the National Nuclear Security Administration's Office of Nonproliferation and International Security; I am deeply honored and grateful for the opportunities this fellowship has provided me. In addition, I also wish to gratefully acknowledge the Russell Family Foundation for their continued support which has made much of this research possible.

TABLE OF CONTENTS

LIST OF TABLES

LIST OF FIGURES

LIST OF ABBREVIATIONS

AA attribute analysis.

AHP analytical hierarchical process.

APA Adversary Pathway Analysis.

BSCM bare sphere critical mass.

CANDU **Can**adian **d**euterium **u**ranium.

DOE Department of Energy.

DUPIC **d**irect **u**se of spent **P**WR fuel **i**n **C**ANDU.

FBR fast burner reactor.

FLB Fuzzy Logic Barrier.

FOM Figure of Merit.

GUI graphical user interface.

HEU highly-enriched uranium.

HWR heavy water reactor.

LEU low-enriched uranium.

LWR light water reactor.

LWR-OT light water reactor, once-through.

MAUA multi-attribute utility analysis.

MC&A material control & accountability.

MOX **m**ixed **o**xide.

MTHM metric tons of heavy metal.

MTU metric tons of uranium.

NASAP Nonproliferation and Alternatives System Assessment Program.

NDA non-destructive analysis.

PR proliferation resistance.

PRA probabilistic risk assessment.

PRPP Proliferation Resistance and Physical Protection.

PRPPWG Proliferation Resistance and Physical Protection Evaluation Methodology Working Group.

PUREX **P**lutonium-**Ur**anium **Ex**traction.

PWR pressurized water reactor.

RGP reactor-grade plutonium.

SFN spontaneous fission neutron.

SQ significant quantity.

TRU **tr**ans**u**ranic materials.

CHAPTER 1

Introduction

With the growing interest in the development and expansion of nuclear energy systems, proliferation resistance (PR) assessment has become an essential tool in supporting the development of new and more proliferation resistant nuclear fuel cycles. In particular, the U.S. government has made PR a paramount priority in new fuel cycle development (being a key factor in decisions regarding the future of the U.S. nuclear fuel cycle). Considerations of the various technical options for used fuel management are inextricably tied to evaluations of relative proliferation resistance, thus driving the need for the development of new and more robust tools for fuel cycle PR assessment. Such a need is acutely important in light of the fact that the intrinsic proliferation resistance can vary substantially between different fuel cycle configurations.

The fact that different fuel cycles carry substantial differences in intrinsic PR is not a new conclusion; this has been a key finding in many studies of the nuclear fuel cycle dating back to the the U.S. Department of Energy (DOE)'s Nonproliferation and Alternatives System Assessment Program (NASAP) report in 1980, which first made such an identification, particularly among non-nuclear weapons states [58].

The IAEA defines nuclear fuel cycle proliferation resistance as follows [25]:

> Proliferation resistance is that characteristic of a nuclear energy system (NES) that impedes the diversion or undeclared production of nuclear material or

misuse of technology by the Host State seeking to acquire nuclear weapons or other nuclear explosive devices.

The discussion of fuel cycle proliferation resistance shall be limited to host state-level threats (e.g., excluding actors such as sub-national groups, which fall more into the domain of physical protection than proliferation resistance). The nature of host-state threats shall be evaluated both by assumed host-state capability (e.g., a sophisticated state with a relatively advanced industrial and indigenous fuel cycle infrastructure versus a less sophisticated state lacking such facilities), which affects the relative prominence of different proliferation barriers and adversary intent (e.g. relative sensitivity to reliable weapons yield). These considerations shall be evaluated across a series of different fuel cycle classes (e.g., including scenarios involving no actinide recovery to those involving complete actinide recycling) and configurations (e.g., fuel burnup, cooling time, actinide recovery strategies, etc.)

1.1 Existing methods for fuel cycle PR analysis

Several methods for characterizing proliferation resistance in the nuclear fuel cycle have been developed. The recognized standard for PR evaluations has been in probabilistic risk assessment (PRA)-based methods, which evaluate potential vulnerabilities in different fuel cycles through a detailed, scenario-based analysis of fuel cycle facilities [42, 46]. The most prominent example of such an analysis in this category is the Proliferation Resistance and Physical Protection (PRPP) methodology developed by the Proliferation Resistance and Physical Protection Evaluation Methodology Working Group (PRPPWG) [46]. A variation on PRA-based methods includes assessment of proliferation risk through use of Markov chain analysis; i.e., evaluating proliferation risk by contingent risk of adversary success and subsequent non-detection probabilities for different fuel cycle facilities and pathways [65]. Such an approach explores the impact of intrinsic (e.g., physical features and facility design) and extrinsic (e.g., safeguards) barriers to proliferation on relative risk. This focus on intrinsic barriers to proliferation represents a common feature across many models, although the interpretation of these barriers as well as their corresponding effectiveness can vary substantially between models.

However, in addition to being resource-intensive and explicitly reliant upon expert evaluations, PRA methods often rely upon sensitive, non-public data, thus limiting their usefulness for preliminary evaluations of novel fuel cycles. In light of this, complementary approaches

are warranted for such tasks as preliminary analysis of proposed fuel cycles. An alternative to PRA-based methods is attribute-based assessment, i.e., attribute analysis (AA) and multi-attribute utility analysis (MAUA). Examples of such include Charlton's MAUA approach [9], the TOPS barrier framework [22, 57], AREVA's SAPRA methodology [20], and the Fuzzy Logic Barrier (FLB) framework used for this study [35], as well as the IAEA's INPRO methodology [64].

Each of these approaches relies upon the study of proliferation resistance of fuel cycle systems as a characteristic of intrinsic features of the fuel, such as material attractiveness for diversion (including isotopic content, chemical form, heat, and radiological hazard), technical features such as the frequency of access to material, along with the bulk and mass of the material form, facility-based features such as the difficulty of modifying the facility for misuse and the skills, expertise, and knowledge required to illicitly divert or produce weapons-usable material at a facility), and finally detection features such as frequency of measurement of materials [64]. The TOPS and INPRO methodologies show an explicit overlap in these categorizations; INPRO goes further to explicitly define a series of extrinsic proliferation barriers based on legal and institutional arrangements controlling access to material and facilities, IAEA and host state-level safeguards, and finally mechanisms for enforcement of violations [57, 64]. TOPS defines three "extrinsic" barriers for these categories; however their interpretation is less explicitly defined than for that of intrinsic barriers [57].

The SAPRA methodology also makes use of the TOPS framework, however its focus is explicitly upon PR as a function of both intrinsic and extrinsic barriers (e.g., IAEA safeguards), rather than intrinsic barriers alone [20]. By contrast, the focus of this study shall be in the performance of intrinsic barriers to proliferation alone. The Fuzzy Logic Barrier method [35] used for this study makes explicit use of the intrinsic barriers defined in TOPS, using definitions for barrier effectiveness based therein, with any explicit alternative barrier effectiveness rankings noted in this paper.

One issue identified with attribute-based methods such as TOPS has been in how to combine what amounts to linguistic assessments of barrier performance for multiple barriers and fuel cycle stages; overcoming this constraint in order to provide comparative assessments of fuel cycle PR performance has been the basis of the design behind the Fuzzy Logic Barrier model (as well as Charlton's method). The Fuzzy Logic Barrier model and the MAUA methodology share a similar analysis framework in that different fuel properties (such as isotopic attractiveness and radiological hazard) are assigned a utility value, using a continuous utility

function in the former and discrete linguistic "fuzzy values" corresponding to different barrier effectiveness levels in the latter case.

1.2 Motivation for PR dynamics analysis

Another significant issue identified in prior assessments [9, 53] has been in the problem of how to represent the dynamic nature of the properties of nuclear materials in the system, particularly when making comparisons between different fuel cycle configurations. Given that nuclear fuel cycle PR is inherently related to the nuclear, radiological, and thermal characteristics of the isotopic inventories in the system, PR assessment exercises require ready access to the changing isotopic inventories throughout the system under consideration. As a result, PR is an explicitly dynamic quantity, given that changes in nuclear fuel properties permeate through the system. A method for addressing this issue has been to thus track the material flow throughout each phase of the nuclear fuel cycle, providing an evaluation of PR as a function of changing nuclear fuel properties [9, 35, 55].

While these methods have sought to address the fact that the evolving physical inventory of nuclear materials must be considered in PR analysis, such methods still ultimately evaluate PR as a function of fixed operational parameters between cycles. Yet given the fact that isotopic inventories (and associated physical features, such as radiological hazard and heat production rates) are generally a direct function of high-level system parameters (such as enrichment, burnup, reactor type, and isotopic separation strategies), PR can logically be evaluated as a function of such cycle parameters. As a result, not only are comparisons between different cycle configurations warranted (e.g., open vs. closed cycles), but comparisons of the dynamics of PR within fixed cycle configurations can also be made, given the effect that system operating parameters may have upon cycle PR. Furthermore, given the "cascade effects" of varying parameters at earlier stages in the cycle, fuel cycle PR dynamics can be expected to vary between different cycle configurations.

Part of the methodology proposed in this study extends the logic of accounting for evolving system inventories in PR assessment exercises by directly coupling isotopic characterization software such as ORIGEN-S [43] with a given PR metric. As a result, the process of tracking changing material properties as they flow through the cycle is not only automated but extended to the next level where the higher-order effects of cycle operational parameters can be directly evaluated as to their impact upon overall system PR.

From this, the specific dynamics of cycle parameters (such as burnup, reactor type, and reprocessing strategies) can be explicitly characterized. Likewise, the dynamics of PR behavior can also be compared between different fuel cycle categories as a means of further characterizing PR sensitivity. The study of PR dynamics in this context can thus further serve to inform the safeguards community as to the sensitivity of PR assessments as a function of cycle parameters, particularly as to the conditions under which the greatest sensitivity to PR response exists. Such a characterization would thus serve to inform as to the conditions under which more detailed system characterizations are warranted in PR assessment, as well as in demonstrating overall trends in system PR behavior as a function of said cycle parameters.

While the Fuzzy Logic Barrier model shall be used as the demonstration platform for this effort [35, 54, 55], it should be emphasized that such a technique could be applied to many other approaches of PR assessment.

1.3 Selection of fuel cycles for PR dynamics evaluation

Three general categories of nuclear fuel cycles shall be considered for this analysis: a traditional "open" cycle, consisting of direct disposal of fuel following irradiation (i.e., no actinide recovery); "modified open" cycles, consisting of limited/partial actinide recovery (e.g., PUREX and advanced UREX-series treatments), followed by limited re-irradiation in the form of **m**ixed **o**xide (MOX) fuel and subsequent disposal; and finally, "closed" cycles consisting of full actinide recovery and recycle (i.e., only fission products are disposed of) through the use of a fast-spectrum reactor, in which all actinides are continuously recycled until they are consumed.

Each of these fuel cycle classes represents an overall branch of fuel cycle alternatives, with considerations extending into areas including waste management, economics and resource utilization, as well as the focus of this analysis: proliferation resistance. Several different configuration parameters within each fuel cycle class can be evaluated, particularly for their impact upon fuel cycle PR. The motivation for each class of fuel cycle shall be considered here, along with a brief overview of the types of parameters which shall be evaluated for each fuel cycle class.

1.3.1 Open cycles

The open cycle ("once-through") represents the default nuclear fuel cycle configuration and thus serves as a useful baseline for fuel cycle studies. Given that no separation of plutonium is involved in these fuel cycles, they represent the standard for proliferation resistance against which other fuel cycles are evaluated.

Two different types of reactors are considered for the case of open cycles: a light water reactor (LWR), which uses ordinary water as a neutron moderator and thus requires enriched uranium as fuel; second, the Canadian heavy water reactor (HWR): **Can**adian **d**euterium **u**ranium (CANDU). The CANDU uses "heavy water" (D_2O, i.e. water in which hydrogen has been replaced by the heavier stable isotope deuterium). Because of the much more favorable scatter-to-absorption cross-section ratio for neutrons in heavy water, the CANDU reactor can use natural uranium as fuel, and thus the CANDU cycle requires no enrichment stages.

Overall, the main parameter of interest for these types of cycles shall be the uranium fuel burnup, which directly corresponds with the amount of plutonium produced through neutron capture in ^{238}U, as well as the "quality" of the plutonium vector (i.e., the fraction of the plutonium vector consisting of ^{239}Pu, which is desirable for weapons purposes), which decreases through subsequent neutron capture reactions (producing higher plutonium species). For the LWR cycles considered, this study has been limited to the evaluation of pressurized water reactor (PWR) designs, due to the overall small differences in void fraction (i.e., the fraction of steam to coolant in the moderator) as a function of axial position along the fuel bundle, which can produce changes in the neutron spectrum (and thus variance in the fuel isotopics as a function of position). While theoretically any combination of enrichments and burnups could be considered for the LWR cycle, a fixed series of burnup/enrichment combinations are used for this study (provided in [60]) in order to simulate the dynamics of realistic core loadings for a civilian fuel cycle as much as possible.

1.3.2 Modified open cycles

In the so-called "modified open" fuel cycle strategy, a limited degree of actinide recovery is employed. Generally this involves the recovery of plutonium (PUREX) for re-fabrication into MOX fuel; however, other advanced treatments include the coextraction of uranium with plutonium (COEX) in order to provide additional proliferation resistance to the extracted product, as well as advanced UREX-series treatments which involve the partition and possible

coextraction of other actinides (e.g., neptunium, americium, and curium) with plutonium [15].

For example, neptunium can be coextracted with plutonium in order to "dope" MOX fuel with neptunium in order to produce additional ^{238}Pu (an intense heat generator) during irradiation (e.g., "heat spiking"), thus reducing the latent attractiveness of the plutonium vector [39]. Other treatments involve the coextraction of plutonium with minor actinides (e.g., Am, Cm, and Np) in order to increase the total heat generation rate of the stream (UREX+1a, UREX+1b). Finally, an additional strategy considered is the coextraction of lanthanides with transuranics, thus providing a radiological barrier with sensitive materials (UREX+1) [15].

In each of the strategies involving the production of MOX fuel, a limited degree of recycling is assumed; e.g., it is assumed that plutonium and other actinides are recycled only once before ultimate disposal (due to the increasing difficulty of working with multiply-recycled plutonium).

An alternative to the MOX cycles evaluated is a fuel cycle being developed by researchers in South Korea referred to as **d**irect **u**se of spent **P**WR fuel **i**n **C**ANDU (DUPIC) [30, 44]. The DUPIC fuel cycle involves the dry processing of spent PWR fuel in order to remove volatile fission product gases; this fuel is then re-sintered into fuel for limited re-irradiation in a CANDU reactor, followed by subsequent disposal. Such a strategy is designed to increase the utilization of energy resources in uranium fuel while avoiding the separation of plutonium, thus increasing the overall proliferation resistance.

1.3.3 Closed cycles

The separation and transmutation of long-lived actinides in fast-spectrum reactors is a matter of key interest in nuclear waste management. The partitioning and separate transmutation of long-lived actinides can potentially result in both significant expansion of repository capacity and mitigation of potential repository risks [34, 41]. However the full destruction of long-lived actinides requires the use of fast-spectrum reactors, rather than thermal spectrum reactors, which are significantly less efficient at such a task, given the much lower overall fission-to-capture ratio of a thermal spectrum [23]. The "fully closed" fuel cycle represents this contingency of full actinide recycle.

In the "burner" configuration evaluated in this study, there is a net consumption of fissile materials (e.g., plutonium) input into the fast reactor system. Following irradiation, actinides present in fast reactor fuel are reprocessed and "topped off" with actinides from LWR fuel;

only fission products are separated for disposal (i.e., no actinides are disposed of).

While fast reactor technology currently remains in a demonstration stage, such reactors are a likely technological alternative for long-term waste management solutions. Therefore, an evaluation of the relative proliferation resistance of such cycles is of a particular interest to the policymaking community.

1.4 Introducing Adversary Pathway Analysis

One of the chief advantages of attribute analysis / multi-attribute utility analysis (AA/MAUA) approaches to proliferation resistance assessment is in the lack of requirement for specific (often sensitive) details of nuclear fuel cycle facilities, compared to more conventional PRA methods. Making use of general characteristics of fuel cycle facilities by characterizing features such as mass flow, isotopic attractiveness, and specific facility characteristics such as the relative difficulty of modifying facilities for illicit diversion or misuse, it is possible to make a relative comparison of PR among different fuel cycle configurations, and even the dynamics of PR as a function of operational system parameters such as fuel burnup, cooling time, enrichment, and isotopic separation strategies. Such methods are thus often useful for general, preliminary comparisons of relative PR between different fuel cycle configurations.

However, by employing a basic understanding of both potential adversary capabilities and attack pathways within a generalized fuel cycle model, it is possible to provide a level of "fine-tuning" to AA/MAUA methods. In particular, it is a working assumption in PR analysis (both in PRA and AA/MAUA-based methods) that adversary capabilities drive potential proliferation pathways, in addition to the relative importance of particular intrinsic barriers to proliferation [57].

Given the varying capabilities of potential adversary states, the resulting differences in the importance of particular barriers can result in significantly different evaluations of intrinsic system PR for different threat profiles. An analysis of potential attack pathways thus affords the ability to tailor the analysis of facility PR based upon the specific threat profile, including the specific PR evaluation criteria. Examples of this would include potential diversion scenarios both before and after fuel irradiation, which involve remarkably different attack profiles (i.e., diversion of uranium for re-enrichment, diversion of spent fuel or failed fuel pins for separation, or diversion of actinides from reprocessing facilities for direct use), similar to the methodology used in traditional PRA analysis [47]. Adversary pathway analysis

can thus be thought of as a "bridge" technique between traditional pathway-based PRA methods and simpler attributed-focused techniques.

In Chapter 5, Adversary Pathway Analysis (APA) shall be presented as a means of augmenting existing AA frameworks. Using the Fuzzy Logic Barrier model as a demonstration platform, the use of Adversary Pathway Analysis (APA) to enhance PR analysis shall be discussed. This will include an analysis of system PR behavior both as a function of adversary characteristics (sophisticated vs. unsophisticated, yield-sensitive vs. yield-insensitive) as well as by target material type (Pu, **tr**ans**u**ranic materials (TRU), or minor actinides).

1.4.1 Motivation for Adversary Pathway Analysis

A common premise underlying many PR models is that proliferation pathways are contingent upon the capabilities of a given adversary. Differing levels of sophistication among actors results in a varying level of proliferation capabilities. For AA/MAUA models, this can correspond both to varying prominence of particular barriers to a proliferation attempt [57], depending upon an adversary's technical capabilities (e.g., physical barriers, such as isotopic attractiveness, play a larger role for less sophisticated actors) as well as adversary intent (e.g., an unsophisticated actor desiring a reliable weapons yield will be more constrained by material properties than one without such a requirement) [6]. As a result, the evaluated proliferation resistance of a given fuel cycle can vary substantially based upon these characterizations of the adversary threat profile. Likewise, the nature of the adversary can impact such aspects as sensitivity to operating conditions (e.g., burnup, actinide co-extraction strategies, etc.), with less sophisticated actors showing a greater overall sensitivity to these factors.

An additional key feature in AA/MAUA approaches to fuel cycle PR evaluation is that assumptions about the nature of both the adversary and the intended target are inherent to the model (and corresponding choice of attribute performance criteria) itself. For example, in a barrier framework approach like TOPS or INPRO [57, 64], the criteria for barrier performance inherently relies upon an assumption of the target material form being diverted – e.g., whether an intact fuel assembly itself or the plutonium contained therein.

The character of the target material (e.g., intact assemblies, plutonium, etc.) can guide how the barrier criteron themselves are applied – i.e., a varying criteria can be used for unique pathways (e.g., diversion of plutonium from spent fuel versus re-enrichment of fresh fuel assemblies). APA thus prompts an explicit characterization of these underlying assumptions,

facilitating a more full exploration of the possible spaces under which a proliferation event can occur, including how these pathways evolve with changing system conditions (e.g., fuel enrichment, burnup, etc.).

By comparison, PRA approaches frequently involve the characterization of a series of contingencies required for a successful diversion (or other acquisition) attempt. These types of analysis characterize pathways to proliferation by evaluating both a target material and its successful acquisition by a proliferator in a fuel cycle facility, including through both abrupt and prolonged diversion scenarios [47, 65]. Such targets can then be characterized by features such as target material attractiveness and proliferation technical difficulty and cost [47].

In this sense, APA can be thought of as a generalization of the approach employed in PRA assessments, grouping together common diversion pathways by target type, and subsequently adjusting the emphasis of particular intrinsic barriers to proliferation by the adversary type. Ultimately, APA is not intended to supplant PRA-based approaches (which are still effectively the benchmark for PR analysis), but rather as a framework to enhance other, less resource-intensive AA/MAUA methodologies by capitalizing on the strengths of PRA in a more accessible context, thus enabling such models to serve a more useful role in initial scoping evaluations using open-source data and analysis tools.

1.4.2 Cases to be considered in Adversary Pathway Analysis

For the Adversary Pathway Analysis evaluation, each of the fuel cycle classes listed above shall be evaluated under a series of different adversary types as well as target material pathways. The adversary types considered will include a sophisticated state (one with a well-developed industrial infrastructure and indigenous nuclear fuel cycle) operating under an overt and covert breakout scenario (e.g., parallel to the “abrupt” versus ”protracted” diversion scenarios seen in other analyses [47]), as well as an unsophisticated state (i.e., a state lacking well-developed nuclear fuel cycle facilities) under a scenario of sensitivity and insensitivity to weapons yield. The choice of adversary type (sophisticated vs. unsophisticated, covert vs. overt) affects the relative prominence of proliferation barriers, while yield sensitivity impacts the evaluation of the isotopic barrier performance.

Material pathways considered include a plutonium-only pathway, a TRU-based pathway, and finally a minor actinides-based pathway. Each of these target pathways represents the convergence of different diversion scenarios; for example, the plutonium-based pathway

represents the diversion of materials in whole form from any given fuel cycle stage and subsequent separation in an undeclared reprocessing facility. As a result, while the material attractiveness of the pathway is controlled by the final product; other barriers (such as the amount of material required for the diversion of one significant quantity of the target material, etc.) are determined by the gross amount of material require for the diversion of the target stream. Alternate material target pathways, such as the TRU and minor actinides pathways, similarly represent the convergence of different diversion scenarios. For example, the TRU-based pathway represents the recovery of the sum of transuranic materials; for example, diversion of intact material from a reprocessing stream or other cases involving less effective material separation. By examining the performance of the system via the material target pathway, such an analysis can also reveal where systems both show the greatest vulnerability (i.e., weighting different changes in barriers such as small changes in isotopic attractiveness versus an increase in overall available mass, etc.) as well as providing a "baseline" for evaluation of minimum fuel cycle PR. For example, the consideration of the plutonium-only pathway indicates what additional PR gains are achieved (if any) under coextraction scenarios assuming an adversary which would subsequently reprocess diverted materials to obtain a pure product, etc. Thus, such an evaluation provides an evaluation of the greatest possible system vulnerability while accounting for changing system conditions (e.g., the effect of varying cycle configuration parameters).

CHAPTER 2

The Fuzzy Logic Barrier Model

2.1 Overview of the Fuzzy Logic Barrier Model

In this chapter, the FLB model used for proliferation resistance evaluation shall be discussed. This includes both a discussion of how PR evaluation is performed using the FLB model, as well as substantial improvements to the FLB methodology from its original development by Dr. Jun Li [35].

2.1.1 The barrier framework

The basis for the Fuzzy Logic Barrier framework is the set of intrinsic proliferation barriers as identified in [57]. TOPS defines 11 intrinsic barriers to proliferation in a given fuel cycle, representing a different intrinsic feature of the nuclear fuel cycle system which must be overcome for a successful proliferation event. These barriers are then divided into two categories: "physical" barriers, which represent intrinsic features of the nuclear materials themselves, and "technical" barriers, which represent characteristics of the nuclear fuel cycle facilities, listed as Table 2.1.

Each barrier is evaluated as to its relative effectiveness, on a scale of "Ineffective" to "Very High" effectiveness, based on an independent performance criterion for each barrier, some

Table 2.1: Intrinsic barriers to proliferation in nuclear energy systems, as defined in [57].

Physical barriers	Technical barriers
Isotopic attractiveness	Facility unattractiveness
Chemical separation difficulty	Facility accessibility
Radiological hazard	Available mass
Material mass & bulk	Facility diversion detectability
Material detectability	Skills, expertise, & knowledge
	Time

of which shall be discussed in this chapter.

The isotopic barrier represents the relative utility of a given material for direct weapons use – for example, weapons-grade plutonium and highly-enriched uranium (HEU) represent the lowest intrinsic PR, whereas natural uranium would be of the highest. The chemical separation difficulty represents the relative difficulty in obtaining a pure, usable chemical form of the material, with pure metals presenting the least difficulty and vitrified mixtures representing the greatest. The radiological barrier represents the relative radiological hazard to personnel in handling materials; the higher the radiological hazard, the greater the barrier effectiveness. Material mass and bulk measure the relative difficulty of diverting material in terms of the total bulk of the physical form. For example, full assemblies of fuel rods require significantly more equipment and personnel for diversion than for example a canister of separated plutonium. Material detectability indicates the relative ease with which material can be detected; materials with easily identifiable signatures (which are not easily shielded) represent a much higher intrinsic PR than those with no detectable signatures, or those more easily shielded. Finally, the time barrier is simply a measure of residence time; it is generally assumed that the longer a material remains in a facility, the greater opportunities for a diversion attempt exist (hence, longer times represent lower PR).

Of the technical barriers, facility unattractiveness represents the relative difficulty (in terms of cost and safety) of modifying a facility to produce materials suitable for diversion. Facility accessibility is measured in terms of the relative access of personnel to a given facility; facilities where material is handled infrequently only by remote access represent a much higher intrinsic PR than those in which personnel have regular access (for example, online refueling systems). The available mass represents the total number of available material for diversion; facilities with multiple significant quantities of material (defined by the IAEA as

8 kg of Pu and 25 kg of low-enriched uranium (LEU)) represent a lower barrier than those with fewer. The facility diversion detectability represents the relative ability of an outside observer to detect modifications of a facility for a diversion attempt (e.g., intrinsic signatures of the facility). Finally, the skills, expertise, & knowledge barrier represents the relative degree for which skills to a given process have the potential for "carry-over" to producing weapons-usable materials. For example, the skills to operate a uranium enrichment facility have a natural carry-over to producing higher enrichments (e.g., HEU), therefore this barrier represents a minimal effectiveness for such a facility.

2.1.2 Advantages of the barrier framework approach

The use of a barrier framework approach to evaluating nuclear fuel cycle proliferation resistance is not a novel concept; several methods, from the TOPS barrier framework [57], AREVA's SAPRA methodology [20], Chartlon's MAUA framework [9] are all examples of this type of attribute-based approach to PR evaluation. Such frameworks evaluate proliferation resistance by composing the problem as a series of complementary "barriers" to proliferation (based both on intrinsic features of the fuel as well as characteristics of the facilities themselves. By evaluating these characteristics at each individual fuel cycle stage, modelers can then draw conclusions regarding the relative proliferation resistance of different fuel cycle configurations.

The main advantage of AA/MAUA models (and the subsequent motivation for their use) over PRA-based approaches is in that evaluations of fuel cycle PR can be made entirely through data and methods available in the open literature; this is in marked contrast to PRA-based methods, which can be both resource-intensive and often rely upon non-public (often sensitive) data. However, the goal of models such as the FLB approach is not as a replacement to traditional PRA-based approaches, but rather as a means to perform basic scoping analysis on novel fuel cycles without the need for sensitive information.

Another advantage of attribute analysis approaches such as TOPS [57] and the FLB approach is in that such approaches reproduce the process by which experts make decisions, namely by assigning linguistic rankings to independent criteria which are then weighed against one another. However, a difficulty in employing such analysis has been in the difficulty of combining disparate linguistic quantities, a task which does not easily lend itself to quantitative approaches.

The fuzzy logic barrier model was designed to solve this difficulty. Fuzzy logic is uniquely

suited to handling quantities which can be linguistically defined, such as the rank assignments inherent in an attribute analysis approach (e.g., “high” and “low” barrier effectiveness) which do not readily correspond to crisp quantification or binary true-false values. Each barrier ranking is thus assigned a fuzzy number corresponding to the linguistic rank, which can then be operated upon using well-defined fuzzy operations to produce a quantitative result.

Despite PRA’s scenario-based focus, fundamentally barrier framework models (such as TOPS and the Fuzzy Logic Barrier approach) and coarse-path PRA approaches share a similar analytical framework, particularly in the assignment of linguistic variables to similar proliferation barriers [46, 47]

2.1.3 Challenges to attribute analysis methods

One of the main challenges in the use of attribute-based methods has been in quantitatively analyzing the linguistic values which result from such an approach. Methods such as Charlton’s [9] resolve this through the use of “utility functions” which use functions to create a 1:1 mapping of barrier performance to physical values. However, an issue identified with this approach is in how to specifically make this mapping; i.e., while the “endpoints” are known in terms of barrier performance, it is often difficult to distinguish barrier performance in a granular or precise fashion. In as much, an alternative is the use of fuzzy logic to represent the inherently linguistic nature of such evaluations, particularly the uncertainty in particular assignments.

An additional challenge to attribute-based approaches has been the perceived subjectivity introduced by expert judgments inherent to such a framework, such as in the choice of weight criteria (especially compared to more traditional PRA models). This problem is twofold: the model designer must both produce a reasonably robust system of weights for both the contributions of individual barriers as well as stages to the system as a whole. Each of these shall be discussed in detail in this chapter.

For the contributions of individual stages, this can be made reasonably objective through the use of physical data such as heavy metal inventories and concentrations in order to determine relative stage prominence.

However, the relative weights of individual barriers are somewhat more problematic. In order to create a consistent process for barrier weight selection, an Analytical hierarchical process (AHP) was employed based on pairwise evaluations of barrier importance, which

shall be discussed in detail in this chapter.

Additionally, the domain of all possible barrier weight combinations can be constrained through a calibration process, limiting the possible space of barriers by evaluating the behavior of stage-level PR in a well-characterized system. Given the fact that the relative stage-to-stage PR behavior is understood for well-characterized systems such as a Light water reactor, once-through (LWR-OT) (despite the absolute performance remaining unknown), the relative stage-to-stage PR performance evaluation can be used as a rejection criterion for barrier weight sets. For example, barrier weight sets which produce PR vector behavior that fails to conform to intuitive understandings of PR performance (e.g., certain stages, such as enrichment, are well-known to be sensitive) are rejected. Thus, the space of possible barrier weights is constrained.

By using these methods, the envelope of subjectivity of this approach can be greatly constrained, thus largely answering this objection.

2.2 Definition and interpretation of fuzzy numbers

2.2.1 Interpretation of fuzzy numbers

Fuzzy numbers are best interpreted as "truth" functions, indicating the possibility that the system is represented by a particular state (in this case, a particular PR ranking). Unlike binary logic, in which there is only "false" (0) and "true" (1), fuzzy logic tolerates a truth value in between 0 and 1, with 0 representing complete impossibility and 1 denoting absolute possibility [50].

For this analysis, relative PR performance of particular barriers, stages, and systems is represented on a scale of 0 to 1, with 0 representing the least possible intrinsic proliferation resistance and 1 representing the greatest.

Each fuzzy function corresponds to a membership function ($\mu(x)$), which ranges from 0 to 1 for any given value of the relative PR (represented as x). Thus, a PR fuzzy number (for a barrier, fuel cycle stage, or fuel cycle system) has a "truth function" for each relative value of PR (from 0 to 1), with a corresponding "membership value" (also from 0 to 1), where a value of $\mu(x) = 0$ represents no possibility (i.e., no possibility that the PR value is "x") and a value of $\mu(x) = 1$ represents the maximum possibility (i.e., absolute possibility that the PR value is "x"). Thus, the fuzzy number for each barrier, stage, and system represents the distribution of

possible PR values for the given quantity.

These fuzzy number can then be reduced down to a "centroid" fuzzy number, rendering it as a "crisp" singular value for simplified comparison [33, 62, 63] by taking the arithmetic mean, as shown in Eq. 2.1.

$$F(\widetilde{u}) = \frac{\int x\mu_{\widetilde{u}}(x)dx}{\int \mu_{\widetilde{u}}(x)dx} \tag{2.1}$$

An example of a system fuzzy number is shown as Figure 2.1. In this example, the system fuzzy number generally spans the space of $\approx$ 0.4–0.6, with all other values showing no possibility. Likewise, the maximum possibility appears to be around $x = 0.5$, corresponding to a linguistic fuzzy value of approximately "High-minus (H-)" to "High (H)."

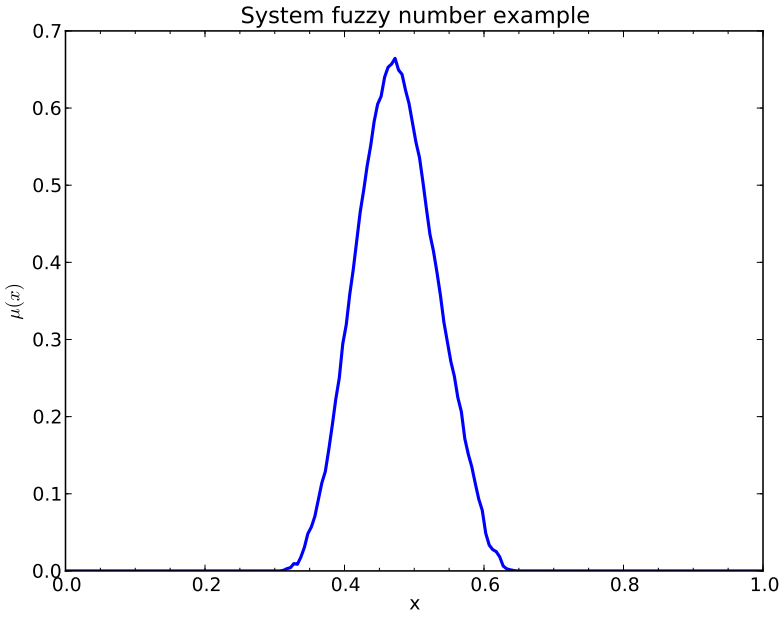

Figure 2.1: An example of a system fuzzy number.

The general utility of this approach is less in the absolute quantification of a single system in isolation, but rather in the comparison of systems across different operating conditions

and configurations (e.g., open vs. closed, varying burnup, etc.).

2.2.2 Linguistic barrier definitions

Similar to the prior work performed by Li [33, 35], the eleven intrinsic barriers to proliferation (based on the barriers defined in [57]) are assigned a linguistic ranking of "Ineffective" (I), "Low" (L), "Medium" (M), "High" (H), or "Very High" (VH). These fuzzy numbers are represented by triangular membership functions, spanning the range of [0,1], as illustrated in Figure 2.2a. The primary barriers each increase in width by 25% per primary level, thus producing a logarithmic scale.

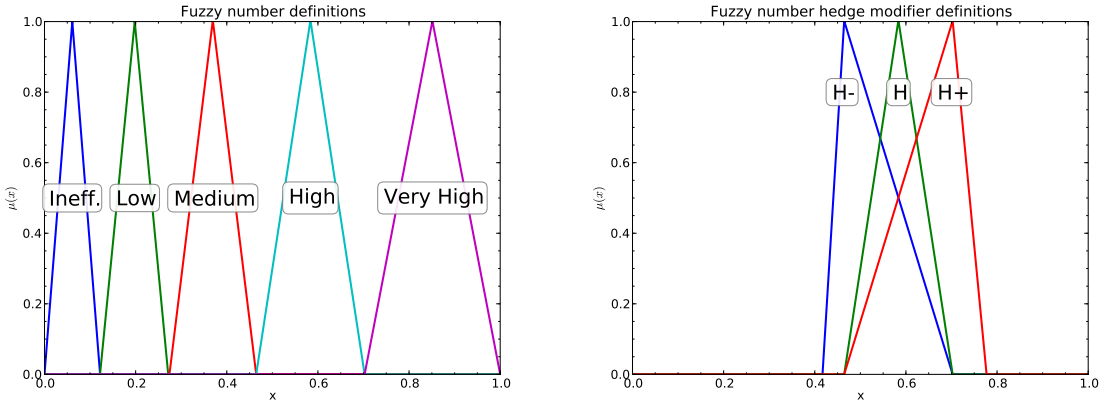

(a): Base fuzzy numbers

(b): Fuzzy "hedge" values

Figure 2.2: Linguistic value fuzzy number definitions, with the "base" fuzzy number definitions and fuzzy "hedge" values.

To increase the level of granularity in the evaluation, a series of fuzzy "hedge" modifiers (e.g., ±) were introduced. These hedge values (illustrated as Figure 2.2b) are "skewed" in the direction of the hedge; for example, the H– hedge value spans the space from 25% into the adjacent "Medium" barrier to the right edge of the "High" membership function.

The ranges of each of the fuzzy functions (including hedge values) are given as Table 2.2.

Table 2.2: Linguistic fuzzy value definitions used in the Fuzzy Logic Barrier model.

Level	Low	Peak	High
I–	0.00000	0.00000	0.12185
I	0.00000	0.06093	0.12185
I+	0.00000	0.12185	0.15993
L–	0.09139	0.12185	0.27146
L	0.12185	0.19801	0.27146
L+	0.12185	0.27146	0.32041
M–	0.23609	0.27416	0.46455
M	0.27416	0.36936	0.46455
M+	0.27416	0.46455	0.52405
H–	0.41696	0.46455	0.70254
H	0.46455	0.58355	0.70254
H+	0.46455	0.70254	0.77691
VH–	0.64305	0.70254	1.00000
VH	0.70254	0.85128	1.00000
VH+	0.70254	1.00000	1.00000

2.3 Barrier evaluation

In this section, the evaluation of the PR performance of specific individual barriers will be discussed, including the data and criteria used to evaluate individual barrier performance.

2.3.1 Isotopic barrier evaluation

The isotopic barrier is considered to be of cardinal importance to the system PR calculation; thus, its evaluation merits the closest scrutiny. For the purpose of the FLB model used in this demonstration, the isotopic barrier is evaluated through an adaptation of the Figure of Merit (FOM) approach developed by Bathke et. al. at Los Alamos National Laboratory [6]. The FOM approach carries the virtue of being developed in consultations with weapons experts, thus making it a highly useful metric for evaluating material attractiveness for purposes of diversion to weapons programs. In addition to functioning as a *de facto* standard for material attractiveness evaluation, the FOM approach also affords a highly granular means of determining material attractiveness, thus making it extremely appropriate for techniques

such as the PR dynamics approach explored in this analysis using the Fuzzy Logic Barrier model.

FOM_1 is evaluated based upon three physical parameters: the material bare sphere critical mass (BSCM), radiological dose at one meter (from one-fifth of the critical mass), and finally the heat generation rate of the material (in W/kg). The calculation of FOM_1 is given as Eq. 2.2, where M is the BSCM in kg, D is the dose at 1 meter from the surface of one-fifth of the critical mass ($0.2 \cdot M$, in rad/hr), and h is the heat generation rate of the material (in W/kg).

$$FOM_1 = 1 - \log_{10}\left(\frac{M}{800} + \frac{Mh}{4500} + \frac{M}{50}\left[\frac{D}{500}\right]^{\frac{1}{\log_{10} 2}}\right) \tag{2.2}$$

For the special case of an unsophisticated state adversary desiring a reliable weapons yield, a second form of the Figure of Merit equation is employed (FOM_2), accounting for the spontaneous fission neutron rate, which can introduce pre-detonation ("fizzle") into a nuclear explosive device; this is given as Eq. 2.3, where S is the spontaneous fission neutron (SFN) generation rate, given in $\frac{\text{n}}{\text{sec}\cdot\text{kg}}$.

$$FOM_2 = 1 - \log_{10}\left(\frac{M}{800} + \frac{Mh}{4500} + \frac{MS}{6.8 \cdot 10^6} + \frac{M}{50}\left[\frac{D}{500}\right]^{\frac{1}{\log_{10} 2}}\right) \tag{2.3}$$

The material attractiveness ratings of the FOM_1 range from 0 (unattractive) to 3.0 (preferred); these values were translated into linguistic values roughly corresponding to those found in [6], given as Table 2.3.

The fuzzy correspondence for FOM_2 is the same as that used for FOM_1 (Table 2.3).

While the radiological dose and heat generation rate (in addition to the SNF rate, when necessary) can be calculated directly from the material inventories themselves (as given in ORIGEN-S), the calculation of the BSCM is not easily automated. Creating a broad space of burnup and material mixture combinations, the BSCM was found for each configuration in a criticality search using MCNPX [32].

From this data, a regression analysis was performed to produce a correlation for the bare sphere critical mass. For this correlation (presented as Eq. 2.4), the mass fraction of plutonium in the stream was found to first order to be the most significant term, showing an inverse-power relationship with the BSCM. The ^{239}Pu vector was found to be a second-order scaling factor, also showing an inverse power relationship. Between these two variables, an

Table 2.3: Fuzzy number correspondence to FOM_1 [6].

FOM_1	Fuzzy Rank	Weapons utility[6]
> 3.00	I	Preferred
2.66 – 3.00	L–	
2.33 – 2.66	L	
2.00 – 2.33	L+	
1.66 – 2.00	M–	Attractive
1.33 – 1.66	M	
1.00 – 1.33	M+	
0.66 – 1.00	H–	Unattractive
0.33 – 0.66	H	
0.00 – 0.33	H+	
< 0.00	VH	

extremely good fit to the BSCM values observed across the broad space of material mixtures can be achieved.

$$\mathrm{BSCM} = 11.5828 \cdot (\mathrm{MF_{Pu}})^{-2.2238} (\mathrm{fr_{Pu239}})^{-0.2731} \tag{2.4}$$

The quality of fit for the BSCM correlation is shown in Figure 2.3; in general, one observes that the correlation provides an excellent fit to the BSCM data obtained in MCNPX for a wide range of mixture conditions, with $\bar{R}^2 = 0.9940$. The quality of the fit declines slightly for very high dilution factors (i.e., lower values of the plutonium mass fraction), however overall the fit shows a very good agreement over the space of the data, thus enabling an automated calculation of the FOM_1 value for any isotopic mixture.

Application of the isotopic attractiveness criteria

One drawback to the use of the FOM approach is in that it is generally unhelpful for intact fuel characterization; i.e., given the fact that in intact form, the bare sphere critical mass will be extremely large or infinite; likewise, coupled with the very high radiological and thermal emission rates, all FOM_1 values will be < 0. Therefore, using the FOM approach for intact fuel provides little resolution in discriminating potential material attractiveness levels. However, by estimating the potential attack pathway by a hypothetical malefactor, it is possible to make

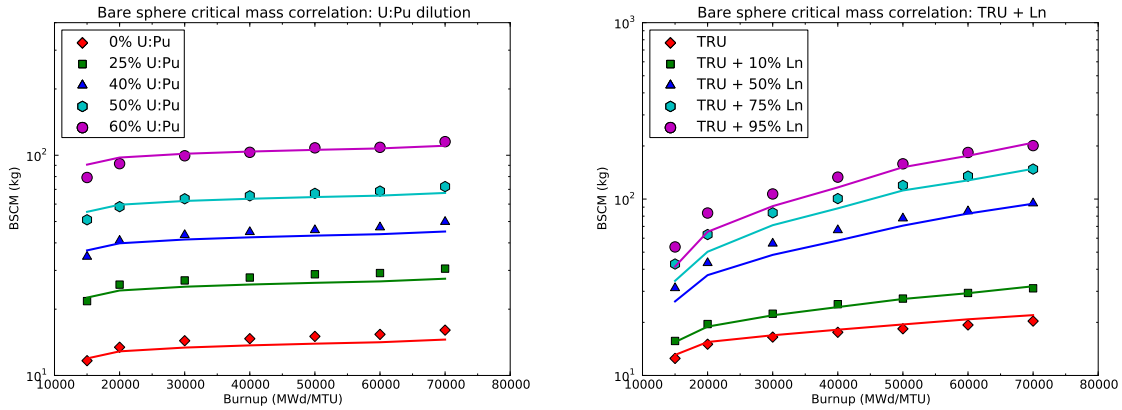

(a): U:Pu (b): TRU + Ln

Figure 2.3: Regression analysis fits (lines) to bare-sphere critical mass data (points) obtained through criticality searches upon material mixtures using MCNPX; BSCM data in kg [32]. Nuclear composition data generated using SCALE [43]. $\bar{R}^2 = 0.9940$.

a discrimination of the latent isotopic attractiveness within different spent fuel forms (i.e., as a function of burnup and initial enrichment) and for different co-extraction techniques.

For this analysis, the assumed attack pathway for intact fuel forms (such as spent uranium oxide as well as fresh and spent mixed-oxide fuels) is the diversion and direct separation of plutonium from the fuel form. For streams of material from reprocessing, it is assumed that an attacker would divert the intact stream for direct use (e.g., including all coextractants, such as uranium or minor actinides). The merits of this evaluation are explored in greater depth later; however, in all cases, the PUREX fuel cycle (involving only plutonium separation) is a useful baseline.

2.3.2 Radiological barrier evaluation

The evaluation of the radiological barrier for intact fuel forms is a relatively straightforward process; using gamma spectra obtained from ORIGEN-S, an exposure is calculated at 1 meter for a line source geometry consisting of a 4 meter fuel bundle. For separated fuel forms (e.g., reprocessing), the dose can be estimated using dose estimations at 1 meter for actinides calculated for a 8 kg bare sphere geometry determined in [1].

The levels of the radiological barrier performance are based upon the assumption of a

radiological self-protection standard of 500 rem/hr [6, 10, 57] and inferred downward from this point. Table 2.4 gives the correspondence of radiation levels in rem/hr to rated barrier performance used in the model.

Table 2.4: Fuzzy ranking of radiological barrier performance, based on dose rate at 1 meter (rem/hr).

Dose rate $\left(\frac{\text{rem}}{\text{hr}}\right)$	Rank
> 1000	VH
> 500	H+
> 100	H
> 50	H–
> 10	M+
> 1	M
> 0.5	M–
> 0.35	L+
> 0.1	L
≤ 0.1	I

2.3.3 Chemical barrier evaluation

The chemical extraction difficulty barrier does not have a specific numeric correspondence in the FLB model; rather, an inferred linguistic quantity is used to determine the performance of said barrier, based upon the levels given in [57]. Given that the chemical form of materials are generally "fixed" based upon the particular fuel cycle facility type, the chemical barrier was thus determined largely by the facility type, with additional criteria added for material mixtures (such as those found in reprocessing streams). The levels used for this analysis are given as Table 2.5.

2.3.4 Mass & bulk barrier

The mass and bulk barrier described in [57] gives quantities in roughly linguistic form (e.g., in a descriptive form based upon the relative difficulty of handling material). This was reduced to a rough estimate based on the mass of the material required itself (in kg). To account for

Table 2.5: Fuzzy ranking of chemical barrier performance, based on [57].

Rank	Description
I	Pure metals
L	Separated plutonium(oxide powder)
L+	Separated plutonium with > 0.5% minor actinides (oxide powder)
M–	Separated plutonium with > 5% uranium (oxide powder)
M	Intact, fresh UO_2, MOX, and FBR fuel Separated plutonium with any amount of fission products Separated plutonium with > 5% uranium **and** > 0.5% minor actindies
M+	Separated TRU with > 5% uranium **and** > 15% fission products
VH	Intact spent nuclear fuel and vitrified wastes

the additional "bulk" factor of less compact material forms (e.g., spent fuel rods, etc.), the calculated mass is in terms of the total required mass required to be diverted in order to acquire one significant quantity (8 kg for plutonium/TRU, 25 kg for uranium). For example, if plutonium is 1% of a material form by mass, an attacker would be required to divert 800 kg of material total (hence applying an overall penalty for the dilute form of plutonium). Table 2.6 gives the relative ranking levels used for the evaluation of the mass & bulk barrier.

Table 2.6: Fuzzy ranking of mass & bulk barrier performance, based on required mass for diversion of 1 SQ [57].

Mass (kg)	Rank
< 10	I–
< 15	I
< 30	I+
< 100	L–
< 250	L
< 2000	M
< 4000	H–
< 6000	H
> 10000	VH

2.3.5 Available mass barrier

The available mass barrier is quantified based upon the calculated bare sphere critical mass of the target material (Figure 2.3) and the mass loading of one reactor cycle (e.g., about 21.3 metric tons of uranium (MTU) fresh fuel or 21.3 metric tons of heavy metal (MTHM) MOX fuel for a typical one-third core loading); the available mass criteria developed for barrier rankings (based on [57]) is given as Table 2.7.

Table 2.7: Fuzzy ranking of available barrier performance, based on required mass for diversion of 1 SQ [57].

N_{CM}	Rank
> 25	I–
> 10	I
> 1	L
> 0.1	M
> 0.01	H
≤ 0.01	VH

2.3.6 Time barrier

The residence time barrier can be directly inferred from the time in residence of materials in a given nuclear fuel cycle facility. The correspondence used for this metric is given as Table 2.8.

2.3.7 Other barriers

Other barriers defined in the TOPS barrier framework [57], including the material detectability, facility unattractiveness, facility accessibility, facility diversion detectability, and the skills, expertise, & knowledge inherent to the process itself are difficult to explicitly quantify and are generally categorized by use of expert elicitation. For the purposes of this analysis, an evaluation using the TOPS barrier framework carried out by Hassberger shall be used as the reference values for these barriers [22], along with the criteria outlined within TOPS [57].

Table 2.8: Fuzzy ranking of residence time barrier performance, based on [57].

Time (years)	Rank
> 50	I
> 15	L
> 5	M
> 2.5	M+
> 1.0	H–
> 0.5	H
> 0.1	H+
≤ 0.1	VH

2.4 Stage and system fuzzy number evaluation

The process of synthesizing the stage and system fuzzy numbers is essentially unchanged from the method outlined in the original development of the Fuzzy Logic Barrier model [33, 35]. Therefore, the process for calculating these fuzzy values shall only be presented in brief in this section.

Given the barrier fuzzy effectiveness function $\mu_i(x)$ (for $i = 1 \ldots N_b$, and $N_b = 11$), the barrier fuzzy number for each barrier is defined as the ordinate-abscissa pair $\widetilde{A_i} = \left[\left(x_{\widetilde{A}_i}\ ,\ \mu_{\widetilde{A}_i}(x_{\widetilde{A}_i})\right)\right]$, where $i = 1 \ldots N_b$. Similarly, the stage fuzzy number for each stage $\widetilde{S}_j$ is given as $\widetilde{S}_j = \left[\left(x_{\widetilde{S}_j}\ ,\ \mu_{\widetilde{S}_j}(x_{\widetilde{S}_j})\right)\right]$. The stage fuzzy number is thus calculated using a fuzzy "AND" operation, calculated as Eq. 2.5 and Eq. 2.6 [33, 50].

$$x_{\widetilde{S}_j} = \frac{\sum_{i=1}^{N_b} x_{\widetilde{A}_i} w_i}{\sum_{i=1}^{N_b} w_i} \tag{2.5}$$

$$\mu_{\widetilde{S}_j}\left(x_{\widetilde{S}_j}\right) = \max_{x_{\widetilde{A}_i}} \left[\min\left(\mu_{\widetilde{A}_i}(x_{\widetilde{A}_i})\right)\right], i = 1 \ldots N_b \tag{2.6}$$

In Eq. 2.5, w_i represents the relative weight for each individual barrier (determined in the following section). This calculation is implemented through the use of a Monte Carlo calculation; for each barrier fuzzy number $\widetilde{A}_i$, a value x_i is generated, along with a corresponding $\mu_{\widetilde{A}_i}(x_i)$. From this, a value $x_{\widetilde{S}_j}$ is calculated (Eq. 2.5). Dividing the domain of

fuzzy numbers [0,1] into individual bins for $x_{\widetilde{S}_j}$, the maximum value of $\mu_{\widetilde{S}_j}$ is calculated for each bin (Eq. 2.6).

This process is then repeated for each stage j, producing a stage fuzzy number $\widetilde{S}_j$ for each fuel cycle stage.

These stage fuzzy numbers are then combined into a system fuzzy number through use of a fuzzy "OR" operation, which is implemented as Eq. 2.7 [33, 50], where W_j is the calculated stage weight (discussed in a following section).

$$\mu_{sys}(x) = \frac{\sum_{j=1}^{N_s} W_j \mu_j(x)}{\sum_{j=1}^{N_s} W_j} \tag{2.7}$$

This process is repeated over the entire domain of the fuzzy number (i.e., $\mu(x)$ is calculated for each of the x bins spanning the domain on [0,1]). From this, a system fuzzy number is constructed for the fuel cycle.

2.5 Barrier weight selection

Barrier weight selection was done through a pairwise comparison of the relative importance of different barriers to particular types of threats, as outlined by the TOPS committee: these include a relatively industrially advanced state in an overt breakout (sophisticated state, overt: SSO), a sophisticated state in a covert breakout (sophisticated state, covert: SSC), and a relatively less developed nation making a covert breakout attempt (unsophisticated state, covert: USC) [57].

The idea that different proliferation barriers would show different levels of importance for different adversary types, particularly on the basis of national capabilities, is well-established in the literature [3, 42, 58]. In particular, NASAP identifies that physical barriers such as the radiological hazard, chemical form, and isotopic attractiveness would present a much more significant barrier to relative unsophisticated states lacking spent fuel reprocessing facilities compared to sophisticated states with such facilities, given the substantial "out-of-system" facilities required to recover plutonium [58]; however, barriers such as the radiological barrier are far less effective for a sophisticated state with such facilities. Likewise, strategies such as co-processing (e.g., affecting the isotopic and chemical barriers) are of minimal effectiveness

for an "abrupt" diversion event (e.g., an overt breakout) [58]. Ergo, "physical" barriers such as the isotopic, radiological, and chemical barriers play a more diminished role for the sophisticated state, particularly in an overt breakout scenario.

In order to make an effective pairwise comparison of the individual barriers, they were first divided into four subordinate groups, based on the groupings found in the SAPRA methodology [20]. These groupings are given as Table 2.9.

Table 2.9: Barrier groupings used for pairwise comparisons in relative weight analysis.

Grouping	Barrier
Material properties	Isotopic Chemical Radiological
Design features	Facility access Mass & bulk Material detectability
Undeclared production	Skills, expertise, & knowledge Facility unattractiveness
Verifiability	Facility diversion detectability Available mass Time

Each barrier was assigned a value from 1 (low importance) to 9 (high importance) based on the relative importance to a given adversary type given in [57]; these assignments were then used to construct a pairwise comparison of both individual barriers within each subcategory and the subcategories themselves. The pairwise comparisons were constructed using the *difference* in the weight values for the pairwise comparison; a similar procedure was used with the sums of individual barrier importances for the subordinate category comparisons (e.g., differences in sums were used to compare relative category rankings).

Saaty's method was used to calculate the barrier weights [48]. Five matrices were constructed (four for the barriers of each subcategory and one for the subcategory matrices); the diagonal elements of these matrices were 1 and the respective upper and lower elements

were inverses of one another. For example, given items A, B, and C, if A is assigned an outrank difference over B of 5 and A over C of 3, and C is assigned an outrank difference of B of 7, this would produce the following matrix:

$$\begin{bmatrix} A \\ B \\ C \end{bmatrix} = \begin{bmatrix} 1 & 5 & 3 \\ \frac{1}{5} & 1 & \frac{1}{7} \\ \frac{1}{3} & 7 & 1 \end{bmatrix} \begin{bmatrix} w_1 \\ w_2 \\ w_3 \end{bmatrix}$$

Taking the real eigenvalues of this matrix would yield relative weights of [0.6018, 0.07460, 0.3236] for elements A, B, and C.

Thus, the relative rankings were used to populate each matrix accordingly through this process. Weights were calculated by finding the real eigenvector for each matrix, and then multiplying the eigenvector for each coefficient matrix by the corresponding eigenvalue term for the subcategory ranking matrix, producing relative weight values for each barrier. The barrier weights were then normalized to unity to produce the final weight values.

The barrier weight assignments produced using this method are given as Table 2.10.

Table 2.10: Relative barrier weights for proliferation attempts by a: sophisticated state, overt (SSO); sophisticated state, covert (SSC); and an unsophisticated state, covert (USC), based upon values in [57].

Barrier	SSO	SSC	USC
Isotopic	0.1688	0.1047	0.4029
Radiological	0.06845	0.05563	0.06019
Chemical	0.02775	0.01970	0.1349
Mass & Bulk	0.01338	0.01449	0.01236
Material detectability	0.01338	0.01449	0.02471
Facility unattractiveness	0.1013	0.04140	0.01303
Facility access	0.01338	0.01449	0.02471
Available mass	0.4310	0.3304	0.1807
Facility diversion detectability	0.08620	0.3304	0.06023
Skills, expertise, & knowledge	0.01567	0.008280	0.02606
Time	0.06070	0.06608	0.06023

2.6 Stage weight selection

Weighting of the various stages within the fuel cycle system is accomplished through a multi-step process. First, taking the assumption that the heavy metal inventory is relatively constant for non-reactor stages (a generally defensible assumption given the half-lives of most actinides), the nuclear energy system can be broken up into constituent "subsystems" based upon the heavy metal inventory. For example, for a LWR-OT system, two subsystems exist: one of the stages before irradiation (e.g., enrichment, fuel fabrication, etc.), and the second consisting of irradiation and post-irradiation stages (e.g., spent fuel handling and disposal). For modified open cycles and closed cycles, additional subsystems are added based upon the concurrent irradiation stages; for example, a MOX system would consist of the pre-reactor subsystem, the post-LWR subsystem (including reprocessing and MOX fuel fabrication), and then a third subsystem consisting of MOX fuel irradiation and disposal. An example of the subsystem breakdown is shown as Figure 2.4.

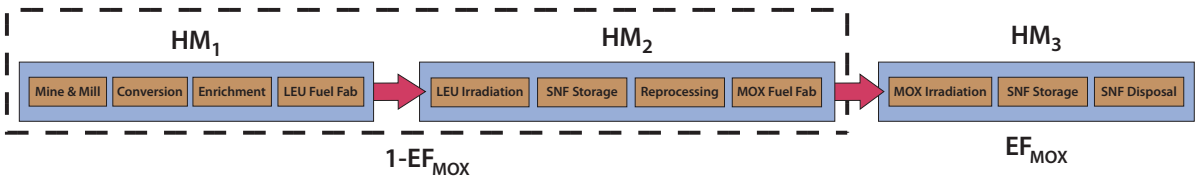

Figure 2.4: Example of mass weighting calculation for a modified open cycle with MOX fuel. HM_i represents the total heavy metal inventory at each subsystem, while EF_{MOX} represents the relative fraction of total electricity generated from MOX fuel, based upon the actinide inventory available for recycling.

Second, a mass balance is applied to the system in order to account for material flow, namely by the calculation of the required fuel mass input per unit of electricity produced (i.e., $\frac{\text{kg}}{\text{TWhe}}$), similar to studies performed by the NEA [40]. For the modified open cycle and closed cycle, this mass balance is used to then calculate the equilibrium share of electricity production by calculating the amount of available TRU for MOX and Fast burner reactor (FBR) fuel fabrication. The mass flow required (and hence available electricity fraction) is thus a function of two parameters: the TRU inventory of LWR fuel and the burnup of fuel in the secondary irradiation stage (dictating the amount of fuel required per unit energy). Assumptions of reactor electrical conversion efficiency are taken as those given in [40].

The weighting between subsystems is thus the ratio of heavy metal inventories scaled by the electricity production factor; this relationship is given explicitly by Equation 2.8, where $\mathrm{EF}_{\mathrm{reirrad.}}$ is the electricity fraction from the re-irradiation cycle (calculated from the available mass flow), HM_i is the heavy metal mass inventory in the given subsystem, and N_{SS} is the number of subsystems.

$$\mathrm{W}_i = \begin{cases} \mathrm{MF_i} \cdot \dfrac{\mathrm{HM_i}}{\sum_{\mathrm{i}}^{\mathrm{N_{SS}}} \mathrm{HM_i}} \cdot (1 - \mathrm{EF_{reirrad.}}) & \text{Pre-reactor \& LWR stages} \\ \mathrm{MF_i} \cdot \dfrac{\mathrm{HM_i}}{\sum_{\mathrm{i}}^{\mathrm{N_{SS}}} \mathrm{HM_i}} \cdot (\mathrm{EF_{reirrad.}}) & \text{Re-irradiation stages (MOX \& FBR)} \end{cases} \tag{2.8}$$

A mass flow parameter, MF_i, accounts for the heavy metal mass flow per unit energy for each subsystem. This parameter, in units of mass per unit energy ($\frac{\mathrm{kg}}{\mathrm{TWhe}}$) is calculated as Eq. 2.9.

$$\mathrm{MF}_i = \begin{cases} \dfrac{24 \cdot 10^9}{\mathrm{BU} \cdot \epsilon} & i > 1 \\ 1 & i = 1 \end{cases} \tag{2.9}$$

In Eq. 2.9, ϵ is the reactor thermal efficiency (taken from [40] and given as Table 2.11) and BU is the fuel burnup in units of $\frac{\mathrm{MWd}}{\mathrm{MTHM}}$, producing a final mass flow in $\frac{\mathrm{kgHM}}{\mathrm{TWhe}}$.

Table 2.11: Thermal and electrical power assumed for each reactor type in this study with corresponding thermal efficiency (ϵ), from [40].

Reactor	Thermal power (MW)	Electrical power (MW)	Efficiency (%)
LWR-UO_2	4250	1450	34.1
LWR+MOX	4250	1450	34.1
CANDU HWR	713	2159	33.0
FR-MOX	600	1575	38.1

The electricity fraction is used for fuel cycles involving partial or full recycling of actinides in order to calculate the relative energy contribution from energy production achieved from recycled fuels, and thus the relative contribution to the overall system (in terms of relative weight). For example, if the electricity production ratio from MOX fuel is 11% (as would be the case for equilibrium mass flow with UO_2 and MOX fuel burnups of 60 $\frac{\text{GWd}}{\text{MTU}}$ / $\frac{\text{GWd}}{\text{MTHM}}$ [40]), the weight of each subsystem is calculated from the subsystem heavy metal inventory (based on the equilibrium material mass flow) and then scaled accordingly by the electricity fraction. Thus, the MOX weight would be scaled by 0.11, and the pre-reactor and post-LWR weights would be scaled by 0.89. The subsystem weighting thus takes into account varying mass flow, giving greater prominence to stages with a higher overall flow of fissile materials.

The electricity fraction for partially and fully closed cycles is calculated as a ratio of the available actinides for recycle (dictating the amount of energy which can be obtained from the recycled actinides) and the relative energy produced (in terms of mass times burnup) of the UO_2 and recycled fuel. An example application of this calculation is Eq. 2.10.

$$\text{EF}_{\text{MOX}} = \frac{\text{Pu}_{\text{LWR}}}{\text{Pu}_{\text{MOX}}} \cdot \frac{\text{M}_{\text{MOX}} \cdot \text{BU}_{\text{MOX}} \cdot \epsilon_{\text{MOX}}}{\text{M}_{\text{MOX}} \cdot \text{BU}_{\text{MOX}} \cdot \epsilon_{\text{MOX}} + \text{M}_{\text{UO}_2} \cdot \text{BU}_{\text{UO}_2} \cdot \epsilon_{\text{UO}_2}} \tag{2.10}$$

In Eq. 2.10, EF_{MOX} is the electricity fraction produced by MOX fuel, Pu_{LWR} is the total amount of plutonium available in LWR fuel, Pu_{MOX} is the total amount of plutonium required for a MOX core loading (i.e., the fraction of plutonium in MOX fuel multiplied by the total mass of MOX fuel in the core), M_{MOX} and M_{UO_2} are the mass loadings of the MOX and UO_2 cores, respectively, while BU_{MOX} and BU_{UO_2} are the fuel burnups of the MOX and UO_2 fuel respectively and ϵ_{MOX} and ϵ_{UO_2} are the thermal efficiencies of the MOX and UO_2 reactors.

The rationale for this choice of weighting system is twofold: first, the goal of such a system is to be able to account for differences in heavy metal mass flow between different systems. That is, for systems with higher fuel burnups, the overall mass flow per unit electricity ($\frac{\text{kg}}{\text{TWhe}}$) decreases, thus shifting the overall balance of the system heavy metal inventory. Second, it is generally valid to assume that the total heavy metal inventory in the system (normalized to electricity production) only changes upon the transmutation of heavy metal in the reactor, thus creating a neat delineation between different subsystems. The electricity fraction component (EF) accounts for the mass balance in fuel cycles with actinide recycle under equilibrium; i.e., given the fact that a limited actinide inventory is discharged from once-burned UO_2 fuel, the mass inventory of the re-irradiation portion of the fuel cycle is controlled by the mass balance itself (e.g., the electricity fraction).

To adjust for the difference in critical mass requirements between ^{235}U and Pu, the IAEA standard of 25 kg for one significant quantity (SQ) of ^{235}U is used with 8 kg for Pu. Given that mixtures of Pu and minor actinides show little difference in the overall size of the BSCM, the sum of TRU is taken from the subsystem inventory and thus scaled by $\frac{25}{8}$ in order to compare enriched uranium inventories to TRU inventories.

Individual constituents of the subsystems (stages) are then weighted by the fraction of fissile material within the total mass flow (i.e., the fraction of ^{235}U and ^{239}Pu to the total mass flow). The net result is that stages with higher concentrations of fissile materials (such as post-enrichment, post-irradiation, and reprocessing) show a higher importance than those with relatively low concentrations (e.g., pre-enrichment and reprocessing wastes).

The stage weights within each subsystem are normalized for the individual subsystem, as are the subsystem weights themselves. Each stage weight is scaled by its corresponding subsystem weight to produce a net stage weight; thus, the total sum of stage weights is unity.

2.7 Application of the Fuzzy Logic Barrier model

2.7.1 Comparative system analysis

One of the chief uses of the FLB model is in the comparative evaluation of different fuel cycle systems (including both different fuel cycle configurations as well as the evolution of system PR for a fixed system over given parameter such as burnup). An example of such a comparison is given as Figure 2.5.

The comparative system evaluation is the primary level of analysis, affording an overview of system PR behavior between different fuel cycle configurations, in addition to PR evolution over parameters such as burnup. Such an analysis is particularly useful for rough rank-ordering of fuel cycle configurations. For example, in Figure 2.5, one will observe that the LWR-OT cycle is clearly of the highest intrinsic PR, due to the lack of plutonium separation and self-protecting features such as the high radiological field. By contrast, a cycle with PUREX-based recycling for MOX fuel shows the lowest intrinsic PR, due to the lack of effective intrinsic barriers during actinide recovery stages. However, one observes an overlap between common portions of the once-through and MOX cycles, due to the identical PR behavior of the two systems prior to reprocessing.

Likewise, one observes that the fast reactor cycle appears to show slightly greater intrinsic

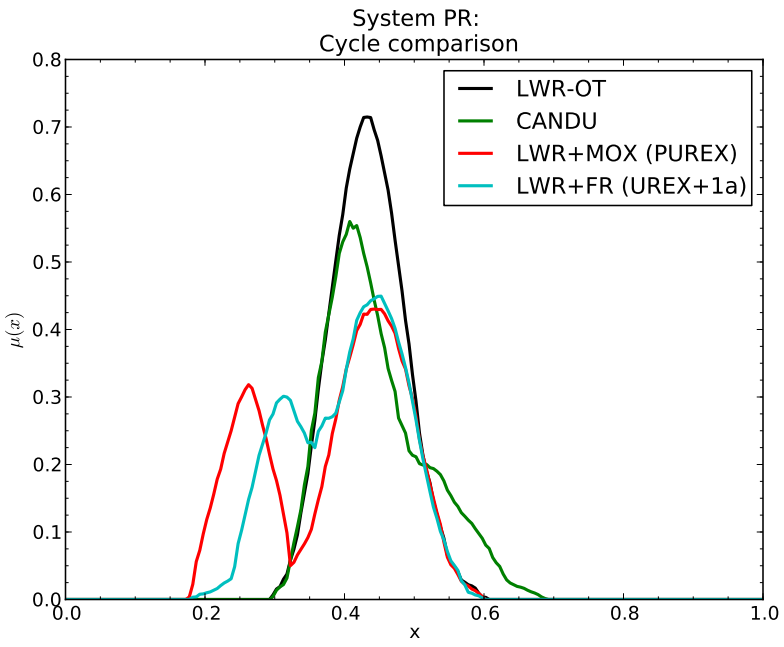

Figure 2.5: Comparative system PR assessment for a LWR once-through cycle, a CANDU HWR cycle using natural uranium fuel, a LWR + MOX cycle (PUREX), and a LWR + fast reactor cycle using advanced UREX series separation (UREX+1a).

PR than the MOX cycle, due to both the co-extraction of other actinides which slightly diminish the attractiveness of the separated stream (such as minor actinides) as well as the less attractive end form of the spent fast reactor fuel.

Finally, showing only slightly less intrinsic PR than the LWR once-through cycle is the CANDU HWR cycle. Despite the lack of an enrichment stage in the CANDU cycle (which is a more sensitive stage in LWR-based cycles), the end plutonium vector of CANDU stages is slightly more attractive than that of LWR cycles due to lower burnup. CANDU cycles also suffer a PR penalty due to the online refueling capabilities, affording greater overall access to materials during a sensitive stage (e.g., reactor irradiation).

For this analysis, comparative system assessment shall be one of the primary methods for comparing overall system PR behavior.

2.7.2 System ranking analysis

Several methods have been proposed for the ranking of fuzzy numbers [7, 14, 16, 36] including the possibility/necessity of strict dominance method proposed by DuBois and Prade [14] which was used by Li [33, 35]. However, in addition to being somewhat ambiguous in terms of producing actual rankings (relative to the barriers defined in Table 2.2 and Figure 2.2), there are particular problems with producing consistent rankings using this approach.

Instead, the approach identified in [16] shall be used, which was found to generally deliver more consistent fuzzy rankings. The advantages of this approach are in its relative simplicity of implementation, consistency of rankings, and in the fact that it was explicitly designed for the ranking of triangular fuzzy numbers (which are used for the fuzzy rankings used in the FLB approach).

For this approach, the "pessimistic" ranking estimate described in [16] is used, namely to give a least upper bound to the rankings. The pessimistic rank preference function is defined as Eq. 2.12. The pessimistic estimate is described as the "worst results that could be obtained from a fuzzy number [...] suitable for a risk-averse decision maker" [16]; it thus appears to be most appropriate for this context.

$$\Phi_P(A,B) = \max_x \{\min(\mu_{Low(A)}(x), \mu_B(x))\} \tag{2.11}$$

$$= \min\left\{\max\left(\frac{a_2-b_1}{a_2-a_1+b_2-b_1}, 0\right), 1\right\} \tag{2.12}$$

In Eq. 2.12, $\mu_A(x)$ is defined by the triplet (a_1, a_2, a_3), which can also be expressed as Eq. 2.13.

$$\mu_A(x) = \begin{cases} 0 & 0 \le x \le a_1 \\ \dfrac{x-a_1}{a_2-a_1} & a_1 \le x \le a_2 \\ \dfrac{x-a_3}{a_2-a_3} & a_2 \le x \le a_3 \\ 0 & x \ge a_3 \end{cases} \tag{2.13}$$

$\mu_{Low(A)}(x)$ is defined as a characteristic function of $\mu_A(x)$, given as Eq. 2.14.

$$\mu_{Low(A)}(x) = \begin{cases} 1-\mu_A(x) & x \le a_2 \\ 0 & \text{otherwise} \end{cases} \tag{2.14}$$

The correspondence between $\mu_A(x)$ and $\mu_{Low(A)}(x)$ is shown as Figure 2.6.

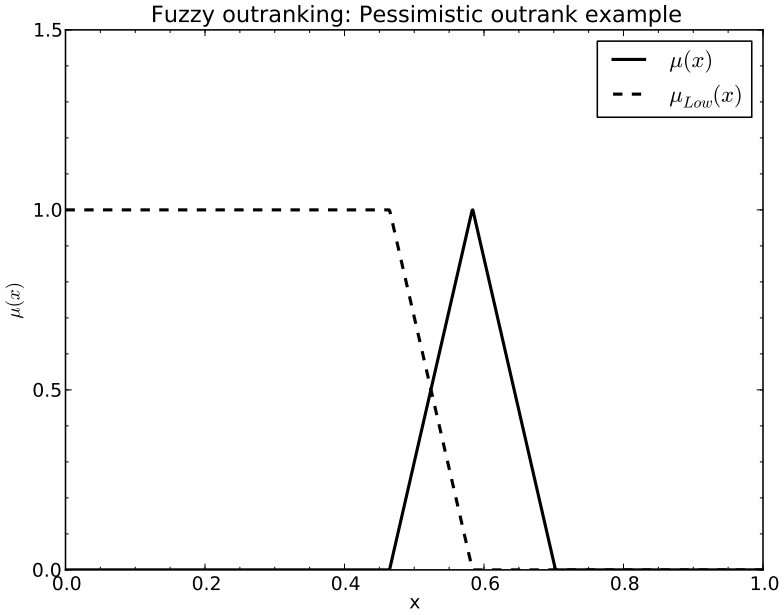

Figure 2.6: Example of the relative quantities used for fuzzy outranking of triangular fuzzy numbers ($\mu_A(x)$) using the pessimistic outrank criteria ($\mu_{Low(A)}(x)$), based on [16].

A preference function for ranking fuzzy functions A and B is defined as Eq. 2.15 [16].

$$A \succ_P B \iff \Phi_P(A,B) > \frac{1}{2} \tag{2.15}$$

For each fuel cycle system, the system fuzzy number was ranked against each of the triangular fuzzy numbers making up the linguistic rankings (Table 2.2 and Figure 2.2); i.e., the linguistic fuzzy number in this context is "A" and the system fuzzy number (e.g., $\mu_{sys}(x)$) is "B." Thus, the assigned system ranking is the highest ranking for which $\phi_P((A,B)) > \frac{1}{2}$. This ranking can thus be used as a simple means of comparing differences in PR between different fuel cycle configurations and parameters (e.g., burnup, enrichment, etc.).

2.7.3 System decomposition analysis

Another useful means of characterizing the behavior of system PR behavior is through the decomposition of the fuel cycle system into its respective stage fuzzy numbers. This can be accomplished in two ways, each with its own purpose: first, a "cross-section" of the stage fuzzy number centroid values can be evaluated, giving a rough indication of the relative behavior of system PR behavior. Such a process is illustrated for a LWR + MOX cycle as Figure 2.7.

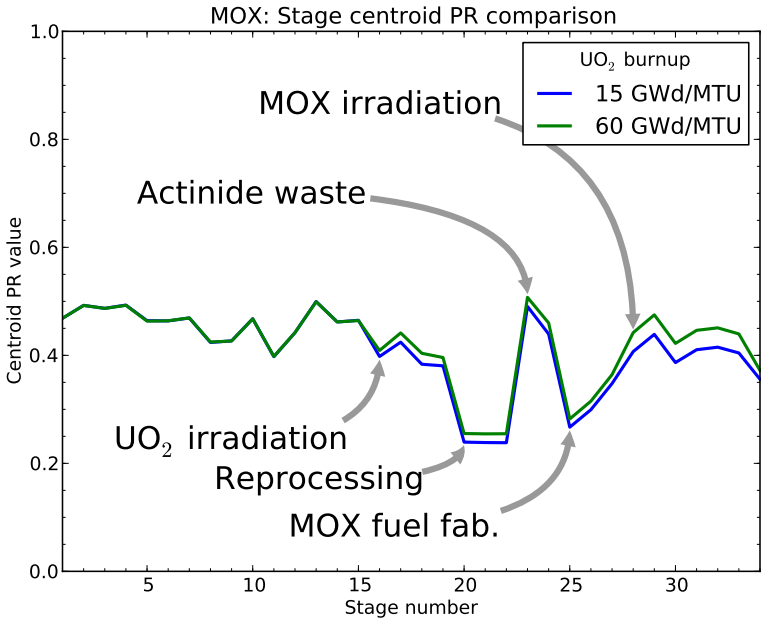

Figure 2.7: Example of decomposition of system PR into level fuzzy centroid values for a LWR + MOX (PUREX) cycle.

This process is particularly useful for characterizing relative PR behavior between individual stages; i.e., the PR *vector*. Such a process is particularly useful for applications such as barrier weight calibration; given that relative PR behavior between particular stages is well-understood for well-characterized systems (such as a LWR once-through cycle), system PR cross-section analysis can be used as a "veto" mechanism for weight sets which produce uncharacteristic evaluations of relative PR (e.g., increases in PR in sensitive stages such as

enrichment).

A second process which can be employed is a decomposition of the system fuzzy number into the relative stage fuzzy numbers. Such a process can be useful for understanding trends in system PR behavior, particularly for bifurcated behaviors (which are often present for fuel cycles involving plutonium separation). An example of this is shown as Figure 2.8.

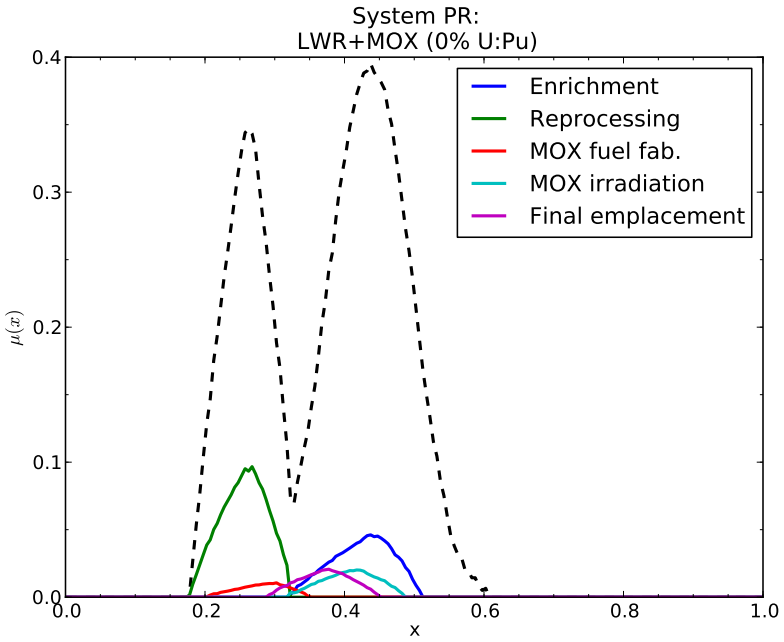

Figure 2.8: Decomposition of system PR fuzzy number into weighted respective stage fuzzy numbers for a LWR + MOX (PUREX) cycle. System fuzzy number shown as black, dashed.

As one observes in Figure 2.8, reprocessing-related stages contribute to the lower PR peak observed in a PUREX-based MOX system, due to the general lack of intrinsic PR barriers for separated plutonium. Given the material concentrations in these stages, these stages thus contribute significantly to the overall shape of the system PR. A second peak is composed of stages consisting of intact fuel, both pre-irradiation (where LEU must be subsequently re-enriched for weapons utility) and intact fuel post-irradiation (where radiological and chemical barriers are most effective).

2.7.4 Stage decomposition analysis

A final level of analysis can be performed through a decomposition of the stage into the weighted constituent barrier fuzzy rankings. Such an approach is useful for characterizing the behavior of intrinsic barriers at a particular fuel cycle stage, especially as a function of fuel cycle parameters of interest (e.g., burnup, enrichment, etc.). Such an analysis likewise has utility for evaluating safeguards effectiveness, namely by characterizing the driving behavior behind stage (and subsequently system) PR at the individual barrier level.

An example of this process is given as Figure 2.9. Three barriers are examined as a function of burnup in this breakdown: isotopic attractiveness (solid line), available mass (dashed line), and time (dot-dashed line); all other barriers are constant.

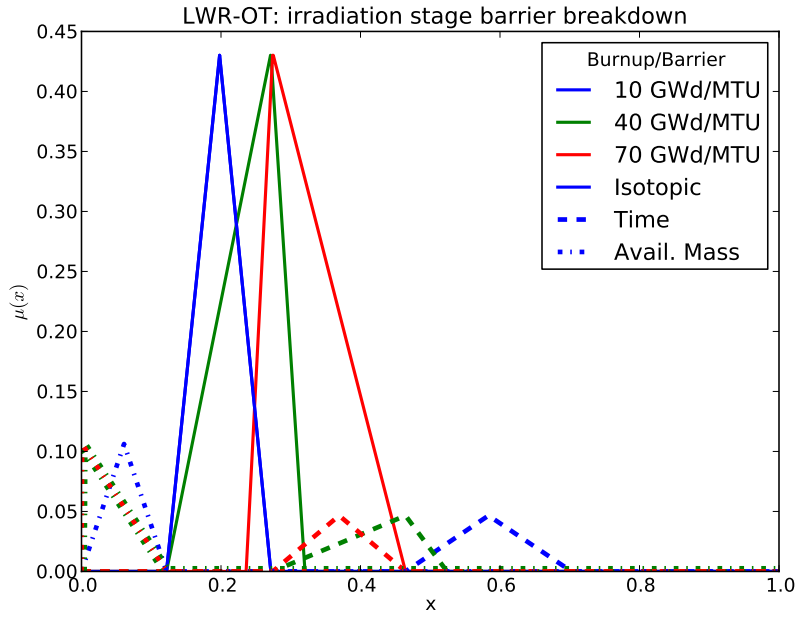

Figure 2.9: Example of barrier decomposition analysis, as applied to the irradiation stage of a LWR fuel cycle for varying burnup. (Blue): 10 $\frac{\text{GWd}}{\text{MTU}}$, (Green) 40 $\frac{\text{GWd}}{\text{MTU}}$, (Red) 70 $\frac{\text{GWd}}{\text{MTU}}$; (Solid) Isotopic barrier, (Dashed) Time barrier, (Dot-dashed) Available mass barrier.

For increasing burnup, the isotopic attractiveness slowly increases; however, the available mass barrier decreases (as more plutonium is produced) and the time barrier decreases

slightly (due to the longer residence time). The chief advantage of decomposition analysis is that it allows for a direct comparison of trends in barrier performance as a function of input parameters. Such an evaluation can be thus used for targeting safeguards by type and efficacy.

As evident in this case, the evolution of barriers is often not in concert (and in fact can be at cross-purposes). For example, given that burnup is both directly associated with time and less directly so with isotopic attractiveness (i.e., due to the ingrowth of higher plutonium species, etc.), in irradiation stages the isotopic and time barriers will often move oppositely with respect to burnup. Likewise, the production of greater plutonium inventories can cause a small drop in the available mass barrier with increasing burnup (although this barrier saturates much more quickly in this context).

CHAPTER 3

Coupling isotopic characterization with PR analysis

3.1 Introduction

One particular problem that arises in attempting to couple nuclear fuel analysis codes such as SCALE directly into fuel cycle PR models is in the difficulty of constructing case inputs. Interfaces such as the ORIGEN-ARP graphical user interface (GUI) provide an excellent means to solve this problem, but do not easily lend themselves to automated case construction or embedding within other analysis codes.

However, by developing and implementing a new interface module to simplify the process of evaluating nuclear fuel depletion and decay, it is possible to construct a generalized fuel cycle model composed of modular cycle stages. The new interface module for ORIGEN-S (called OASIS) uses high-level keywords to construct the input files used by ORIGEN-S, eliminating much of the difficulty of constructing case input [52]. It also allows one to construct a series of modular fuel cycle levels which can be then chained together as one coherent fuel cycle system.

In this chapter, a method for directly coupling nuclear fuel analysis via ORIGEN-S into a fuel cycle model of interest (e.g., the FLB model) shall be presented. This shall include an overview of the OASIS module created to simply ORIGEN-S input as well as the generalized fuel cycle framework designed to represent different fuel cycle facility types, thus enabling a

direct tracking of the evolution of nuclear materials throughout the system from within the model.

3.2 OASIS overview

The OASIS module for SCALE[1] is a new user interface for ORIGEN-S designed to radically simplify the process of nuclear fuel depletion and decay evaluation, along with providing greatly enhanced capabilities for chained case analysis [52]. One of the drawbacks to the FIDO input system for ORIGEN-S is its steep learning curve with input that is far from easily user-friendly (or human-readable). Such disadvantages are a frequent reason why individuals continue to use older, obsolete codes such as ORIGEN2. Alternatively, many use the ORIGEN-ARP GUI provided with SCALE; while this provides for an excellent solution for standalone analysis, it does not easily lend itself to chained analysis cases or to automation and embedding into other codes.

The OASIS module was designed to solve several of these problems. OASIS uses high-level keywords to construct the traditional FIDO input files used by ORIGEN-S, thus eliminating much of the difficulty of constructing case input. In particular, the capabilities of the OASIS module and its vastly simplified interface allow one to construct a series of modular fuel cycle levels which can be then chained together as one coherent fuel cycle system. Likewise, given the streamlined nature of the OASIS input, the construction of the modular input deck can be largely automated to allow for coupling into general fuel cycle models.

An example of OASIS input for a simple irradiation case is given as Figure 3.1. In this particular example, OASIS can easily construct an irradiation case and subsequent decay in a mere 13 lines, compared to the over 50 lines required for a traditional FIDO input file.

Thus, using the OASIS module, it is possible to draw upon the sophistication of ORIGEN-S and its depletion model for direct evaluation of spent fuel characteristics as a function of time, including such features as isotopic composition, radiation signatures (gamma and neutron), thermal power, etc. As a result, fuel cycle PR models can automate input deck construction for OASIS and directly draw upon SCALE data to perform analysis.

Current plans entail the public release of the OASIS module with the release of the SCALE 6.1 update.

[1] See Appendix B for a more detailed treatment of the functionality of the OASIS module for SCALE.

```
=oasis
  title= sample PWR irradiation
  id=cz205
  lib=w17x17_ofa
  mod= 0.7332
  enrich= 3.965
  lightel= o 135.95 cr 5.91975 mn 0.328875 fe 12.9358
           co 0.074545 ni 9.86625 nb 0.7016 sn 3.508 end
  read radhist
          power= 40.2  burn= 331.675  down= 54.7264 end
          power= 40.2  burn= 331.675  down= 54.7264 end
          power= 40.2  burn= 331.675  down= 1 end
  end radhist
end
```

Figure 3.1: Example of a simple irradiation case in OASIS.

3.3 Implementing coupled PR evaluation

With the OASIS module, it is possible to produce a direct coupling of nuclear fuel depletion and decay analysis with a given fuel cycle model. Using a generalized model for fuel cycle facilities (e.g., based on specialized level "types" for individual facilities), the process of creating a coupled analysis framework based upon generalized fuel cycle facilities shall be presented in brief.

3.3.1 A generalized fuel cycle model

Given the streamlined nature of the OASIS input, the construction of the modular input deck can be largely automated, allowing for direct coupling into general fuel cycle models. By drawing upon the sophistication of ORIGEN-S and its depletion model for direct evaluation of spent fuel characteristics as a function of time, including such features as isotopic composition, radiation signatures (gamma and neutron), thermal power, etc., the fuel cycle model can perform PR analysis directly as a function of high-level parameter input, such as total fuel burnup, specific power, cooling time, and isotope separation strategies.

Thus by making use of OASIS, it is possible to construct a generalized fuel cycle model

composed of modular cycle stages. In the generalized model, stages are broken down into generic "types" with configurable input parameters. These level types include a "generic" level (i.e., for non-OASIS/SCALE stages, such as pre-reactor operations), fuel irradiation (UO_2 and MOX), decay, reprocessing, fuel batching, and MOX fuel fabrication.

Constructing the generalized model in C++ has allowed for each generalized level type to be instantiated as it is own class, each deriving from a generalized fuel cycle class, with specialized functions for particular stage types. C++'s polymorphism and inheritance features allow the user to create a logical hierarchy of related level types (i.e., inheriting related parameters and functionality). The general inheritance structure of the level types used for this integration work is shown as Figure 3.2.

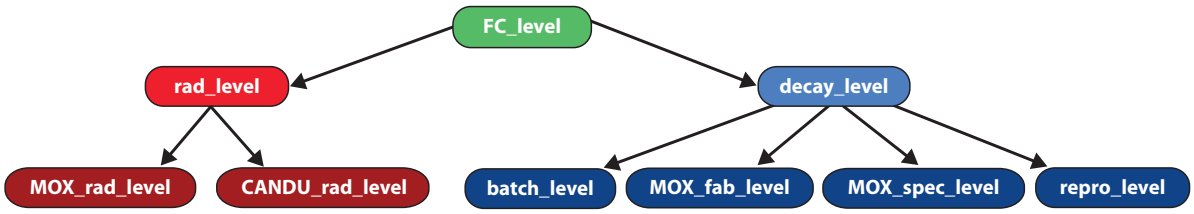

Figure 3.2: Inheritance hierarchy of generalized fuel cycle classes used for fuel cycle evaluation and analysis.

Each fuel cycle class inherits generic functions to track such features such as the position on the binary ORIGEN-S output, handle such functions such as stage weighting (e.g., tracking the heavy metal inventory), etc. Specialized classes handle features such as the construction of the appropriate OASIS input for a given stage type (e.g., irradiation versus reprocessing), processing relevant stage input, and other stage-specific features (e.g., calculation of the radiological source term).

A particular advantage in using the inheritance-based framework is in its natural scalability; new specialized level "types" can easily be added to expand upon the existing capabilities of the framework. For example, a class for a fast-spectrum reactor (FBR_RAD_LEVEL) as well as re-irradiation in CANDU (e.g., DUPIC: DUPIC_RAD_LEVEL) were added, based upon the functions of RAD_LEVEL. Other specialized level types can also be added; for example, a voloxidation process was added (VOLOX_LEVEL) as a special case of the reprocessing level class (REPRO_LEVEL).

The sum result of this integration is a model in which information from ORIGEN is directly accessible to PR models without user intervention; this allows for a much more sensitive means of analysis using physically verified data with a far more streamlined user interface. This integration thus affords a great deal of automation capability within the analysis, a particular advantage for evaluating the specific impact of cycle parameters upon system PR in many models, as shall be demonstrated in the following chapters.

3.3.2 Generalized fuel cycle levels

Each level type in the analysis inherits from a master "generic" fuel cycle level (FC_LEVEL), which contains a generic set of data structures and function definitions for calculating barrier definitions, stage weights, etc.

Two specialized child classes implement basic OASIS/ORIGEN-S functionality: RAD_LEVEL and DECAY_LEVEL, which correspond to a basic LWR irradiation and a generalized decay stage. Each of these child classes contains respective functions to build an OASIS string for their corresponding function (e.g., irradiation or decay of a prior case).

The irradiation level takes in parameters corresponding to enrichment, specific power, burn time, and irradiation cross-section library (for use with ARP interpolation or user cross-section libraries), total burnup, number of irradiation cycles, down time, and decay time following irradiation. These parameters are then assembled to produce both input for ARP cross-section library interpolation in addition to the OASIS string.

Further specialized levels build upon the functions created in RAD_LEVEL and DECAY_-LEVEL to perform other tasks. For example, REPRO_LEVEL takes in parameters of separation fractions of plutonium, minor actinides, lanthanides, and a uranium dilution fraction (i.e., the dilution factor of the stream with uranium from spent fuel), and finally a decay time following separation. MOX fuel fabrication levels (MOX_BLEND_LEVEL and MOX_SPEC_LEVEL) create a mixture of MOX fuel either from blending of prior streams (MOX_BLEND_LEVEL) or through direct user specification of the constituent elements such as the plutonium fraction and plutonium vector (MOX_SPEC_LEVEL).

Derivative classes of RAD_LEVEL are used to produce other types of reactor irradiation scenarios, including the irradiation of natural uranium in a heavy-water CANDU reactor (CANDU_RAD_LEVEL), irradiation of MOX fuel (MOX_RAD_LEVEL), and the irradiation of fast reactor fuel (FBR_RAD_LEVEL). Each reactor class contains both the specialized functions to create the necessary OASIS string for depletion analysis as well as built-in error checking

based on the built-in bounds for ARP interpolation (e.g., lower and upper thresholds for burnup, enrichment, etc.).

Each of these classes also contains general information about the chemical form of the fuel (e.g., as a single compound, mixed oxide, or spent fuel), thus allowing the chemical barrier to be directly evaluated as part of the fuel cycle level class. Various aliases are used with FC_LEVEL and DECAY_LEVEL in order to simplify differentiation of various intermediate process stages, such as material transport, disposal, and various pre-reactor stages such as uranium enrichment and fuel fabrication.

Making use of the stream tracking capabilities of OASIS, each level has the capability of "picking up" concentrations from a prior, user-specified stream to operate on. Thus changes in nuclear materials as a function of time (e.g., due to transmutation and decay) can be followed directly in PR models using this method.

3.4 Coupled PR evaluation

Once each fuel cycle level has been processed and the appropriate OASIS strings have been constructed for each stage, the OASIS strings are combined together into a single OASIS master input deck for the system, where the cases are then sequentially executed. Results from analysis cases are stored upon sequential file positions within the binary SCALE output, thus enabling chained evaluation of material properties in both ORIGEN-S and the PR model (i.e., given that the generalized levels are designed to be able to follow the binary file positions of preceding fuel cycle stages).

Each generalized fuel cycle level stage contains the respective file position on the ORIGEN-S binary for the respective fuel properties data for said stage. Thus, using a data accessor function[2], the relevant physical attributes for each stage are retrieved directly from the ORIGEN-S binary file, including isotopic inventories and gamma/neutron emission rates in (user-configurable) energy groups (which can be used both for calculations of dose rate as well as directly modeling detector response for specific safeguards applications). Built-in regular expressions retrieve thermal output data (in units of W/kg) from the ORIGEN-S text output for plutonium, minor actinides, and the total heat generation rate; thermal data can also be directly incorporated into the PR evaluation.

Following the execution of the master OASIS deck in SCALE, the model then cycles

[2]See Appendix C for greater details on the retrieval of data from the ORIGEN-S binary output.

through each level class to perform the relevant PR analysis, retrieving the corresponding physical data from the ORIGEN binary. Figure 3.3 summarizes the process of constructing the OASIS deck from user input and the subsequent evaluation of system PR.

3.5 Conclusion

As a result of the coupling technique proposed in this chapter, fuel cycle analysis can thus be performed directly upon the entire inventory of physical data output from ORIGEN-S. Such a coupling affords numerous analytical capabilities, including the evaluation of fuel cycle performance as a function of high-level system parameters such as reactor type, fuel burnup, enrichment, cooling time, etc. Likewise, the coupling process allows for new avenues of analysis, including a direct evaluation of the radiological (gamma and neutron) spectrum (from user-configurable energy bins), thus allowing for a direct evaluation of aspects such as detector response. Such an evaluation has several useful potential applications, including the evaluation of safeguards performance of non-destructive analysis (NDA) systems and other measures for material control & accountability (MC&A) in fuel cycle facilities (particularly for reprocessing facilities) [18].

Likewise, such a coupling technique has obvious applications beyond the metric of fuel cycle PR considered in this study; e.g., the technique could conceivably be applied to such applications as overall fuel cycle analysis (similar to models such as VISION [28, 61]) and models for fuel cycle mass loading and overall repository performance [34]. Unlike VISION however, which tracks only 81 isotopes [28], ORIGEN-S tracks over 2000 radioisotopes [43]. While simulation frameworks such as VISION explicitly perform neutronics calculations "out-of-model" in order to simplify the user experience, the coupling technique proposed in this methodology demonstrates that such trade-offs of flexibility and accuracy for a streamlined user interface need not be made.

Additionally, unlike fuel cycle models such as NFCSim [5], which uses the obsolete ORIGEN2 package, the proposed coupling technique relies upon the more accurate and up-to-date ORIGEN-S package, with a far greater number of interpolated cross-section libraries to draw upon (including the option for users to create additional depletion libraries using TRITON) [43]. In addition to a lack of updated cross-section libraries, the use of ORIGEN2 carries several disadvantages with respect to the accuracy of actinide concentration calculations, even compared to earlier versions of ORIGEN-S [45]. A particular drawback of the ORIGEN2

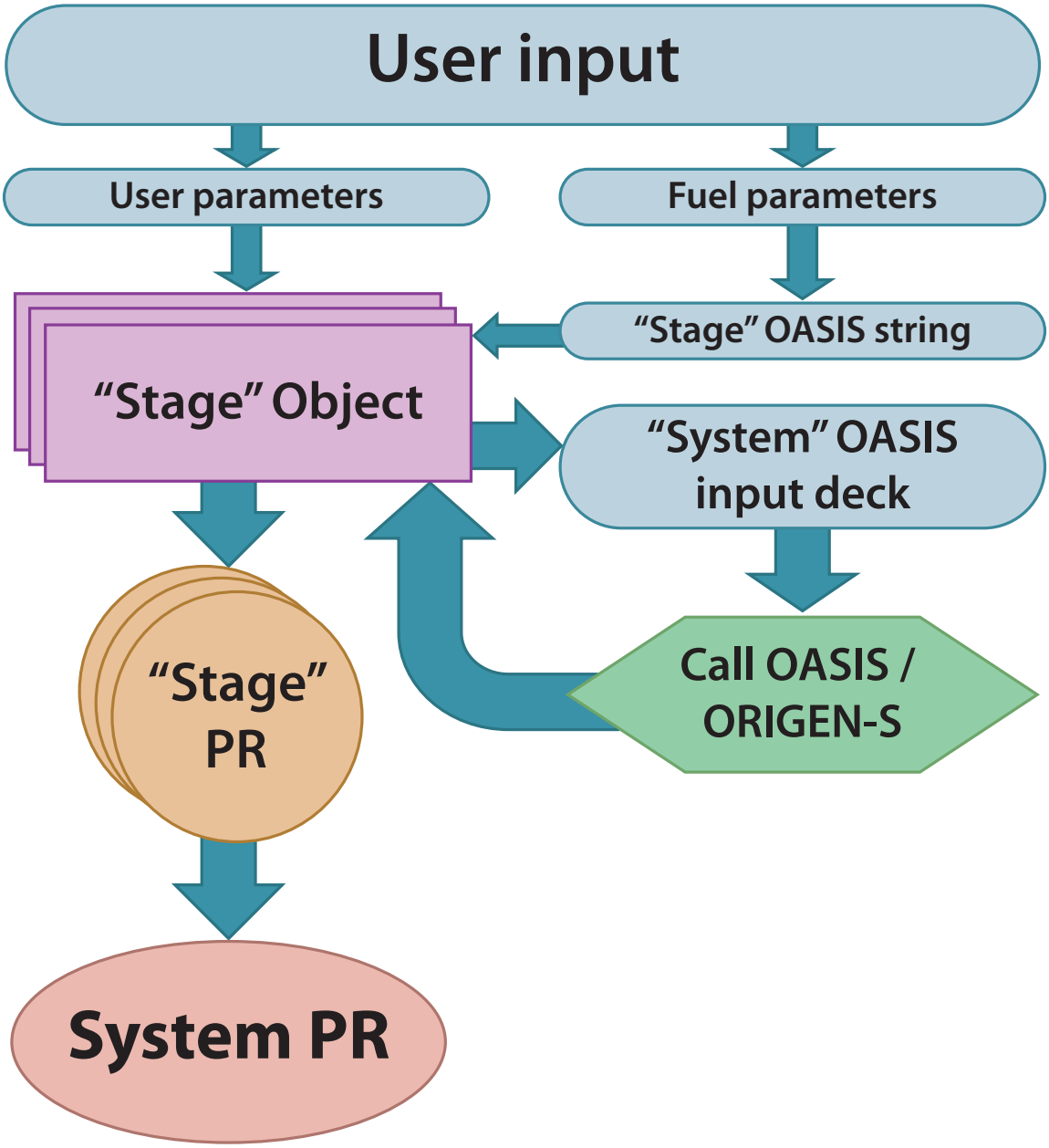

Figure 3.3: Schematic of process used to couple isotopic characterization with PR analysis. User data is used to generate fuel depletion and decay cases for analysis for each stage, which are combined to evaluate nuclear materials properties throughout the system. Nuclear materials data is then imported back from SCALE into the PR model at each stage for barrier effectiveness evaluation.

code is in the limitations on the available parameter space (such as enrichment) and the (lack of) availability specialized cross-section libraries, such as those for MOX fuel irradiation) [17, 45]; this can lead to noticeably less accurate results in spent fuel characterization.

The use of the OASIS module (particularly in the coupled context proposed in this work) resolves many of the difficulties in using ORIGEN-S (prompting users to continue to use the obsolete ORIGEN2 package). Likewise, the coupled framework developed in this methodology allows for the flexibility of the deployment of new reactor cross-section libraries developed using TRITON and COUPLE [43], thus affording the broadest possible evaluation of fuel cycle and proliferation resistance assessment. As a result, the coupling process proposed in this methodology bears the capability of bringing enormous new analytical power to fuel cycle evaluation models.

CHAPTER 4

System PR dynamics evaluation

4.1 Introduction

In this chapter, an exploration as to the dynamics of fuel cycle PR shall be made in response to several fuel cycle parameters of interest, including aspects such as fuel cycle type (open vs. closed), reactor type, fuel burnup/enrichment, and actinide recovery strategy employed. Using the coupled technique outlined prior, it is possible to evaluate the "cascade" effects of changes in material properties due to changes such as fuel burnup, etc. As a result, PR can be evaluated as a truly dynamic system property, in contrast with prior efforts which have sought to characterize fuel cycle system PR solely as a static system property (with parameters assumed to be fixed).

For all cases in this section, unless otherwise noted the assumed adversary is a yield-insensitive, unsophisticated state adversary engaged in a covert breakout attempt; the appropriate weights from Table 2.10 were used for this purpose and FOM_1 is used for isotopic attractiveness evaluation (Eq. 2.2).

4.2 Open fuel cycles

The two open fuel cycles considered for this analysis shall be the LWR-OT cycle, fueled by uranium enriched from 1.5–6% ^{235}U, and the CANDU HWR, fueled by natural uranium. Each of these fuel cycles shall be evaluated as to their relative system PR as a function of fuel burnup.

The stages composing each generalized fuel cycle for the two cases are generally the same as those outlined in [57]. Specific stages of interest to each process, which are examined in the system cross-sections, are listed as Table 4.1.

Table 4.1: Selected stage numbers for CANDU and LWR–OT cycles.

CANDU	LWR–OT	Stage
1	1	Mining
5	5	Conversion
—	8	Enrichment
8	11	LEU fuel fabrication
13	16	Reactor irradiation
15	18	SNF wet storage
16	19	SNF dry storage
22	25	Final emplacement

4.2.1 LWR once-through cycle

The LWR once-through cycle is perhaps the simplest cycle to evaluate and is also regarded as the standard for intrinsic proliferation resistance against which other fuel cycles are evaluated. The once-through cycle was evaluated across a range of burnups from 10 $\frac{\text{GWd}}{\text{MTU}}$ to 70 $\frac{\text{GWd}}{\text{MTU}}$; corresponding loading values for enrichments were obtained from [24, 60].

The system PR of the LWR-OT cycle as a function of fuel burnup is shown as Figure 4.1. One observes that burnup has a nominal, positive effect on system PR (e.g., system PR increases slowly with increasing burnup). A decomposition of the LWR-OT system fuzzy number into the constituent stage fuzzy numbers is shown as Figure 4.2.

In general, the stage weights are relatively evenly distributed for the LWR-OT system; in

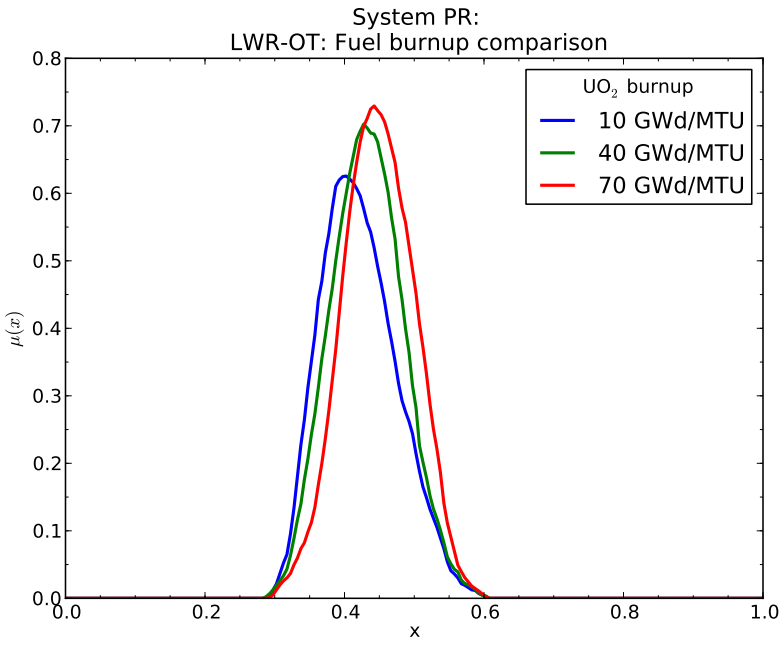

Figure 4.1: Intrinsic system proliferation resistance for a LWR-OT cycle as a function of fuel burnup. Higher abscissa values represent increasing PR.

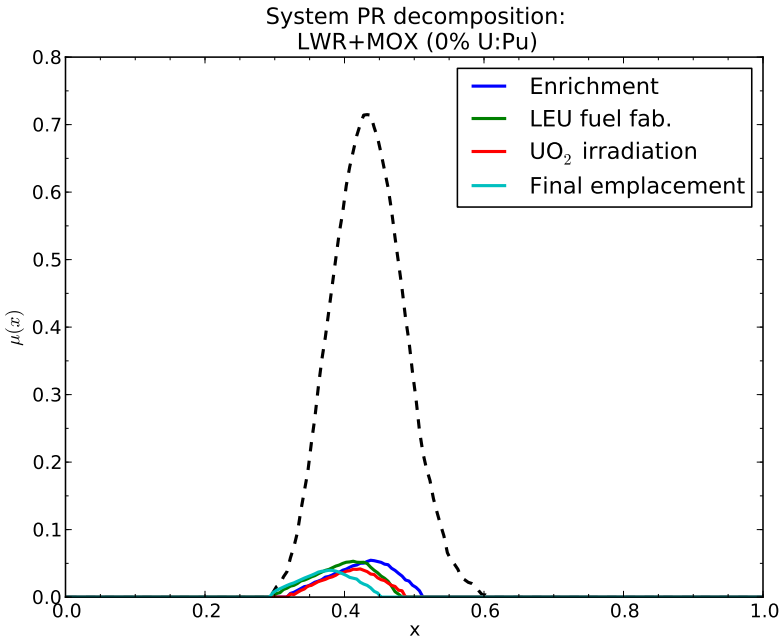

Figure 4.2: Decomposition of the system fuzzy PR value into the constituent stage fuzzy numbers for the LWR-OT cycle, 60 $\frac{\text{GWd}}{\text{MTU}}$ burnup.

as much, all stages with enriched LEU fuel or spent fuel contribute on roughly the same order to the shape of the system PR fuzzy function. Likewise, although a noticeable drop in the stage PR is observed for post-irradiation stages (particularly for lower burnups), the overall separation in stage PR between pre-irradiation and post-irradiation stages is not large. Such is evident from an analysis of the system PR cross-section (in terms of stage fuzzy centroid values), shown as Figure 4.3.

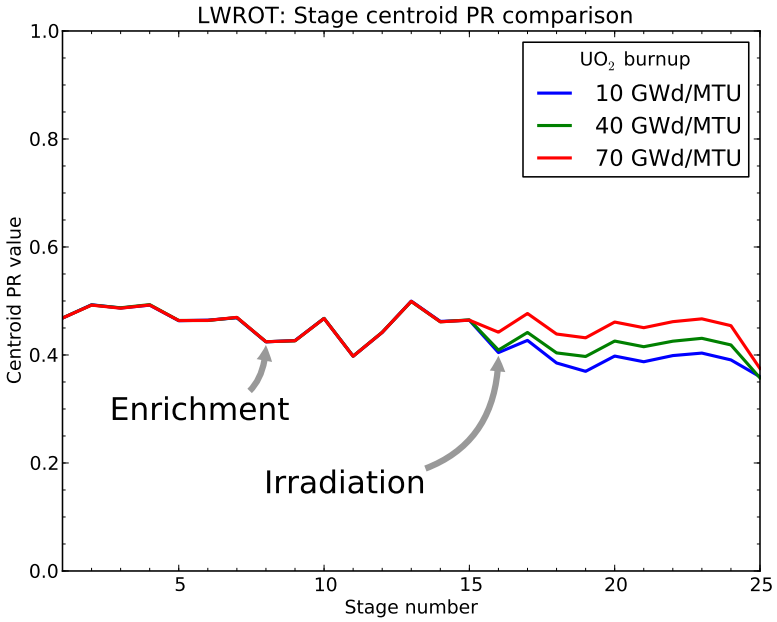

Figure 4.3: Cross-section view of system PR (e.g., level fuzzy number centroid values) for a LWR-OT as a function of fuel burnup. Higher ordinate values represent increasing PR.

Overall, one observes nominal, expected drops in PR at particularly sensitive stages, such as enrichment and irradiation (as well as a small drop at LEU fuel fabrication). Post-irradiation, a small increase in the PR is observed, namely due to the difference in capabilities for undeclared production (e.g., short-cycling, etc.) combined with the high radiological and chemical barriers presented by the the spent fuel. Additionally, one observes a uniform drop in PR at the final geologic emplacement stage, both due to the declining radiological barrier with time and the ineffective time barrier. These barrier dynamics are illustrated as Table 4.2.

Finally, the differences in overall system PR as a function of fuel burnup are entirely

Table 4.2: Barrier performance rankings for selected stages and burnup values of the LWR once-through cycle.

	Isotopic			Radiological			Time		
Stage / Burnup ($\frac{GWd}{MTU}$)	10	40	70	10	40	70	10	40	70
Irradiation	L	L+	M–	VH	VH	VH	H	M+	M
SNF dry storage	L	L+	M–	M	H	H	M	M	M
Final emplacement	L	L	L+	M	M	M	I	I	I

attributable to post-irradiation stages (i.e., due to changes in the plutonium attractiveness at higher burnups). Changes to the material characteristics "cascade" through the remainder of the system, building up the observed difference in system PR. "Cascade" effects such as that observed in Figure 4.3 are ultimately what drive PR dynamics effects, as will be demonstrated in the additional analysis cases presented in this chapter.

A breakdown of the system PR centroid and ranking values are given as Table 4.3.

Table 4.3: System PR centroid values and rankings as a function of uranium fuel burnup for the LWR once-through cycle.

Burnup ($\frac{GWd}{MTU}$)	Centroid	Rank
10	0.4213	M
20	0.4245	M
30	0.4315	M
40	0.4327	M+
50	0.4339	M+
60	0.4344	M+
70	0.4489	M+

Effect of varying lattice type

An additional effect which can be considered for LWR fuels is the impact of varying lattice geometry. Seven different lattice geometries for PWR fuel were considered, based on the available ARP cross-section libraries provided with SCALE: a Combustion Engineering (CE)

14x14 and 16x16 array, a Siemens 14x14 array, and a Westinghouse (W.House) 14x14, 15x15, 17x17, and 17x17 optimized fuel array (OFA) [43]. These seven geometries were evaluated for three different burnups: 10 $\frac{\text{GWd}}{\text{MTU}}$, 40 $\frac{\text{GWd}}{\text{MTU}}$, and 70 $\frac{\text{GWd}}{\text{MTU}}$. Figure 4.4 shows the results of this study.

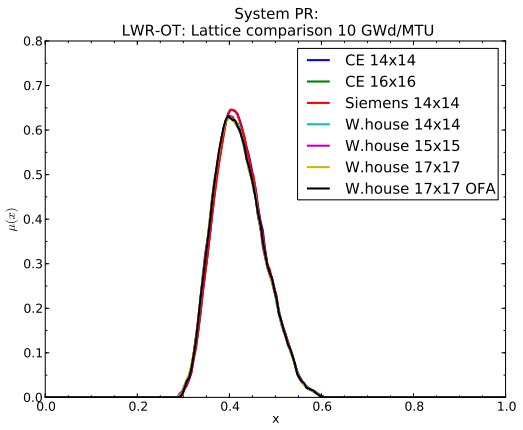

(a): 10 $\frac{\text{GWd}}{\text{MTU}}$

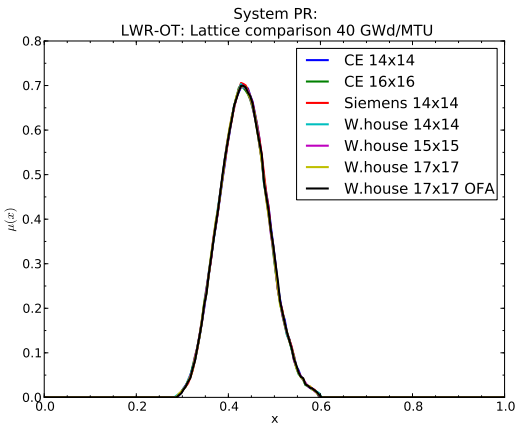

(b): 40 $\frac{\text{GWd}}{\text{MTU}}$

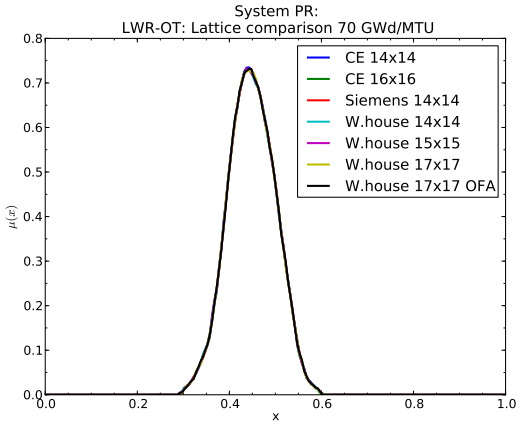

(c): 70 $\frac{\text{GWd}}{\text{MTU}}$

Figure 4.4: Intrinsic system PR evaluation for PWR fuel as a function of varying lattice geometry for three burnups: 10 $\frac{\text{GWd}}{\text{MTU}}$, 40 $\frac{\text{GWd}}{\text{MTU}}$, and 70 $\frac{\text{GWd}}{\text{MTU}}$. Higher abscissa values represent higher intrinsic PR.

As one observes from Figure 4.4, the choice of lattice geometry has little to no effect on

evaluated system PR; i.e., the changes introduced by lattice geometry are generally on too microscopic of a level to significantly impact parameters of interest to material attractiveness, particularly across constant burnup and enrichment.

4.2.2 CANDU HWR cycle

The **Can**adian **d**euterium **u**ranium (CANDU) reactor uses a heavy-water moderator (deuterium oxide; i.e., D_2O) rather than "light water" (H_2O) as a neutron moderator, and thus is capable of using natural uranium fuel, rather than the enriched uranium required for light water reactors. Several other features are unique to the CANDU design as well, including an online refueling capability where fuel is continuously cycled through the reactor (rather than batch loads, as is used in LWR cycles). With respect to intrinsic PR, online refueling acts as a slight penalty for CANDU designs, given the greater facility access by individuals due to online refueling.

The analysis of system PR for the CANDU cycle is given as Figure 4.5.

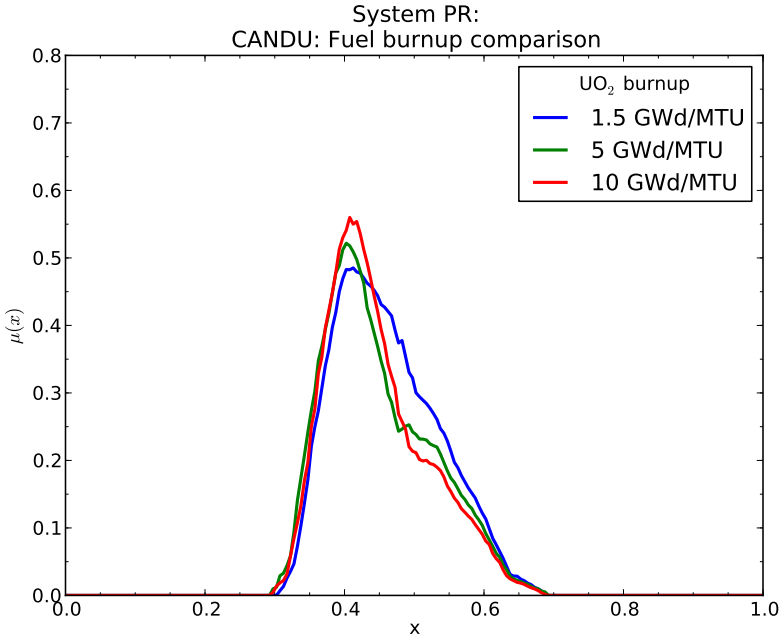

Figure 4.5: Intrinsic system proliferation resistance for a CANDU HWR cycle fueled with natural uranium as a function of fuel burnup. Higher abscissa values represent increasing PR.

While the lack of an enrichment stage is a PR benefit to the CANDU cycle, overall the material is burned for a shorter period of time. The plutonium produced in spent CANDU fuel is thus of a nominally higher attractiveness than that produced in LWR fuel, namely due to the lower overall buildup of higher plutonium species (which contribute to a higher heat generation rate and thus lower attractiveness). Additionally, the relatively narrow space of burnup evaluated in a CANDU cycle results in a minimal change in system PR as a function of burnup; this can be observed in Figure 4.6.

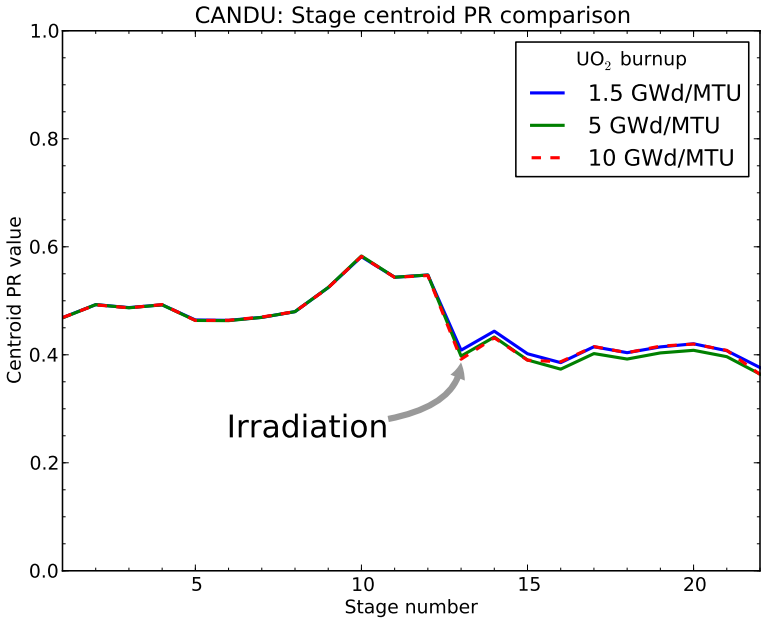

Figure 4.6: Cross-section view of system PR (e.g., level fuzzy number centroid values) for a CANDU HWR cycle as a function of fuel burnup. Higher ordinate values represent higher intrinsic PR.

As one observes from Figure 4.6, the intrinsic PR of the material (and subsequently, fuel cycle stages) changes very little over the burnup range considered.

Additionally, the careful observer will notice a small artifact: while the level PR for higher burnups is slightly greater for higher burnups in the CANDU cycle, the system fuzzy number (and corresponding centroid value) appears to slightly *decrease*. This is due to the change in material mass flow as a function of burnup; because fuel is burned for longer at higher

Table 4.4: Barrier performance rankings for selected stages and burnup values of the CANDU HWR once-through cycle.

	Isotopic			Mass & Bulk			Available Mass		
Stage / Burnup ($\frac{GWd}{MTU}$)	1.5	5	10	1.5	5	10	1.5	5	10
Irradiation	L–	L	L	H+	H	H–	L	I	I
SNF dry storage	L–	L	L	H+	H	H–	L	I	I
Final emplacement	L–	L	L	H+	H	H–	L	I	I

burnups, greater weight is placed on the post-irradiation stages (i.e., lower mass flow from pre-reactor to post-reactor stages). However, the overall PR is lower in post-irradiation stages for CANDU than in pre-irradiation stages (Figure 4.6), thus explaining this minor artifact; this is evident in Table 4.4.

As one observes in Table 4.4, while the isotopic attractiveness of material decreases with burnup in the CANDU cycle, the amount of fissile material per unit fuel mass increases with burnup, as well as the total available fissile mass (thus, decreasing the available mass and mass & bulk barriers). Likewise, the decreasing mass flow with burnup increases the relative model emphasis upon post-irradiation stages, accounting for the overall trend in decreasing PR with burnup for CANDU.

The system PR centroid values and rankings for the CANDU system are given as a function of uranium fuel burnup as Table 4.5.

Table 4.5: System PR centroid values and rankings as a function of uranium fuel burnup for the CANDU HWR cycle.

Burnup ($\frac{GWd}{MTU}$)	Centroid	Rank
1.5	0.4602	M
5	0.4486	M
10	0.4462	M

An interesting contradiction is revealed in the CANDU centroid and ranking results in Table 4.5, particularly compared to those of the LWR once-through cycle (Table 4.3). Despite the fact that the centroid mean value of the PR is in fact notably higher for the lowest

CANDU burnup configuration (and generally high compared to lower LWR-OT burnups), the system ranking of the CANDU system is equivalent or lower than that of the LWR-OT system (particularly at high LWR burnups). This contradiction appears to be attributable to the lack of an enrichment stage in the CANDU cycle (augmenting the overall system PR), while the PR from post-irradiation stages is lower than that from high-burnup fuel in LWR cycles (owing to the attractiveness of the ejected material from CANDU). Thus, the CANDU cycle appears to show a greater "spread" in PR values; this is evident from the system PR cross-section seen in Figure 4.6, where the overall PR drops between PRe and post-irradiation stages.

4.3 "Modified open" fuel cycles

For the so-called "modified open" fuel cycle strategies, a limited degree of actinide recovery is employed. The cases considered for this evaluation include a plutonium-only extraction (PUREX), co-extraction of plutonium and uranium (COEX), and other advanced aqueous processes involving the co-recovery of other minor actinides with plutonium/uranium (UREX series).

For the MOX-based cycles, the electricity fraction produced by MOX fuel (of total nuclear energy produced) at equilibrium is calculated by evaluating the available amount of actinides from UO_2 fuel and a corresponding mass balance based on burnup; this relation is given as Eq. 4.1.

$$\mathrm{EF_{MOX}} = \frac{\mathrm{Pu_{LWR}}}{\mathrm{Pu_{MOX}}} \cdot \frac{\mathrm{M_{MOX}} \cdot \mathrm{BU_{MOX}} \cdot \epsilon_{\mathrm{MOX}}}{\mathrm{M_{MOX}} \cdot \mathrm{BU_{MOX}} \cdot \epsilon_{\mathrm{MOX}} + \mathrm{M_{UO_2}} \cdot \mathrm{BU_{UO_2}} \cdot \epsilon_{\mathrm{UO_2}}} \tag{4.1}$$

In Eq. 4.1, $\mathrm{EF_{MOX}}$ is the electricity fraction produced by MOX fuel, $\mathrm{Pu_{LWR}}$ is the total amount of plutonium available in LWR fuel, $\mathrm{Pu_{MOX}}$ is the total amount of plutonium required for a MOX core loading (i.e., the fraction of plutonium in MOX fuel multiplied by the total mass of MOX fuel in the core), $\mathrm{M_{MOX}}$ and $\mathrm{M_{UO_2}}$ are the mass loadings of the MOX and UO_2 cores, respectively, while $\mathrm{BU_{MOX}}$ and $\mathrm{BU_{UO_2}}$ are the fuel burnups of the MOX and UO_2 fuel respectively and ϵ_{MOX} and $\epsilon_{\mathrm{UO_2}}$ are the thermal efficiencies of the MOX and UO_2 reactors (each taken to be 34.1%) [40].

For each recycle scenario, a fixed fuel cooling time of 15 years following discharge was assumed (e.g., 10 years in wet storage and 5 years in dry storage); extraction efficiencies of 99% for plutonium and neptunium were assumed, with 95% efficiency for americium and curium extraction (as appropriate) [2, 59].

The MOX cross-section libraries used were those provided with SCALE; SCALE provides for an automatic interpolation of cross-sections based on interpolated assembly-average plutonium content [17].

In addition to the MOX-based modified open cycles, a DUPIC fuel cycle which involves the re-irradiation of LWR fuel in a CANDU reactor will also be considered. The details of this fuel cycle will be more fully explored in the corresponding subsection.

The stage structure for each of the modified open cycles considered again is based upon those outlined in [57]; some adaptation is made to account for the differences in the DUPIC-based cycle. Key stage numbers of interest for the modified open cycles are given as Table 4.6.

Table 4.6: Selected stage numbers for LWR + MOX and DUPIC cycles.

#	MOX	DUPIC
1	Mining	”
5	Conversion	”
8	Enrichment	”
11	LEU fuel fabrication	”
16	Reactor irradiation	”
18	SNF wet storage	”
19	SNF dry storage	”
20	Reprocessing	Voloxidation
21	Recovered material storage	”
23	—	DUPIC fuel fabrication
24	Actinide waste disposal	—
25	MOX fuel fabrication	—
26	—	DUPIC fuel irradiation
28	MOX fuel irradiation	—
32	—	Final emplacement
34	Final emplacement	—

4.3.1 Reprocessing with PUREX

The **P**lutonium-**Ur**anium **Ex**traction (PUREX)-based MOX cycle forms the “baseline” of the modified open cycle strategy, both in that it is the most limited actinide recovery strategy (plutonium-only) and that all other advanced recovery strategies essentially “default” back to

the PUREX scenario if one assumes further material processing on the part of an adversary. Further, given that the PUREX process is currently employed in states engaged in reprocessing (including France and Japan), it is a highly relevant fuel cycle alternative for policy considerations.

Figure 4.7 gives a comparison of the overall system PR as a function of LWR fuel burnup for a PUREX-based MOX cycle (MOX fuel burnup is held at a constant 60 $\frac{\text{GWd}}{\text{MTHM}}$ for this case).

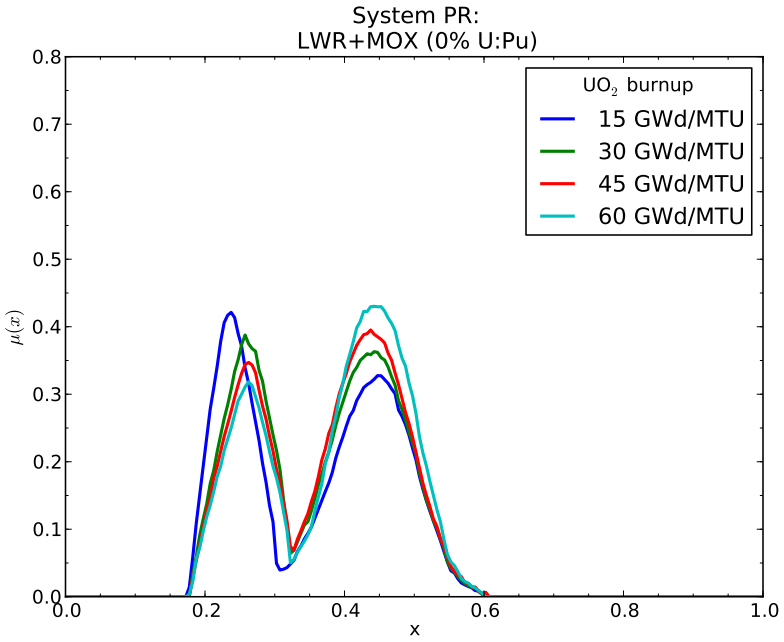

Figure 4.7: Intrinsic system proliferation resistance for a LWR + MOX cycle employing PUREX for plutonium recovery as a function of UO_2 fuel burnup. Higher abscissa values represent higher intrinsic PR.

LWR fuel burnup appears to have a nominal effect upon overall system PR for the PUREX-based cycle; increasing burnups do correlate with the production of higher plutonium species, thus decreasing the plutonium attractiveness. However, this effect is somewhat constrained given the limited space of burnups considered for this study. Using the burnup/enrichment pairs from [60], a minimum burnup of 15 $\frac{\text{GWd}}{\text{MTU}}$ and a maximum burnup of 45 $\frac{\text{GWd}}{\text{MTU}}$ were imposed as constraints due to inherent limitations of the ARP MOX cross-section libraries and the plutonium vector [43]. Higher burnups resulted in a plutonium vector with less than

50% ^{239}Pu, outside the scope of the ARP interpolation range for MOX cross-section libraries. (While adjusting the enrichment values for LWR fuel can compensate for this effect, these enrichments were well beyond the prescribed enrichment/burnup combinations found in [60] and [24]).

In order to compensate for this limitation (and thus evaluate a more full range of burnup values), a minor extrapolation beyond the ARP interpolation limits was used for uranium burnups of up to 60 $\frac{\text{GWd}}{\text{MTU}}$; this approach is justified both in that the ^{239}Pu vector is still very close to 50% (around 49%) and the cross-section variance as a function of the ^{239}Pu vector is relatively flat at lower isotopic fractions [17]. Thus, this can be considered a reasonable estimate of depletion performance in this limiting burnup case.

Prominent among the features of the PUREX-based cycles (and other reprocessing-based strategies) is the "bifurcation" in the system PR fuzzy number. Two trends are apparent: first, a peak at lower PR, consisting of reprocessing-related stages (including fuel separation and MOX fuel fabrication), and then a larger peak at higher PR, consisting of pre-reactor stages and stages where plutonium is kept with intact fuel (i.e., protected by greater intrinsic barriers).

A cross-section of the level PR is given as Figure 4.8. Two significant drops in the stage PR are observed: first, in the reprocessing stage (where intrinsic barriers are largely ineffective, due to the separation of pure plutonium) as well as MOX fuel fabrication (where large stocks of plutonium are found, again with little in the way of intrinsic barriers such as a significant radiological hazard). Post-irradiation, the stage PR rises once more, slightly declining upon disposal (similar to the once-through case, Figure 4.3).

A decomposition of the system PR fuzzy function into the constituent stage PR fuzzy functions is shown as Figure 4.9; fuel burnup is fixed at 60 $\frac{\text{GWd}}{\text{MTU}}$ / 60 $\frac{\text{GWd}}{\text{MTHM}}$ for this case.

As one observes in Figure 4.9, reprocessing and its associated stages both compose the lower "peak" of the system PR function; these stages also carry a greater overall relative weight due to the concentration of fissile materials at these stages compared to other stages (e.g., when fissile material is contained in intact fuel). Changes in the relative attractiveness of the plutonium vector, particularly as it enters the reprocessing-related stages (Figure 4.8) thus "drive" changes in the system PR function for the PUREX-based MOX cycles.

Despite the fact that some plutonium is consumed in the MOX cycle, the post-irradiation stages do not represent a significant gain over the LWR once-through cycle. This is due both to the fact that only about $\frac{1}{3}$ of the total plutonium inventory of the MOX fuel is consumed

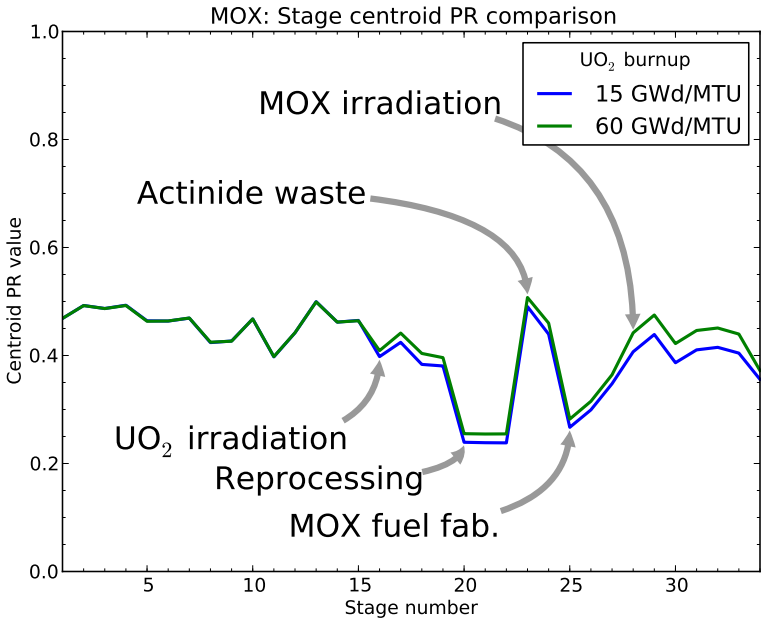

Figure 4.8: Cross-section view of system PR (e.g., level fuzzy number centroid values) for a LWR + MOX cycle employing PUREX for plutonium recovery as a function of UO_2 fuel burnup. Higher ordinate values represent higher intrinsic PR.

during irradiation, as well as the fact that the change in plutonium attractiveness is generally small, as found here and in other studies [6]. This is evident in the barrier rankings as a function of burnup, presented as Table 4.7.

The system centroid values and system rankings for the PUREX-based MOX cycle are presented as Table 4.8.

4.3.2 Uranium coextraction: COEX

One simple alternative to PUREX-based MOX cycles is the COEX process, in which uranium is co-extracted with plutonium. For this study, it is assumed this is at a 50% ratio with plutonium, although this study will also consider other coextraction ratios. An example of this process is at the design of the Rokkasho-mura reprocessing facility in Japan, which is designed to produce an end product of a mixture of plutonium and uranium oxide[1], with

[1]For the sake of accuracy, the process employed at Rokkassho-mura is in fact PUREX-based, however uranyl nitrate is recombined with the plutonium feed to form MOX powder in the accessible product stream [15].

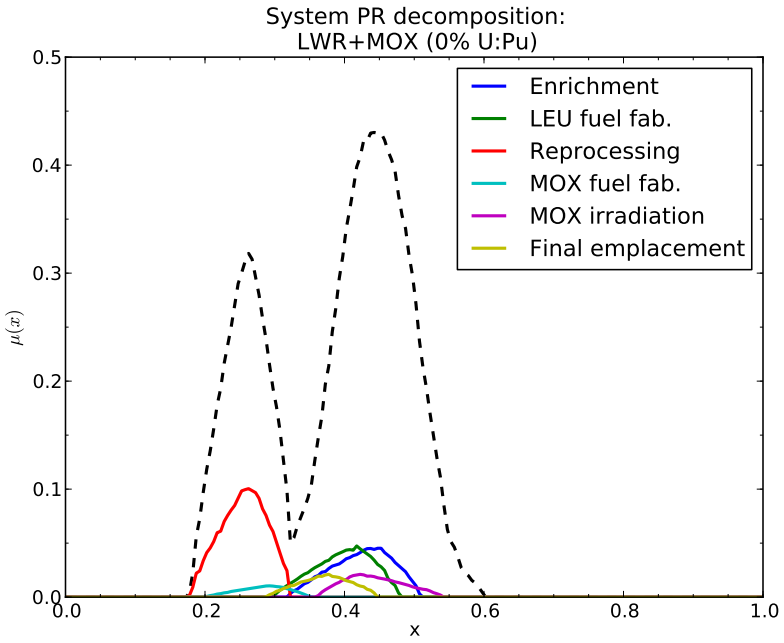

Figure 4.9: Decomposition of the system fuzzy PR value into the constituent stage fuzzy numbers for the LWR+MOX with a PUREX-based actinide recovery strategy; fuel burnup fixed at 60 $\frac{\text{GWd}}{\text{MTU}}$ / 60 $\frac{\text{GWd}}{\text{MTHM}}$.

Table 4.7: Barrier performance rankings for selected stages and burnup values of the PUREX-based MOC strategy.

	Isotopic		Radiological	
Stage / Burnup ($\frac{\text{GWd}}{\text{MTU}}$)	15	60	15	60
UO_2 fuel irradiation	L	L+	VH	VH
SNF dry storage	L	L+	H	H
Reprocessing	L	L+	L	L
MOX fuel fabrication	L	L+	L	L
MOX fuel irradiation	L+	M–	VH	VH
Final emplacement	L	L+	M	M

Table 4.8: System PR centroid values and rankings as a function of LWR fuel burnup for a LWR + MOX cycle using PUREX for plutonium recovery.

Burnup ($\frac{\text{GWd}}{\text{MTU}}$)	Centroid	Rank
15	0.3588	L+
30	0.3677	L+
45	0.3749	L+
60	0.3857	L+

no significant ability (outside of sample extraction) to obtain separated plutonium alone [15]. The final product is nominally a mixture of 50% plutonium (balance assumed to be uranium) [15]; this mixture ratio shall be used as the basis for all assumptions involving uranium stream coextraction.

The COEX cycle is considered as a function of LWR fuel burnup (with a fixed MOX fuel burnup of 60 $\frac{\text{GWd}}{\text{MTHM}}$) as Figure 4.10.

While burnup effects are again quite small (owing to the confined space of burnups considered, as was discussed in the previous section), one observes an overall shift in the PR trend upwards from the PUREX case. In particular, the prominent bifurcated peak due to reprocessing has now shifted over such that while the contribution from reprocessing-related stages is still distinct (i.e., the lower PR "shoulder" of the system PR function), it is no longer a separate peak in the system fuzzy number.

The system centroid values and system rankings for the COEX-based MOX cycle are presented as Table 4.9.

Table 4.9: System PR centroid values and rankings as a function of LWR fuel burnup for a LWR + MOX cycle using COEX for plutonium/uranium recovery.

Burnup ($\frac{\text{GWd}}{\text{MTU}}$)	Centroid	Rank
15	0.3782	L+
30	0.3854	L+
45	0.3902	L+
60	0.4069	M–

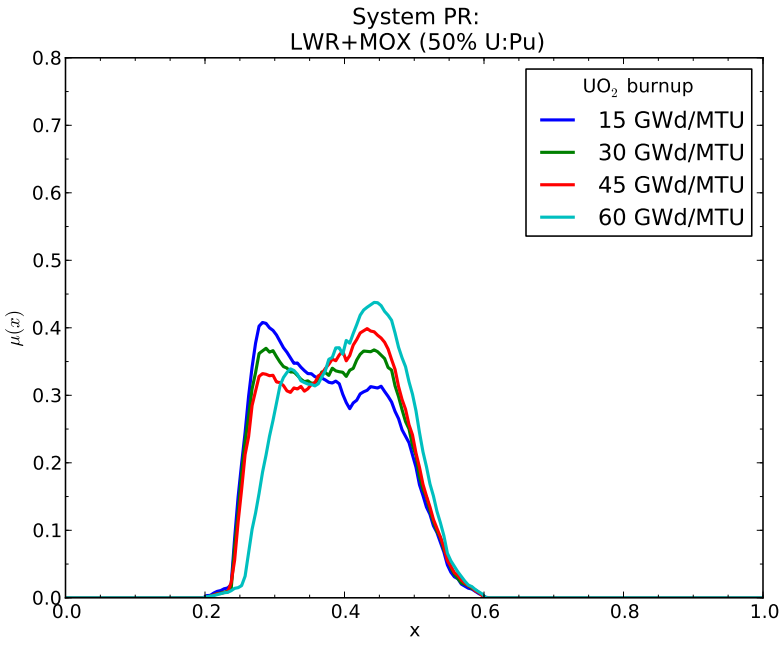

Figure 4.10: Intrinsic system proliferation resistance for a LWR + MOX cycle employing COEX (50% U:Pu) for actinide recovery as a function of UO_2 fuel burnup. Higher abscissa values represent higher intrinsic PR.

A decomposition of the system PR fuzzy function for the COEX case with a fuel burnup of 60 $\frac{\text{GWd}}{\text{MTU}}$ / 60 $\frac{\text{GWd}}{\text{MTU}}$ is shown as Figure 4.11.

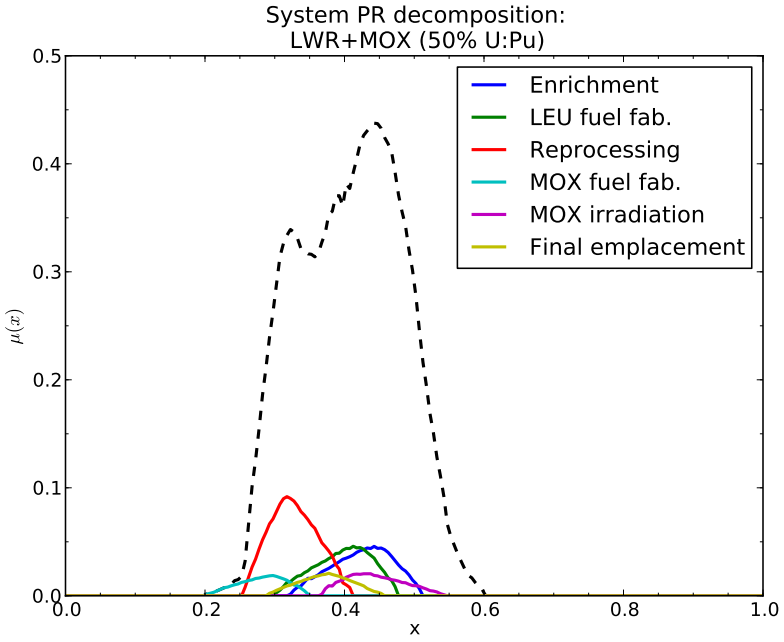

Figure 4.11: Decomposition of the system fuzzy PR value into the constituent stage fuzzy numbers for the LWR+MOX with a COEX-based actinide recovery strategy; fuel burnup fixed at 60 $\frac{\text{GWd}}{\text{MTU}}$ / 60 $\frac{\text{GWd}}{\text{MTHM}}$.

As one observes from Figure 4.11, reprocessing-related stages once again are of primary importance for the COEX-based cycle, similar to the PUREX-based case (Figure 4.9). Thus, the decreasing attractiveness of the intact plutonium vector in a COEX-based scenario produces an observable shift in the stage PR function of the reprocessing-related stages and thus the system PR function overall.

Effect of uranium dilution fraction

The uranium coextraction fraction (relative to the plutonium concentration) can be studied as a separate parameter, particularly given its potent impact upon material attractiveness (by increasing the bare sphere critical mass of the plutonium-bearing stream). Figure 4.12

evaluates the impact of uranium coextraction levels on overall system PR; the centroid PR values and system rankings are expressed as Table 4.10. For this evaluation, the LWR fuel burnup was fixed at 60 $\frac{\text{GWd}}{\text{MTU}}$, with MOX fuel burnup fixed at 60 $\frac{\text{GWd}}{\text{MTU}}$.

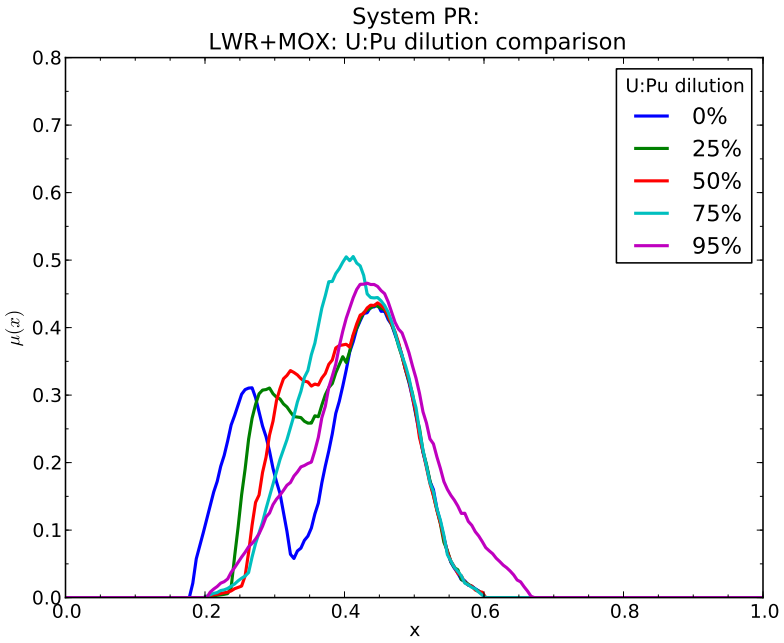

Figure 4.12: Intrinsic system proliferation resistance for LWR + MOX cycle as a function of uranium dilution factor (i.e., ratio of uranium to plutonium in the plutonium-bearing stream). Higher abscissa values represent higher intrinsic PR.

As one observes from both Figure 4.12 and Table 4.10, uranium co-extraction has an immediate, if moderate impact upon overall system PR by decreasing the material attractiveness of the plutonium stream during reprocessing and increasing the overall mass of material required in order to acquire one significant quantity (e.g., mass & bulk). The effect of this is evident in the cross-section view of the system PR for MOX cycles as a function of uranium coextraction fraction, shown as Figure 4.13, as well as the breakdown of barrier performance as a function of dilution, given as Table 4.11.

However, while an immediate gain is realized in overall system PR from even small amounts of uranium dilution, substantial gains are not realized until very high coextraction ratios (on the order of 75% U:Pu and above); levels which appears to be above the currently

Table 4.10: System PR centroid values and rankings as a function of uranium co-extraction fraction with plutonium.

U:Pu (%)	Centroid	Rank
0	0.3862	L+
25	0.3990	M–
50	0.4069	M–
65	0.4089	M–
75	0.4117	M
85	0.4261	M
95	0.4366	M

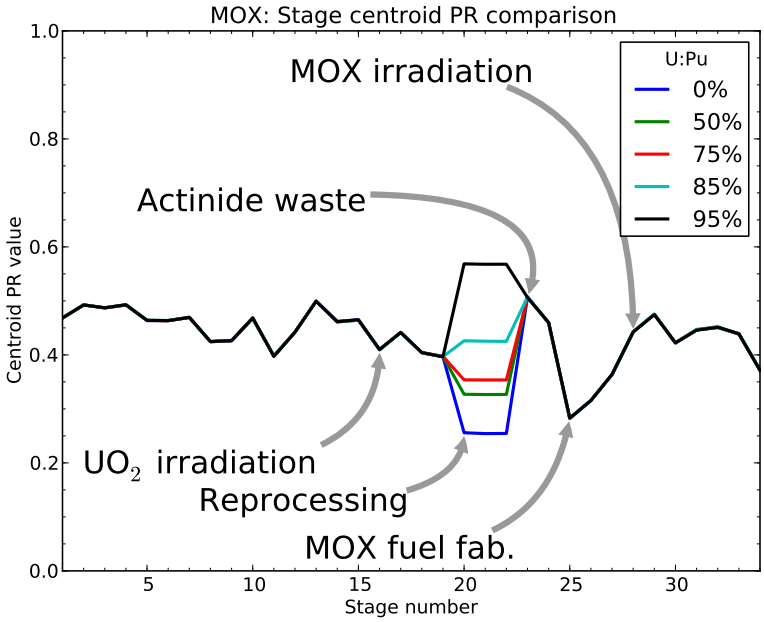

Figure 4.13: Cross-section view of system PR (e.g., level fuzzy number centroid values) for a LWR + MOX cycle as a function of uranium dilution fraction of the plutonium stream during reprocessing. Higher ordinate values represent higher intrinsic PR.

Table 4.11: Barrier performance rankings for selected barriers in the reprocessing stage as a function of uranium coxtraction ratio.

U:Pu (%)	Isotopic	Mass & Bulk
0	L+	I
25	M–	L–
50	M	L
65	M	M
75	M+	M
85	H–	H+
95	VH	VH

proposed coextraction fractions for reprocessing facilities.

4.3.3 Reprocessing with Advanced UREX series

Several advanced UREX series reprocessing scenarios shall be considered for this study. Interest in the advanced UREX series is twofold. First, given the partition and separate disposal of certain long-lived actinides, several benefits can be realized to the capacity and impact of a geologic repository. Heat loading due to americium and curium (in addition to plutonium) can be substantially reduced, greatly increasing the available repository storage capacity and potentially obviating the need for additional repositories [34, 59]. Additionally, neptunium is a key contributor to long-term dose projections in evaluations of a potential geologic repository; its removal and subsequent transmutation could therefore reduce the potential risk to future public health from a repository [41]. Finally, most relevant to this particular analysis, the advanced UREX series treatments involve a co-extraction of actinides, rather than a separate extraction of plutonium alone. The effect of actinide coextraction will be evaluated for this analysis for its effect on PR, both as a function of selected coextraction strategy and the impact of said strategy as a function of uranium fuel burnup.

Some overlap exists between different UREX processes given that the chief stream of interest is the plutonium-bearing stream; these processes are sorted by product stream in Table 4.12. These category groupings are similar to those performed in prior analyses such as [3, 42]; i.e., groupings are based upon similar plutonium-bearing streams (e.g., streams with plutonium and uranium dilution, streams with plutonium and minor actinides, etc.). The studies performed by [3, 42] do not make a distinction between the grouping of plutonium

streams with and without neptunium, finding no nonproliferation benefit; however, an explicit evaluation of the impact of neptunium inclusion has been made for this analysis.

Table 4.12: List of UREX processes evaluated and their associated product streams [12, 13, 42, 59]

Product	process(es)
Pu + Np	UREX+2, UREX+3, UREX+4
Pu + Np + U	UREX+2a, UREX+3a, UREX+4a
TRU	UREX+1a
TRU + U	UREX + 1b
TRU + Ln	UREX + 1

UREX+2/3/4

Figure 4.14 shows the system PR as a function of LWR fuel burnup for the UREX+2/3/4 cycle(s) (MOX fuel burnup is held constant at 60 $\frac{\text{GWd}}{\text{MTHM}}$). The coextraction of neptunium with uranium shows only a very small change in PR over the baseline, noticeable only at 60 $\frac{\text{GWd}}{\text{MTU}}$ LWR fuel burnup (e.g., where the Np inventory is the greatest).

The inclusion of ^{237}Np in both LWR and MOX fuel has been explored previously for the potential for ^{238}Pu "heat spiking" (i.e., selectively increasing the production of ^{238}Pu, thus substantially increasing the heat generation rate of the plutonium), illustrated as Eq. 4.2 [39]. However, the addition of neptunium itself does little to augment the intrinsic PR of plutonium in the reprocessing stream itself; i.e., the heat and dose contribution of Np alone does little to change material attractiveness.

$$^{237}\text{Np} + {}^{1}_{0}\text{n} \longrightarrow {}^{238}\text{Np} \xrightarrow{\beta^-} {}^{238}\text{Pu} \tag{4.2}$$

However, comparing the system cross-sections of the PUREX and UREX+2/3/4 processes, one does observe a small but noticeable increase in the system in the stage centroid PR for post-MOX irradiation stages, shown in Figure 4.15. The effect of this increase is most pronounced for higher burnups, given the higher available neptunium inventory in spent LWR fuel. However, the impact on overall system PR is limited due to the fact both that such

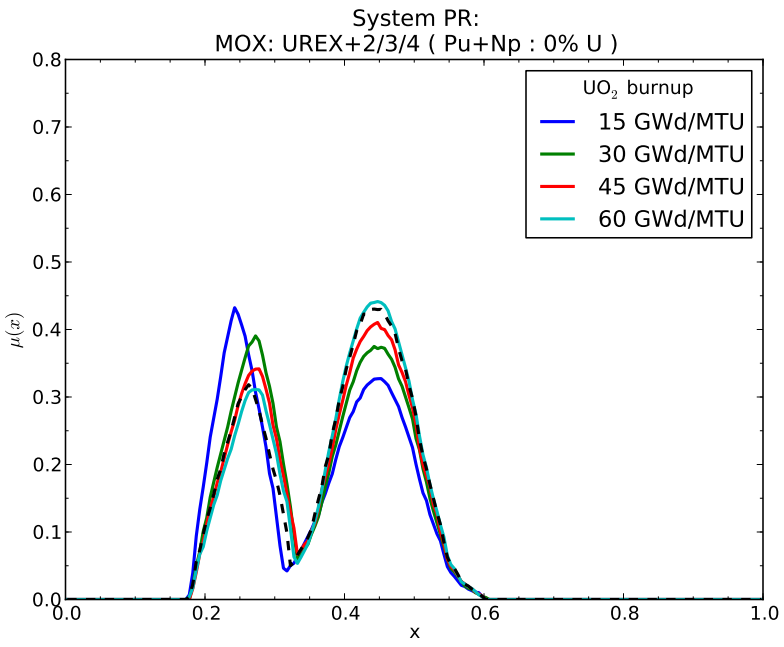

Figure 4.14: Intrinsic system proliferation resistance for a LWR + MOX cycle employing UREX+2/3/4 (Pu+Np) for actinide recovery as a function of UO_2 fuel burnup. Reference PUREX scenario (Pu only) for 60 $\frac{\text{GWd}}{\text{MTU}}$ burnup shown in black, dashed. Higher abscissa values represent higher intrinsic PR.

an increase occurs only at the tail end of the fuel cycle (i.e., a short "cascade length") and does little to ameliorate the most sensitive stage in the fuel cycle process involving separated materials (e.g., reprocessing and related stages).

While the doping of fresh UO_2 fuel with neptunium to produce additional ^{238}Pu was not considered for this study, such a process may produce a more profound overall impact on system PR given the longer "cascade" effect as well as influencing the material attractiveness of plutonium in separations-related stages [29, 39, 49]

The relative system rankings of the UREX+2/3/4 system as a function of burnup are provided as Table 4.13.

UREX+2a/3a/4a

The UREX+2a/3a/4a process flows are similar to that of the UREX+2/3/4 with the addition of uranium to the stream. For this evaluation, the uranium co-extraction ratio was assumed

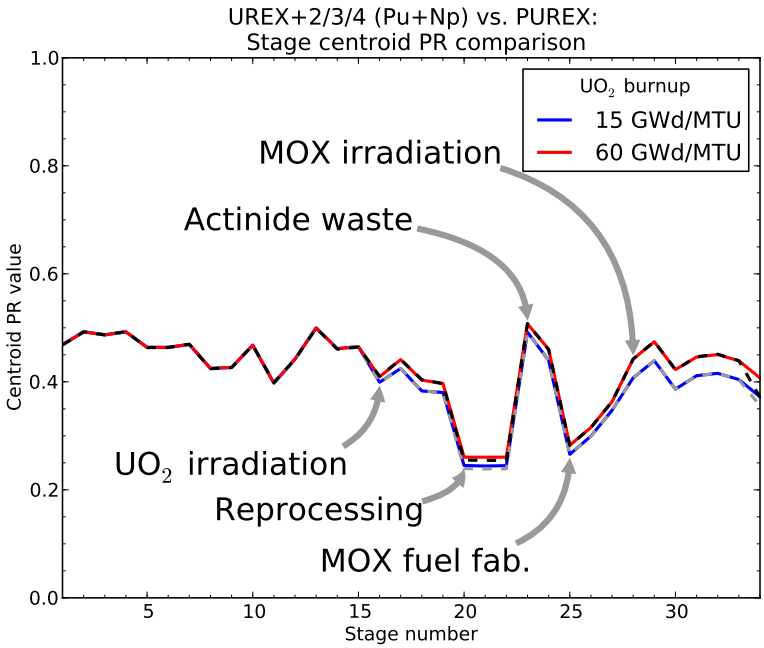

Figure 4.15: Stage PR cross-section comparison for UREX+2/3/4 (Pu + Np) versus PUREX (Pu) as a function of burnup; UREX+2/3/4 shown as solid lines, PUREX as dashed.

Table 4.13: System PR centroid and rankings as a function of LWR fuel burnup for a LWR + MOX cycle with UREX+2/3/4.

UO_2 burnup ($\frac{GWd}{MTU}$)	Centroid	Rank
15	0.3592	L+
30	0.3725	L+
45	0.3804	L+
60	0.3872	L+

to be 50%; MOX fuel burnup was again held to 60 $\frac{\text{GWd}}{\text{MTHM}}$, while PR was evaluated across LWR fuel burnup, presented as Figure 4.16.

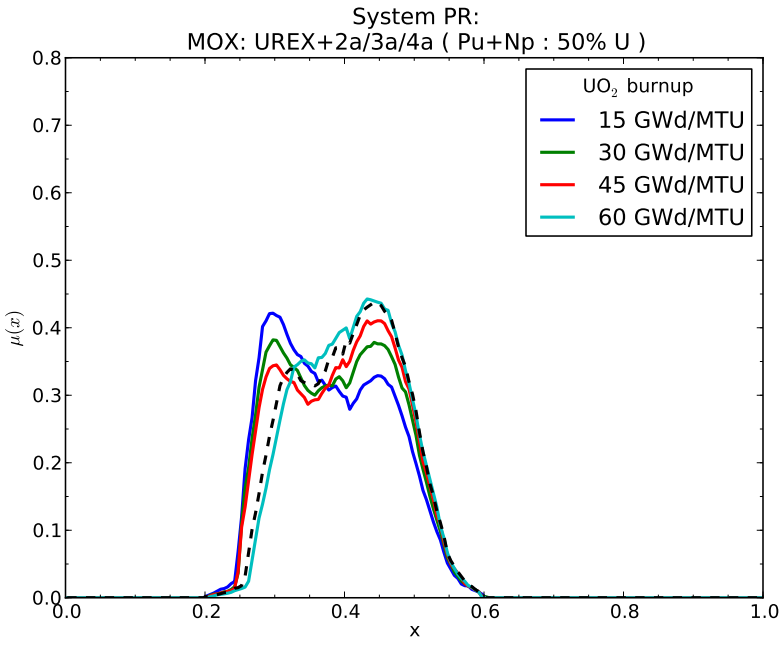

Figure 4.16: Intrinsic system proliferation resistance for a LWR + MOX cycle employing UREX+2a/3a/4a (Pu+Np + 50% U) for actinide recovery as a function of UO_2 fuel burnup. Reference COEX scenario (50% U:Pu) for 60 $\frac{\text{GWd}}{\text{MTU}}$ burnup shown in black, dashed. Higher abscissa values represent higher intrinsic PR.

Similar to the case of the UREX+2/3/4 process, the co-extraction of neptunium introduces a minor decrease in the material attractiveness for the spent MOX fuel. However, in terms of overall impact on system PR, the addition of uranium to the extraction stream appears to have a far greater impact; this is apparent from a comparison of the UREX+2a/3a/4a/ system PR to the baseline COEX scenario (black, dashed line), where one observes the change from the baseline COEX scenario to be small, while the difference between UREX+2/3/4 and UREX+2a/3a/4a (due to the addition of uranium) appears to be substantial. The relative system rankings of the UREX+2a/3a/4a system as a function of burnup are provided as Table 4.14.

Table 4.14: System PR centroid and rankings as a function of LWR fuel burnup for a LWR + MOX cycle with UREX+2a/3a/4a.

UO_2 burnup ($\frac{GWd}{MTU}$)	Centroid	Rank
15	0.3820	M–
30	0.3920	M–
45	0.3974	M–
60	0.4098	M–

Table 4.15: Isotopic barrier performance ranking for selected stages and burnup values of the UREX+1a-based MOC strategy.

Stage / Burnup ($\frac{GWd}{MTU}$)	15	30	45	60
Reprocessing	L+	M–	M–	M
MOX fuel fabrication	L	L+	L+	L+
MOX fuel irradiation	M–	M–	M	M
Final emplacement	L+	M–	M–	M–

UREX+1a

The UREX+1a process involves the co-extraction of minor actinides (Np, Am, and Cm) with plutonium. UREX+1a shows a higher impact on overall system PR, primarily due to the fact that the introduction of americium and curium (particularly ^{244}Cm) substantially increasing the stream heat generation rate (thus lowering the material attractiveness). The assumed extraction efficiencies for Am/Cm are assumed to be 95%, with 99% efficiency for Pu/Np. Figure 4.17 illustrates the overall system PR as a function of LWR fuel burnup (MOX fuel burnup is held constant at 60 $\frac{GWd}{MTHM}$).

The impact of minor actinide co-extraction relative to the PUREX baseline (black, dashed) is more noticeable than neptunium coextraction alone (UREX+2/3/4). This effect becomes particularly pronounced with burnup (as the inventories of minor actinides scale markedly with increasing burnups, thus increasing the heat generation rate). This manifests in the isotopic barrier performance as a function of burnup, as seen in Table 4.15.

The system PR centroid values and relative system rankings of the UREX+1a system as a function of burnup are provided as Table 4.16.

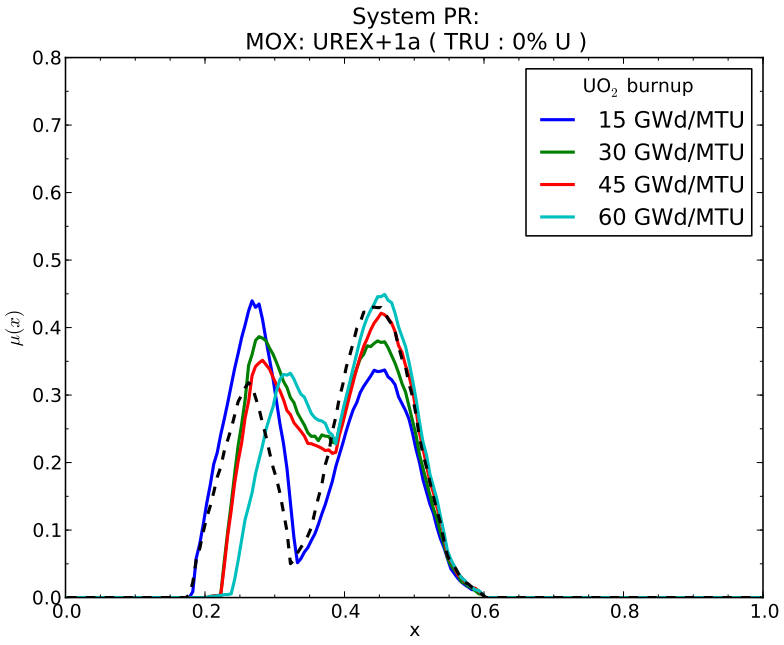

Figure 4.17: Intrinsic system proliferation resistance for a LWR + MOX cycle employing UREX+1a (TRU) for actinide recovery as a function of UO_2 fuel burnup. Reference PUREX scenario (Pu only) for 60 $\frac{\text{GWd}}{\text{MTU}}$ burnup shown in black, dashed. Higher abscissa values represent higher intrinsic PR.

Table 4.16: System PR centroid and rankings as a function of LWR fuel burnup for a LWR + MOX cycle with UREX+1a.

UO_2 burnup ($\frac{\text{GWd}}{\text{MTU}}$)	Centroid	Rank
15	0.3628	L+
30	0.3841	L+
45	0.3921	L+
60	0.4060	M–

UREX+1b

Extending the logic of minor actinide co-extraction found in UREX+1a is the UREX+1b process, in which uranium is also coextracted with transuranic elements. Uranium is again assumed to be coextracted at a 50% ratio, while the extraction efficiency ratios for Pu/Np and Am/Cm are again taken as 99% and 95%, respectively. Figure 4.18 gives the breakdown of system PR as a function of LWR burnup (with a fixed MOX burnup of 60 $\frac{\text{GWd}}{\text{MTHM}}$).

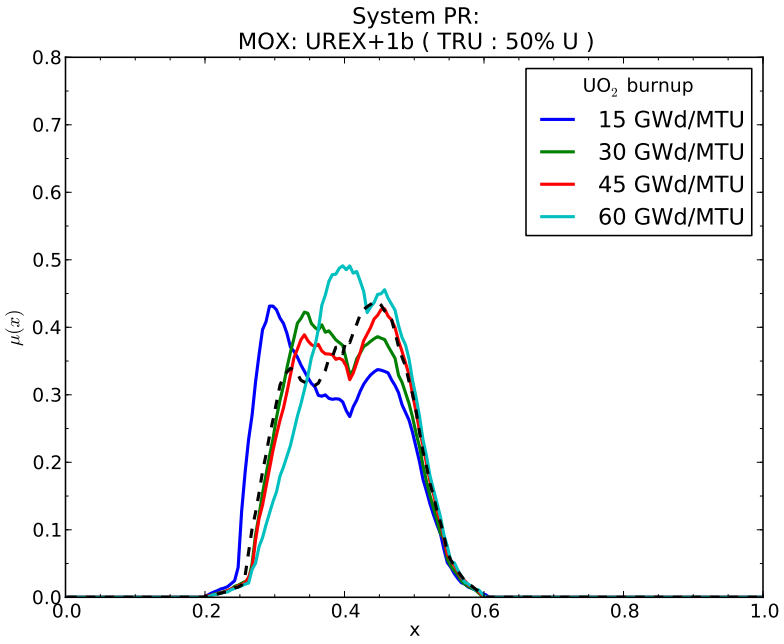

Figure 4.18: Intrinsic system proliferation resistance for a LWR + MOX cycle employing UREX+1b (TRU + 50% U) for actinide recovery as a function of UO_2 fuel burnup. Reference COEX scenario (50% U:Pu) for 60 $\frac{\text{GWd}}{\text{MTU}}$ burnup shown in black, dashed. Higher abscissa values represent higher intrinsic PR.

One observes that again the PR impact of uranium coextraction appears to be substantially greater than the impact (compared to the baseline COEX scenario) of minor actinide coextraction. However, these two effects also appear to be additive; i.e., while uranium dilution strongly increases the bare sphere critical mass, it contributes very little to the heat generation rate, while conversely minor actinides contribute little the bare sphere critical mass (making up a small fraction of the mass fraction) but contribute greatly to the heat

Table 4.17: Isotopic barrier performance rankings for selected stages and burnup values of the UREX+1b-based MOC strategy.

	Isotopic	
Stage / Burnup ($\frac{GWd}{MTU}$)	15	60
Reprocessing	M–	M+
MOX fuel fabrication	L	L+
MOX fuel irradiation	M–	M
Final emplacement	L+	M–

generation rate, particularly at higher burnups. This is illustrated in Table 4.17; the isotopic barrier is the primary barrier evolving both between this fuel cycle strategy and the baseline PUREX/COEX and as a function of fuel burnup.

The system PR centroid values and relative system rankings of the UREX+1b system as a function of burnup are provided as Table 4.18.

Table 4.18: System PR centroid and rankings as a function of LWR fuel burnup for a LWR + MOX cycle with UREX+1b.

UO_2 burnup ($\frac{GWd}{MTU}$)	Centroid	Rank
15	0.3846	M–
30	0.4025	M–
45	0.4088	M–
60	0.4163	M

UREX+1

A final UREX series considered is UREX+1, in which transuranics are coextracted with lanthanides, providing a radiological barrier to protect the fissile nuclides. This scenario is evaluated across the same burnup space (with a fixed MOX burnup of 60 $\frac{GWd}{MTHM}$) and likewise compared against the baseline PUREX scenario (60 $\frac{GWd}{MTU}$ LWR fuel burnup; black, dashed line) as Figure 4.19.

UREX+1 again presents a non-trivial departure from the PUREX baseline scenario, par-

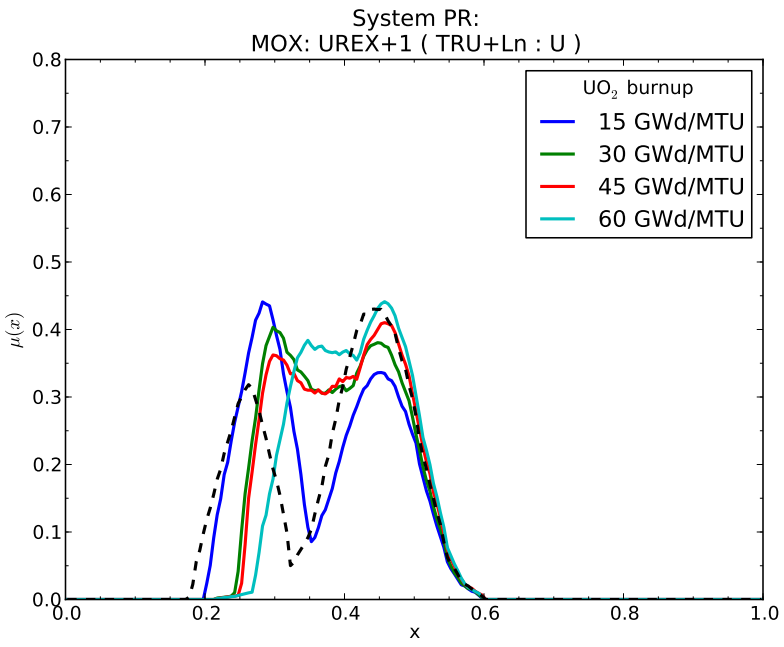

Figure 4.19: Intrinsic system proliferation resistance for a LWR + MOX cycle employing UREX+1 (TRU + Ln) for actinide recovery as a function of UO_2 fuel burnup. Reference PUREX scenario (Pu only) for 60 $\frac{\text{GWd}}{\text{MTU}}$ burnup shown in black, dashed. Higher abscissa values represent higher intrinsic PR.

ticularly with increasing burnup. The burnup dependence of the PR gains are tied to the fact that both lanthanide inventories as well as TRU inventories both increase as a function of burnup; thus, the plutonium-bearing stream material attractiveness subsequently diminishes with increasing burnup; this is evident in the isotopic and radiological barrier performance, given as Table 4.19. The relative system rankings of the UREX+1 system as a function of burnup are provided as Table 4.20.

4.3.4 System PR as a function of MOX fuel burnup

Evaluating the system PR as a function of MOX fuel burnup (with UO_2 fuel burnup held constant at 60 $\frac{\text{GWd}}{\text{MTU}}$), one finds that the level of MOX fuel burnup has very little effect upon the overall system PR, as evinced in Figure 4.20. Evaluating the effect of MOX fuel burnup on the post-MOX irradiation level PR values (Figure 4.21), it is clear that MOX fuel burnup has little discernible impact upon PR; i.e., while plutonium is consumed in MOX fuel, the

Table 4.19: Barrier performance rankings for the isotopic and radiological barriers for selected stages and burnup values of the UREX+1-based MOC strategy.

	Isotopic		Radiological	
Stage / Burnup ($\frac{GWd}{MTU}$)	15	60	15	60
Reprocessing	M–	M+	L	M
MOX fuel fabrication	L	L+	M	M
MOX fuel irradiation	M–	M	VH	VH
Final emplacement	L+	M–	M	M

Table 4.20: System PR centroid and rankings as a function of LWR fuel burnup for a LWR + MOX cycle with UREX+1

UO_2 burnup ($\frac{GWd}{MTU}$)	Centroid	Rank
15	0.3710	L+
30	0.3923	M–
45	0.4008	M–
60	0.4148	M–

plutonium vector changes very little, therefore the material attractiveness of the remaining plutonium remains largely unchanged. Likewise, while some plutonium is consumed, sufficient amounts of plutonium remain in spent MOX fuel rods as to produce no change in the available mass barrier.

However, even if changes in the post-MOX irradiation PR were observed, the overall impact upon system PR would likely be constrained. In particular, this owes to two factors: the first being that the MOX fuel burnup occurs at the "tail end" of the fuel cycle, creating a short "cascade" for changes in material properties to propagate, and second owing to the relative small electricity fraction produced by MOX fuel at equilibrium (e.g., around 10–13%), making the contribution from post-MOX irradiation stages comparatively small to the overall system PR.

4.3.5 System PR as a function of cooling time (pre-separation)

The cooling time before actinide separation has been raised as a potential proliferation concern, namely due to the balance of the ease of separation (which increases with time) versus the effectiveness of the radiological barrier (which decreases with time). Fuel cycle

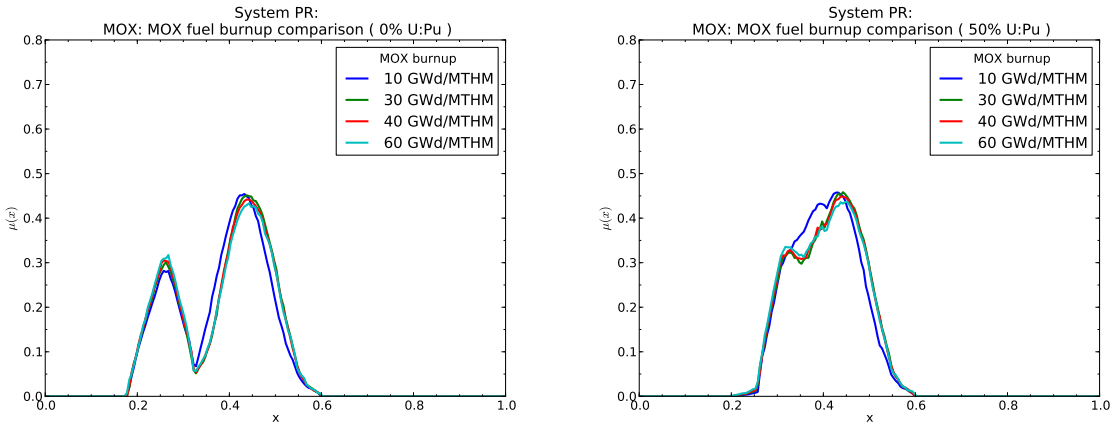

(a): PUREX (0% U:Pu) (b): COEX (50% U:Pu)

Figure 4.20: Intrinsic system proliferation resistance for a LWR + MOX fuel cycle as a function of MOX fuel burnup (with a fixed UO_2 burnup of 60 $\frac{\text{GWd}}{\text{MTU}}$) for a PUREX and COEX extraction process, respectively. Higher abscissa values represent higher intrinsic PR.

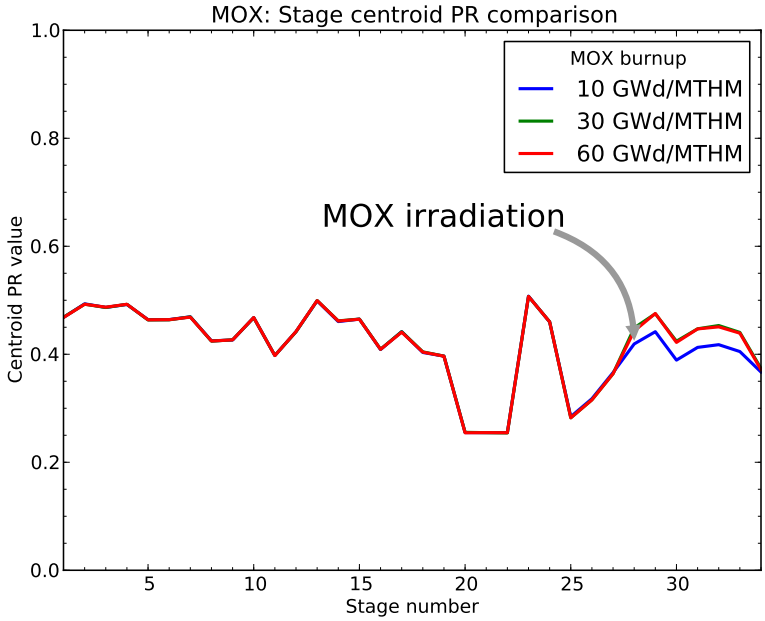

Figure 4.21: Cross-section view of system PR for a LWR + MOX cycle using PUREX for plutonium recovery as a function of MOX fuel burnup (UO_2 fuel burnup fixed at 60 $\frac{\text{GWd}}{\text{MTU}}$). Higher ordinate values represent increasing PR.

experts such as Emory Collins note that the radiological barrier becomes insufficient around 70 years cooling time [11], making spent fuel more susceptible to theft and diversion.

Thus, the cooling time before actinide separation is of relevant interest to PR considerations, given the potential link between radiological barrier performance and cooling time. This factor is thus evaluated as Figure 4.22 over the range of 1 to 100 years total cooling time before separation.

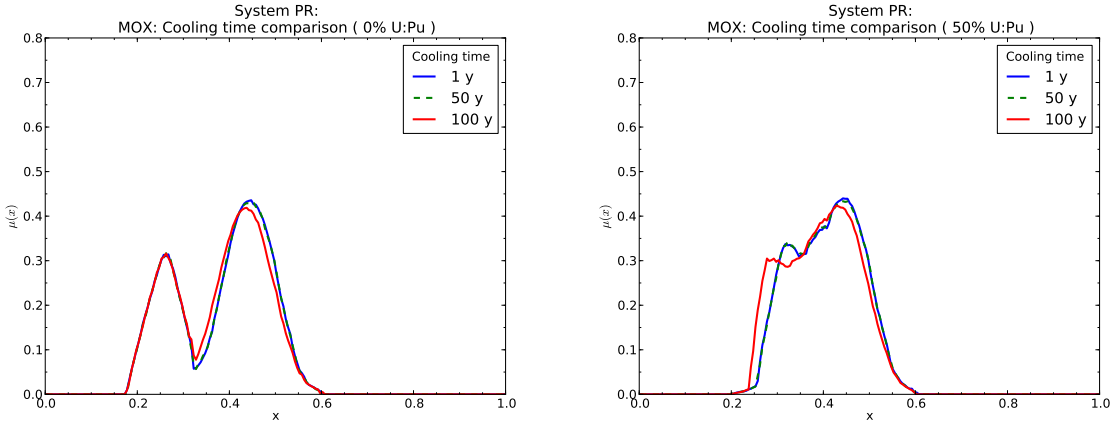

(a): PUREX (0% U:Pu)

(b): COEX (50% U:Pu)

Figure 4.22: Intrinsic system proliferation resistance for a LWR + MOX fuel cycle as a function of cooling time before separation (with a fixed UO_2 burnup of 60 $\frac{\text{GWd}}{\text{MTU}}$), for a PUREX and COEX cycle, respectively. Higher abscissa values represent higher intrinsic PR.

As one observes in Figure 4.22, cooling time before separation only has a small impact upon overall system PR, where a slight decrease in overall system PR is observed between the period of 50 and 100 years cooling time before separation for both the PUREX-based and COEX-based scenarios. Thus, while cooling time is a direct factor in the radiological hazard (as well as other factors such as the heat generation rate in the fuel), this is but one of many factors in the PR calculation, the majority of which remain largely unchanged with cooling time. While minor changes are observed in the isotopic composition of the plutonium vector (i.e., changes in the ^{241}Pu content, which has a half-life of 14 years), these changes are insufficient to cause a significant difference in the latent material attractiveness of the plutonium vector.

4.3.6 DUPIC fuel cycle

The **d**irect **u**se of spent **P**WR fuel **i**n **C**ANDU (DUPIC) is a novel fuel cycle concept proposed by researchers in South Korea [30, 44]. Normally, one constraint upon the extended use of LWR fuel is the buildup of particular fission products which act as "neutron poisons," parasitically absorbing neutrons without producing additional energy through fission. One example is the production of ^{135}Xe, a decay product of the fission product ^{135}I (Eq. 4.4). ^{135}Xe is a highly effective neutron absorber, producing ^{136}Xe (which is stable). The buildup of "neutron poisons" like ^{135}Xe (which reaches an equilibrium during irradiation) produce a gradual decline in the neutron economy of nuclear fuel until it is otherwise impractical to continue irradiation, despite an abundance of remaining fissionable materials in the fuel.

$$^{135}\mathrm{I} \xrightarrow{\beta^-} {}^{135}\mathrm{Xe} \tag{4.3}$$

$$^{135}\mathrm{Xe} + {}^{1}_{0}\mathrm{n} \longrightarrow {}^{136}\mathrm{Xe} \tag{4.4}$$

The DUPIC fuel cycle is designed to extract additional energy out of spent PWR fuel through the use of "dry" processing. Through voloxidation, spent fuel is reduced to a powder form, releasing volatile fission product gases; the specific concentrations removed are taken as those from [30] and reproduced as Table 4.21. This powder is then re-formed into fuel pellets and fashioned into CANDU fuel for irradiation in a CANDU reactor. No actinides are separated during this process, and the powder remains highly radioactive, requiring the work to be done in a hot cell. Thus, the DUPIC fuel process is designed to maximize proliferation resistance while facilitating additional energy recovery from fuel.

Table 4.21: Volatile fission product removal fractions (RF) for voloxidation, as taken from [30]

Element	RF (%)	Element	RF (%)
H	100	C	100
Kr	100	Ru	100
Cd	75	Te	75
Ir	75	I	100
Xe	100	Cs	100

The system PR of the DUPIC process is evaluated as a function of LWR fuel burnup (with a fixed DUPIC burnup of 10 $\frac{\text{GWd}}{\text{MTU}}$) as Figure 4.23.

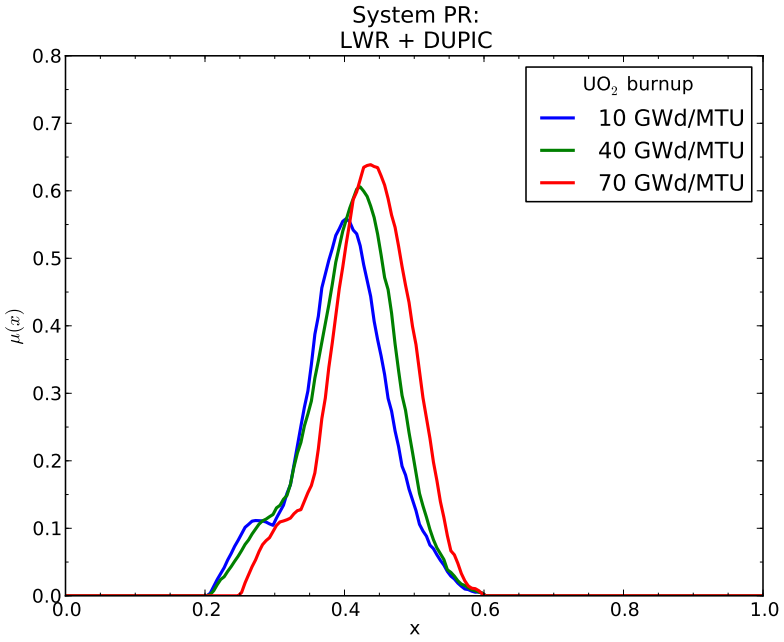

Figure 4.23: Intrinsic system proliferation resistance for a DUPIC fuel cycle as a function of UO_2 fuel burnup. Higher abscissa values represent higher intrinsic PR.

From Figure 4.23, the overall system PR of the DUPIC cycle compares favorably with the MOC alternatives, approaching the intrinsic PR of the LWR once-through system. Likewise, the DUPIC system shows an overall elevated response to burnup, given the consumption of plutonium in the re-irradiation stages (e.g., further degrading the final plutonium vector).

A cross-section of the DUPIC fuel cycle is given as Figure 4.24.

As one observes in the system PR cross-section, the "dry processing" (voloxidation) carries a higher overall intrinsic PR compared to aqueous reprocessing techniques, namely due to the fact that the fuel remains mixed with radioactive fission products (i.e., no plutonium is separated). However, a noticeable drop in PR is observed, due to the substantial decline in the radiation barrier with the removal of volatile fission product gases. This barrier remains significantly higher than that of separated TRU (which presents a negligible overall radiological barrier), however the removal of these products does carry a small penalty to

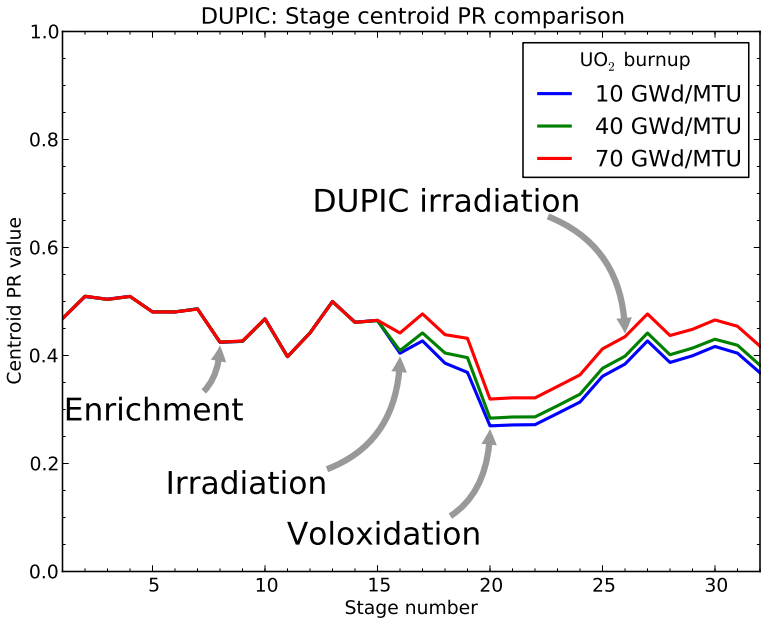

Figure 4.24: Cross-section view of system PR for a DUPIC as a function of UO_2 fuel burnup (DUPIC fuel burnup fixed at 10 $\frac{\text{GWd}}{\text{MTHM}}$). Higher ordinate values represent increasing PR.

overall system PR.

A decomposition of the system PR function for the DUPIC cycle at a UO_2 burnup of 60 $\frac{\text{GWd}}{\text{MTU}}$ is shown as Figure 4.25. The DUPIC cycle much more closely resembles the system PR behavior of once-through cycles due to the lack of isolation of plutonium (i.e., voloxidation only removes volatile fission product gases, leaving actinides with other radioactive fission products). The voloxidation-related stages thus make up the smaller, slightly lower "shoulder" in the system PR function, due to the fact that the materials are still relatively unattractive. Additionally, the DUPIC re-irradiation stages show a slightly higher PR than the UO_2 fuel irradiation due to the further degradation of the isotopic vector following re-irradiation.

The breakdown of system PR centroid values and rankings is given as Table 4.22.

4.3.7 Plutonium disposition alternative: "Storage MOX"

An alternative plutonium disposition strategy which has been proposed as a means of handling excess stockpiles of separated reactor-grade plutonium (RGP) has been so-called "storage MOX" [37]. The storage MOX concept takes separated RGP for fabrication into MOX fuel

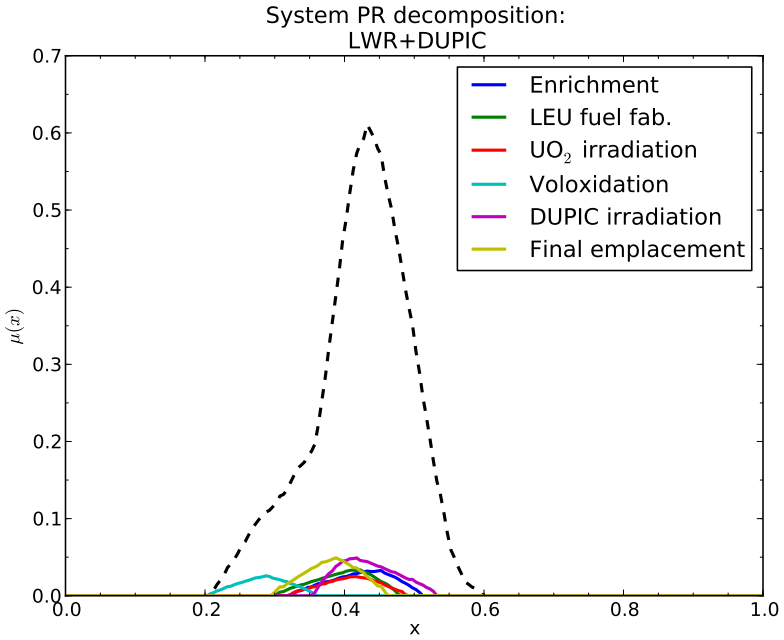

Figure 4.25: Decomposition of the system fuzzy PR value into the constituent stage fuzzy numbers for the LWR + DUPIC fuel cycle; fuel burnup fixed at 60 $\frac{\text{GWd}}{\text{MTU}}$ / 10 $\frac{\text{GWd}}{\text{MTHM}}$.

Table 4.22: System PR centroid values and rankings as a function of uranium fuel burnup for the DUPIC cycle

Burnup ($\frac{\text{GWd}}{\text{MTU}}$)	Centroid	Rank
10	0.3971	M
20	0.4040	M
30	0.4075	M
40	0.4085	M
50	0.4223	M+
60	0.4231	M+
70	0.4335	M+

rods with roughly double the amount of ordinary plutonium content (e.g., about 10-15% in storage MOX rods), with more relaxed manufacturing tolerances. These "storage MOX" rods are then permanently bonded with spent fuel rods (to provide for a radiological barrier) and placed in a neutron-absorbing cask (for criticality safety) for permanent disposal. The storage MOX concept is thus designed as an alternative to consumption of separated plutonium in light water reactors via MOX fuel.

The "storage MOX" scenario is considered to two plausible alternatives: a PUREX-based scenario and a COEX-based scenario (50% U:Pu), in order to simulate the plausible fuel cycles where this alternative would be employed (e.g., in France and Japan, respectively). These evaluations are given as Figure 4.26 and Figure 4.27, respectively. The "baseline" scenario for each (LWR fuel burned for 60 $\frac{\text{GWd}}{\text{MTU}}$ and burned for 60 $\frac{\text{GWd}}{\text{MTHM}}$ as MOX fuel) is indicated with an equivalent separation strategy as a black, dashed line.

For this evaluation, an equivalent fuel cycle to the MOX fuel cycles is considered through MOX fuel fabrication. The "storage MOX" fuel is then fabricated with 15% plutonium (balance of depleted uranium). This "storage MOX" fuel is then "batched" with an inventory of spent LWR fuel, cooled for 10 years (in order to calculate the appropriate radiological barrier). The remaining steps are then identical to the end stages of the MOX cycle (e.g., disposal-related stage).

As one observes from Figures 4.26 and Figure 4.27, the "storage MOX" scenario does not represent a viable pathway for increasing intrinsic fuel cycle PR; for all cases except for the outermost extremes of burnup (e.g., 70 $\frac{\text{GWd}}{\text{MTU}}$, where the plutonium vector has notably changed in attractiveness during reprocessing-related stages), the "storage MOX" scenario fails to achieve any higher intrinsic PR than the reference MOX fuel-based scenario. The reasons are of course twofold: not only is plutonium not consumed (but rather simply disposed of), but likewise the chemical form of the plutonium remains in an overall more accessible state than in spent fuel; i.e., while processing would be required to recover the plutonium, the difficulty of removing plutonium from mixed-oxide rods (assuming they were safely separated from the cask) is substantially easier than separating plutonium from intact spent fuel rods. This of course does not speak to the argument of whether "storage MOX" is a more viable means of clearing excess separated RGP inventories as an economic or technical argument, but simply as to the question of relative PR gains compared to the next available alternative, i.e. the consumption of RGP in MOX fuel rods.

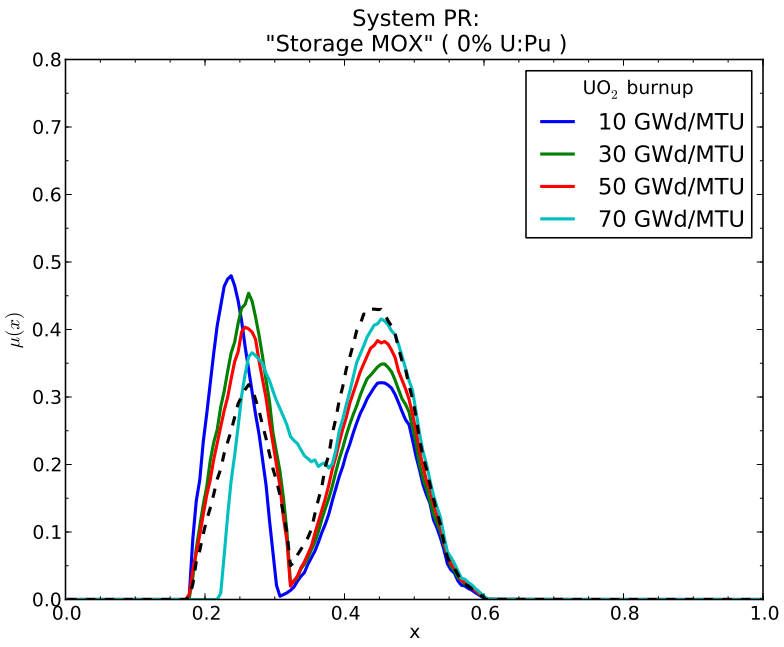

Figure 4.26: Intrinsic system proliferation resistance for a "storage MOX" scenario, assuming a PUREX-based reprocessing strategy (0% U:Pu), as a function of UO_2 fuel burnup. LWR + MOX (PUREX) scenario (60 $\frac{\text{GWd}}{\text{MTU}}$ UO_2 burnup and 60 $\frac{\text{GWd}}{\text{MTHM}}$ MOX fuel burnup) shown as black, dashed.

4.4 Closed fuel cycles

Fully closed fuel cycles represent the logical endpoint of nuclear fuel cycle technology in that they harness the full uranium energy resources available through the multiple recycle of actinides in nuclear fuel. Likewise, such a strategy has enormous potential for waste management considerations by eliminating much of the longest-lived elements found in spent fuel. These elements also represent the most significant contributors to long-term heat projections in the repository; their partition and destruction in fast reactors would thus enable a significant increase in overall repository capacity and minimization of overall risk [34, 41]. The fast reactor cycle thus represents an extension of the proliferation resistance and nuclear waste management considerations introduced in the advanced UREX series treatments.

The relative PR of fast reactor cycles can be evaluated across several parameters: the input burnup of the LWR fuel, the separation strategy employed for actinide recovery, and

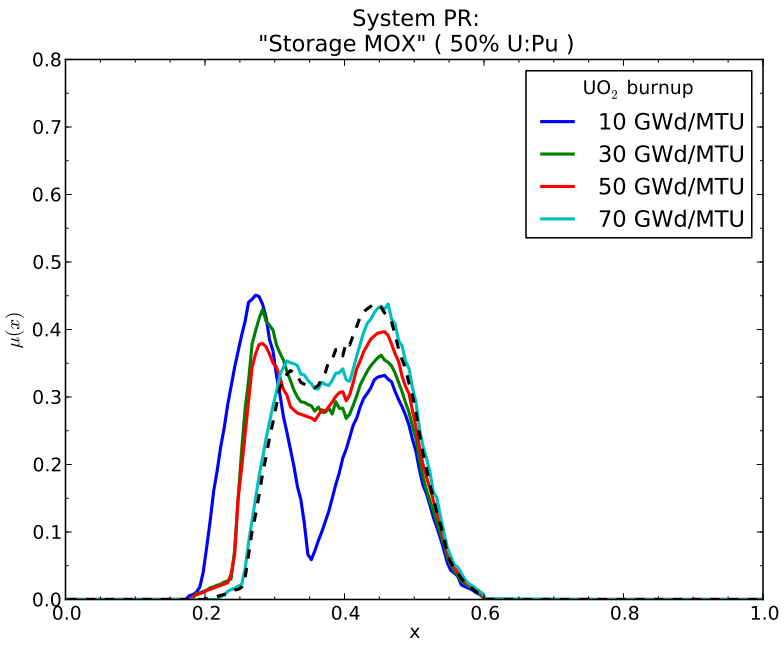

Figure 4.27: Intrinsic system proliferation resistance for a "storage MOX" scenario, assuming a COEX reprocessing strategy (50% U:Pu), as a function of UO_2 fuel burnup. Reference LWR + MOX (COEX) scenario (60 $\frac{\text{GWd}}{\text{MTU}}$ UO_2 burnup and 60 $\frac{\text{GWd}}{\text{MTHM}}$ MOX fuel burnup) shown as black, dashed.

the burnup of the fast reactor fuel itself. Two separation strategies are considered to this end: an advanced UREX series treatment (UREX+1a) as well as electro-metallurgical separation (e.g., "pyroprocessing").

The electricity fraction for the FR portion of the cycle is calculated in a similar fashion to the MOX cycle (Eq. 4.1); this is given as Eq. 4.5

$$\text{EF}_{\text{TRU}} = \frac{\text{TRU}_{\text{LWR}}}{\text{TRU}_{\text{FR}}} \cdot \frac{\text{M}_{\text{FR}} \cdot \text{BU}_{\text{FR}} \cdot \epsilon_{\text{FR}}}{\text{M}_{\text{FR}} \cdot \text{BU}_{\text{FR}} \cdot \epsilon_{\text{FR}} + \text{M}_{\text{LWR}} \cdot \text{BU}_{\text{LWR}} \cdot \epsilon_{\text{LWR}}} \tag{4.5}$$

In Eq. 4.5, TRU_{LWR} and TRU_{FR} are the TRU inventories found in LWR fuel and in an initial FR core loading, respectively. Likewise, M_{LWR} and M_{FR} are the mass loadings of the light water and fast reactors while BU_{LWR} and BU_{FR} are the fuel burnups of the LWR and FR fuel, respectively. Finally, ϵ_{LWR} and ϵ_{FR} are the thermal efficiencies of the thermal and fast reactors, assumed respectively as 34.1% and 38.1% [40].

Eq. 4.5 gives the fast reactor electricity fraction for a single initial core-startup, requiring a

significantly higher TRU inventory than subsequent top-offs. Thus, in the case of the top-off, one would simply replace TRU_{FR} with ΔTRU_{FR}, where this quantity represents the amount of "top-off' fuel required for a full core. The net effect of this change is to shift the relative weighting of the FR stages (i.e., the relative fraction of electricity from FR increases, increasing the relative weight of the post-FR irradiation stages).

For all FR loadings, a conversion ratio of 50% (CR=0.5) was used for the mass loading (e.g., $MF_{TRU} = 0.330$) [40].

The ORIGEN-S fast reactor library used for the calculation is based on the ABTR spectrum [43], using a collapsed one-group energy spectrum in order to calculate reaction rates [23]; an ARP-compatible library was provided courtesy of Ian Gauld of Oak Ridge National Laboratory.

The stage structure of the fast reactor cycles is similar to that of the modified open cycles, also based on [57]. The exception to this is in the lack of disposal-related stages: the stage breakdown for closed cycles is given as Table 4.23.

Table 4.23: Selected stage numbers for closed cycles.

#	Stage
1	Mining
5	Conversion
8	Enrichment
11	LEU fuel fabrication
16	Reactor irradiation
18	SNF wet storage
19	SNF dry storage
20	Reprocessing
21	Recovered material storage
24	Actinide waste disposal
25	FBR fuel fabrication
28	FBR fuel irradiation
30	FBR SNF storage

4.4.1 System PR as a function of LWR fuel burnup & separation strategy

The first realm of analysis for PR impact in the LWR + FR cycle is in the burnup of LWR fuel used for FR loading. For each scenario, LWR fuel was cooled for 10 years before separation; FR fuel burnup was held fixed at 90 $\frac{\text{GWd}}{\text{MTHM}}$.

Figure 4.28 shows the system PR dynamics of a LWR + FR system using a UREX+1a (i.e., TRU: Pu + MA) recovery strategy.

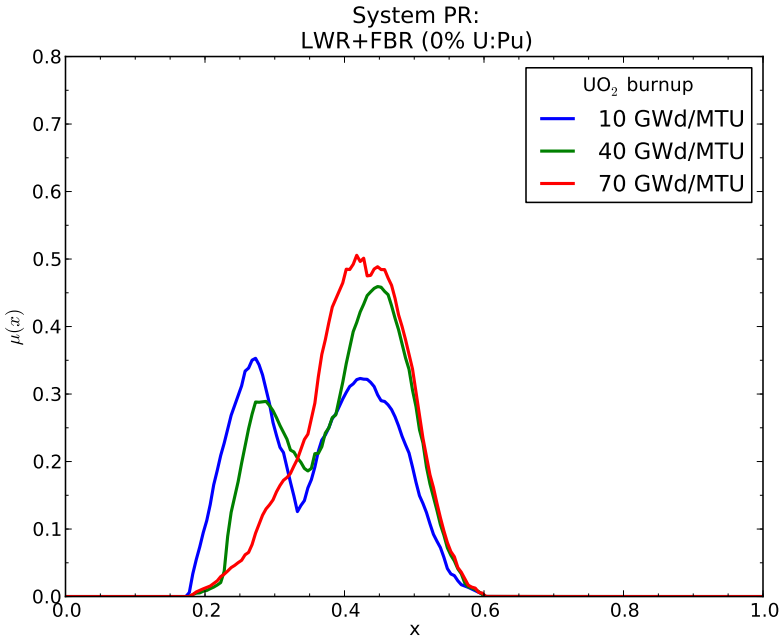

Figure 4.28: Intrinsic system proliferation resistance for a LWR + FBR cycle employing UREX+1a (TRU) for actinide recovery as a function of UO_2 fuel burnup. Higher abscissa values represent higher intrinsic PR.

Unlike the MOC strategies, one observes a far more clear UO_2 burnup dependence in the fast reactor cycle (Figure 4.28). This is due both to the higher space of burnups evaluated (up to 70 $\frac{\text{GWd}}{\text{MTU}}$) as well as the general dependence of minor actinide inventories (such as Am/Cm) on burnup; these actinides contribute substantially to the heat generation rate (lowering intrinsic material attractiveness), while their inventories are strongly burnup-dependent.

Evaluating a cross-section of the UREX-based FR cycle (Figure 4.29), one observes both

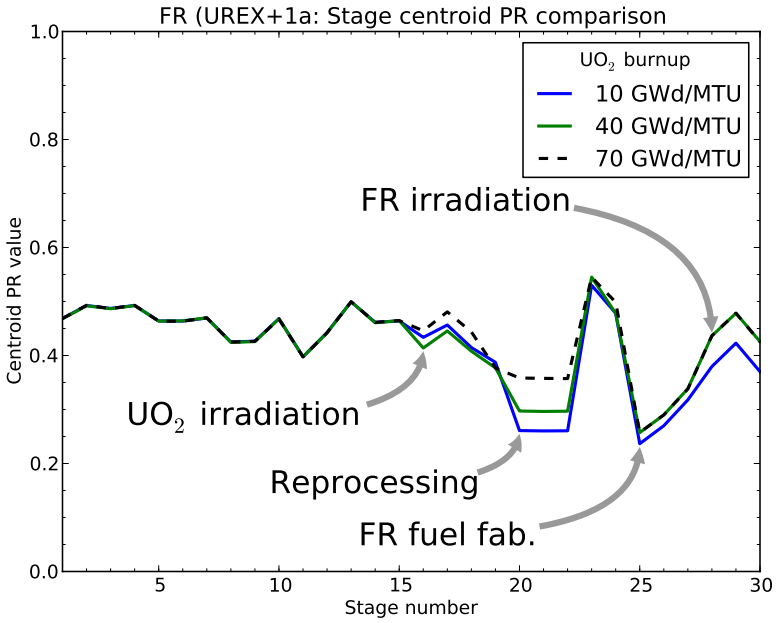

Figure 4.29: Cross-section view of system PR for a LWR + FR cycle employing UREX+1a (TRU) for actinide recovery as a function of UO_2 fuel burnup; FR burnup fixed at 90 $\frac{\text{GWd}}{\text{MTHM}}$. Higher ordinate values represent higher intrinsic PR.

that the higher actinide inventory (as a function of burnup) has positive consequences for PR both at the actinide recovery stages as well as corresponding "cascade" effects throughout the FBR fuel fabrication and irradiation. This corresponds not only with the higher minor actinide inventory, but in particular the degradation of the plutonium vector attractiveness as a function of burnup, where higher burnups result in a greater ingrowth of higher plutonium species (particularly ^{240}Pu and ^{242}Pu), greatly increasing the overall material heat generation rate.

In this respect, the FR cycle is perhaps one of the best demonstrations of the utility of the PR dynamics analysis technique and the value of coupled isotopic analysis. One clearly observes in this case how "cascade effects" in material properties (such as the inventories of plutonium and minor actinides) carry through to further stages of the system, thereby influencing system PR.

The breakdown of the system centroid PR and rankings are given as Table 4.24.

From Table 4.24, one observes a relative large space of potential system rankings, from "Low-plus" at low burnup (equivalent to a PUREX-based MOX cycle) to "Medium" at very

Table 4.24: System PR centroid and rankings as a function of LWR fuel burnup for a LWR + FR cycle using UREX+1a for actinide recovery

UO_2 burnup ($\frac{GWd}{MTU}$)	Centroid	Rank
10	0.3640	L+
20	0.3735	L+
30	0.3852	L+
40	0.3988	M–
50	0.4011	M–
60	0.4030	M–
70	0.4157	M

high burnup (equivalent to the CANDU cycle and just under a LWR once-through cycle).

A decomposition of the FBR fuel cycle (with UREX+1a for actinide recovery) is shown as Figure 4.30. Due to the aggregation of fissile materials at the "back end" of the cycle in the LWR+FBR system (i.e., due to the continuous recycle of actinides), post-FBR irradiation stages begin to show a nearly equal contribution as the reprocessing-related stages.

Additionally, given the dynamic nature of the fissile material inventories (particularly in the fast reactor system), the relative weight of these stages (and thus contribution to the system PR) changes as a function of burnup. This is evident in the comparison featured as Figure 4.31; not only does one observe a progressive increase in the PR of reprocessing-related stages with burnup, but likewise a small but observable decline in the weight of these stages with increasing burnup.

A second scenario for fast reactors considered was in the recovery of actinides through use of electrochemical separation, also known as "pyroprocessing" [31]. In pyrprocessing, fuel assemblies are dismantled and individual fuel rods are chopped into short pieces and loaded into an anode basket. This basket is then loaded into a molten salt solution. Electrical potential is then applied across the anode and a corresponding cathode in order to facilitate the reduction of uranium and plutonium from the solution as a solid metal, thus facilitating their recovery. Other minor actinides, such as neptunium, americium, and curium can also be recovered this way. Finally, a small amount of lanthanides tend to be drawn up with the uranium and plutonium (about 5000 ppm, or 0.5%) [51]; this is accounted for in the simulation. The relatively low level of material decontamination thus requires pyroprocessing materials be handled in a hot cell [21, 31]; this is thus also accounted for in the barrier

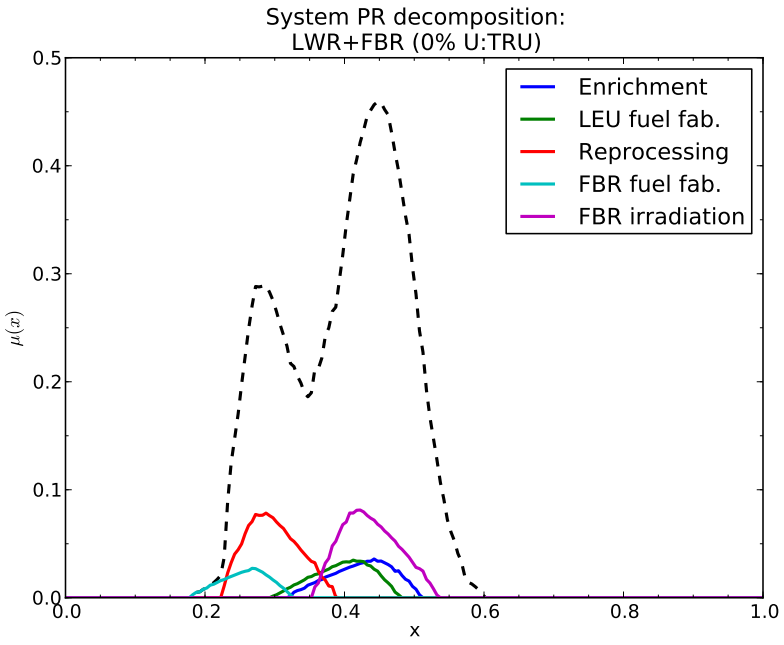

Figure 4.30: Decomposition of the system fuzzy PR value into the constituent stage fuzzy numbers for the LWR + FBR fuel cycle employing UREX+1a for actinide recovery; fuel burnup fixed at 40 $\frac{\text{GWd}}{\text{MTU}}$ / 90 $\frac{\text{GWd}}{\text{MTHM}}$.

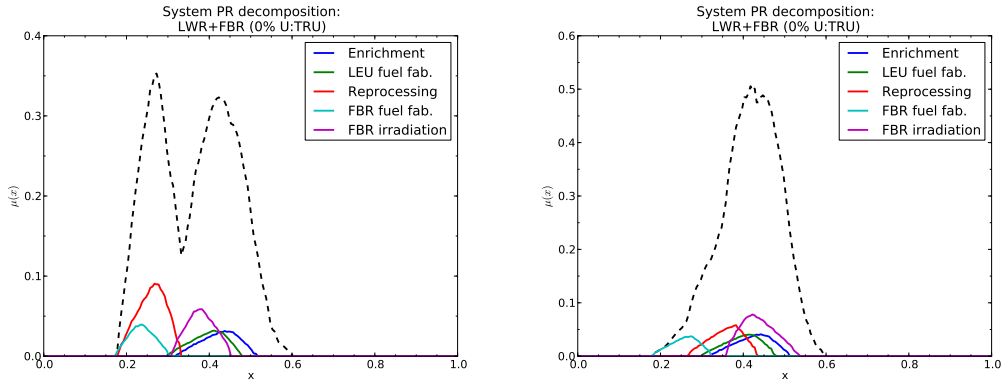

(a): 10 $\frac{\text{GWd}}{\text{MTU}}$ (b): 70 $\frac{\text{GWd}}{\text{MTU}}$

Figure 4.31: Comparison of the system decomposition for the LWR + FBR cycle (using UREX+1a for actinide recovery) as a function of UO_2 fuel burnup; FBR fuel burnup fixed at 90 $\frac{\text{GWd}}{\text{MTHM}}$.

performance rankings used in the Fuzzy Logic Barrier model.

Figure 4.32 gives the system PR dynamics of the pyroprocessing-based FBR cycle.

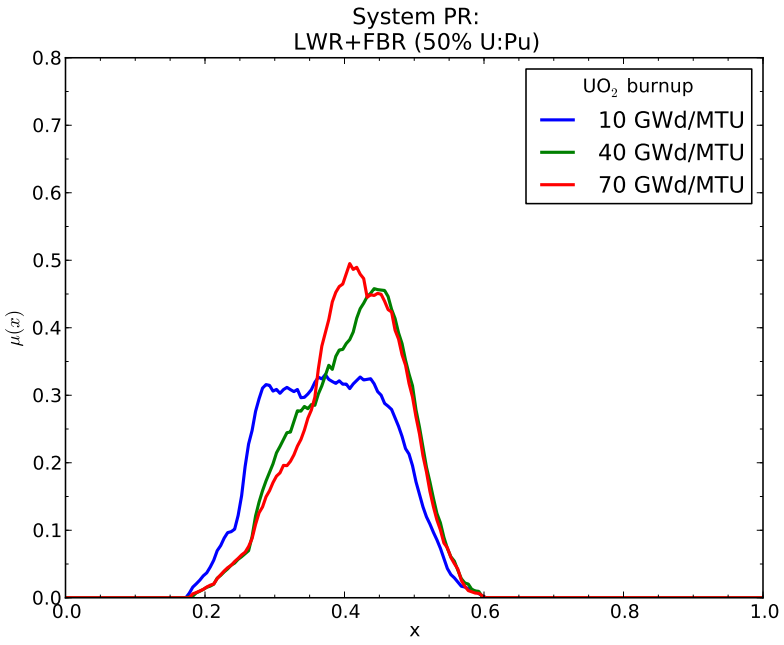

Figure 4.32: Intrinsic system proliferation resistance for a LWR + FBR cycle employing pyroprocessing for actinide recovery as a function of UO_2 fuel burnup. Higher abscissa values represent higher intrinsic PR.

The observed PR dynamics effects are somewhat weaker for the pyroprocessing scenario (Figure 4.32); this appears to be due to a "saturation" effect of the relative PR during actinide recovery stages; i.e., the addition of uranium and small amounts of lanthanides "saturate" the FOM calculation, where the marginal impact of additional minor actinide inventories due to burnup is thus smaller. This can be observed in the system cross-section, given as Figure 4.33.

In Figure 4.33, the "baseline" PR of the actinide recovery stages is clearly greater than that found in the advanced UREX scenario (save for UREX at very high burnups), as seen in Figure 4.29. However, one still observes the "cascade" effects due to burnup as seen before in the post-reprocessing and irradiation stages, due to the decreasing attractiveness of the plutonium vector.

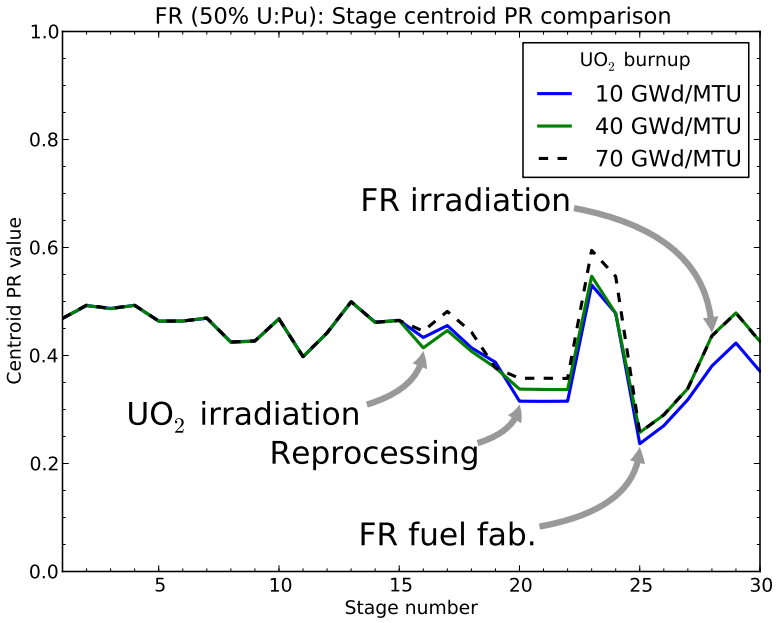

Figure 4.33: Cross-section view of system PR for a LWR + FR cycle employing pyroprocessing for actinide recovery as a function of UO_2 fuel burnup; FR burnup fixed at 90 $\frac{\text{GWd}}{\text{MTHM}}$. Higher ordinate values represent higher intrinsic PR.

The system PR centroid values and rankings for the pyroprocessing-based FR cycle are given as Table 4.25.

As one observes from Table 4.25, the overall system PR of the fast reactor cycle employing pyroprocessing is higher than that of one employing conventional UREX for actinide recovery, approaching the "medium" effectiveness ranking at substantially lower burnups. Overall, this cycle represents the highest PR of any partially closed or closed system with the exception of the DUPIC cycle.

Likewise, similar to the UREX-based FBR cycle (Figure 4.30), the pyroprocessing-based system PR function can also be decomposed into its respective stage fuzzy numbers for analysis; this is presented as Figure 4.34.

Additionally, the dynamics of the system decomposition can again be evaluated as a function of UO_2 fuel burnup; this is presented as Figure 4.35. Overall, given the relative dilution of the fissile material stream for pyroprocessing, the reprocessing-related stages show a lower weight and a more rapid decline as a function of burnup as compared to the corresponding UREX+1a case (Figure 4.31). Finally, PR in the reprocessing stages appears to

Table 4.25: System PR centroid and rankings as a function of LWR fuel burnup for a LWR + FR cycle using pyroprocessing for actinide recovery

UO_2 burnup ($\frac{GWd}{MTU}$)	Centroid	Rank
10	0.3779	L+
20	0.3922	M–
30	0.3959	M–
40	0.4090	M–
50	0.4099	M
60	0.4096	M
70	0.4094	M

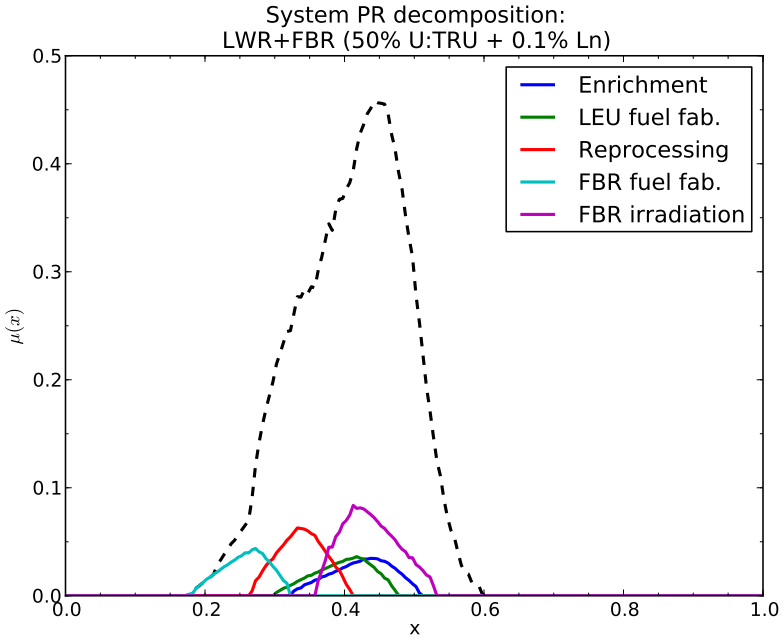

Figure 4.34: Decomposition of the system PR fuzzy number into the constituent stage fuzzy numbers for the LWR + FBR cycle with a pyroprocessing-based actinide recovery strategy; fuel burnup fixed at 40 $\frac{GWd}{MTU}$ / 90 $\frac{GWd}{MTHM}$.

"saturate" somewhat more quickly for the pyroprocessing-based case. This owes to the behavior of the isotopic barrier, which is affected both by the uranium dilution (increasing the bare sphere critical mass) and the increasing inventory of transuranics with burnup (increasing the heat generation rate). Given the inclusion of uranium dilution (in addition to the auxiliary radiological factor introduced by only partial decontamination, e.g. lanthanide inclusion), the reprocessing-related stages thus manifest a higher PR at lower burnups. (However, the final PR value for the reprocessing-related stages of both the UREX and pyroprocessing-based systems appears to converge upon a common value at very high burnups.)

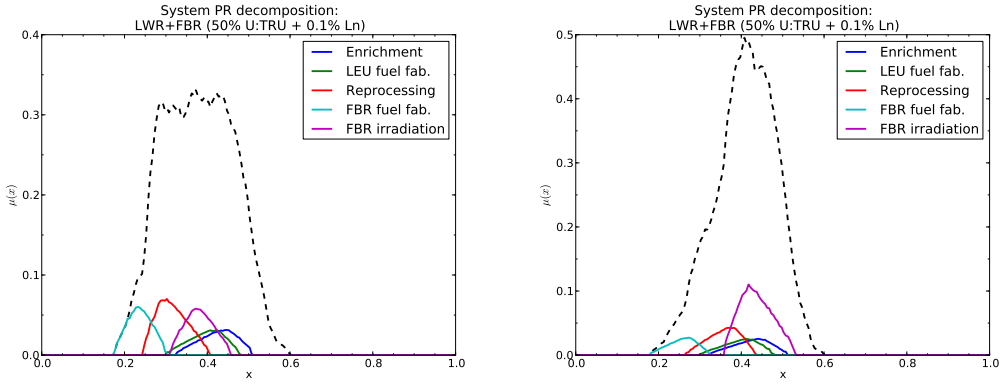

(a): 10 $\frac{\text{GWd}}{\text{MTU}}$ (b): 70 $\frac{\text{GWd}}{\text{MTU}}$

Figure 4.35: Comparison of the system decomposition for the LWR + FBR cycle (using pyroprocessing for actinide recovery) as a function of UO_2 fuel burnup; FBR fuel burnup fixed at 90 $\frac{\text{GWd}}{\text{MTHM}}$.

4.4.2 System PR as a function of FBR fuel burnup

The fast reactor cycles can also be evaluated as a function of fast reactor fuel burnup, holding the UO_2 burnup as a constant. For these scenarios, UO_2 fuel burnup is held constant at 60 $\frac{\text{GWd}}{\text{MTU}}$. Figure 4.36 gives the comparative system evaluation as a function of FBR fuel burnup for both the UREX-based and pyroprocessing-based scenarios.

Similar to the case of MOX fuel burnup, the burnup of fast reactor fuel has little overall impact upon system PR, as is evident from Figure 4.36. Taking the system cross-section

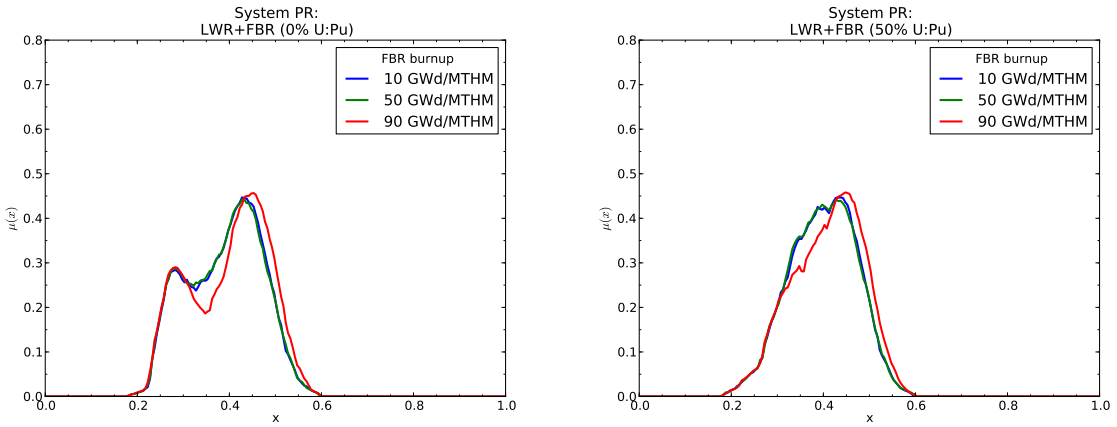

(a): UREX+1 (TRU+Ln)

(b): Pyroprocessing

Figure 4.36: Intrinsic system proliferation resistance for a LWR + FBR fuel cycle as a function of FBR fuel burnup (with a fixed UO_2 burnup of 60 $\frac{\text{GWd}}{\text{MTU}}$) for a UREX+1a and pyroprocessing extraction process, respectively. Higher abscissa values represent higher intrinsic PR.

(Figure 4.37), one observes that FR fuel burnup does not appear to appreciably change over the burnup range considered. Similar to the MOX case, while greater amounts of fissile materials are consumed with burnup, this effect does not appear to be (sufficiently) isotopically biased in a way to produce noticeable changes in material attractiveness or radiological hazard and subsequently proliferation resistance.

4.5 Conclusion

Based upon the evaluations performed in this chapter, a comparative evaluation of fuel cycles can be made as to relative proliferation resistance. This summation is presented as Figure 4.38, and further summarized in terms of ranking and centroid behavior as Table 4.26.

An overall comparison of fuel cycles indicates that in general, the LWR once-through cycle remains the most proliferation resistant cycle overall, with DUPIC ranking as the next-closest alternative (although it should be clearly noted here that no cycle studied in this analysis is "proliferation-proof"). The PUREX-based MOX cycle has the weakest proliferation resistance overall, given the separation of pure plutonium in the reprocessing stages. Fast cycles appear to exist as a "middle ground," given that both a greater amount of fissionable materials are ultimately consumed as well as the fact that plutonium is kept with other actinides, thus

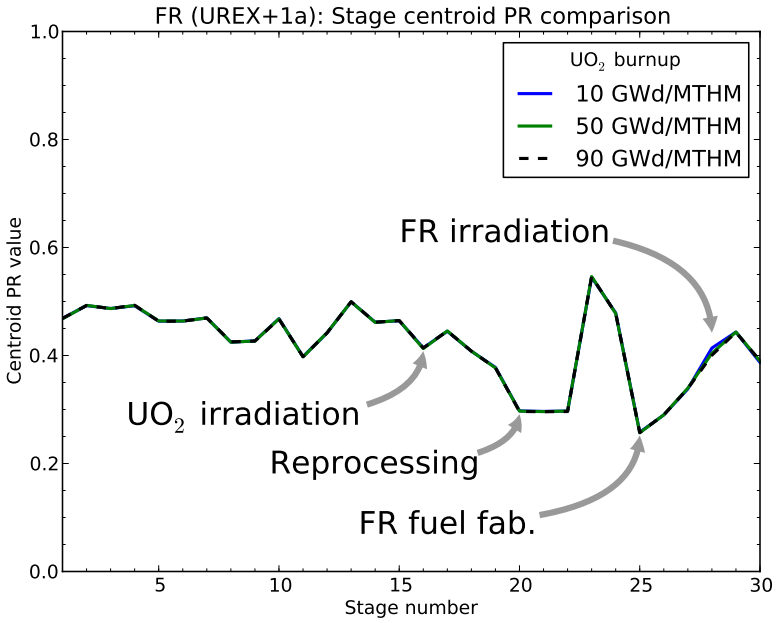

Figure 4.37: Cross-section view of system PR (e.g., level fuzzy number centroid values) for a LWR + FR cycle employing UREX+1 for plutonium recovery as a function of FR fuel burnup. Higher ordinate values represent higher intrinsic PR.

decreasing the overall material attractiveness. A specific comparison can also be made with respect to the separations strategies employed for the "modified open" cycle; such a comparison is given both as Figure 4.39 and Table 4.27.

The evaluation of MOC separation strategies can be divided roughly into three categories: pure plutonium (PUREX), plutonium and other minor actinides (UREX+2/3/4, UREX+1a, UREX+1), and plutonium (and other actinides) diluted with uranium (COEX, UREX+2a/3a/4a, UREX+1b). Each of these levels roughly corresponds with a $\frac{1}{3}$ level "step" change in attractiveness. The addition of uranium on its own during reprocessing appears to be a far more potent means of increasing PR than in the co-extraction of minor actinides, however advanced UREX scenarios which coextract minor actinides with plutonium do appear to have a minor impact upon overall system PR.

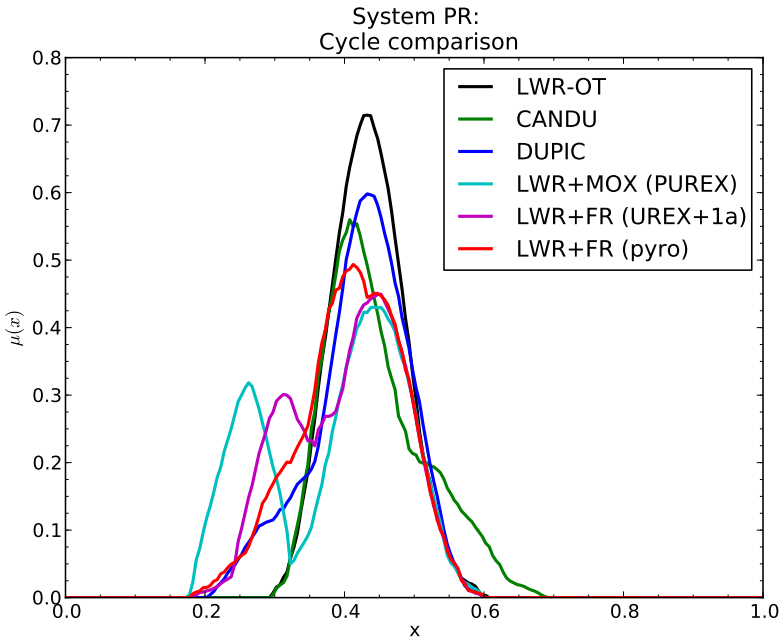

Figure 4.38: Overall comparison of intrinsic system PR for fuel cycle systems considered; burnup fixed at 60 $\frac{\text{GWd}}{\text{MTU}}$ / $\frac{\text{GWd}}{\text{MTHM}}$ for LWR and MOX fuel, 10 $\frac{\text{GWd}}{\text{MTU}}$ for CANDU/DUPIC fuel, and 90 $\frac{\text{GWd}}{\text{MTHM}}$ for FBR fuel. Higher abscissa values represent higher intrinsic PR.

Table 4.26: Summary of system centroid PR and rank values for selected fuel cycle systems.

System	Burnup ($\frac{\text{GWd}}{\text{MTU}}$/ $\frac{\text{GWd}}{\text{MTHM}}$)	Centroid	Rank
LWR-OT	40 / —	0.4327	M+
	70 / —	0.4489	M+
CANDU HWR	10 / —	0.4462	M
MOX: PUREX	60 / 60	0.3853	L+
MOX: COEX	60 / 60	0.4069	M–
MOX: UREX+1a	60 / 60	0.4060	M–
DUPIC	40 / 10	0.4085	M+
	70 / 10	0.4335	M+
FBR: UREX+1a	40 / 90	0.3988	M–
	70 / 90	0.4157	M
FBR: Pyro	40 / 90	0.4090	M
	70 / 90	0.4094	M

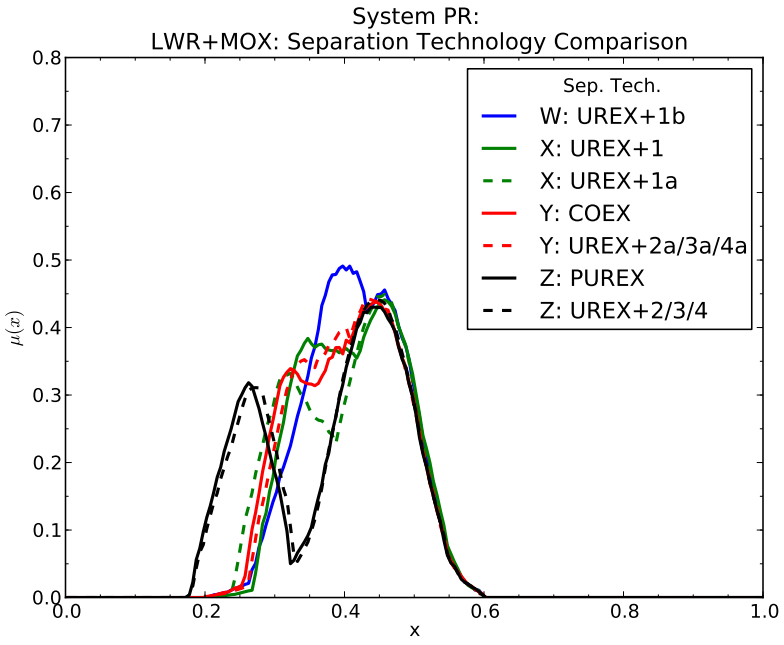

Figure 4.39: Comparison of intrinsic PR for LWR + MOX fuel cycles by separation strategy, with a fixed LWR fuel burnup of 60 $\frac{\text{GWd}}{\text{MTU}}$ and MOX fuel burnup of 60 $\frac{\text{GWd}}{\text{MTHM}}$. Higher abscissa values represent higher intrinsic PR.

Table 4.27: Summary of system centroid PR and rank values for each of the separation strategies considered for the "modified open" cycle. Burnup held fixed at 60 $\frac{\text{GWd}}{\text{MTU}}$ / 60 $\frac{\text{GWd}}{\text{MTHM}}$.

System	Product(s)	Centroid	Rank
PUREX	Pu	0.3853	L+
UREX+2/3/4	Pu + Np	0.3872	L+
UREX+1a	TRU	0.4060	M–
UREX+1	TRU + Ln	0.4148	M–
COEX	Pu + U (50%)	0.4069	M–
UREX+2a/3a/4a	Pu/Np + U (50%)	0.4098	M–
UREX+1b	TRU + U (50%)	0.4163	M

CHAPTER 5

Adversary Pathway Analysis

5.1 Introduction

In this section, the development and use of Adversary Pathway Analysis (APA) shall be presented. This process involves the concurrent evaluation of nuclear fuel cycles while considering such aspects as the capabilities of the adversary host state (impacting the relative importance of particular barriers, such as physical barriers like isotopic attractiveness, radiological hazard, etc.), adversary intent (e.g., sensitivity to reliable weapons yield) and the target material pathway (e.g., plutonium, transuranics, or minor actinides). Such an evaluation can be used as a "fine-tuning" process to AA methods such as the Fuzzy Logic Barrier model used in this study.

The premise of APA is twofold. First, the application of particular criteria such as the isotopic attractiveness of material (as well as other physical barriers, such as the radiological hazard, etc.) depend upon the assumed final form of the target material being diverted. For example, plutonium coextracted with uranium manifests a significantly different material attractiveness under an assumed direct-use scenario compared to one in which plutonium is subsequently re-extracted, as well as other factors (e.g., mass & bulk, radiological hazard, etc.); a similar evaluation can be made for any facility or material stream in the nuclear fuel cycle. PRA-based assessments such as PRPP characterize all such pathways by the

sequence of events which result in such material diversions; APA can thus be thought of as a "bridge" technique which evaluated convergent pathways through the evaluation of changing attributed based upon the material diversion pathway. Second, adversary capabilities (and intent) are assumed to impact the relative prominence of particular barriers (e.g., physical barriers are less important to advanced industrial states with a fully developed indigenous fuel cycle). Likewise, the "overt" versus "covert" breakout scenarios can be taken as analogous to "abrupt" versus "protracted" diversion scenarios seen in other analyses [47]. Finally, assumptions of adversary intent for the unsophisticated state actor (e.g., sensitivity to reliable weapons yield) can impact the evaluation of factors such as the isotopic barrier.

This chapter shall thus explore the development and use of Adversary Pathway Analysis as a means of enhancing PR analysis using attribute-based approaches such as AA and MAUA models for nuclear fuel cycle PR assessment.

5.1.1 Application of the isotopic attractiveness criteria

A particular drawback to the use of the FOM approach is in that it is generally unhelpful for intact fuel characterization; i.e., given the fact that in intact form, the bare sphere critical mass will be extremely large; coupled with the very high radiological and thermal emission rates, all FOM_1 values will be < 0. Therefore, using the FOM approach for intact fuel provides little resolution in discriminating potential material attractiveness levels. If instead however the latent potential attractiveness is determined by assuming the intended adversary target material (e.g., Pu, TRU, etc.), the FOM can provide an extremely useful means of discriminating on material attractiveness based on different operational parameters (such as burnup, enrichment, and co-extraction strategies).

5.1.2 Implementation of APA in PR analysis

The assumed choice of target material by an adversary in the nuclear energy system touches on many of the intrinsic "physical" barriers, from the isotopic attractiveness of the target material itself to the radiological hazard of the bulk material being diverted (in order to obtain the target material), as well as the amount of bulk material required for diversion (affecting both the available mass as well as mass & bulk).

Thus, for a given target material, the assumption within this analysis begins with a diversion of the total material form containing the target material (for example, a spent fuel

pin or canister containing mixed oxide powder). The isotopic attractiveness is calculated from the end target material itself (e.g., Pu, TRU, etc.), while the radiological hazard is calculated from the "intact" diversion path (e.g., the radiological hazard from the spent fuel pin, containing highly radioactive fission products). Other barriers, such as the mass and bulk and overall available mass shall also follow a similar characterization (thus accounting for the barrier presented by more bulky, dilute forms of target material).

For this analysis, a "nominal" scenario shall be employed where the latent attractiveness of plutonium is considered for all intact fuel forms (i.e., the default attack pathway is assumed to be one where the malefactor separates only plutonium from intact fuel) and the "whole stream" for separated forms (for example, co-extraction of uranium with plutonium in reprocessing).

However, the assumption of the adversary characteristics also factors heavily into the model considerations. Two issues with be addressed with respect to this: the first being the relative importance of various barriers to different adversary types. For example, isotopic attractiveness poses a lower overall barrier to a sophisticated state capable of processing or otherwise compensating for sub-optimal weapons utility of a material, compared to a less sophisticated state. These differences are outlined in the TOPS report [57], which is used as a basis for creating different barrier weight sets for four different adversary types: a sophisticated state in an overt breakout attempt, a sophisticated state in a covert breakout, and finally an unsophisticated state in a covert proliferation attempt (under yield-sensitive and yield-insensitive conditions). The relative barrier weights identified in Table 2.10 are used for the respective PR evaluation by adversary type for this analysis.

For the case of the unsophisticated state, an additional branch of analysis is introduced in terms of reliability of yield. For such a nation desiring a high/reliable yield, FOM_2 is used as a measure of material attractiveness; for such a state unconcerned with yield (and for every other adversary type), FOM_1 will be used as the measure of material attractiveness [6].

5.2 PR assessment by target type

The following assessments evaluate PR by the target material type within the nuclear energy system. The "nominal" case outlined in the previous sections (i.e., plutonium target for intact fuel and whole-stream diversion for separated fuel forms). Each case uses the assumption of an unsophisticated state in a yield-insensitive context (e.g., FOM_1); this case is the most

sensitive to isotopic changes in the fuel. (Thus, other cases will show a lower overall sensitivity to isotopic changes as a function of burnup and enrichment).

5.2.1 Plutonium-only target pathway

The plutonium-only pathway assumes an adversary for which material is diverted and subsequently reprocessed to obtain exclusively plutonium. The isotopic barrier is evaluated based on the plutonium attractiveness, while other barriers (e.g., mass & bulk, radiological, chemical, etc.) are evaluated based upon the quantity of source material required for a diversion of 1 SQ of plutonium.

Given that the nominal case for once-through cycles exclusively relies upon a plutonium-only pathway, this case is identical to the nominal case. The reader is directed to the previous chapter, specifically Figures 4.1 and 4.5, for these cases.

Modified open cycles

Figure 5.1 shows a comparison of several recycle scenarios: PUREX (with plutonium-only separation), and several UREX alternatives (including the extraction of TRU, U, and lanthanides), and finally the DUPIC scenario.

The PUREX case remains unchanged from the baseline "nominal" scenario. For the UREX systems lacking uranium coextraction, the system PR function appears to converge to the PUREX baseline; i.e., few differences in the isotopic barrier of the target product exists, while other barriers (such as mass & bulk, chemical form, and radiological hazard) provide at best a small increase in intrinsic PR over the baseline PUREX case. Likewise, for such cases, a "bifurcation" in the system PR fuzzy number appears in the system PR function, where two clearly distinguishable peaks exist: one peak from the common stages to the once-through case (i.e., all stages prior to reprocessing) followed by a second peak at lower PR from the reprocessing-related stages (such as separation, recovery, and MOX fuel fabrication) where intrinsic barriers are least effective. Finally, uranium burnup appears to show little impact for the plutonium-only target case (e.g., given the very small changes in attractiveness

For cases involving uranium coextraction, the difference in system PR is nominally greater (due to the substantial increase in mass & bulk). However this change is still quite small if the assumption that an adversary will seek to reprocess diverted material for plutonium-only diversion. The DUPIC case appears to change only slightly from the "nominal" case scenario,

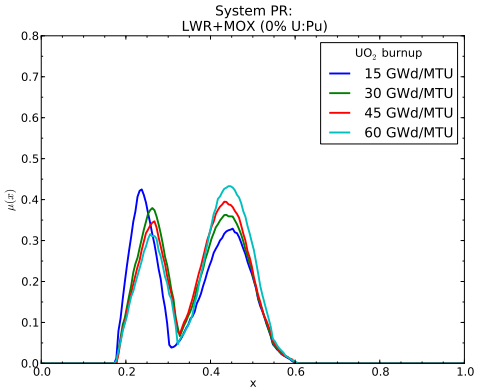

(a): PUREX (Pu only)

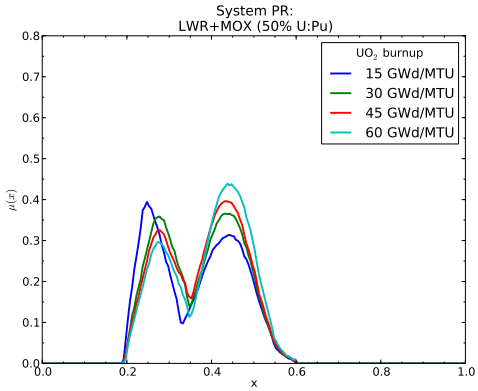

(b): COEX (Pu + 50% U)

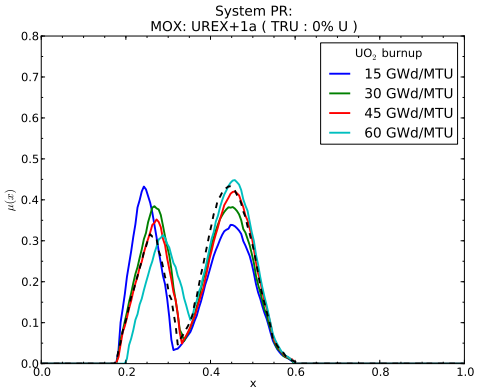

(c): UREX+1a (TRU)

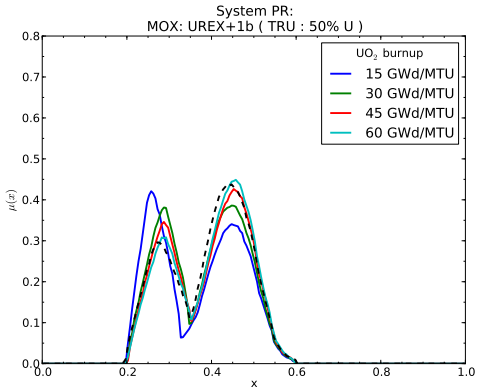

(d): UREX+1b (TRU + 50% U)

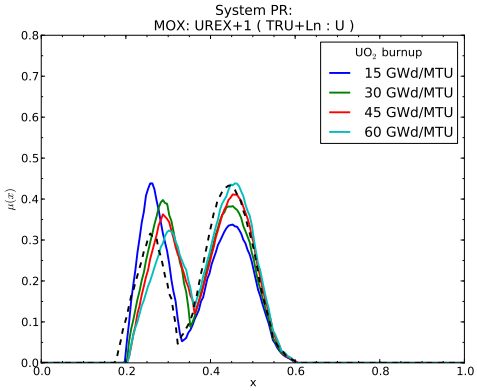

(e): UREX+1 (TRU+Ln)

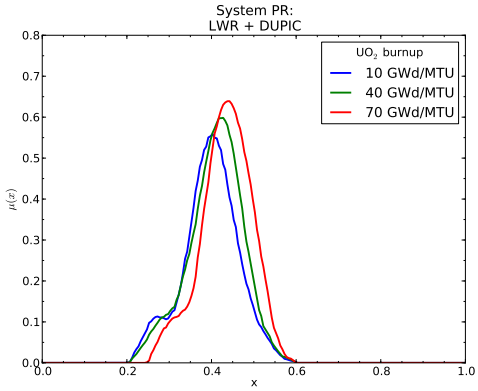

(f): DUPIC

Figure 5.1: System PR comparison for the plutonium-only target pathway for selected "modified open" cycles, assuming an unsophisticated state, covert (yield-insensitive). Higher abscissa values indicate higher intrinsic PR.

Table 5.1: Summary of system centroid PR and rank values for "modified open" cycle strategies, assuming a plutonium-only target pathway. Burnup held fixed at 60 $\frac{\text{GWd}}{\text{MTU}}$ / 60 $\frac{\text{GWd}}{\text{MTHM}}$ for MOX cycles and 60 $\frac{\text{GWd}}{\text{MTU}}$ / 10 $\frac{\text{GWd}}{\text{MTHM}}$ for DUPIC.

System	Product(s)	Centroid	Rank
PUREX	Pu	0.3859	L+
UREX+1a	TRU	0.3959	L+
UREX+1	TRU + Ln	0.3974	M–
COEX	Pu + U (50%)	0.3916	L+
UREX+1b	TRU + U (50%)	0.3960	L+
DUPIC	—	0.4231	M+

showing only a small change due to the target pathway.

The relative system PR centroid values and rankings for each of these MOC systems is presented as Table 5.1. In this scenario, it is clear that while actinide co-extraction provides a nominal benefit over plutonium-only separation (PUREX) for the MOX-based cycles, the gain from co-extraction is quite small under this set of assumptions, with no significant gains over the simple coextraction of uranium and plutonium (COEX) achieved by other processes.

The overall system PR for the plutonium-only pathway is evaluated as a function of the uranium co-extraction ratio as Figure 5.2.

For the plutonium-only pathway, one observes that the uranium dilution factor has a much weaker (although still nominally observable) effect upon system PR, due to the increase in other barriers such as the mass & bulk required for a successful diversion attempt. Nonetheless, the intrinsic benefit introduced by uranium coextraction largely disappears (as intuition would expect) if subsequent reprocessing of diverted material is performed, consistent with the findings involving the coextraciton of other actinides (Figure 5.1 and Table 5.1).

Closed cycles

Figure 5.3 shows the overall system PR comparison for the fast reactor-based closed cycles as a function of uranium fuel burnup. Several features are apparent in the plutonium-only pathway for the closed cycle. First, given the more extended burnup range, changes in the system PR due to plutonium vector changes appear to be more prominent; likewise, these changes have an impact on the post-FR irradiation stages as before. However, the plutonium-

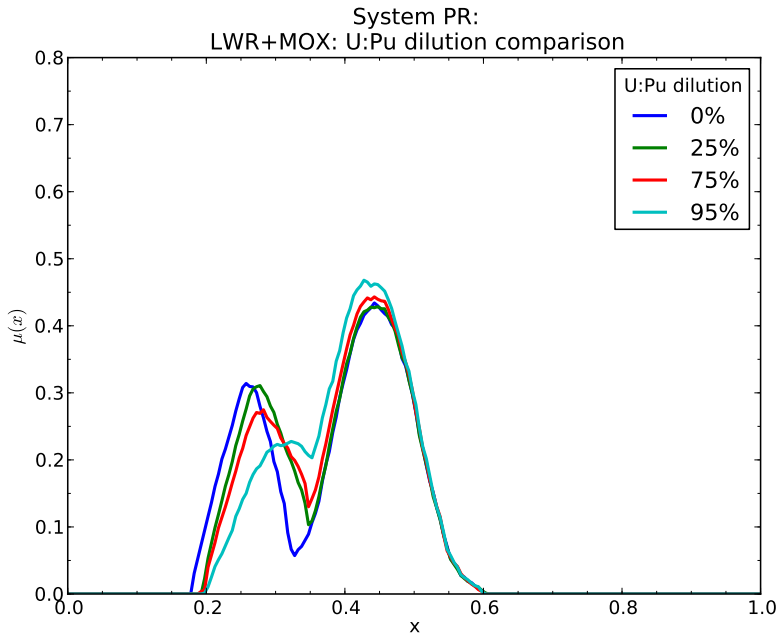

Figure 5.2: System PR comparison for the plutonium-only target pathway MOX cycles as a function of uranium dilution ratio during plutonium extraction, assuming an unsophisticated state, covert (yield-insensitive). Higher abscissa values indicate higher intrinsic PR.

Table 5.2: Summary of system centroid PR and rank values for closed cycle strategies for selected UO_2 fuel burnups (FR fuel burnup held constant at 90 $\frac{GWd}{MTHM}$), assuming a plutonium-only target pathway.

System	Burnup ($\frac{GWd}{MTU}$)	Centroid	Rank
LWR + FR: UREX+1a	10	0.3652	L+
	40	0.3919	L+
	70	0.4041	M–
LWR + FR: Pyro	10	0.3712	L+
	40	0.3977	M–
	70	0.4044	M–

only pathway also appears to introduce the "bifurcation" once more in system PR, where the lower PR peak is roughly equivalent to those found in the conventional "modified open" cycle strategies. In as much, it would appear that some of the PR gains inherent to a closed cycle, particularly one employing advanced separation techniques such as pyroprocessing, are eroded if the assumption of subsequent reprocessing of diverted materials to acquire pure plutonium is made.

Table 5.2 gives a breakdown of the system PR centroid and rank for the closed cycles at selected uranium fuel burnups.

5.2.2 TRU target pathway

Similar to the plutonium-only pathway, the TRU pathway assumes an adversary for which material is diverted and subsequently reprocessed for all transuranic species. The isotopic barrier is evaluated based on the attractiveness of all TRU materials in the fuel form, while other barriers are evaluated similarly to the plutonium-only case (e.g., the amount of material required for diversion of 1 SQ of material).

Once-through cycles

Figure 5.4 compares the two once-through cycles (LWR and CANDU) as a function of uranium fuel burnup for a TRU-based adversary target in each stage.

For the TRU pathway, a small increase in system PR is observed for the once-through cycles over the nominal "plutonium-only" recovery scenario. This occurs despite the increase

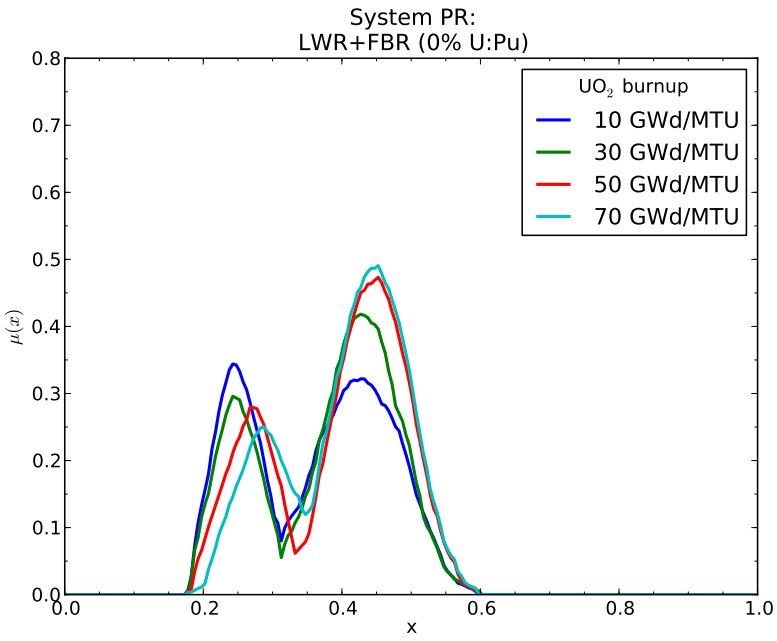

(a): LWR + FR (UREX+1a)

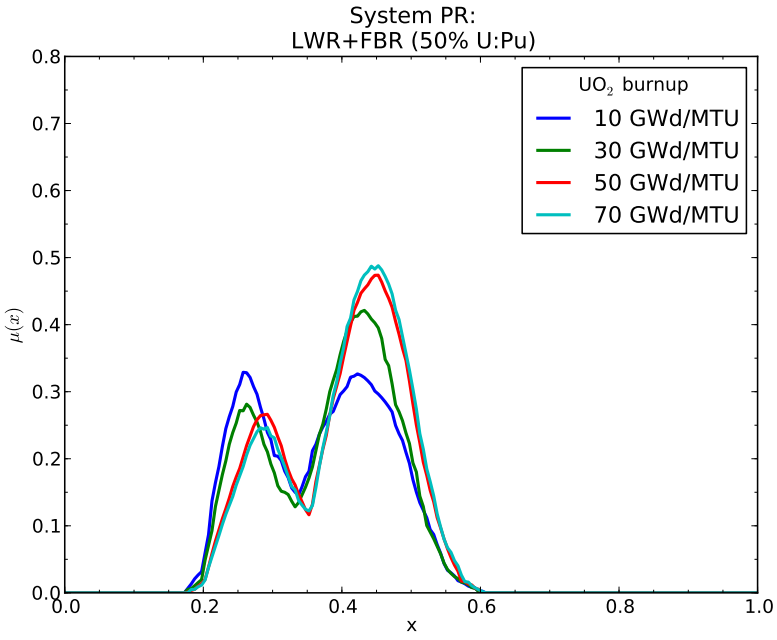

(b): LWR + FR (Pyro)

Figure 5.3: System PR comparison for the plutonium-only target pathway for closed cycles (unsophisticated state, covert; yield-insensitive). Higher abscissa values indicate higher intrinsic PR.

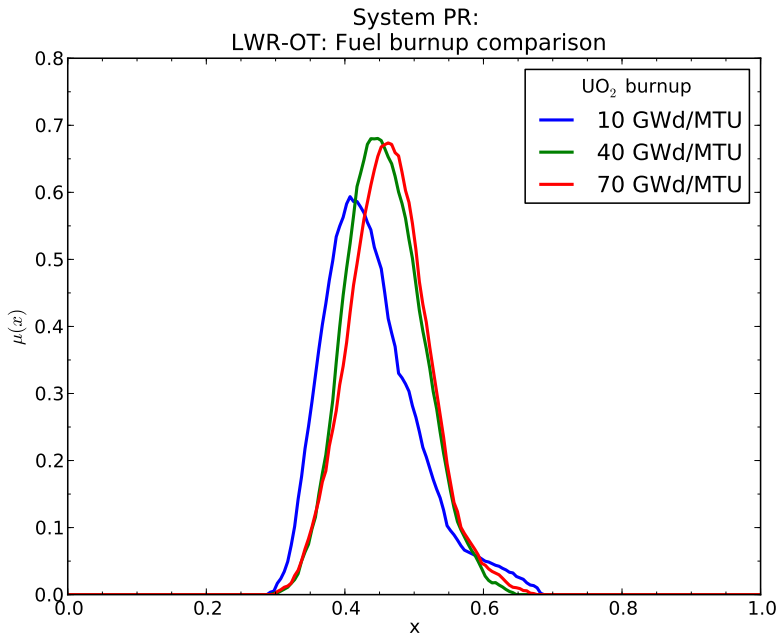

(a): LWR-OT

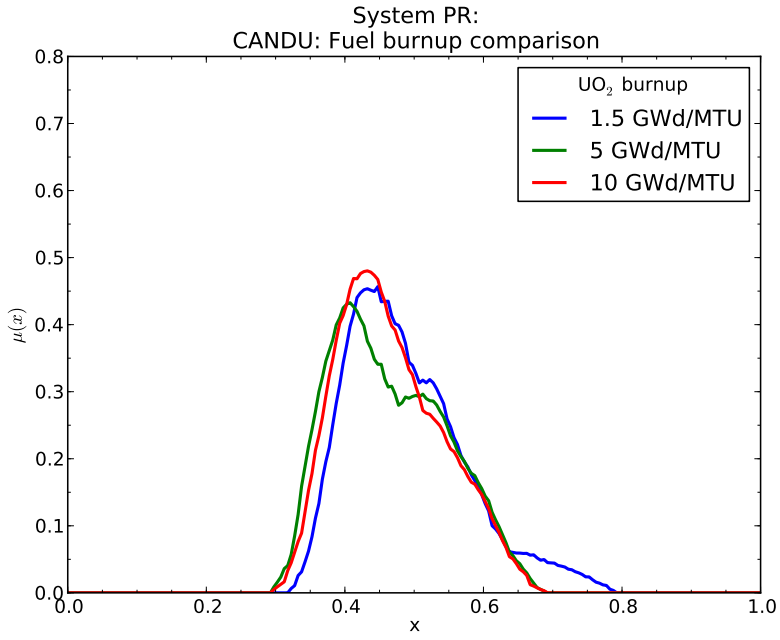

(b): CANDU

Figure 5.4: Comparative system PR as a function of UO_2 fuel burnup for the TRU diversion target pathway for once-through systems, assuming an unsophisticated state, covert (yield-insensitive). Higher abscissa values indicate higher intrinsic PR.

Table 5.3: Summary of system centroid PR and rank values for open cycles (LWR-OT and CANDU) for selected UO_2 fuel burnups, assuming a TRU-based diversion target pathway.

System	Burnup ($\frac{GWd}{MTU}$)	Centroid	Rank
LWR-OT	10	0.4389	M
	40	0.4577	M+
	70	0.4639	M+
CANDU HWR	1.5	0.4892	M+
	5	0.4649	M
	10	0.4658	M

in overall available material; i.e., the small increase in available mass is outweighed by the decrease in material attractiveness.

The ranking and PR centroid behavior of the once-through systems in the TRU-based diversion pathway scenario are given as Table 5.3.

As observed in the plutonium-based pathway, the intrinsic PR rank of the LWR-OT system increases slowly with burnup, showing the highest PR effectiveness at very high burnups, while the PR of the CANDU cycle slightly declines with increasing burnup (due to the increasing fissile material inventories).

Modified open cycles

Figure 5.5 compares the selected partially closed cycles for a TRU-based diversion target at each stage. The TRU target pathway shows a small overall "shift" toward higher overall PR for each fuel cycle configuration evaluated. This shift appears to be burnup-dependent, with a higher shift observed for higher uranium fuel burnups, given the fact that the higher actinide inventories scale with higher burnups, leading to a higher heat generation rate and subsequently lower material attractiveness.

Two distinct shifts are observed for the partially-closed fuel cycle cases; the first in the "intact" peak (i.e., due to decreased attractiveness of spent UO_2 and MOX fuel), and the second in the reprocessing-related peak (including MOX fuel fabrication). As is expected, the reprocessing peak changes little for the PUREX case (i.e., given that no other actinides from plutonium are present), while this peak does show a burnup response for advanced UREX series (where other actinides are part of the reprocessing stream). Following on this,

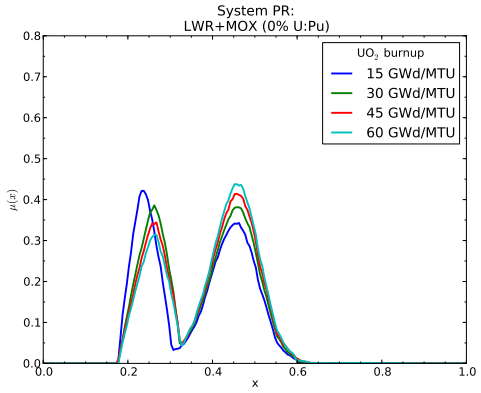

(a): PUREX (Pu only)

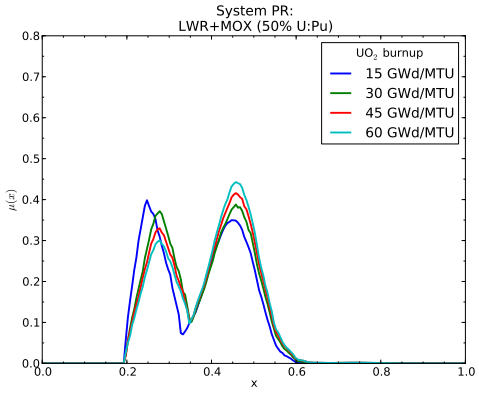

(b): COEX (Pu + 50% U)

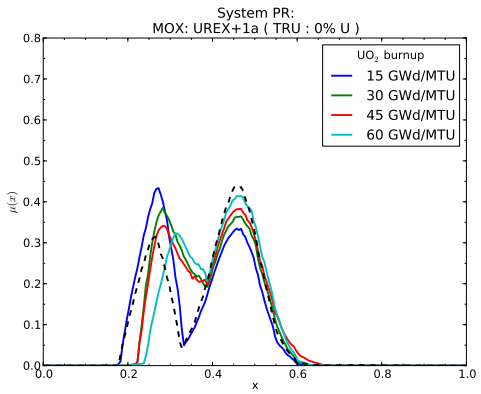

(c): UREX+1a (TRU)

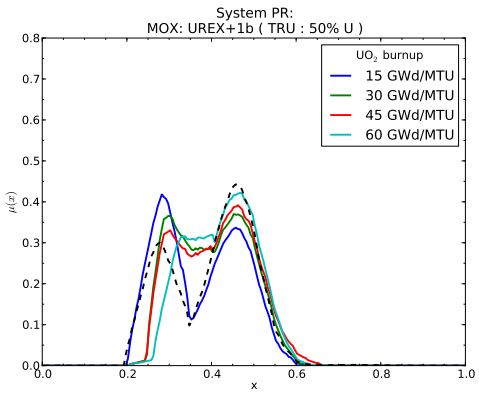

(d): UREX+1b (TRU + 50% U)

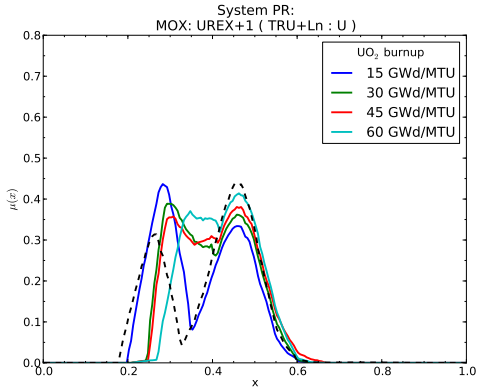

(e): UREX+1 (TRU+Ln)

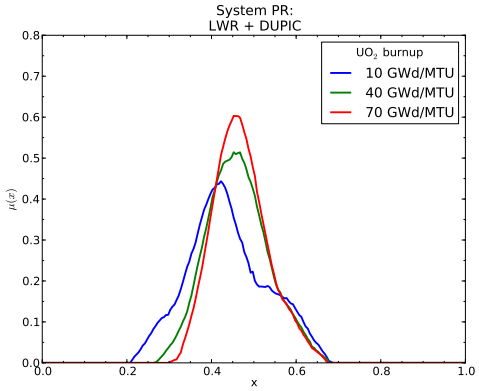

(f): DUPIC

Figure 5.5: Comparative system PR as a function of UO_2 fuel burnup for the TRU diversion target pathway for partially-closed systems, assuming an unsophisticated state, covert (yield-insensitive). Higher abscissa values indicate higher intrinsic PR.

Table 5.4: Summary of system centroid PR and rank values for "modified open" cycle strategies, assuming a TRU target pathway. Burnup held fixed at 60 $\frac{\text{GWd}}{\text{MTU}}$ / 60 $\frac{\text{GWd}}{\text{MTHM}}$ for MOX cycles and 60 $\frac{\text{GWd}}{\text{MTU}}$ / 10 $\frac{\text{GWd}}{\text{MTHM}}$ for DUPIC.

System	Product(s)	Centroid	Rank
PUREX	Pu	0.3944	L+
UREX+1a	TRU	0.4164	M–
UREX+1	TRU + Ln	0.4242	M–
COEX	Pu + U (50%)	0.3999	L+
UREX+1b	TRU + U (50%)	0.4237	M–
DUPIC	—	0.4648	M+

one observes a restored sensitivity to the coextraction of minor actinides in the UREX-based cases, as well as a nominal burnup sensitivity (i.e., as the minor actinide inventories scale with burnup).

The comparative rankings and system centroid PR values for fixed burnup for the modified open cycle cases under the TRU target pathway are given as Table 5.4.

One notable artifact observed in the TRU pathway case, particularly in the rank and centroid behavior (Table 5.4), is in the comparative impact of minor actinide coextraction versus uranium coextraction. While a PR sensitivity for co-extraction of minor actinides appears (i.e., due to minor actinides being included in the final target pathway), the sensitivity to uranium coextraction is again quite small, insufficient to produce a significant change over the baseline PUREX scenario.

Additionally, with the assumption of a TRU target pathway, the DUPIC fuel cycle once again shows a similar proliferation resistance as the LWR once-through cycle.

Closed cycles

Figure 5.6 gives a comparison of the TRU target pathway for the closed cycles, assuming an actinide recovery strategy of UREX+1a and pyroprocessing.

For the TRU-based pathway, a clear burnup dependence appears in the closed cycles, with the overall system PR increasing as a function of uranium fuel burnup. Likewise, for this particular pathway, there appears to be little difference between the UREX+1a and pyroprocessing scenarios; i.e., these scenarios appear to show parallel PR values as a function of burnup. This is evident in Table 5.5, in which a listing of the system PR ranking and

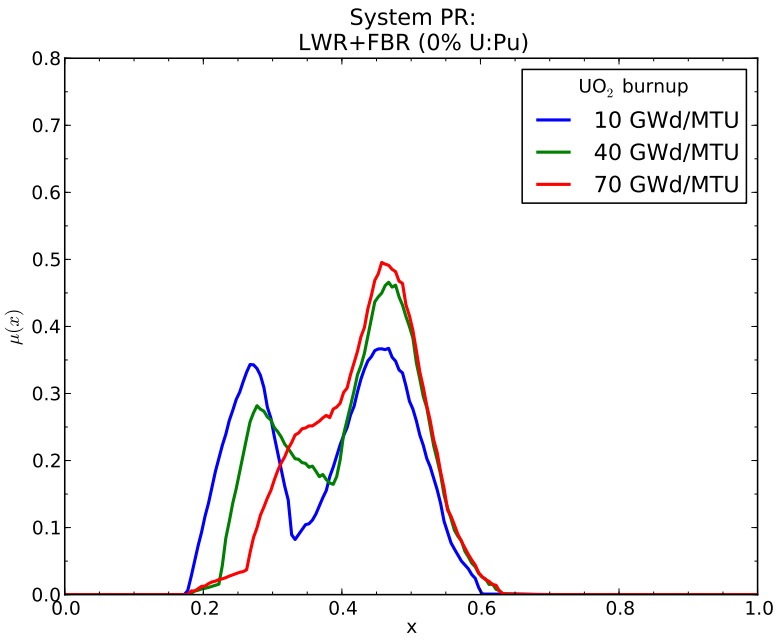

(a): LWR + FR (UREX+1a)

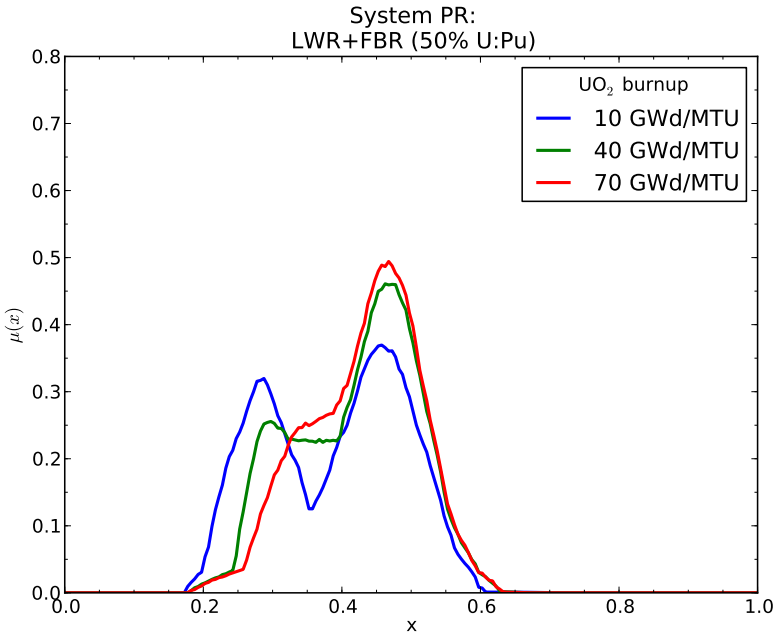

(b): LWR + FR (Pyro)

Figure 5.6: System PR comparison for the TRU target pathway for closed cycles, assuming an unsophisticated state, covert (yield-insensitive). Higher abscissa values indicate higher intrinsic PR.

Table 5.5: Summary of system centroid PR and rank values for closed cycle strategies for selected UO_2 fuel burnups (FR fuel burnup held constant at 90 $\frac{GWd}{MTHM}$), assuming a TRU diversion target pathway.

System	Burnup ($\frac{GWd}{MTU}$)	Centroid	Rank
LWR + FR: UREX+1a	10	0.3811	L+
	40	0.4203	L+
	70	0.4370	M–
LWR + FR: Pyro	10	0.3882	L+
	40	0.4265	M–
	70	0.4370	M–

centroid values is given.

As one observes from Table 5.4, the differences between the UREX+1a and pyroprocessing fuel cycles is quite small for the TRU diversion pathway, with the pyroprocessing-based cycle showing a slight advantage in intrinsic system PR over the UREX+1a case; this difference disappears at very high burnups (e.g., 70 $\frac{GWd}{MTU}$).

5.2.3 Minor actinides-only pathway

A final target scenario considered is the diversion of minor actinides only (e.g., no plutonium). While somewhat unorthodox, it is a useful illustration particularly for "modified open" cycles, given the presence of actinide waste streams which frequently contain minor actinides (and little plutonium). In general, one observes that the system PR for the minor actinide target case is a reversal over the plutonium and TRU-based pathways; i.e., the minor actinides (absent plutonium) do not represent an attractive proliferation target overall, showing a lower overall attractiveness than fresh uranium fuel. What this appears to demonstrate is that a minor actinide diversion scenario does not appear to be a main pathway of interest compared to the Pu/TRU target pathways. This is fully explored in the following subsections.

Open cycles

Figure 5.7 compares the two once-through cycles (LWR and CANDU) with the two partially closed cycles (PUREX and UREX+1) for a TRU-based adversary target in each stage.

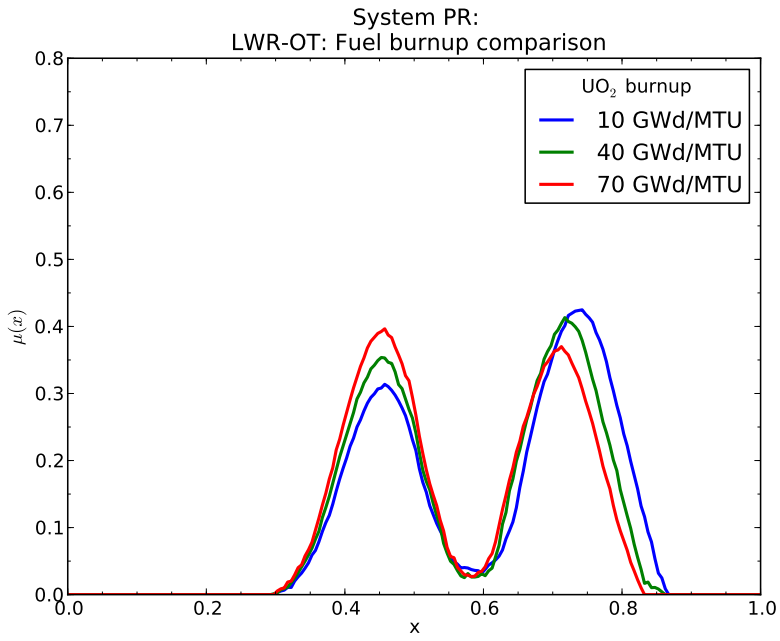

(a): LWR-OT

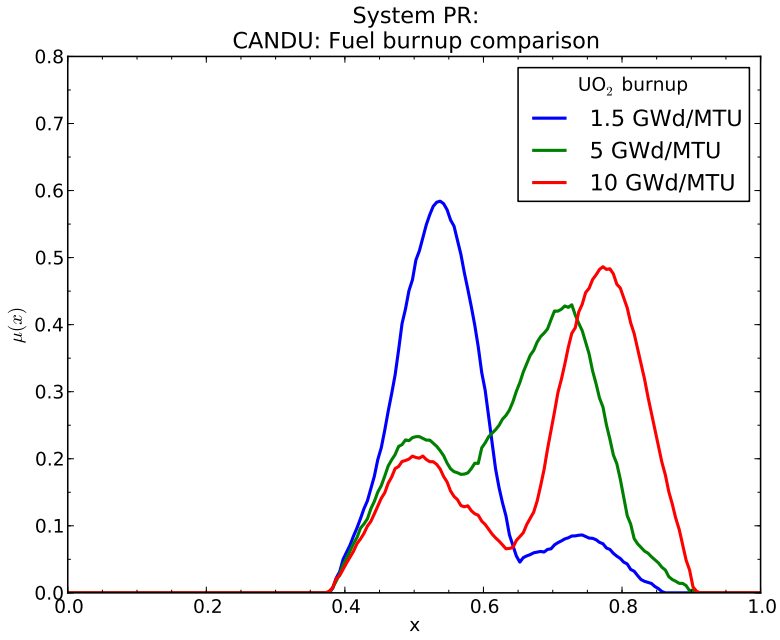

(b): CANDU

Figure 5.7: Comparative system PR as a function of UO_2 fuel burnup for the minor actinides-only diversion target pathway for once-through systems, assuming an unsophisticated state, covert (yield-insensitive). Higher abscissa values indicate higher intrinsic PR.

Table 5.6: Summary of system centroid PR and rank values for open cycles (LWR-OT and CANDU) for selected UO_2 fuel burnups, assuming a minor actinide-based diversion target pathway.

System	Burnup ($\frac{GWd}{MTU}$)	Centroid	Rank
LWR-OT	10	0.6209	M+
	40	0.5942	M+
	70	0.5730	M+
CANDU HWR	1.5	0.5562	H–
	5	0.6421	H–
	10	0.6925	H – VH–

For the LWR once-through case, two distinct peaks appear: the first being of the pre-reactor stages (i.e., given that no minor actinides exist, the only plausible pathway is fresh uranium diversion and re-enrichment), and the second being from minor actinide inventories present in post-irradiation stages. The system PR for post-irradiation stages decreases slightly, given that the minor actinide inventories build up with burnup, however the intrinsic attractiveness of these materials is substantially lower than that of plutonium-bearing mixtures (e.g., plutonium and TRU).

For the CANDU case, the system PR increases with burnup; this would appear to be due to the buildup of higher actinide species (such as curium) not present at extremely low burnups, thus increasing the heat generation rate of the material and subsequently decreasing its intrinsic attractiveness. The increase in the isotopic barrier appears to substantially outweigh the increase in available mass (and thus decreasing barrier effectiveness), thus resulting in a higher overall system PR. Again in this case the system PR for the minor actinides-based pathway appears to be substantially higher in all cases than for plutonium-based pathways.

An analysis of the system PR centroid values and corresponding system rankings for the once-through cycles in a minor actinides diversion scenario is given as Table 5.6.

Modified open cycles

Figure 5.8 gives a comparison of the partially closed fuel cycles for a target of minor actinides only (i.e., no plutonium).

The resulting system PR function shapes appear to fall into three categories: plutonium-based streams (e.g., PUREX & COEX), TRU-based streams (UREX series), and the DUPIC

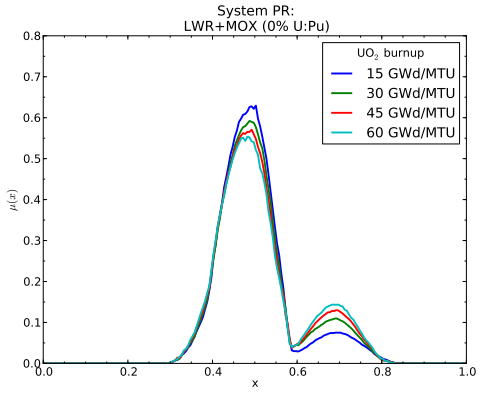

(a): PUREX (Pu only)

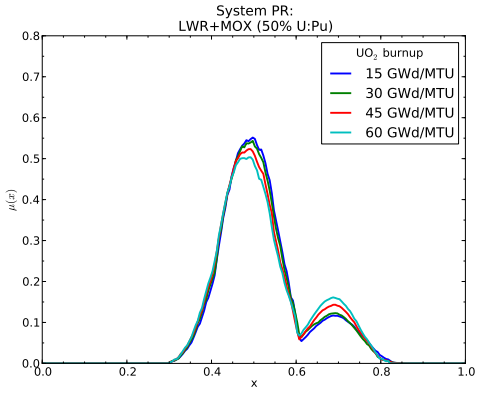

(b): COEX (Pu + 50% U)

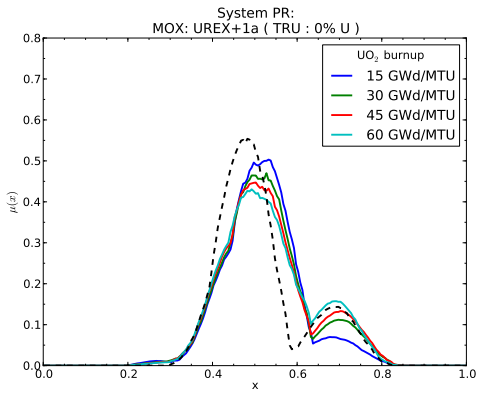

(c): UREX+1a (TRU)

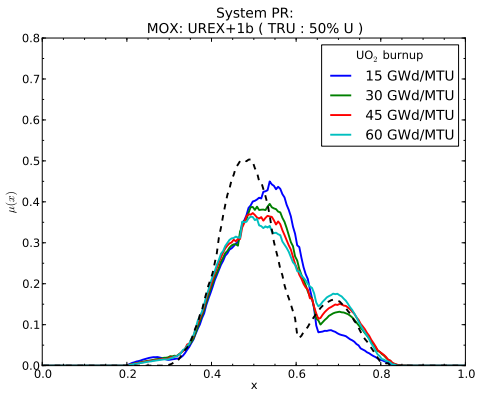

(d): UREX+1b (TRU + 50% U)

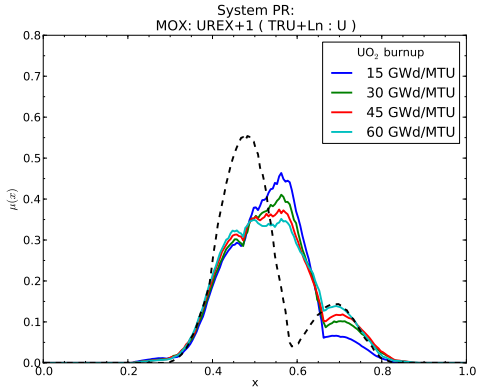

(e): UREX+1 (TRU+Ln)

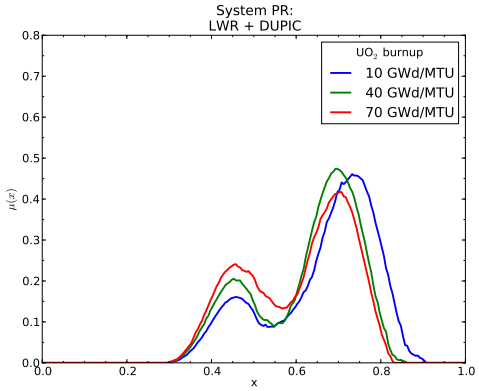

(f): DUPIC

Figure 5.8: Comparative system PR as a function of UO_2 fuel burnup for the minor actinides-only diversion target pathway for partially-closed systems, assuming an unsophisticated state, covert (yield-insensitive). Higher abscissa values indicate higher intrinsic PR.

Table 5.7: Summary of system centroid PR and rank values for "modified open" cycle strategies, assuming a minor actinides-based target pathway. Burnup held fixed at 60 $\frac{\text{GWd}}{\text{MTU}}$ / 60 $\frac{\text{GWd}}{\text{MTHM}}$ for MOX cycles and 60 $\frac{\text{GWd}}{\text{MTU}}$ / 10 $\frac{\text{GWd}}{\text{MTHM}}$ for DUPIC.

System	Product(s)	Centroid	Rank
PUREX	Pu	0.5118	M+
UREX+1a	TRU	0.5324	M+
UREX+1	TRU + Ln	0.5392	M+
COEX	Pu + U (50%)	0.5156	M+
UREX+1b	TRU + U (50%)	0.5402	M+
DUPIC	—	0.6096	M+

cycle, with the respective centroid values increasing respectively among these categories. Each of these cycles again shows a substantially higher intrinsic PR than the corresponding plutonium or transuranic-based pathways. Each system appears to only show a very weak relationship between system PR and burnup for this case as well, particularly for MOX cycles; i.e., the minor actinide inventory does not appear to change enough to produce significant changes in the system PR for these cycles.

Further, no obvious low-PR peak appears (which would indicate a uniquely vulnerable stage for the minor actinide pathway); i.e., each fuel cycle and burnup combination evaluated appears to show uniformly higher PR for the minor actinide pathway than the plutonium-bearing counterparts.

A breakdown of the ranking and system PR centroid behavior for the partially closed cycles is given as Table 5.7.

Closed cycles

Figure 5.8 gives a comparison of the fully closed fuel cycles for a target of minor actinides only, for a UREX+1a and pyroprocessing-based actinide recovery strategy.

Again one observes that the minor actinide pathway shows substantially higher PR for the closed cycles than the plutonium-bearing pathways. A weak dependence on UO_2 fuel burnup appears, showing the most substantial (although limited) effect at very high burnups. Overall, the minor actinide pathway does not appear to represent a viable attack pathway for closed cycles compared to the more attractive plutonium-based routes; this is evident in the overall system PR values and rankings given as Table 5.5. However, while the minor

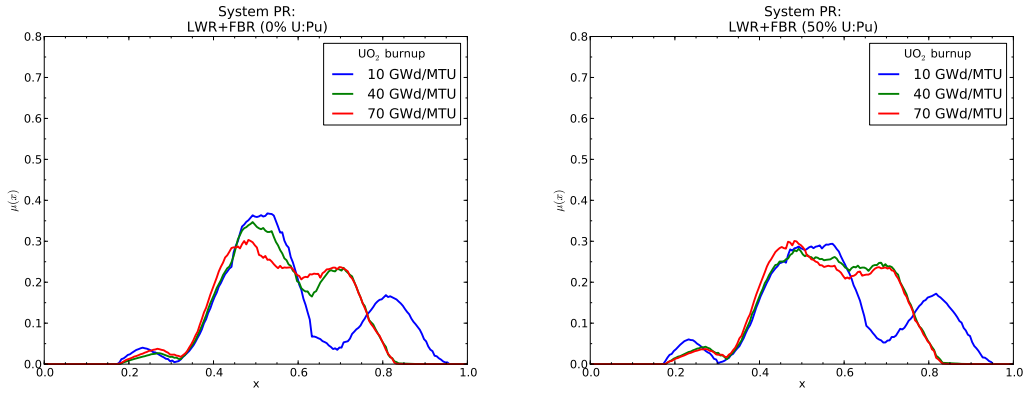

(a): LWR + FR (UREX+1a) (b): LWR + FR (Pyro)

Figure 5.9: System PR comparison for the minor actinides-only target pathway for closed cycles, assuming an unsophisticated state, covert (yield-insensitive). Higher abscissa values indicate higher intrinsic PR.

Table 5.8: Summary of system centroid PR and rank values for closed cycle strategies for selected UO_2 fuel burnups (FR fuel burnup held constant at 90 $\frac{\text{GWd}}{\text{MTHM}}$), assuming a minor actinides-based diversion target pathway.

System	Burnup ($\frac{\text{GWd}}{\text{MTU}}$)	Centroid	Rank
LWR + FR: UREX+1a	10	0.5659	M+
	70	0.5616	M+
LWR + FR: Pyro	10	0.5692	M+
	70	0.5618	M+

actinide-based pathway does show substantially elevated intrinsic PR, this evaluation of non-viability should in no way be taken to indicate that such a pathway is "proliferation proof," (it is clearly not), but simply that other pathways represent a more attractive diversion route.

5.2.4 Summary of results by target pathway type

An overall summary of rankings for selected systems studied across each of the target pathways along with a comparison of the ranking for the "nominal" evaluation case is given as Table 5.9.

Table 5.9: Summary of system rank values for selected fuel cycle systems as a function of target pathway: "nominal" (e.g., plutonium only for intact fuel and whole stream for separated materials), plutonium (Pu) only, transuranics (TRU) only, and minor actinides (MA) only.

System	Burnup ($\frac{GWd}{MTU}$ / $\frac{GWd}{MTHM}$)	System rank Nominal	Pu only	TRU only	MA only
LWR-OT	40 / —	M+	M+	M	M+
	70 / —	M+	M+	M+	M+
CANDU HWR	10 / —	M+	M+	M	H – VH–
MOX: PUREX	60 / 60	L+	L+	L+	M+
MOX: COEX	60 / 60	M–	L+	L+	M+
MOX: UREX+1a	60 / 60	M–	L+	L+	M+
MOX: UREX+1b	60 / 60	M	L+	M–	M+
MOX: UREX+1	60 / 60	M–	L+	M–	M+
DUPIC	40 / 10	M	M+	M+	H – H+
	70 / 10	M+	M+	M+	M+
FBR: UREX+1a	40 / 90	M–	L+	L+	M+
	70 / 90	M	M–	M	M+
FBR: Pyro	40 / 90	M–	L+	L+	M+
	70 / 90	M	M–	M	M+

Under most cases, the "nominal" target pathway rank evaluation matches closely with that of the plutonium-only and TRU-only pathways.

This same pattern also appears to be true for the closed cycle cases; in this case, it appears to be due to the higher overall available material in a TRU diversion scenario, necessitating lower amounts of material to be diverted over a plutonium-only pathway.

The "minor actinides" only target pathway consistently shows the highest overall system PR, substantially higher than the nominal, Pu-only, or TRU-only pathways. Thus, while the general PR rankings indicate that minor actinide pathways still represent a *possible* proliferation pathway, such pathways are far less attractive than pathways involving the diversion of plutonium, TRU, or even intact reprocessing streams.

5.3 PR assessment by adversary type

Given the fact that substantial differences exist in the capabilities of different host states for nuclear energy facilities, it is apparent that the relative weightings for barriers to proliferation will vary with the capabilities of the adversary state [57]. Such relative contributions to proliferation resistance will also vary given whether the adversary is concerned with factors such as non-detection (e.g., overt vs. covert) and for relatively unsophisticated adversaries, sensitivity to reliable yield (which introduces a sensitivity to the spontaneous fission neutron rate produced by the material). The relative barrier weights for each adversary type are those identified in Table 2.10.

Each of these factors shall be explored for their relative effect upon intrinsic system proliferation resistance in the following sections.

5.3.1 Sophisticated state, overt

In the case of the sophisticated state, it is generally assumed that the host state has a well-developed industrial infrastructure with potentially a full compliment of indigenous fuel cycle facilities and expertise. Thus, particular physical barriers such as the isotopic, chemical, and radiological barriers present a lower overall barrier to such actors, given the latent ability to overcome such factors.

Additionally, for an overt breakout attempt, issues such as detectability also play a diminished role; rather, the main quantities of interest for such a scenario are ultimately the available mass at a given facility, followed secondarily by the isotopic attractiveness and the difficulty and expense in modifying such a facility for a diversion attempt (facility unattractiveness).

The results for this scenario evaluation for each of the three fuel cycle classes (open cycles, modified open cycles, and closed cycles) are presented in the following subsections.

Open cycles

Figure 5.10 gives a comparison as a function of burnup of the system PR for the LWR once-through and CANDU cycles.

For each of these cases in the sophisticated state, overt category, the physical barriers play only a secondary role in the relative barrier weights; therefore the burnup dependence is relatively small. An exception is the case of the CANDU cycle, in which the available material

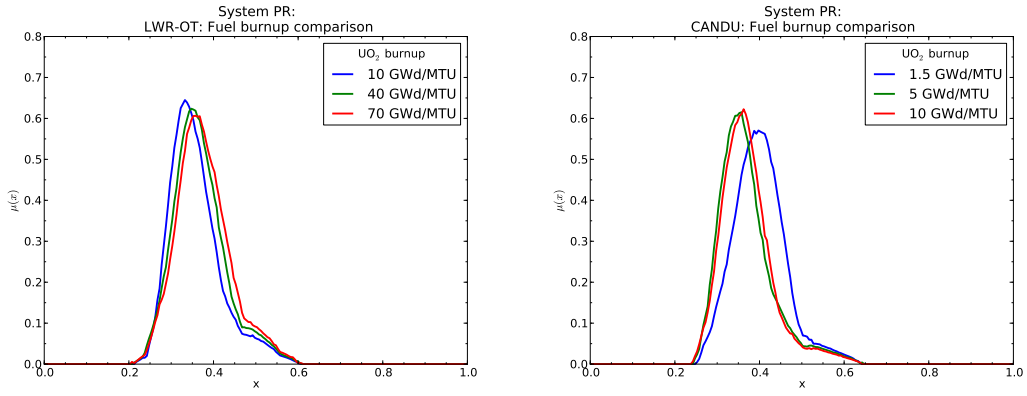

(a): LWR-OT (b): CANDU HWR

Figure 5.10: System PR as a function of fuel burnup for once-through cycles (LWR-OT and CANDU) for a sophisticated state (overt).

Table 5.10: System PR centroid value and ranking for the once-through systems, assuming a sophisticated state (overt).

System	Burnup ($\frac{\text{GWd}}{\text{MTU}}$)	Centroid	Rank
LWR-OT	10	0.3585	M–
	70	0.3771	M–
CANDU	1.5	0.4012	M
	10	0.3719	M–

increases with burnup; given that available mass is of primary importance, an increase in fissile material inventories thus produces a downward shift in system PR with burnup for the CANDU cycle. Outside of this exception, the variance in system PR as a function of burnup for these systems is relatively small.

A comparison of the relative rankings and system centroid PR values of the two systems is given as Table 5.10.

Modified open cycles

Figure 5.11 gives a comparison of the open and partially closed fuel cycles for the assumption of a nation with relatively sophisticated industrial capacity (including well-developed indigenous nuclear fuel cycle capacities), under conditions of an overt breakout attempt.

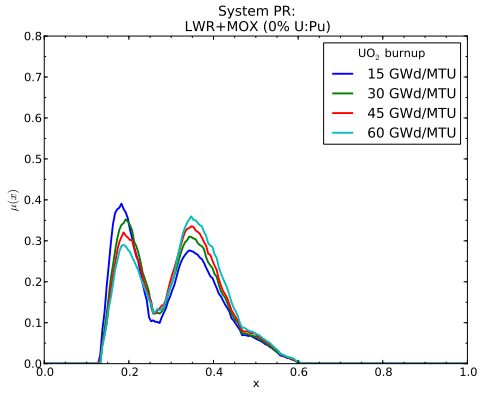

(a): PUREX (Pu only)

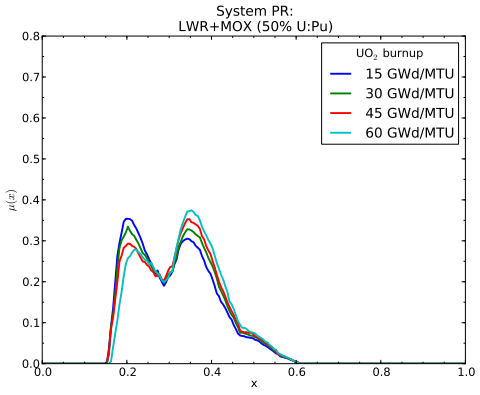

(b): COEX (Pu + 50% U)

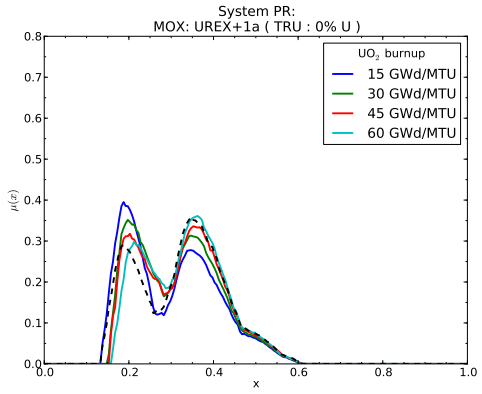

(c): UREX+1a (TRU)

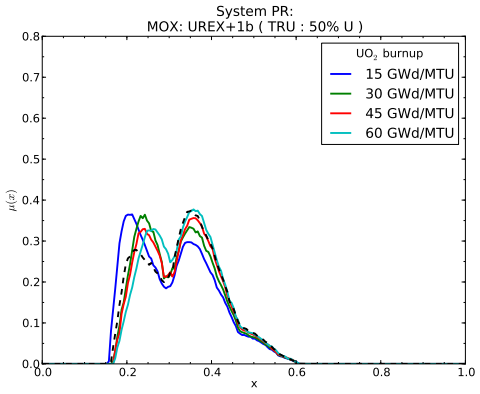

(d): UREX+1b (TRU + 50% U)

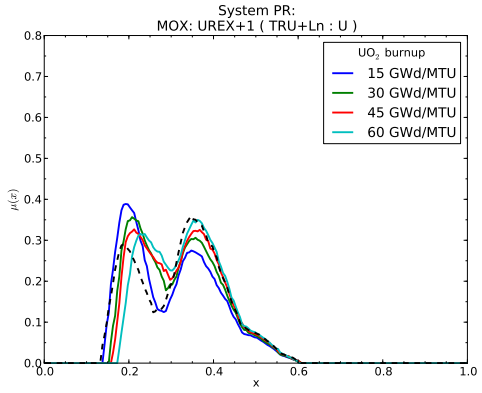

(e): UREX+1 (TRU+Ln)

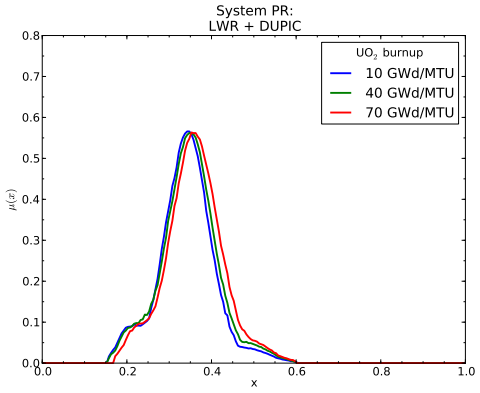

(f): DUPIC

Figure 5.11: System PR as a function of fuel burnup for modified open cycles as a function of uranium fuel burnup for a sophisticated state (overt).

Table 5.11: Summary of system centroid PR and rank values for "modified open" cycle strategies, assuming a sophisticated state (overt) adversary. Burnup held fixed at 60 $\frac{\text{GWd}}{\text{MTU}}$ / 60 $\frac{\text{GWd}}{\text{MTHM}}$ for MOX cycles and 60 $\frac{\text{GWd}}{\text{MTU}}$ / 10 $\frac{\text{GWd}}{\text{MTHM}}$ for DUPIC.

System	Product(s)	Centroid	Rank
PUREX	Pu	0.3234	L
UREX+1a	TRU	0.3330	L
UREX+1	TRU + Ln	0.3381	L+
COEX	Pu + U (50%)	0.3354	L
UREX+1b	TRU + U (50%)	0.3407	L+
DUPIC	—	0.3546	M–

Given the relatively low importance of the isotopic barrier for this case (i.e., assuming the state's ability to overcome limitations with the isotopic material itself in the design of a potential weapon), the system PR shows minimal sensitivity to burnup. Additionally, one observes the relative prominence of the reprocessing-related stages for this case, given the relative ease at which materials can be obtained for diversion within these stages, particularly if non-detection is not a concern. Coextraction of materials (e.g., uranium, minor actinides, etc.) has only a minor impact on overall system PR relative to traditional PUREX-based processes as well, as is evident from the centroid and ranking values presented in Table 5.11.

An evaluation of the system PR as a function of uranium dilution in reprocessing (Figure 5.12) indicates that dilution of the plutonium-bearing stream with uranium has only a small impact on overall system PR, given the secondary importance of physical barriers to the sophisticated state adversary. (i.e., it is assumed that the sophisticated state can easily overcome these barriers through the use of existing industrial and fuel cycle facilities and expertise.) Noticeable changes in the system PR do not appear to manifest until dilution levels of 75% and above, well above the current COEX standard of 50% uranium dilution.

Closed cycles

The evaluation system PR for closed cycles (e.g., a LWR + FR cycle) is evaluated under the UREX+1a and pyroprocessing actinide recovery strategies as a function of uranium fuel burnup assuming a sophisticated state adversary in an overt proliferation attempt is given as Figure 5.13.

Similar to other cycles for the sophisticated state engaged in an overt breakout, burnup

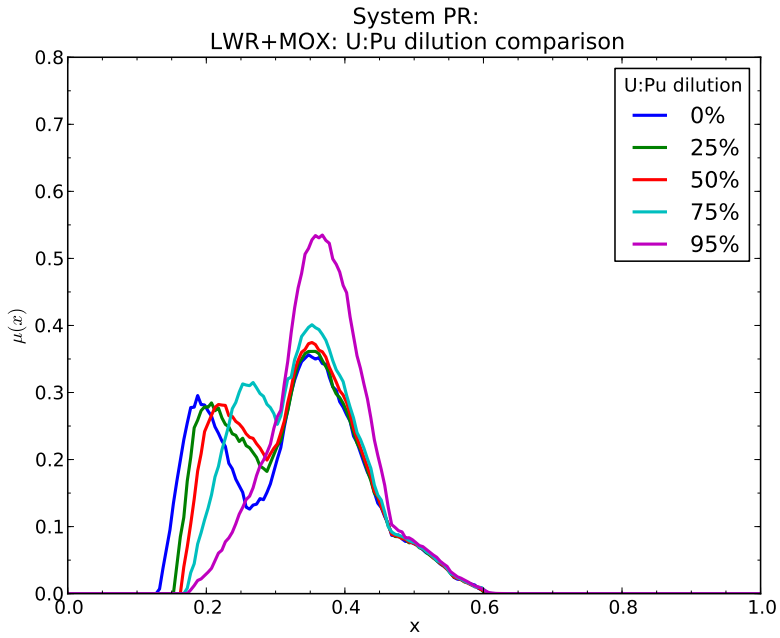

Figure 5.12: System PR as a function of uranium dilution during reprocessing for an unsophisticated state (overt).

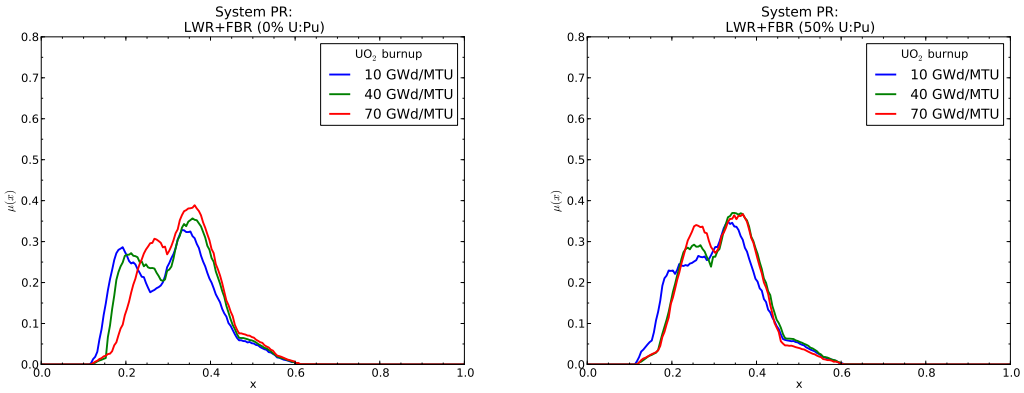

(a): LWR+FR (UREX+1a)

(b): LWR+FR (Pyro)

Figure 5.13: System PR as a function of fuel burnup for LWR + FR cycle, based on UREX+1a and pyroprocessing actinide recovery strategies, for an sophisticated state (covert).

Table 5.12: Summary of system centroid PR and rank values for closed cycle strategies for selected UO_2 fuel burnups (FR fuel burnup held constant at 90 $\frac{GWd}{MTHM}$), assuming a sophisticated state (covert).

System	Burnup ($\frac{GWd}{MTU}$)	Centroid	Rank
LWR + FR: UREX+1a	10	0.3048	L–
	70	0.3420	L+
LWR + FR: Pyro	10	0.3121	L
	70	0.3309	L+

shows a very small impact upon system PR, given the relatively low importance of physical barriers. As a result, the fast reactor cycles, which do not involve the direct isolation of plutonium, show little overall intrinsic PR gain over the modified open cycles which involve plutonium separation through traditional aqueous processes. This is further evident in the system centroid and ranking evaluation for the closed cycles, given as Table 5.12.

As one observes from Table 5.12, comparatively little difference exists between the pyroprocessing-based and aqueous-based UREX+1 cycles for the sophisticated state (overt) scenario, particularly at higher fuel burnups.

5.3.2 Sophisticated state, covert

In the case of a sophisticated state undertaking a covert proliferation attempt, it is again assumed that the host state would have access to a relatively advanced industrial and fuel-cycle related infrastructure. A particular change in emphasis in the covert scenario is upon the diversion detectability within the facility; physical barriers (such as the isotopic, chemical, and radiological barriers) play a diminished role in this case; rather, it is the available mass and facility diversion detectability which are considered to be preeminent in this scenario.

The following sections will once again evaluate the three fuel cycle classes in terms of relative PR using this set of assumptions to guide the barrier weight selection.

Open cycles

Figure 5.14 gives the system PR comparison for the LWR once-through and CANDU cycles as a function of uranium fuel burnup. Given the relative low emphasis on physical barriers, little in the way of burnup-dependence is observed in the system PR; again the exception

Table 5.13: System PR centroid value and ranking for the once-through systems, assuming a sophisticated state (covert).

System	Burnup ($\frac{\text{GWd}}{\text{MTU}}$)	Centroid	Rank
LWR-OT	10	0.4514	M+
	70	0.4627	M+
CANDU	1.5	0.4784	H–
	10	0.4641	M+

is in the case of CANDU, where system PR nominally drops from the 1.5 $\frac{\text{GWd}}{\text{MTU}}$ case to higher burnups, due to the larger available mass, similar to the overt case.

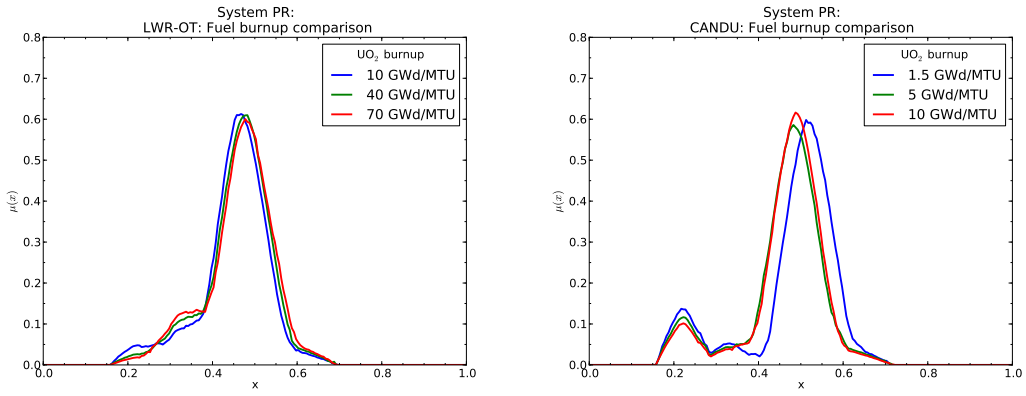

(a): LWR-OT (b): CANDU

Figure 5.14: System PR as a function of fuel burnup for open cycles as a function of uranium fuel burnup for a sophisticated state (covert).

A comparison of the relative rankings and system centroid PR values of the two systems is given as Table 5.13.

Modified open cycles

Figure 5.15 makes a comparison across the four featured fuel cycles for a sophisticated state in a covert diversion attempt. For this case, the isotopic barrier is of greater importance

Table 5.14: Summary of system centroid PR and rank values for "modified open" cycle strategies, assuming a sophisticated state (covert) adversary. Burnup held fixed at 60 $\frac{\text{GWd}}{\text{MTU}}$ / 60 $\frac{\text{GWd}}{\text{MTHM}}$ for MOX cycles and 60 $\frac{\text{GWd}}{\text{MTU}}$ / 10 $\frac{\text{GWd}}{\text{MTHM}}$ for DUPIC.

System	Product(s)	Centroid	Rank
PUREX	Pu	0.4057	L+
UREX+1a	TRU	0.4117	L+
UREX+1	TRU + Ln	0.4143	L+
COEX	Pu + U (50%)	0.4140	L+
UREX+1b	TRU + U (50%)	0.4183	M–
DUPIC	—	0.4474	M+

(although still not predominant), thus again one observes minimal sensitivity to burnup. However, one does observe a nominal sensitivity to the reprocessing product stream (i.e., Pu vs. TRU), given the additional weight placed upon the isotopic and chemical barriers. However, the change from the "overt" breakout case is generally small.

Overall, the intrinsic PR values of the modified open cycle systems for the covert proliferation case of the sophisticated states appear to shift in relatively uniform fashion to higher overall PR, due to the non-detection considerations introduced. This is evident in the rankings and system PR centroid values given for these system as Table 5.14, particularly when compared to the overt case (Table 5.11).

An evaluation of the effect of uranium dilution during reprocessing (Figure 5.16) indicates that dilution effects are relatively limited until such dilution factors are at or over 75%; i.e., the COEX case of 50% dilution shows almost no change over the standard PUREX-based case for the sophisticated state, covert, given the assumed ability to re-separate materials. This is in concert with the findings for the overt breakout attempt by a similar state-level threat.

Closed cycles

An evaluation of the comparative system PR values for closed cycles as a function of uranium fuel burnup for the sophisticated state (covert) adversary is given as Figure 5.17.

Similar to the modified open cycles, the closed cycles show a nominal upward shift in intrinsic system PR in the covert scenario compared to the overt case for the sophisticated state adversary, due to the non-detection aspects introduced. However, burnup remains a relatively small effect, given the low importance of physical barriers for the sophisticated

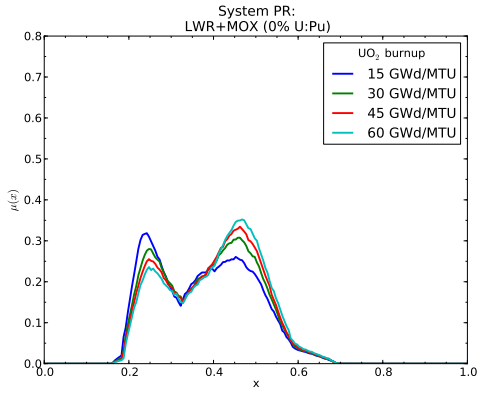

(a): PUREX (Pu only)

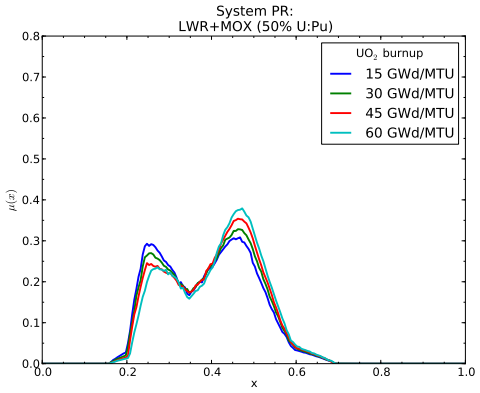

(b): COEX (Pu + 50% U)

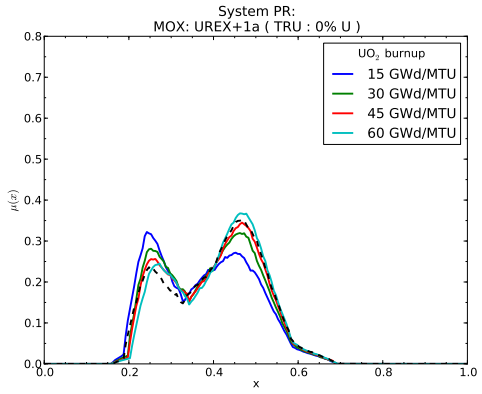

(c): UREX+1a (TRU)

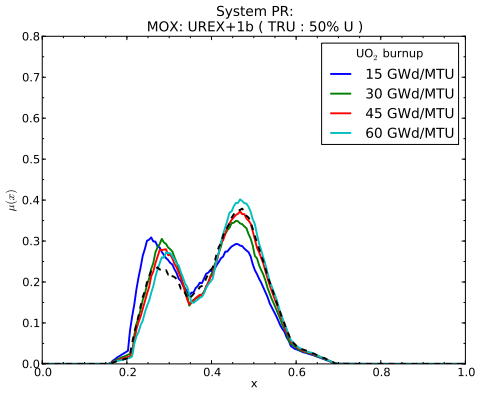

(d): UREX+1b (TRU + 50% U)

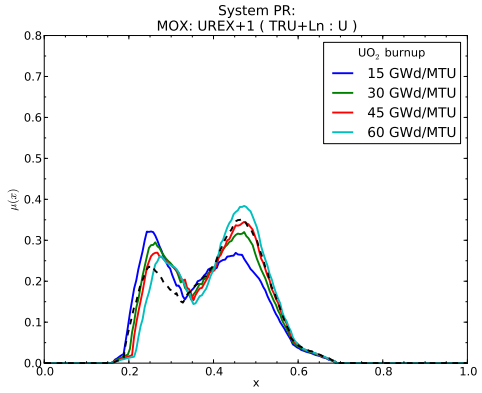

(e): UREX+1 (TRU+Ln)

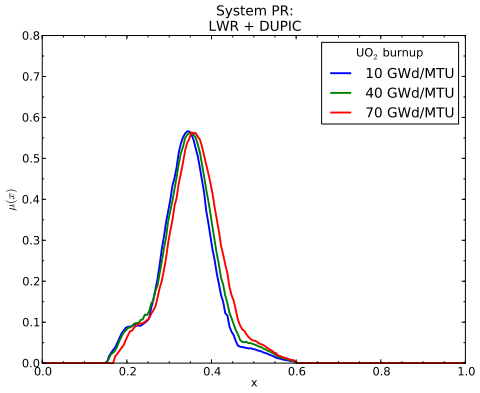

(f): DUPIC

Figure 5.15: System PR as a function of fuel burnup for modified open cycles as a function of uranium fuel burnup for a sophisticated state (covert).

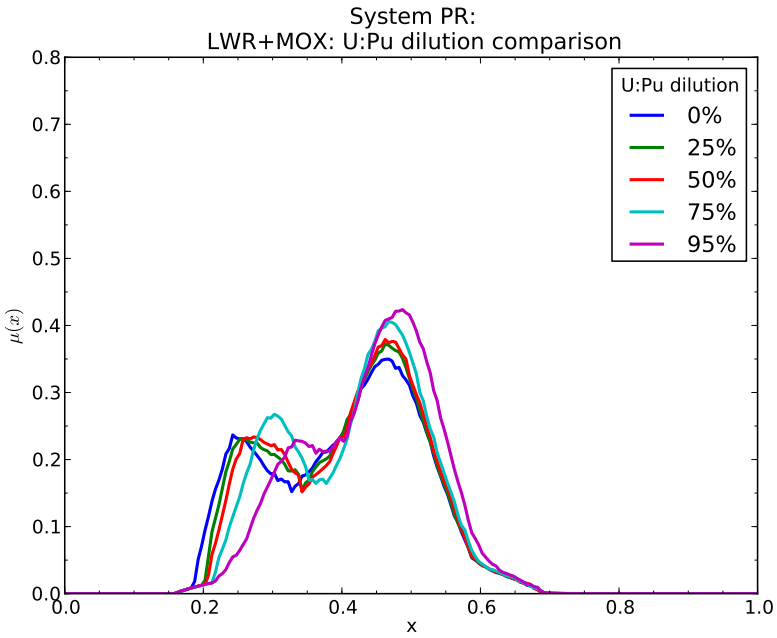

Figure 5.16: System PR as a function of uranium dilution during reprocessing for an unsophisticated state (covert).

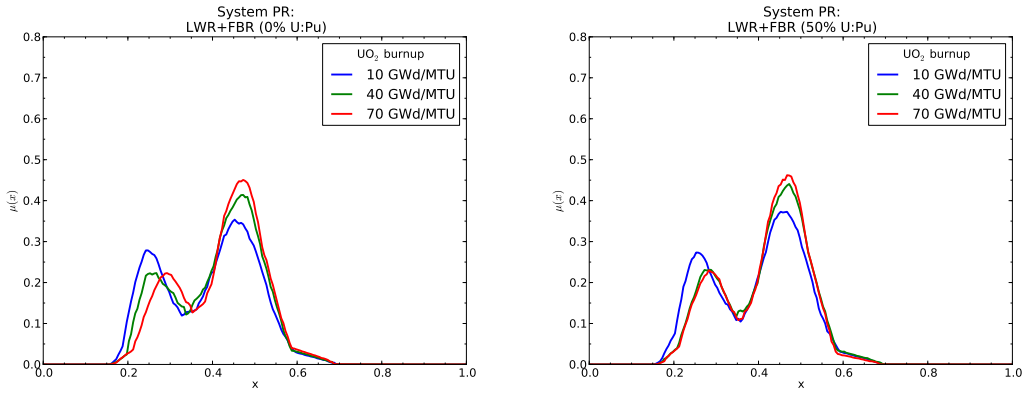

(a): LWR+FR (UREX+1a) (b): LWR+FR (Pyro)

Figure 5.17: System PR as a function of fuel burnup for LWR + FR cycle, based on UREX+1a and pyroprocessing actinide recovery strategies, for an sophisticated state (covert).

Table 5.15: Summary of system centroid PR and rank values for closed cycle strategies for selected UO_2 fuel burnups (FR fuel burnup held constant at 90 $\frac{GWd}{MTHM}$), assuming a sophisticated state (covert).

System	Burnup ($\frac{GWd}{MTU}$)	Centroid	Rank
LWR + FR: UREX+1a	10	0.3899	L+
	70	0.4268	M – M+
LWR + FR: Pyro	10	0.3984	L+
	70	0.4242	M – M+

state adversary. As a result, the effects between the UREX+1a and pyroprocessing actinide recovery strategies on relative system PR remain small (although still present); this again is evident in the system PR centroid and ranking values presented in Table 5.15.

5.3.3 Unsophisticated state, covert

The analysis of the unsophisticated state assumes a still-developing nation, one lacking a well-developed industrial infrastructure or complete indigenous civilian nuclear fuel cycle. As a result, physical barriers play a much more prominent role in the case of a proliferant unsophisticated state, taking a primary role in the proliferation resistance evaluation. Consequently, burnup effects are far more manifest in PR evaluations for such an adversary.

Additionally, two "branch" scenarios are considered for the unsophisticated state: a state unconcerned with reliable weapons yield (yield-insensitive) and one desiring a reliable yield (yield-sensitive). The assumption of yield sensitivity introduces a sensitivity to the SFN rate; i.e., it is assumed that an unsophisticated state would lack the capability to overcome deficiencies in the isotopic character of a target material (thus resulting in a pre-detonation or "fizzle") [6]. Thus, FOM_2 is employed to evaluate material attractiveness for the yield-sensitive adversary, while FOM_1 is used for the yield-insensitive case [6].

Once-through cycles

Figure 5.18 gives a comparison for the case of an unsophisticated state actor (lacking sophisticated indigenous fuel cycle capacities) for a once-through LWR cycle under the conditions of a yield-sensitive (using FOM_2) and a yield-insensitive adversary (using FOM_1); Figure 5.19 makes a similar comparison for a CANDU cycle.

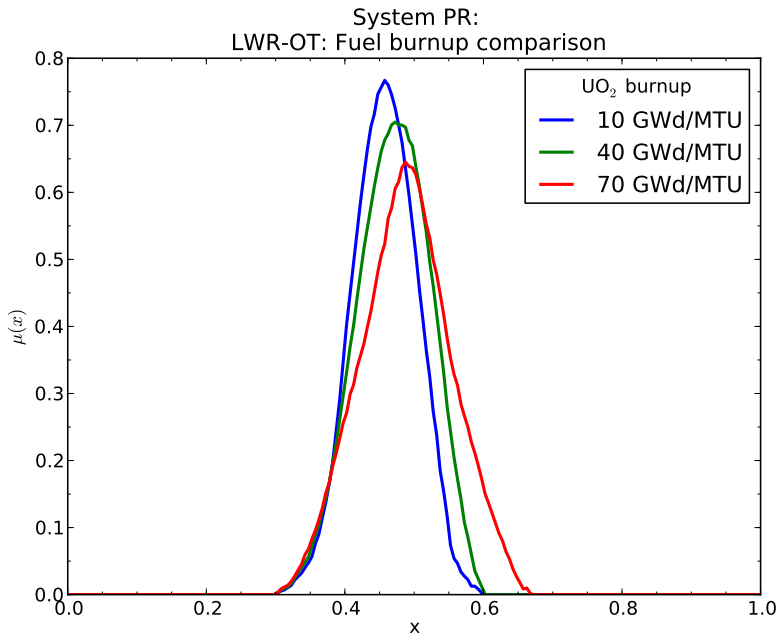

(a): LWR-OT: yield-sensitive (FOM_2)

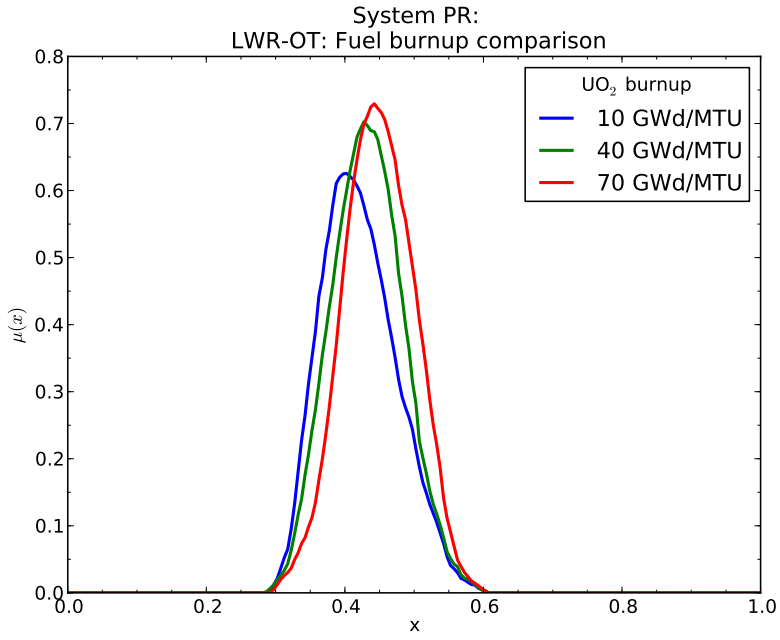

(b): LWR-OT: yield-insensitive (FOM_1)

Figure 5.18: System PR as a function of fuel burnup for once-through LWR cycle, for an unsophisticated state (covert) under a yield-sensitive scenario (FOM_2) and a yield-insensitive scenario (FOM_1).

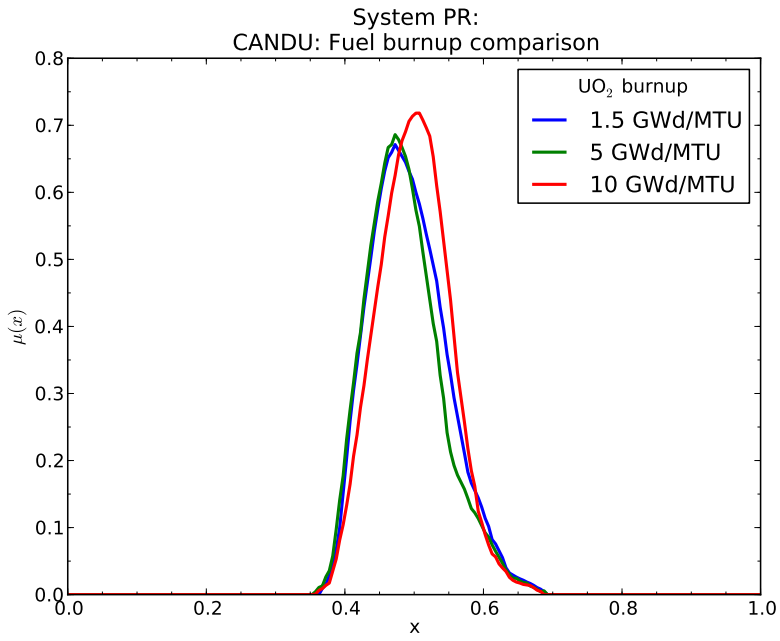

(a): CANDU: yield-sensitive (FOM_2)

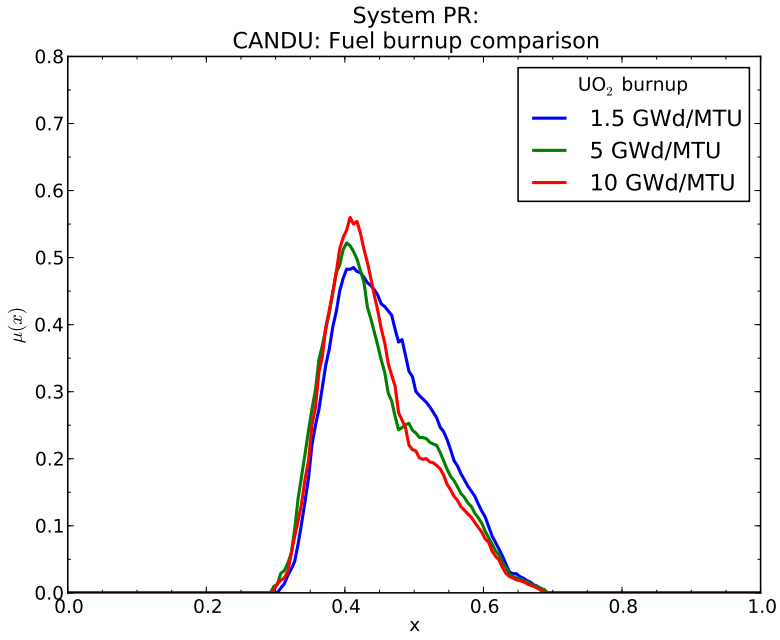

(b): CANDU: yield-insensitive (FOM_1)

Figure 5.19: System PR as a function of fuel burnup for once-through CANDU HWR cycle, for an unsophisticated state (covert) under a yield-sensitive scenario (FOM_2) and a yield-insensitive scenario (FOM_1).

Table 5.16: System PR centroid value and ranking for the once-through systems, assuming an unsophisticated state (covert), for yield-sensitive and yield-insensitive cases.

System	Burnup ($\frac{GWd}{MTU}$)	Yield-sensitive (FOM_2) Centroid	Rank	Yield-insensitive (FOM_1) Centroid	Rank
LWR-OT	10	0.4574	M+	0.4212	M
	40	0.4696	M+	0.4327	M
	70	0.4880	M+	0.4487	M+
CANDU	1.5	0.4928	M+	0.4604	M
	10	0.5001	M+	0.4459	M

The LWR-OT cycle shows a significant burunup effect on PR, particularly for the yield-sensitive case, given the production of higher plutonium species at higher burnup. Likewise, the CANDU cycle shows a marked shift for the yield-sensitive case, given the ingrowth of even-numbered plutonium species with burnup (e.g., dramatically enhancing the spontaneous fission neutron generation rate); in the yield-sensitive case, the CANDU cycle strongly resembles the shape and PR behavior of the LWR cycle, with PR monotonically increasing with burnup.

The comparative evaluation of system centroid PR values and rankings are shown for these systems as Table 5.16.

One observes the effect of the ingrowth of higher plutonium species as a function of burnup for the LWR-OT and CANDU cases both from Figures 5.18 and 5.19 and in the centroid and rank values presented in Table 5.16; i.e., the difference in the relative PR of the yield-sensitive and yield-insensitive cases grows as a function of comparable burnups.

Modified open cycles

A comparison of the relative system PR for the yield-sensitive and yield-insensitive cases of the unsophisticated state (covert) are presented for the aqueous-based PUREX and UREX processes as Figure 5.20; a similar comparison is made for the DUPIC cycle as Figure 5.21. In Figure 5.20, a baseline plutonium extraction case (with a comparable uranium dilution ratio) is indicated as a black, dashed line.

The effect of burnup for the aqueous-based processes (Figure 5.20) is strongest for the yield-sensitive case, particularly with the inclusion of minor actinides (e.g., both as a heat

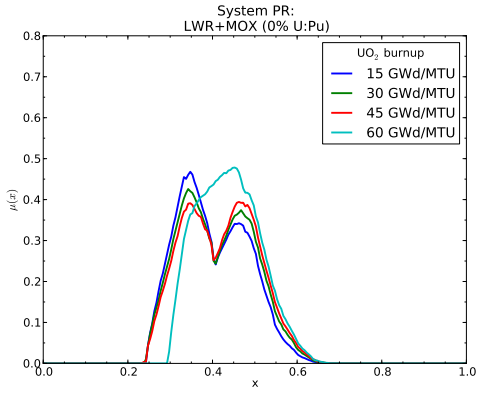

(a): PUREX (Pu only): yield-sensitive (FOM_2)

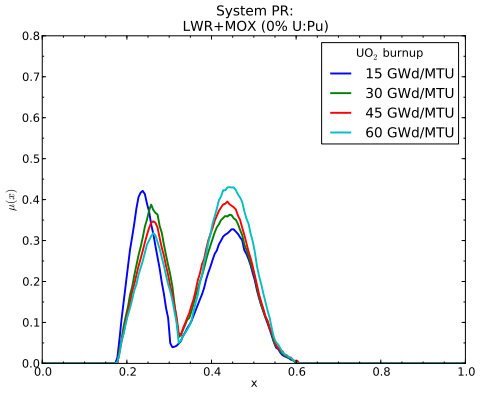

(b): PUREX (Pu only): yield-insensitive (FOM_1)

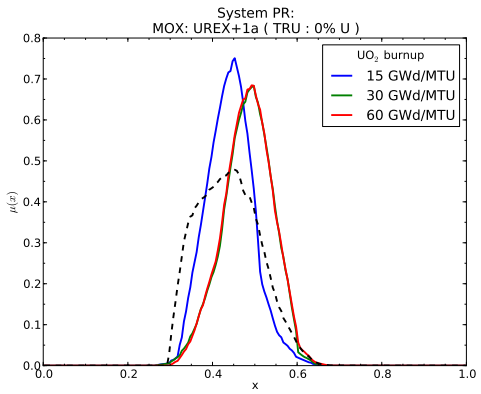

(c): UREX+1a (TRU): yield-sensitive (FOM_2)

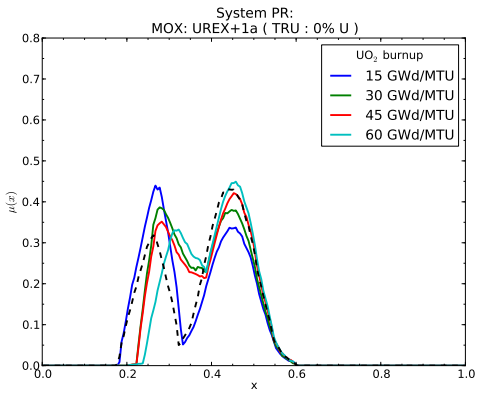

(d): UREX+1a (TRU): yield-insensitive (FOM_1)

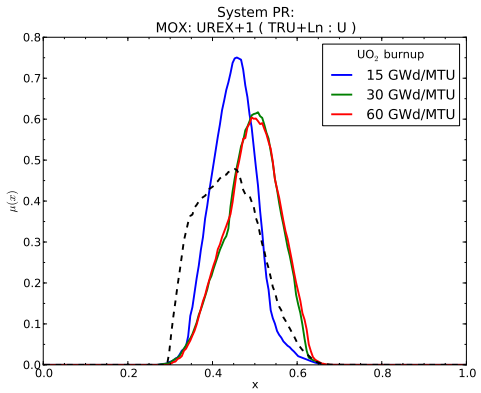

(e): UREX+1 (TRU+Ln): yield-sensitive (FOM_2)

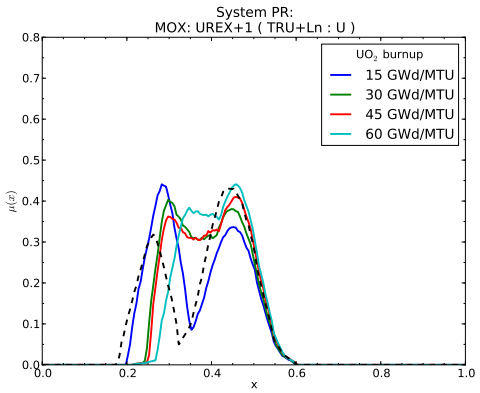

(f): UREX+1 (TRU+Ln): yield-insensitive (FOM_1)

Figure 5.20: System PR as a function of fuel burnup for partially closed cycles, for an unsophisticated state (covert) under (left) a yield-sensitive scenario (FOM_2) and (right) a yield-insensitive scenario (FOM_1).

Table 5.17: Summary of system centroid PR and rank values for "modified open" cycle strategies, assuming an unsophisticated state (covert) adversary, for yield-sensitive and yield-insensitive cases. Burnup held fixed at 60 $\frac{\text{GWd}}{\text{MTU}}$ / 60 $\frac{\text{GWd}}{\text{MTHM}}$ for MOX cycles and 60 $\frac{\text{GWd}}{\text{MTU}}$ / 10 $\frac{\text{GWd}}{\text{MTHM}}$ for DUPIC.

		Yield-sensitive (FOM_2)		Yield-insensitive (FOM_1)	
System	Product(s)	Centroid	Rank	Centroid	Rank
PUREX	Pu	0.4379	M	0.3862	L+
UREX+1a	TRU	0.4834	M+	0.4060	M–
UREX+1	TRU + Ln	0.4937	M+	0.4148	M–
COEX	Pu + U (50%)	0.4538	M	0.4069	M–
UREX+1b	TRU + U (50%)	0.4887	M+	0.4163	M
DUPIC	—	0.4888	M+	0.4231	M+

source and a source of spontaneous fission neutrons). Burnup shows a smaller (but non-trivial) effect for the yield-insensitive adversary; i.e., impact of higher actinide species can change the heat generation rate of material significantly, nominally decreasing the material attractiveness.

For the DUPIC cycle, burnup effects appear to very quickly saturate (Figure 5.21), where the system shows an overall PR effectiveness of "medium-plus" for the yield-sensitive case even at low LWR fuel burnups.

These cases are broken down by system PR centroid values and rankings as Table 5.17.

An evaluation of the effect of uranium coextraction on PR is also evaluated for the yield-sensitive and yield-insensitive cases as Figure 5.22. While the introduction of uranium has only a small impact on the spontaneous fission neutron rate, its inclusion quickly "tips the balance" of material attractiveness (e.g., pushing it lower); the system PR values thus appear to "saturate" at relatively lower uranium dilution fractions for the yield-sensitive adversary, with strong effects becoming manifest at dilution ratios as low as 25%. The effect of uranium dilution is also noticeable at this level for the yield-insensitive state as well, however the full effect of uranium dilution is not achieved for such an adversary until much higher levels of dilution: up to 75% and beyond.

Table 5.18 gives an overall comparison of the system centroid PR values and rankings as a function of uranium dilution for the yield-sensitive and yield-insensitive adversary.

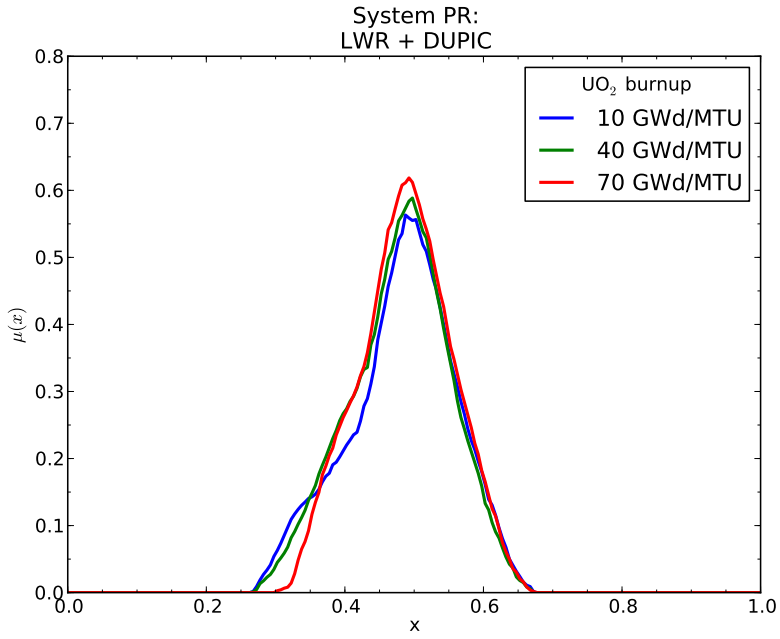

(a): DUPIC: yield-sensitive (FOM_2)

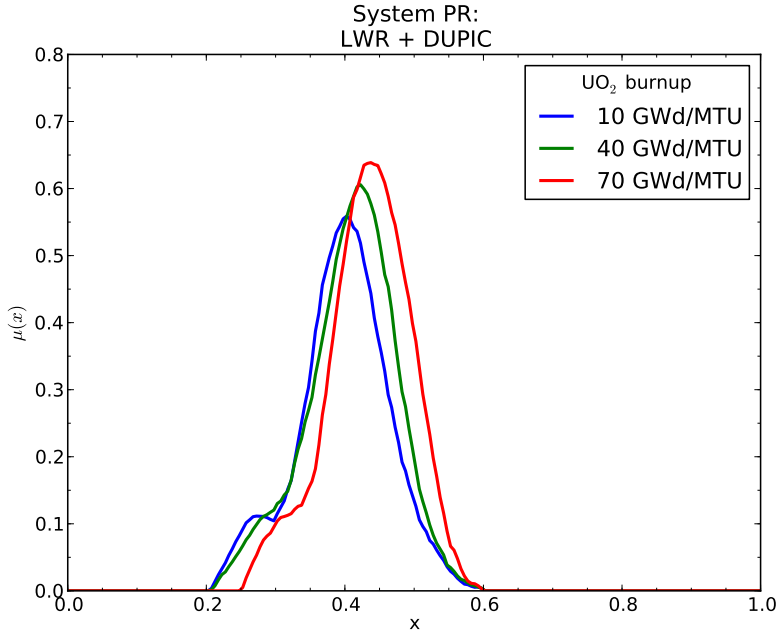

(b): DUPIC: yield-insensitive (FOM_1)

Figure 5.21: System PR as a function of uranium fuel burnup for the DUPIC fuel cycle, for an unsophisticated state (covert) under a yield-sensitive scenario (FOM_2) and a yield-insensitive scenario (FOM_1).

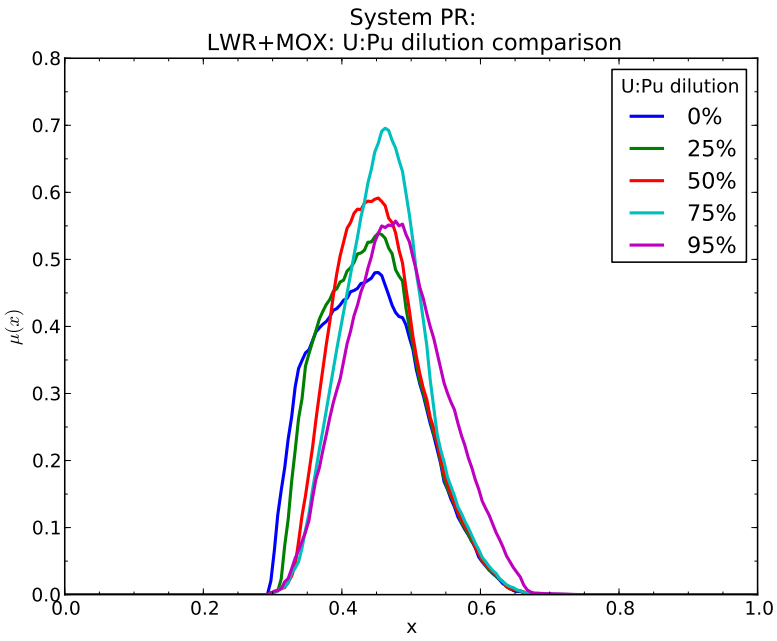

(a): MOX dilution: yield-sensitive (FOM_2)

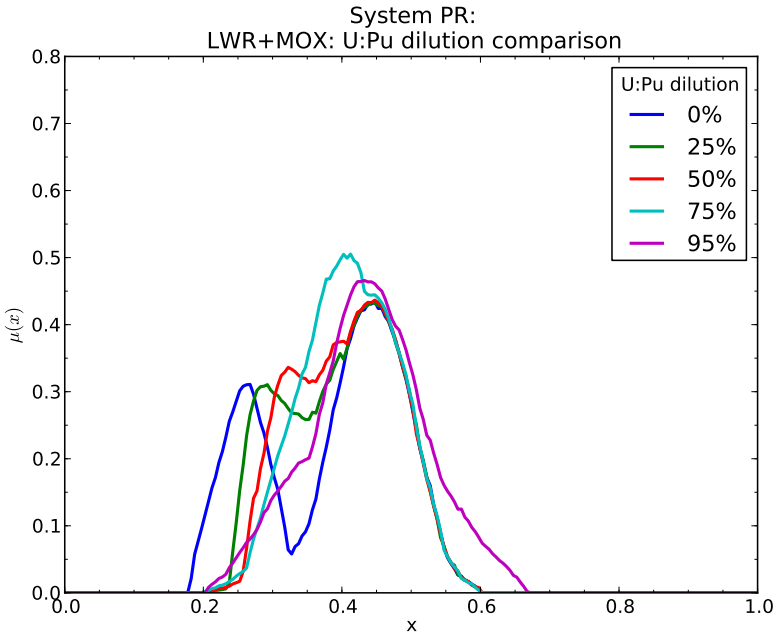

(b): MOX dilution: yield-insensitive (FOM_1)

Figure 5.22: System PR as a function of uranium dilution during reprocessing stages for partially closed cycles, for an unsophisticated state (covert) under a yield-sensitive scenario (FOM_2) and a yield-insensitive scenario (FOM_1).

Table 5.18: Summary of system centroid PR and rank values for as a function of uranium dilution during reprocessing for "modified open" cycle strategies, assuming an unsophisticated state (covert) adversary, for yield-sensitive (FOM_2) and yield-insensitive (FOM_1) cases. Burnup held fixed at 60 $\frac{GWd}{MTU}$ / 60 $\frac{GWd}{MTHM}$.

	Yield-sensitive (FOM_2)		Yield-insensitive (FOM_1)	
U:Pu (%)	Centroid	Rank	Centroid	Rank
0	0.4379	M	0.3862	L+
25	0.4441	M	0.3990	M–
50	0.4536	M	0.4067	M–
65	0.4565	M+	0.4089	M–
75	0.4629	M+	0.4117	M
85	0.4872	M+	0.4261	M
95	0.4793	M+	0.4366	M

Closed cycles

Figures 5.23 and 5.24 show the evolution of system PR as a function of uranium fuel burnup for the unsophisticated state (covert) for closed cycles, assuming a yield-sensitive and yield-insensitive adversary, for the UREX+1a and pyroprocessing actinide recovery strategies, respectively.

Given the dominant importance of the isotopic barrier for case of the unsophisticated state, there is a more pronounced burnup sensitivity with system PR, particularly for higher burnups (e.g., the LWR once-through case). Thus, the sensitivity for the yield-sensitive case appears to be due to the buildup of higher plutonium and transuranic species, each which has a higher SFN emission rate (thus increasing the propensity for pre-detonation). Likewise, the TRU inventory also increases the heat generation rate (hence the marked difference between PUREX and UREX series treatments).

5.3.4 Summary of results by adversary type

An overall summary of rankings for selected systems studied across each of the adversary types is given as Table 5.20.

Several trends in the system rankings are noteworthy. First, for the sophisticated state, overt case, actinide coextraction shows little to no effect upon overall system PR for partially closed cycles, given the relative low importance of the isotopic barrier; i.e., it is assumed

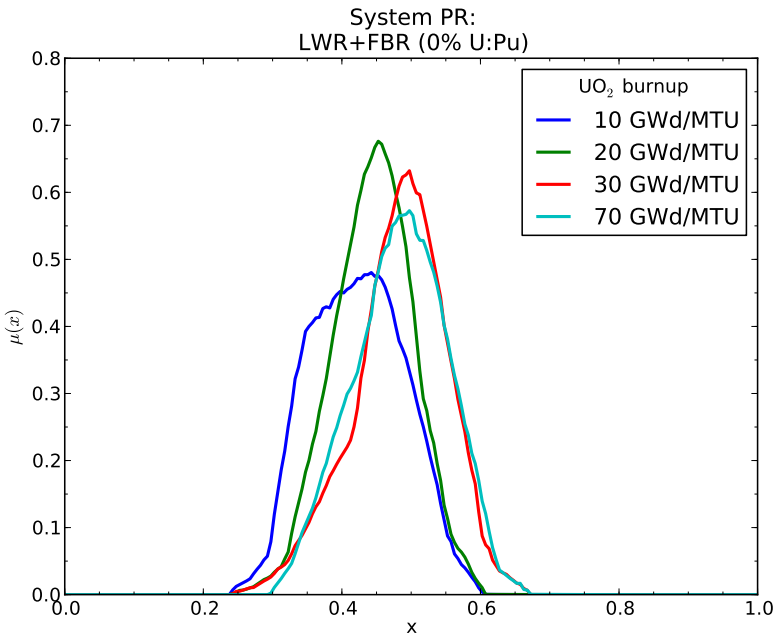

(a): LWR+FR (UREX+1a): yield-sensitive (FOM_2)

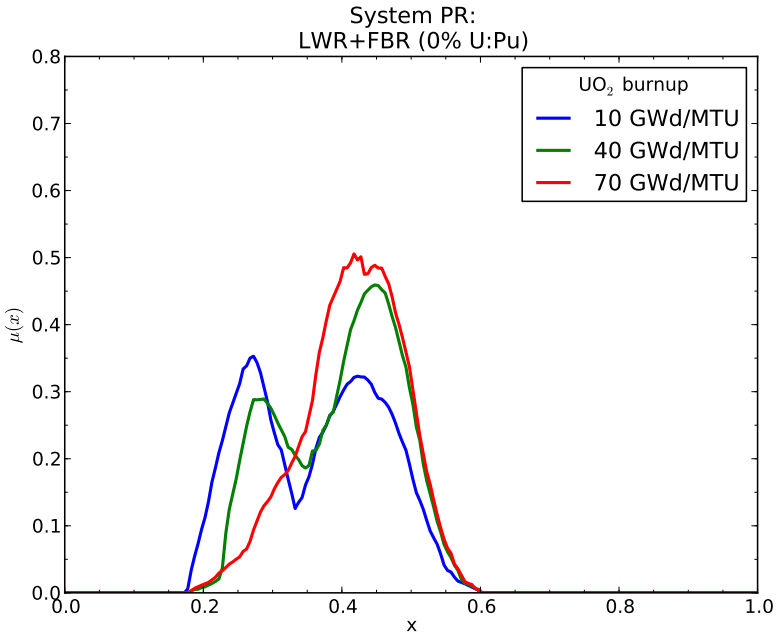

(b): LWR+FR (UREX+1a): yield-insensitive (FOM_1)

Figure 5.23: System PR as a function of fuel burnup for LWR + FR cycle, based on UREX+1a actinide recovery strategy, for an unsophisticated state (covert) under a yield-sensitive scenario (FOM_2) and a yield-insensitive scenario (FOM_1).

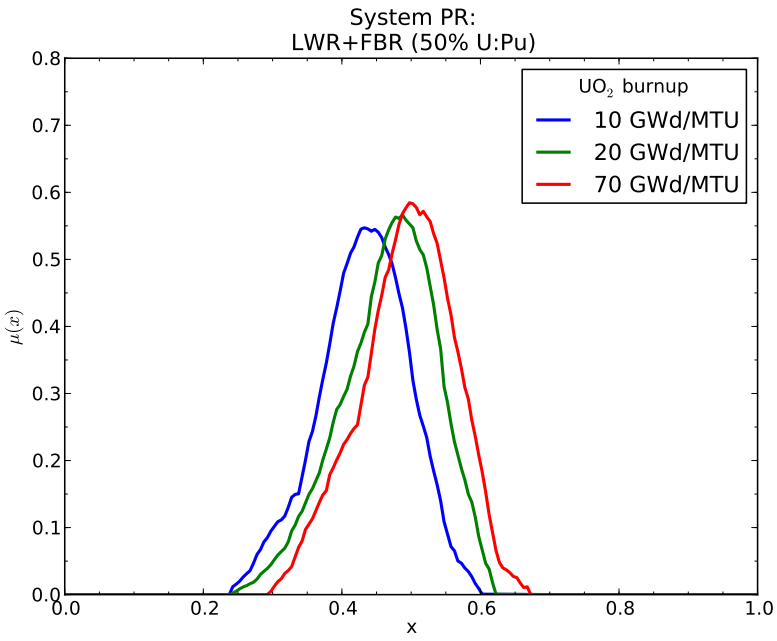

(a): LWR+FR (Pyro): yield-sensitive (FOM_2)

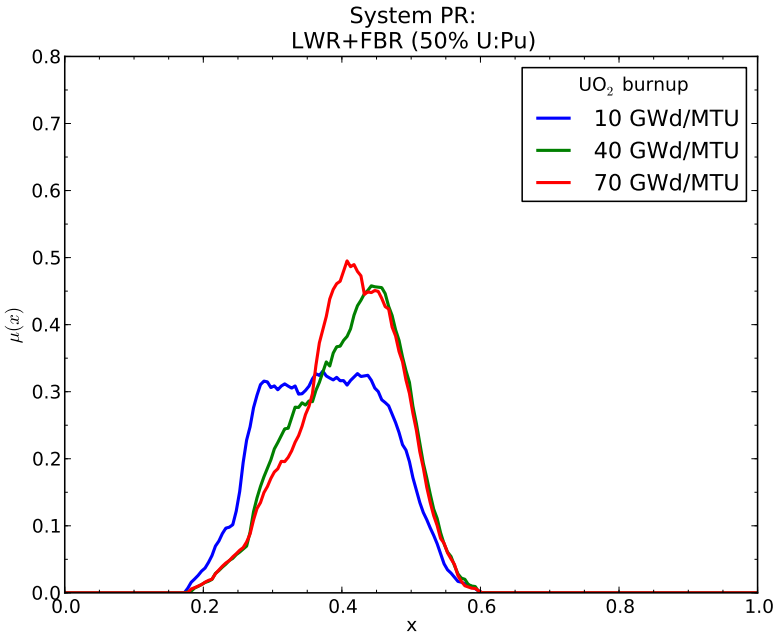

(b): LWR+FR (Pyro): yield-insensitive (FOM_1)

Figure 5.24: System PR as a function of fuel burnup for LWR + FR cycle, based on a pyroprocessing actinide recovery strategy, for an unsophisticated state (covert) under a yield-sensitive scenario (FOM_2) and a yield-insensitive scenario (FOM_1).

Table 5.19: Summary of system centroid PR and rank values for closed cycle strategies for selected UO_2 fuel burnups (FR fuel burnup held constant at 90 $\frac{GWd}{MTHM}$), assuming an unsophisticated state (covert) for yield-sensitive (FOM_2) and yield-insensitive (FOM_1) cases.

		Yield-sensitive		Yield-insensitive	
System	Burnup ($\frac{GWd}{MTU}$)	Centroid	Rank	Centroid	Rank
LWR+FR: UREX+1a	10	0.4225	M–	0.3640	L+
	40	0.4831	M+	0.3988	M–
	70	0.4842	M+	0.4157	M
LWR+FR: Pyro	10	0.4321	M	0.3779	L+
	40	0.4808	M+	0.4090	M–
	70	0.4934	M+	0.4094	M

to be relatively simple for such an adversary to reprocess diverted material to achieve a more attractive isotopic form. Cycles where fuel remains intact or otherwise is not separated (e.g., LWR-OT, CANDU, and DUPIC) show a higher overall PR, however these values are still nominally lower for the sophisticated state in an overt breakout attempt, given the latent presence of potentially usable materials. Finally, fully closed cycles show a nominally higher intrinsic PR than the partially closed cycles, as material is separated in a nominally less attractive form (i.e., TRU vs. Pu) and the material discharged from the fast reactors is overall of a lower attractiveness. Small differences in intrinsic PR are evident between UREX+1a strategies and pyroprocessing at lower burnups (with pyro showing a small advantage); this difference appears to disappear at higher burnups.

For the case of the sophisticated state (covert), the same trends as before with the overt breakout case appear to prevail, with certain notable features. First, once-through cycles (and DUPIC) perform much better in this case, as the detectability of a breakout attempt begins to become a more relevant concern. Material in dilute forms (e.g., with uranium coextraction) present an overall higher PR than mixtures of TRU alone (e.g., UREX+1a). Likewise, the fully closed cycles again show the same behavior trend, both in terms of PR relative to partially closed cycles and in the differences between UREX-based and pyroprocessing-based actinide recovery strategies.

In the case of the unsophisticated state, all fuel cycles with the exception of PUREX and COEX appear to converge upon the “medium-plus” ranking, given the lower overall material attractiveness when spontaneous fission neutron rates are accounted for. (PUREX

Table 5.20: Summary of system rank values for selected fuel cycle systems as a function of adversary type: sophisticated state, overt (SSO); sophisticated state, covert (SSC), and unsophisticated state, covert, yield-sensitive (USC, YS) and yield-insensitive (USC, YI).

System	Burnup ($\frac{GWd}{MTU}$ / $\frac{GWd}{MTHM}$)	System rank SSO	SSC	USC (YS)	USC (YI)
LWR-OT	40 / —	M–	M	M+	M
	70 / —	M–	M+	M+	M+
CANDU HWR	10 / —	M–	M+	M+	M
MOX: PUREX	60 / 60	L	L+	M	L+
MOX: COEX	60 / 60	L	L+	M	M–
MOX: UREX+1a	60 / 60	L	L+	M+	M–
MOX: UREX+1b	60 / 60	L+	M–	M+	M
MOX: UREX+1	60 / 60	L+	L+	M+	M–
DUPIC	40 / 10	M–	M+	M+	M
	70 / 10	M–	M+	M+	M+
FBR: UREX+1a	40 / 90	L	L+	M+	M–
	70 / 90	L+	M – M+	M+	M
FBR: Pyro	40 / 90	L+	M–	M+	M–
	70 / 90	L+	M – M+	M+	M

and COEX show a slightly lower intrinsic PR, ranked as "medium" effectiveness.) For the yield-insensitive case, factors such as burnup and coextractants appear to have the greatest delineating effect, with COEX and UREX+1a showing a nominal advantage over COEX, and several cycles showing a burnup dependence upon PR (e.g., LWR-OT and closed cycles).

Overall, the trend in system PR performance appears to be a near-uniform increase with decreasing adversary sophistication and increasing concern for yield and non-detection (e.g., overt vs. covert). Put another way, fuel cycle system PR performance appears to generally increase moving from the sophisticated state (overt) to the corresponding covert case; from the sophisticated state (covert) to the unsophisticated state (covert); and finally again going from the yield-insensitive unsophisticated state (covert) to the yield-sensitive unsophisticated state (covert). The only exceptions to this trend appear to be in the rankings for the CANDU cycle (where the unsophisticated state, covert shows a slightly lower ranking than the sophisticated state, covert) and in the DUPIC cycle at lower burnup (similar pattern). This appears to be due to the relative importance of other, non-isotopic barriers (e.g., time,

available mass, etc.) which produce this artifact in these very limited cases.

In total, the effect of actinide co-processing on overall system PR appears to be quite limited for sophisticated states with a well-developed industrial and fuel cycle infrastructure. Rather, any intrinsic PR benefits to these types of processes appear to be mainly concentrated in less developed (unsophisticated states), for which physical barriers represent a greater overall obstacle to proliferation. Such a finding agrees with the conclusions of prior studies on this subject [3, 42]. Additionally, in comparing pyroprocessing with advanced UREX series treatments (e.g., UREX+1a) for fast cycles, pyroprocessing appears to show a nominal advantage over conventional UREX-based cycles for low fuel burnups, however these differences largely disappear with higher fuel burnups.

5.4 Analysis and conclusion

In this analysis, the effect of both the material target type (e.g., plutonium, TRU, or minor actinides only) as well as the adversary type (as a measure of relative barrier importance) were evaluated for their effect upon system PR. This analysis was carried out for sevreal different fuel cycle systems: two "open" systems, consisting of a LWR once-through cycle and a HWR CANDU once-through cycle; several iterations of the "modified open cycle" concept, consisting of LWRs with recycling in either a conventional PUREX process or an advanced UREX process, in which PR was evaluated across dimensions of both burnup as well as actinide co-processing strategies; and finally, a "closed cycle" consisting of LWRs and advanced recycling of all actinides using either UREX+1a or pyroprocessing. In as much, the objective has been to characterize the impact of assumptions such as adversary characteristics (a sophisticated or unsophisticated state, sensitivity to yield, material target type, etc.).

From the above results, it would appear that the choice of relative barrier weights (i.e., due to the adversary type) appears to be of primary importance to the overall calculation of system PR, indicating that the assignment of barrier weights based on assumptions of adversary capabilities deserve particular scrutiny.

Conversely, the study of PR by adversary target type appears to indicate that the choice of the "nominal" pathway (e.g., plutonium for intact post-irradiation fuel forms and the "whole stream" for separated forms) would be well-justified. In particular, alternative target pathways (particularly, minor actinides) do not appear to show a credible alternative pathway,

given the substantially lower material attractiveness (and less available mass). From this analysis, it would appear that even balanced against other barriers (e.g., mass and bulk, radiological hazard), the plutonium-only pathway represents the most vulnerable target pathway in each of the fuel cycle cases considered and thus merits the most detailed consideration. For advanced recycle scenarios (e.g., UREX-series), the system PR appears to asymptotically converge to the PUREX case under this scenario; i.e., additional intrinsic barriers introduced by material co-processing are largely mooted if further post-processing is assumed.

Finally, assumptions about adversary intent (i.e., whether or not an unsophisticated state is concerned about weapons yield) have been demonstrated to show a substantial effect upon evaluated system PR, given the substantial differences in spontaneous fission neutron rates, particularly for higher plutonium species and minor actinides. The combination of adversary type and yield sensitivity are determinative to whether secondary system parameters (such as burnup) substantially impact system PR. For cases outside of an unsophisticated state adversary (in a covert diversion attempt), parameters such as burnup were found to have a minimal impact upon system PR (and thus more detailed system characterization does not appear to be warranted). However, for the unsophisticated state case (particularly for the yield-sensitive adversary), these parameters can have a significant impact, thus meriting more detailed system characterization under these very specific circumstances.

By making an explicit exploration of the assumptions about both adversary characteristics and material target type, APA has been shown to be capable of making a more generalized characterization of PR behavior within a nuclear fuel cycle, thus providing a "bridge" between traditional PRA and AA/MAU methods.

CHAPTER 6

Evaluation of uncertainty and simplification effects

6.1 Introduction

The evaluation of material attractiveness for direct weapons proliferation purposes is central to proliferation resistance (PR) analysis. It is well-known that the relative attractiveness of candidate materials for nuclear weapons proliferation purposes degrades as a function of fuel burnup [6, 53]. For such analysis, it is generally a standing assumption that explicit reactor details (such as heterogeneity in neighboring lattice enrichments and other local features such as gadolinium control rods) are of negligible concern and thus can be neglected [4]. As a result, PR assessments generally make use of globally-averaged quantities (such as lattice-averaged burnup) and ignoring specific reactor details (such as lattice effects at the fuel assembly level). Simplified depletion analysis using lattice-averaged burnup (as is the case with reactor libraries in ORIGEN-S [43]) is thus often employed to evaluate the isotopic, thermal, and radiological properties of nuclear fuel, rather than more explicit (and resource-intensive) 2-D lattice physics calculation methods (such as TRITON). However, an open question remains as to whether neglecting local lattice features is a valid assumption for materials attractiveness evaluation in such analyses.

Additionally, a second question arises as to the effect of cross-section uncertainties in said depletion calculations as to the isotopic inventories and the resulting impact on the

uncertainty in the attractiveness calculation, particularly for transuranic inventories.

A review of the existing literature on proliferation resistance assessment [6, 9, 35, 42, 46, 53] indicates that the effect of simplifications in depletion modeling and cross-section uncertainty have generally not been considered with respect to their impact on PR evaluation.

This analysis attempts to resolve both of these questions through a direct benchmarking study using the Figure of Merit (FOM) criteria for material attractiveness [6]. Using the Figure of Merit approach, the effect of simplified reactor models (such as using a lattice-average burnup in ORIGEN-S) on evaluated material attractiveness was explored. This was accomplished by comparing evaluated FOM_1 values of experimental data obtained from spent fuel analysis conducted by Oak Ridge National Laboratory on samples from the Three-Mile Island Unit 1 and Calvert Cliffs reactors along with data from the REBUS and ARIANE programs [26, 27] to values obtained from a simplified lattice depletion model in ORIGEN-S as well as those from a higher-fidelity 2-D lattice physics depletion analysis using TRITON [43].

Additionally, the overall uncertainty in material attractiveness due to cross-section uncertainties was evaluated through the propagation of uncertainty from isotopic inventories to relevant parameters of interest to the FOM calculation (e.g., the bare sphere critical mass and the heat generation rate), based upon a prior study conducted of the effect of cross-section uncertainty on isotopic inventories in ORIGEN-S [56].

From this analysis, an assessment as to the adequacy of simplified reactor models based on depletion analysis in ORIGEN-S (as compared to higher-fidelity 2-D lattice physics models such as TRITON) can be made by comparing the FOM values for identical burnups and lattice configurations. Additionally, uncertainty propagation shall indicate the relative uncertainty in such characterizations due to cross-section uncertainties, and in particular whether a discrimination in material attractiveness can be made between different fuel burnup values.

6.2 Methodology

6.2.1 Data used for analysis

The data used for this analysis was obtained from measurements of spent fuel samples obtained from the TMI-1 reactor and Calvert Cliffs [26] as well as fuel data from the REBUS and ARIANE fuel characterization programs [27]. These studies were conducted as a valida-

tion study of the predictions of the SCALE analysis system; the inventory results from these studies can thus also be used to directly characterize the material properties (such as the bare sphere critical mass, dose at 1 meter, and heat generation rate).

The data from these four reactors covers a wide span of burnups, ranging from around 22 to 60 $\frac{\text{GWd}}{\text{MTU}}$.

In addition, TRITON input for particular samples tested was made available in the above studies [26, 27]; these TRITON input decks were thus used as a basis of comparison for a 2-D lattice calculation to the simplified lattice depletion model carried out using ORIGEN-S [43]. Likewise, the calculation in ORIGEN-S was carried out using provided power history data for the experimental samples [26, 27] in order to provide a reasonable fidelity in the simplified calculation.

Examples of the TRITON lattices for the TMI-1, Calvert Cliffs, ARIANE, and REBUS fuels are shown as Figures 6.1–6.4.

Dose data for plutonium and TRU masses was obtained using estimates obtained from [1], while BSCM data was calculated from the correlation shown in Figure 2.3. Heat generation rate data was obtained from ORIGEN-S output and from calculations based on the standard heat generation rates per isotope.

6.2.2 Uncertainty analysis

For the experimental data, experimental uncertainty was reported on a per-isotope basis for each of the actinides measured in the benchmark studies [26, 27].

For the corresponding depletion data generated via ORIGEN-S, a study on the effect cross-section uncertainties in final isotopic values was employed [56]. This uncertainty data was generated through a propagation of cross-section and number density covariance data via the Efficient Subspace Method (ESM) [56]. In the ESM method, covariance data was decomposed into singular pairs and perturbed along independent directions for uncertainty for the the most significant uncertainty values [56]. Uncertainties in the final isotopic inventories of the depletion calculation were then characterized for a burnup of 40 $\frac{\text{GWd}}{\text{MTU}}$ and an enrichment of 4.5 w/o; these values were used for uncertainty propagation through the FOM calculation. (Values for other PWR enrichment/burnup combinations were unavailable at the time of this study.) The evaluated cross-section uncertainties to isotopic inventories are given as Table 6.1.

For each of the per-nuclide uncertainties, the uncertainty values were then propagated

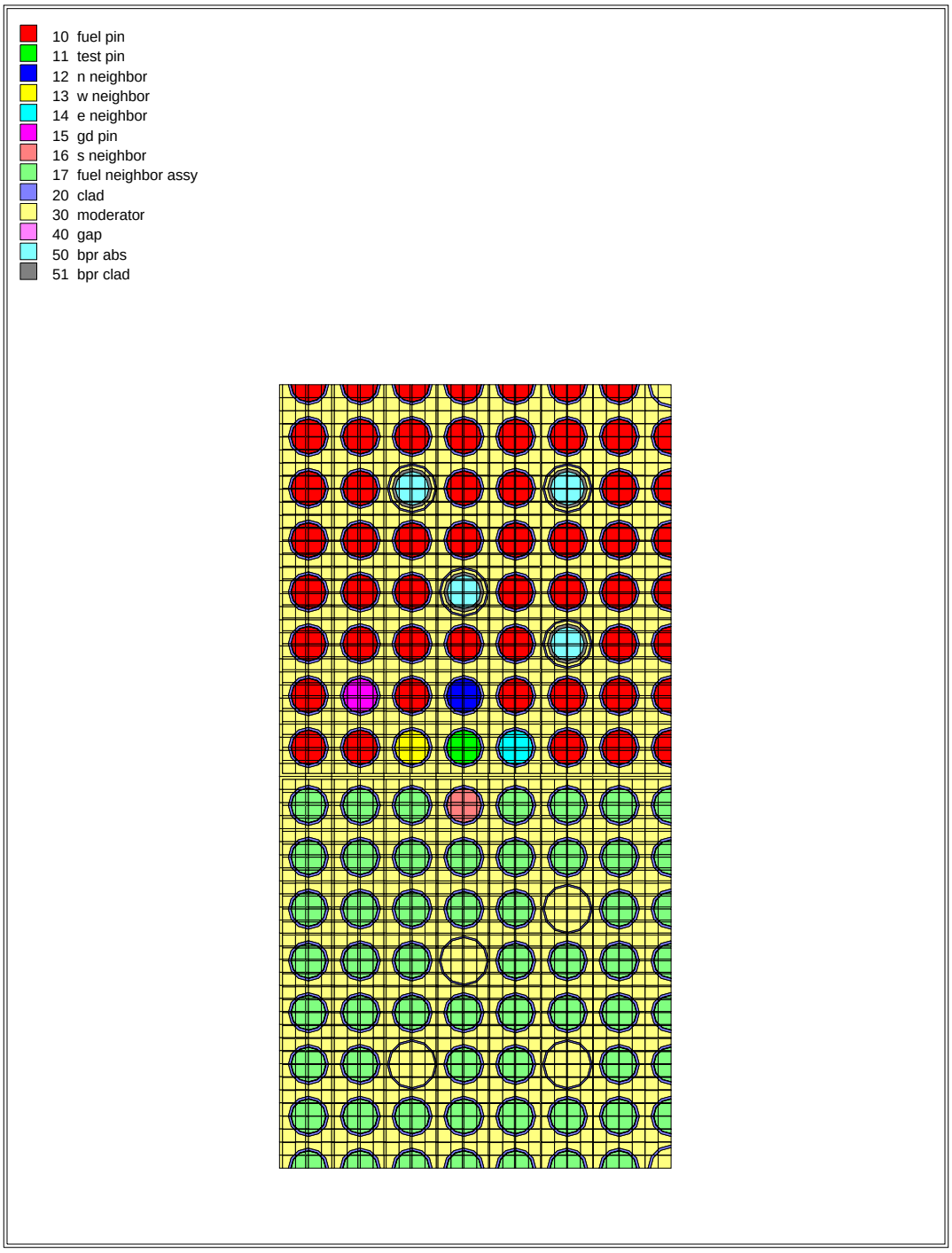

Figure 6.1: TRITON material lattice for the TMI-1 O12S4 sample.

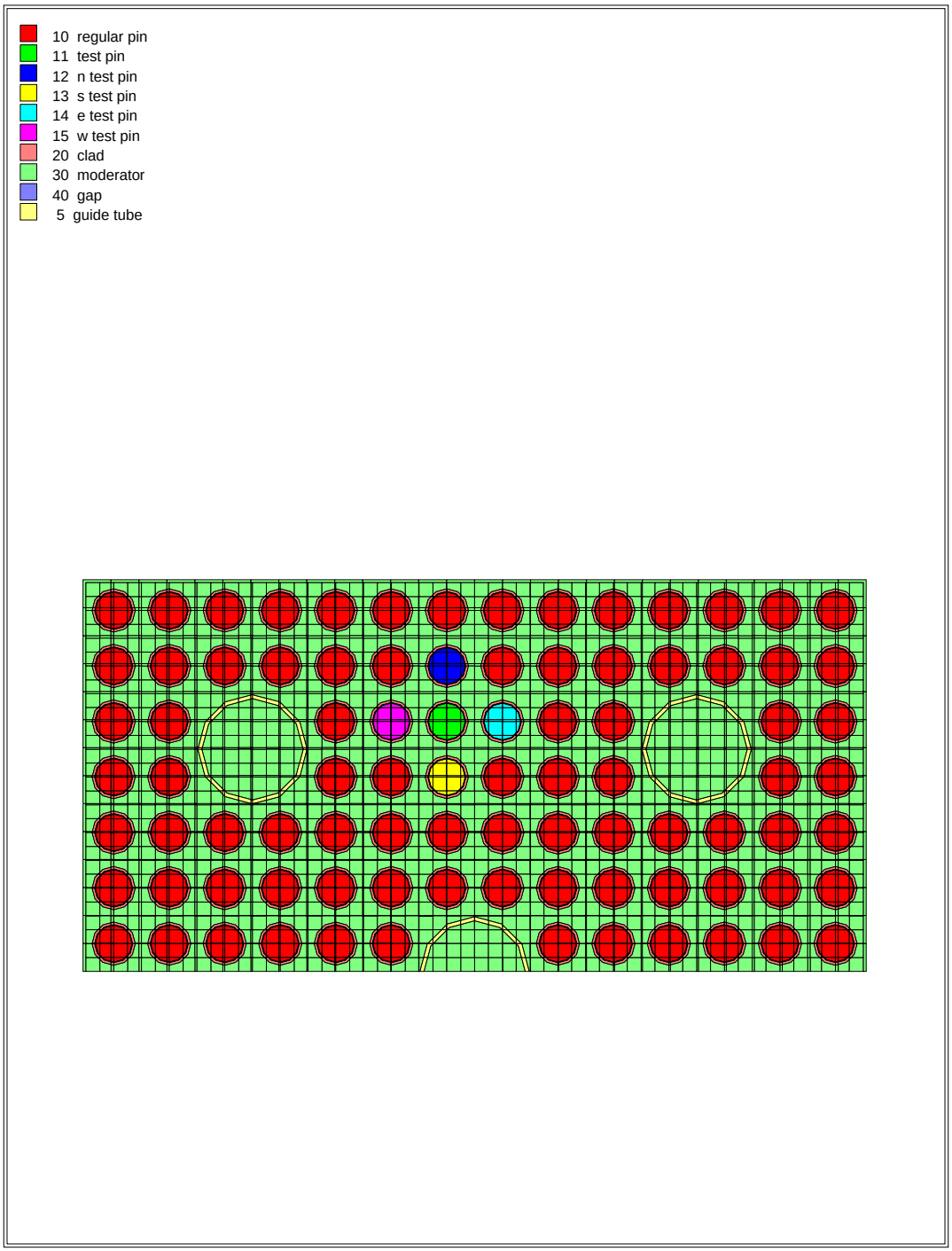

Figure 6.2: TRITON material lattice for the Calvert Cliffs D047 sample.

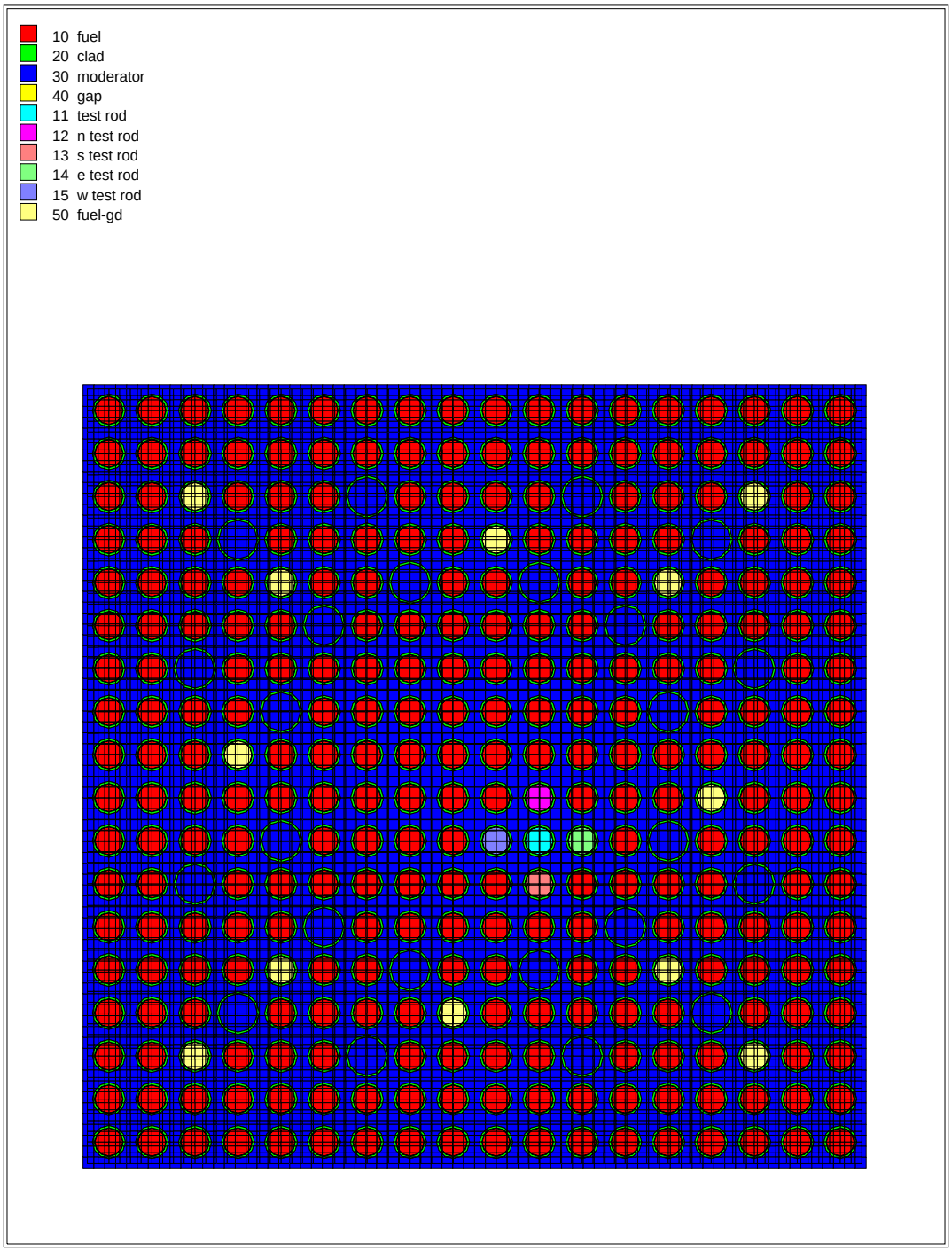

Figure 6.3: TRITON material lattice for the REBUS GK2 sample.

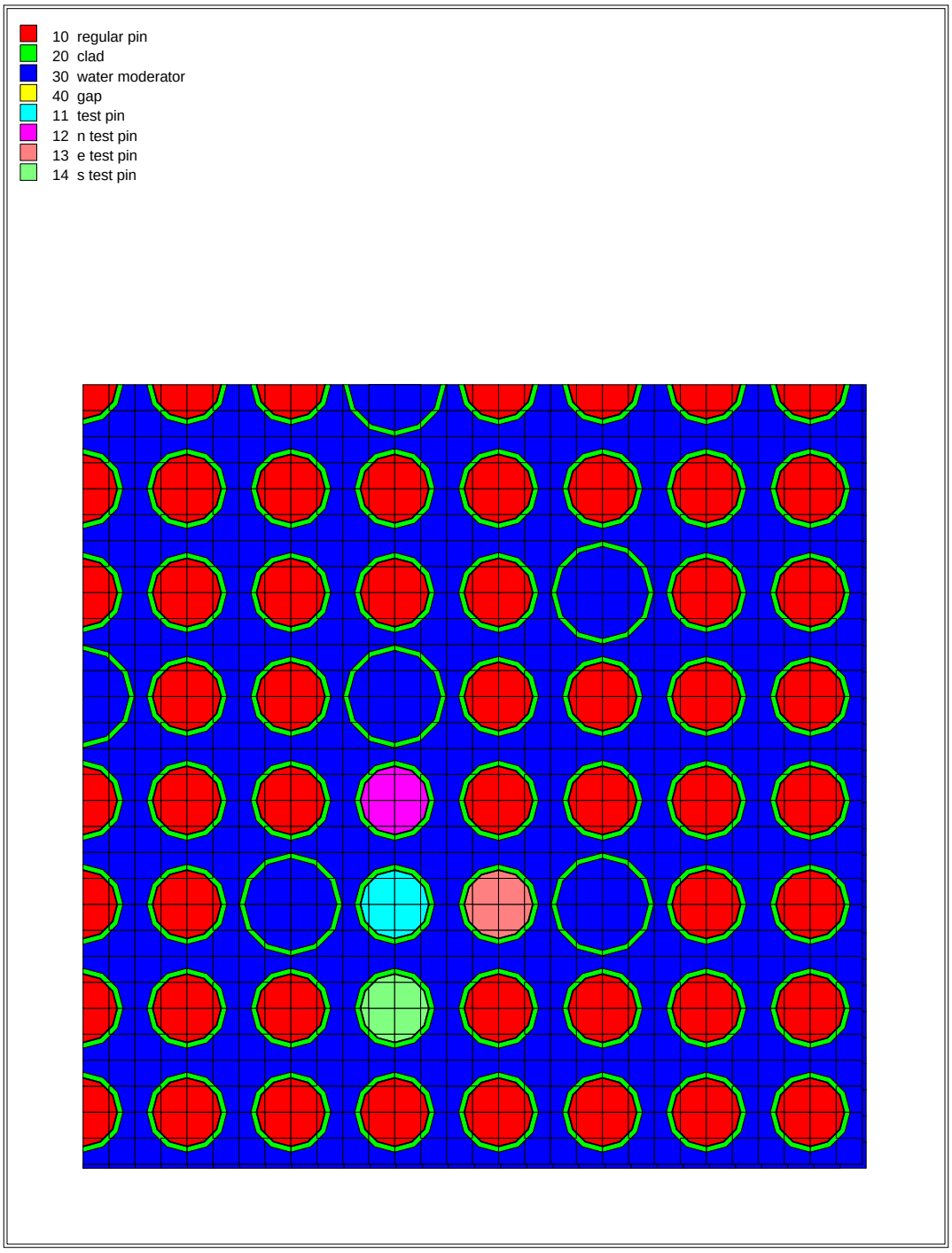

Figure 6.4: TRITON material lattice for the ARIANE GU1 sample.

Table 6.1: Relative mass uncertainties in ORIGEN-S calculated isotopic inventories due to cross-section uncertainties, per calculations performed using the Efficient Subspace Method in [56]. Uncertainty data for a burnup of 45 $\frac{\text{GWd}}{\text{MTU}}$ and enrichment of 4.5 w/o.

Nuclide	Uncertainty (±%)
^{237}Np	0.616
^{238}Pu	1.058
^{239}Pu	0.885
^{240}Pu	2.766
^{241}Pu	2.551
^{242}Pu	2.625
^{241}Am	2.535
^{242m}Am	2.229
^{243}Am	13.870
^{242}Cm	2.229
^{244}Cm	11.670
^{245}Cm	10.600

to produce the relative uncertainties in the plutonium vector (determining the bare sphere critical mass) and the relative fraction of plutonium to other actinides (e.g., for the TRU case, also for BSCM quantification), as well as the relative heat generation rate (calculated as a weighted average per nuclide).

The calculation of the ^{239}Pu vector and corresponding plutonium fraction in the stream (for calculating the bare sphere critical mass) is based on the propagation of uncertainty for the fraction of ^{239}Pu (σ_{fr}^{239}) and the plutonium fraction (σ_{fr}^{Pu}) is given as Equations 6.2 and 6.4.

$$\sigma_{Pu} = \sqrt{\sum_x \left(\sigma_x^{Pu}\right)^2} \tag{6.1}$$

$$\sigma_{fr}^{239} = \sqrt{\left(\frac{\sigma_{239}}{^{239}Pu}\right)^2 + \left(\frac{\sigma_{Pu}}{\sum_x Pu_x}\right)^2} \tag{6.2}$$

$$\sigma_{TRU} = \sqrt{\sum_x \left(\sigma_x^{TRU}\right)^2} \tag{6.3}$$

$$\sigma_{fr}^{Pu} = \sqrt{\left(\frac{\sigma_{Pu}}{\sum_x Pu_x}\right)^2 + \left(\frac{\sigma_{TRU}}{\sum_x TRU_x}\right)^2} \tag{6.4}$$

Uncertainties were then propagated in similar fashion to produce the uncertainties in the BSCM (σ_M) and the heat generation rate (σ_{HGR}), for which the uncertainty in the latter is propagated as Equation 6.6. In Equation 6.6, h_i represents the heat generation rate of the nuclide of interest, and X_i represents the mass of said nuclide and σ_i^x represents the respective uncertainty in nuclide mass.

$$\frac{\partial h}{\partial X_i} = \frac{h_i\left(\sum_{j\neq i} X_j\right) - \left(\sum_{j\neq i} X_j h_j\right)}{\left(\sum_j X_j\right)^2} \tag{6.5}$$

$$\sigma_{HGR} = \sqrt{\sum_i \left(\frac{\partial h}{\partial X_i}\sigma_i^x\right)^2} \tag{6.6}$$

Given the small effect of the dose rate (especially for actinide-only mixtures, such as Pu and TRU), the uncertainty in the dose rate was neglected for this characterization. The uncertainty was thus propagated through the Figure of Merit equation, giving a FOM uncertainty σ_{FOM} calculated per Equation 6.7.

Taking the partial derivatives of Equation 2.2 with respect to the BSCM (M) and heat

generation rate (h) and assuming the relative impact of dose is negligible ($\frac{\partial FOM}{\partial D} \approx 0$), the uncertainty of the FOM is thus calculated as Equation 6.7.

$$\sigma_{FOM} = \sqrt{\left(\frac{1}{M\ln(10)}\right)^2 \sigma_M^2 + \left(\frac{8}{(8\ln(h)+45)\ln(10)}\right)^2 \sigma_h^2} \tag{6.7}$$

6.3 Results and analysis

6.3.1 Effect of lattice simplification and cross-section uncertainties

Figure 6.5 shows the Figure of Merit comparison for two cases: plutonium obtained from spent nuclear fuel and TRU from spent fuel (Pu, Np, Am, Cm), each as a function of burnup. Error bars for the experimental data indicate propagated errors due to reported measurement uncertainties in isotopic concentrations; for the ORIGEN-S results, these are propagated from the cross-section uncertainties evaluated in [56].

Additionally, curium isotopic data was missing from the Calvert Cliffs and some of the TMI-1 experimental sample data for the TRU evaluation; thus, the experimental predictions for the heat generation rate appear to significantly depart from the corresponding ORIGEN-S predictions. For these cases, a second set of "corrected" data (as indicated on the graphs) was calculated by substituting the calculated heat generation rates from ORIGEN-S for the corresponding irradiation histories, while leaving the dose and bare sphere critical mass data unchanged. This correction can be justified in light of separate benchmarking studies performed as to decay heat predictions for ORIGEN-S, which show a high degree of accuracy over a wide range of burnups for decay heat [19].

Correcting for the decay heat term in the TRU data, one observes that in both the plutonium and TRU data that there is generally a very good correspondence between the simplified ORIGEN-S calculation and the lattice physics depletion performed in TRITON to the FOM values of the experimental samples. While moderate differences in composition have been found, these differences are generally small with respect to material attractiveness. Introducing factors such as explicitly modeling surrounding assemblies (of heterogeneous enrichment) and correcting for factors such as gadolinium rod location and rod pitch was found to have a notable reduction in the over-prediction of plutonium species in the TRITON model (from an over-prediction of ^{239}Pu of 10.4% to 1.8%) [26]; however, as one observes from Figure 6.5, even without these corrections the systemic over-prediction is of minor

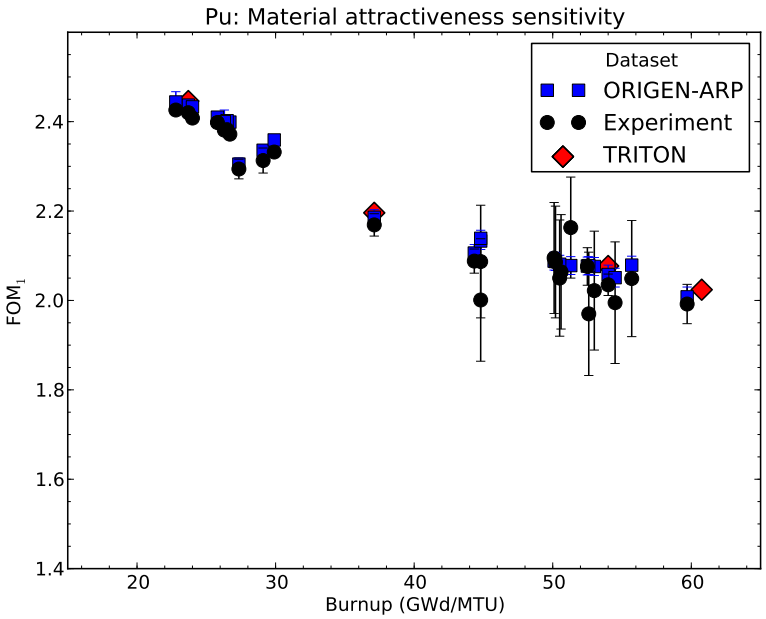

(a): Pu only

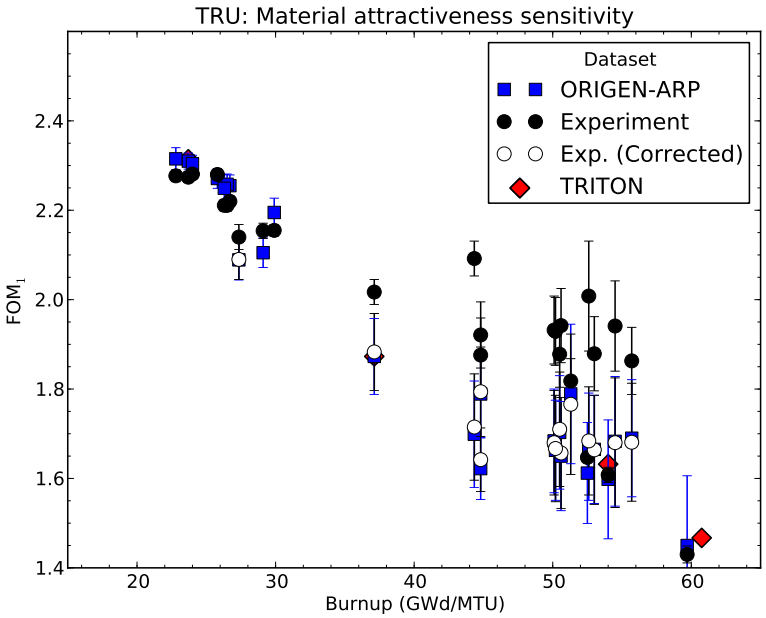

(b): TRU (Pu + MA)

Figure 6.5: Material attractiveness (FOM_1) for plutonium and transuranics in spent fuel as a function of fuel burnup for isotopic data evaluated from experimental samples, TRITON lattice physics analysis, and ORIGEN-S depletion analysis.

consequence to the overall calculated FOM value. In particular, one observes that even the basic depletion calculation performed using a reasonably faithful reproduction of the power history in ORIGEN-S gives a reasonable correspondence to the experimental sample FOM values for the entire range of burnups considered for both the plutonium-only and transuranic cases.

The uncertainty in the ORIGEN-S depletion calculation due to cross-section uncertainties appears to be burnup-dependent, with overall uncertainty magnitude growing as a function of increasing burnup. However, these uncertainties are quite small for plutonium-only mixtures, particularly compared to uncertainties in experimental measurements.

Conversely, mixtures containing transuranic materials show a stronger burnup dependence on uncertainty, given the ingrowth of higher actinides as a function of burnup, which in turn have a higher associated uncertainty. For TRU mixtures, analysis indicates these uncertainties to be chiefly dominated by uncertainties in the inventory of ^{244}Cm, which has both a very high heat generation rate as well as a high overall isotopic uncertainty (both in terms of cross-section and experimental measurements). However, the propagated uncertainty in FOM_1 attractiveness values appears to be on the same order as those from experimental values for higher burnups and do not appear to obviously prevent a useful comparison of material attractiveness for plutonium or TRU mixtures as a function of burnup.

6.3.2 Effect of assumed uniform power history

In addition to considering the impact of simplified assumptions regarding the fuel geometry (e.g., including the enrichments of surrounding assemblies and explicit modeling of features such as gadolinium rod placement), an additional simplification which can be evaluated is the effect of assuming a uniform irradiation history (e.g., a "flat," lower-fidelity power history in which fuel is irradiated at a constant power over the entire burnup) compared to a higher-fidelity approach which attempts to more faithfully reproduce the irradiation power history (e.g., a "high fidelity" power history) for the same total fuel burnup.

Such a comparison was made for a subset of the four experimental datasets evaluated [26, 27] (e.g., data sets with detailed irradiation power histories). For these evaluations, a weighted average power was calculated (based on relative irradiation time); the average power used for each sample and the corresponding burnups are listed as Table 6.2. For each "flattened" irradiation history, an irradiation over 3 cycles was calculated at the calculated average power, assuming a 90% uptime.

Table 6.2: Burnup and averaged irradiation power for samples considered; irradiation history provided in [26, 27].

Reactor / Program	Sample ID	Burnup ($\frac{\text{GWd}}{\text{MTU}}$)	Averaged power ($\frac{\text{MW}}{\text{MTU}}$)
REBUS [27]	GKN II	54.095	38.88
ARIANE [27]	GU1	59.656	46.02
	GU3	52.504	52.66
	GU4	29.067	29.15
Calvert Cliffs [26]	87-63	44.34	27.46
	87-71	37.12	22.99
	87-81	27.35	16.94
TMI-1 NJ05YU [26]	H6 A1B	45.687	34.47
	H6 A2	51.861	38.93
	H6 B1B	51.696	41.93
	H6 B2	52.089	38.55
	H6 B3J	51.861	40.78
	H6 C1	51.545	38.62
	H6 C2B	51.563	40.47
	H6 C3	51.696	39.47
	H6 D1A2	51.53	42.86
	H6 D1A4	50.81	38.86
	H6 D2	48.569	34.47

The material attractiveness evaluation arising from the "flattened" power history ("low-fidelity") was then compared to the material attractiveness calculated more detailed power history ("high fidelity") provided in [26, 27], as well as the experimental measurements. This comparison is presented for both Pu and TRU streams (with associated uncertainties) as Figure 6.6.

The use of an averaged power does introduce small discrepancies in the actinide inventories from the higher-fidelity calculation; such a change most significantly manifests in the calculated heat generation rate. However, as one observes from Figure 6.6, the discrepancies introduced through the use of a uniform, averaged irradiation power do not appear to produce significant departures for the material attractiveness calculation, particularly when compared to the level of uncertainty introduced by cross-section uncertainties on material inventories (especially for transuranic materials). For most cases, the simplified irradiation history appears to closely match the calculated material attractiveness values of both the "high-fidelity" power history calculation and experimental data. Thus, for calculations of material attractiveness, simplifications such as the use of uniform irradiation histories do not appear to introduce unacceptable errors and can thus be used as a reasonable simplification.

6.4 Conclusion

In this study, the effect of using simplified models for nuclear fuel depletion (e.g., ORIGEN-S) compared to more sophisticated 2-D lattice physics models (e.g., TRITON) for material attractiveness was evaluated as well as the impact of cross-section uncertainties upon uncertainty in material attractiveness, using the Figure of Merit method for evaluating material attractiveness [6]. The impact of using simplified depletion models was evaluated both by comparing evaluated material attractiveness values for the simplified model to higher-fidelity lattice physics models as well as experimentally measured benchmark fuel data [26, 27]. For the purposes of materials attractiveness evaluation, such simplifications have an overall minor impact, showing a good agreement with experimental data as well as lattice physics approaches which model local fuel features with greater fidelity. This was true across a wide range of burnups (from approximately 20 to 60 $\frac{\text{GWd}}{\text{MTU}}$) as well as for both plutonium and TRU derived from spent fuel.

The effect of cross-section uncertainties in the depletion calculation on material attractiveness evaluation appears to be fairly limited, particularly for plutonium-only mixtures. For

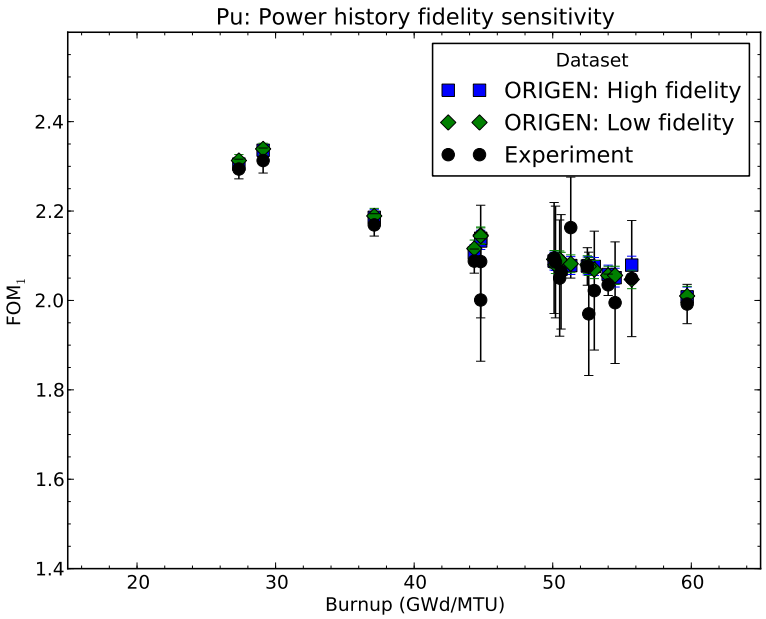

(a): Pu only

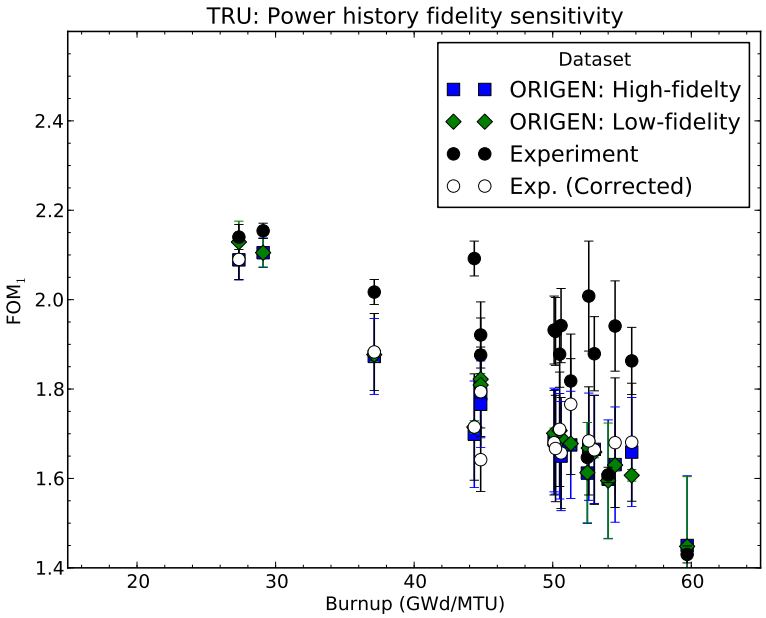

(b): TRU (Pu + MA)

Figure 6.6: Material attractiveness (FOM_1) for plutonium and transuranics in spent fuel as a function of burnup for the actual, non-uniform irradiation history ("high-fidelity") and a simplified irradiation history based on average cycle power ("low-fidelity").

TRU mixtures, the uncertainty effects grow larger with burnup (e.g., with increasing curium inventories), however the effect of these uncertainties is still limited (on the order of 5-10%) and does not appear to be a serious constraint to material attractiveness evaluation and discrimination. The uncertainties introduced at higher burnups for TRU mixtures appear to be dominated by uncertainties in ^{244}Cm, which is a both a significant contributor to the heat generation term as well as having high overall cross-section uncertainty (as well as high levels of uncertainty in experimental characterization).

Each of these conclusions has generally been assumed for the purposes of PR evaluation in the existing literature [4, 6, 9, 35, 42, 46, 53], however the results of this study conclusively indicate that these are valid assumptions in this context.

Additionally, the use of simplified irradiation history data (such as uniform irradiation histories) does not appear to introduce an unacceptable level of error into material attractiveness calculations, particularly compared to calculations based upon more faithful reproductions of the recorded irradiation history in depletion analysis tools such as ORIGEN-S.

As a consequence, the use of simplified models for nuclear fuel depletion (such as lattice-averaged models like ORIGEN-S) appears to be well-justified for the task of materials attractiveness evaluation. Additional simplifications, such as the use of uniform irradiation power histories, also appear to produce reasonable estimates with minimal additional error for material attractiveness calculations.

CHAPTER 7

Summary and Conclusion

A methodology for coupling isotopic characterization of nuclear fuel directly with models for intrinsic proliferation resistance has been developed to evaluate the dynamics of nuclear fuel cycle PR. Such an evaluation has been carried out across three different classes of fuel cycle: an "open" cycle with no actinide recycle, a "modified open" cycle with limited actinide recovery followed by disposal, and finally a "closed cycle" in which all actinides are recovered and recycled. These fuel cycles were then evaluated across a range of parameters, including fuel burnup (both uranium and recycled fuel), actinide coextraction strategies, reactor type, and cooling time before actinide recovery.

7.1 Trends in PR dynamics analysis

In general, the "strongest" PR dynamics effects were found for fuel cycle scenarios with longer "cascade" pathways for material changes; i.e., changes which occur "upstream" in the fuel cycle (such as changes in uranium fuel burnup) show the greatest impact as a function of burnup, particularly for pathways which involve other-burnup-dependent effects (e.g., production of minor actinides, etc.). These changes in the isotopic character of nuclear materials as they pass through the system persist ("cascade") throughout the remainder of the cycle, particularly in cases involving the recovery of actinides for re-irradiation.

By contrast, cycles with "limited" cascade chains (or limited overall burnup spaces) show very few dynamics effects; this is most evident for MOX/FBR fuel burnups (which show very little overall impact on PR, due to the limited cascade length).

In addition to a direct study of PR dynamics, the nature of nuclear fuel cycle PR was explored as a function of the assumed capabilities and intent of an assumed adversary state. For this evaluation, it was found that highly developed states with sophisticated indigenous fuel cycle capabilities are less impacted overall by "physical" barriers to proliferation (e.g., isotopic attractiveness, radiological hazard, etc.) and thus burnup effects appear to be least manifest in these particular scenarios. By contrast, relatively unsophisticated states desiring a reliable weapons yield (thus having sensitivity to the spontaneous fission neutron rate) show the greatest overall sensitivity to burnup effects, given the ingrowth of higher (even-numbered) plutonium species and other minor actinides with burnup, both of which serve both to increase the heat generation and spontaneous fission neutron rates of nuclear materials.

Additionally, overall PR between identical systems appears to decrease as a function of a state's concern over non-detection (e.g., overt vs. covert, where fuel cycles present higher overall PR for covert diversion and misuse scenarios), level of sophistication (i.e., physical barriers become more prominent for less sophisticated states, raising the overall level of proliferation resistance), and sensitivity to yield (i.e., attractiveness of materials found in civilian nuclear fuel cycles more quickly drops as a function of burnup for yield-sensitive adversaries due to the increasing spontaneous fission neutron rate).

7.2 Comparative evaluation of intrinsic fuel cycle PR

In general, the once-through cycles (which do not involve any separation of plutonium) have the highest overall intrinsic proliferation resistance; the DUPIC cycle, which involves only the removal of volatile fission products via dry processing ("voloxidation"), shows a similar overall PR behavior with only a minor penalty over the LWR-OT cycle due to the downgrading of the radiological barrier. Fuel cycles which involve the separation of pure plutonium (e.g., PUREX) show the lowest intrinsic PR, due to the lack of effective intrinsic barriers in the material separation stages. Coextraction of actinides appears to partially mitigate these vulnerabilities. Uranium dilution showing the highest overall single impact in this respect by inflating the bare sphere critical mass of the intact stream, while the coextraction of minor actinides also

appears to have a smaller yet additive effect upon intrinsic PR. Coextraction of neptunium (e.g., UREX+2/3/4 and UREX+2a/3a/4a) does not appear to have a significant effect upon overall system PR; while the addition of neptunium to MOX fuel does nominally decrease the material attractiveness of irradiated MOX fuel (e.g., by "spiking" the plutonium vector, producing additional ^{238}Pu, a high heat generator), such a change does not significantly impact the overall system PR. (Proposals for "plutonium spiking" of fresh uranium fuel were not evaluated in this study, however such a strategy may have a more substantial impact upon system PR given the longer cascade chain.)

Additionally, while the destruction of plutonium in MOX fuel does show some overall benefit in terms of decreasing the material attractiveness (as well as overall fissile material inventories), this benefit alone does not appear to offset the vulnerability introduced due to material separation stages. Further, while actinide coextraction (e.g., uranium and minor actinides) appears to show substantial potential for increasing intrinsic proliferation resistance, such measures do not appear to "restore" the intrinsic system PR to the "once-through" standard, thus indicating that proliferation safeguards would still be warranted under such advanced separations cases.

"Closed" cycles involving full actinide recycle appear to occupy a middle ground in terms of intrinsic PR between the aqueous-based "modified open" cycles (e.g., PUREX and UREX series) and the "open" (once-through) cycles. This is primarily due to the fact that plutonium is not isolated in such cycles (i.e., all actinides are recycled); likewise, such cycles involve a greater overall destruction of fissile material inventories than comparable MOX cycles. Of the separations strategies considered for "closed" cycles, electro-metallurgical separation (e.g., "pyroprocessing") shows a nominal advantage over aqueous-based advanced UREX-series treatments (e.g., UREX+1a) for lower fuel burnups.

7.3 Comparison of findings with prior PR studies

A useful comparison can be made as to the relative evaluations of fuel cycle proliferation resistance compared to prior studies conducted on this topic. In particular, a series of major evaluations of spent-fuel reprocessing alternatives have divided the separation strategies into the following groups, given as Table 7.1 [3, 42, 47].

These studies found little difference in overall proliferation resistance for state-level actors between groups W, X, and Y and only small differences in overall PR between groups

Table 7.1: Groupings of advanced fuel cycle reprocessing alternatives, as found in [3, 42, 47].

Group	Process(es)	Products
W	UREX+1b, Pyroprocessing	U + TRU
X	UREX+1, UREX+1a	TRU (+ Ln)
Y	COEX, UREX+2a/3a/4a	Pu + U (+ Np)
Z	PUREX, UREX+2/3/4	Pu (+ Np)

W, X, and Z and (i.e., group Z representing the baseline of pure plutonium and plutonium with neptunium). These differences are posited to be greater for non-state actors seeking to acquire materials for a nuclear device (which is not considered in this study). Additionally, it was concluded in this study that a state which chose to openly abrogate its international nonproliferation obligations (e.g., an overt breakout attempt) would find little difficulty in converting material from such processes into a usable form for weapons purposes.

Evaluations by Charlton imply a greater PR in UREX-series processes over PUREX treatments, however the significance of this difference is not explicitly quantified [9]. Likewise, NASAP concluded that co-processing could significantly increase intrinsic proliferation resistance by making isolation of plutonium (through illicit modification of facilities) more easily detected; likewise, uranium and plutonium blending (e.g., COEX) was concluded to produce a similar benefit [58]. It was additionally concluded that the addition of radiological barriers (e.g., through partial decontamination or material "spiking") could partially augment the intrinsic proliferation resistance of materials in reprocessing facilities, although such measures would be largely ineffective under an abrupt breakout scenario [58]. (For example, an overt breakout attempt would almost certainly be conducted in an abrupt rather than gradual fashion.)

A useful comparison in the dimensions of this study would be in the consideration of the different adversary classes considered (Table 5.20). For example, no significant differences were observed between the modified open cycles for the sophisticated state adversary engaged in a covert breakout attempt save for the UREX+1b cycle (rated at "low-plus" overall PR, compared to "low" for all other aqueous-based separations processes). This was likewise true for a sophisticated state in a covert proliferation attempt: again the UREX+1b cycle showed a slightly higher proliferation resistance than the alternatives ("medium-minus" compared to "low-plus"); each cycle also showed a nominally higher intrinsic PR for the covert breakout case as compared to the overt case.

For the unsophisticated state, this trend appears to persist; the division between the UREX+1b system appears to be the strongest over the PUREX baseline scenario in this case ("medium" versus "low-plus" for the yield-insensitive adversary). The overall delineation between the identified groups also appears to be the strongest in an adversary assumed to be of limited industrial capabilities; e.g., fuel cycles in Group W show an overall marked advantage over those in X and Y, which in turn also appear to cluster above those in Group Z. This can be seen in Figure 7.1.

As one observes from Figure 7.1, the differences observed per the groups in [3] and [42] appear to manifest in this evaluation as well; although one can also make out small but distinct differences among the groupings for the unsophisticated state. These differences are more stark for the yield-insensitive case (e.g., the UREX+1/1a/1b series, which all involve TRU streams, appear to converge for the yield-sensitive case), however they appear to manifest as discrete groups for both cases.

In as much, the evaluations of comparative proliferation resistance appear to be consistent with findings by [3, 42], with perhaps only minor disagreement over the significance of differences between spent fuel reprocessing alternatives.

A general comparison may also be made with the results of the SAPRA methodology study, with the caveat that such a study accounts explicitly for both proliferation resistance of both intrinsic and extrinsic (e.g., safeguards) barriers. Overall, the SAPRA methodology concluded that a fuel cycle with an an indigenous fuel cycle with reprocessing facilities shows a lower overall PR score than a cycle with only reactors and a fuel cycle with reactors and enrichment facilities (but no reprocessing) showing the lowest overall score [20]. While the methodology in this analysis definitively shows a significant penalty is incurred in terms of intrinsic PR for fuel cycles involving reprocessing (partially mitigated by advanced reprocessing strategies), this analysis found only a smaller detriment for the existence of enrichment facilities. However, it should be noted that this disagreement largely arises due to the accounting for safeguards in the SAPRA methodology; i.e., the SAPRA methodology's calculation of the relative PR due to the "diversion" and "transformation" aspects for materials in reprocessing and MOX fuel fabrication stages are substantially lower than those involving intact fuel [20]. However, SAPRA assigns the absolute lowest intrinsic PR to materials entering the enrichment stage (i.e., due to the comparatively low hazard and difficulty in handling raw uranium ore and corresponding lower level of safeguards associated with such stages).

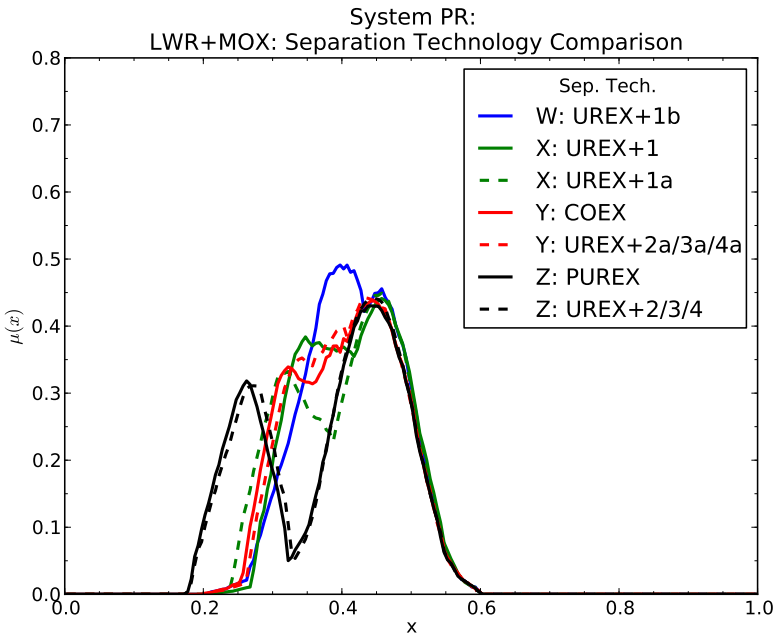

(a): Unsophisticated state, yield-insensitive (FOM_1)

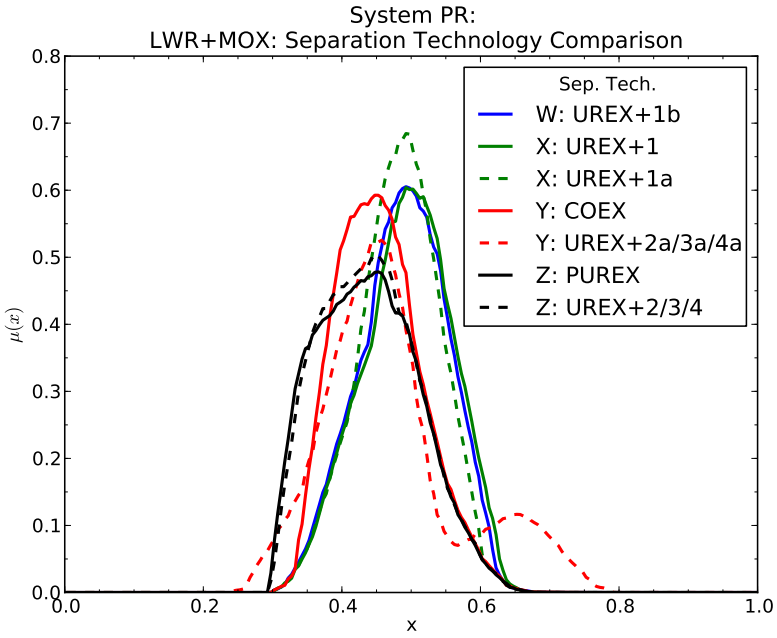

(b): Unsophisticated state, yield-sensitive (FOM_2)

Figure 7.1: Comparison of intrinsic PR for LWR + MOX fuel cycles featuring UREX series separation strategies, with a fixed LWR fuel burnup of 60 $\frac{\text{GWd}}{\text{MTU}}$ and MOX fuel burnup of 60 $\frac{\text{GWd}}{\text{MTHM}}$. Higher abscissa values represent higher intrinsic PR.

7.4 Impact of uncertainty and simplifications

The impact of particular simplifying assumptions used for isotopic calculations was also evaluated in this analysis as well as the relative impact of cross-section uncertainties upon the materials attractiveness calculation. For this analysis, a reaction cross-section (interpolated on variables of reactor power, uranium enrichment, and fuel burnup) based an infinite lattice (e.g., reflective boundary conditions) was used (ORIGEN-S) [43]. A comparison of the evaluated material attractiveness from this calculation was compared to the results from both a two-dimensional lattice physics calculation (TRITON) [43] as well as measured experimental values. This analysis found that for the purposes of material attractiveness calculations, little observed variance was found between the simplified reactor model (e.g., ORIGEN-S) and more sophisticated lattice physics models (such as TRITON); both show an excellent agreement to material attractiveness values calculated from isotopic assays performed upon experimental data. While the effect of features such as heterogeneous enrichment in surrounding lattices has been characterized by others [26, 27] and was evaluated to a limited degree in the lattice physics calculation, the impact of such features is generally small in terms of material attractiveness, insufficient to cause noticeable differences in material attractiveness values. The overall agreement was found to hold for both plutonium and transuranic mixtures (i.e., plutonium with minor actinides).

Additionally, the impact of cross-section uncertainties was evaluated through the use of calculated uncertainties in isotopic inventories, as calculated by Stover via the Efficient Subspace Method [56]. It was found that the impact of cross-section uncertainties upon material attractiveness are very small for plutonium inventories; these uncertainties were on the order of or smaller than uncertainties in experimental assays. Uncertainties associated with the material attractiveness of transuranic mixtures were notably higher (particularly as a function of burnup) due to the higher overall uncertainties in higher actinides (especially ^{244}Cm, which is a primary heat generator and thus strongly significant term in the material attractiveness of TRU mixtures). Such uncertainties were also manifest in the experimental data however, due to uncertainties in the same isotopes (e.g., ^{244}Cm). However, despite larger uncertainties, it nonetheless appears to be possible to adequately discriminate material attractiveness as a function of burnup for both plutonium and transuranic mixtures as a function of fuel burnup.

Finally, an evaluation of the relative impact of using a simplified reactor power history (e.g., a uniform irradiation power history based upon an overall average power) was also

evaluated, both in comparison to a calculation using a higher-fidelity reproduction of the reported irradiation power history as well as isotopic compositions from experimental measurements. This analysis found that the use of simplified power histories introduces some minor deviations in the material attractiveness values (particularly for transuranic mixtures, owing to minor differences in the calculated heat generation rate due to differences in the calculated transuranic isotope production). However, these discrepancies are generally minor and on the order of existing uncertainties introduced due to cross-section uncertainties. Therefore, the use of simplified irradiation histories (such as a uniform average power for the same discharge burnup value) can be justified as a reasonable simplification for such evaluations.

7.5 Recommendations for enhancing intrinsic fuel cycle PR

One well-understood conclusion regarding intrinsic fuel cycle proliferation resistance which is confirmed by this study is that fuel cycle systems which do not involve the separation of plutonium (with or without other actinides) inherently show the highest levels of proliferation resistance. For this study, this includes both the conventional once-through cycles (LWR-OT and CANDU) as well as the DUPIC-based modified open cycle (in which actinides are not separated from most fission products). A limitation of cycles such as the once-through cycles and DUPIC however is in the limited resource utilization; only a small fraction of fissionable uranium resources are consumed in any of these fuel cycles.

Additionally, the issue of proliferation resistance must also be balanced against other competing concerns, such economics (including the recoverable resource present in spent nuclear fuel) as well as long-term management of spent fuel. Given the present political difficulty in opening a permanent geological repository in the United States, it is extremely likely that some use of actinide recovery will be utilized to either partially or fully close the nuclear fuel cycle some time in the future. Thus it is of a key political interest both domestically and as a matter of international policy to pursue and promote fuel cycle strategies which carry the highest intrinsic proliferation resistance.

The findings of this study first confirm findings of prior studies that in the case of an unsophisticated state adversary, the coextraction of other actinides with plutonium (particularly uranium but also minor actinides) can substantially increase the proliferation resistance of materials against direct diversion in reprocessing-related stages, which are some of the most

vulnerable stages in the fuel cycle. Likewise, the inclusion of a radiological barrier through strategies such as limited decontamination (e.g., UREX+1 and pyroprocessing) also appears show nominal positive impact on overall proliferation resistance for unsophisticated states, confirming the findings of studies such as NASAP [58].

Likewise, the pursuit of higher fuel burnups (thus diminishing the overall attractiveness of nuclear material from civilian fuel cycles) appears to be a universal promoter of intrinsic proliferation resistance, particularly for cycles involving the coextraction of minor actinides. Therefore, research and development into strategies for increasing fuel burnup limits (e.g., through novel fuel and materials development) would aid both the objectives of minimizing long-term waste and promoting intrinsic proliferation resistance.

An additional technique not explored in detail in this work but suggested in other literature is the doping of LWR uranium fuel with neptunium for the production of ^{238}Pu (e.g., "protected plutonium production," or P_3) [29, 49]. While the effect of neptunium doping was found to be relatively limited for the MOX-based cycles (e.g., UREX+2/3/4 and UREX+2a/3a/4a in part due to the relatively short "cascade" for the spent MOX fuel), such an effect may be capable of enhancing overall system PR for partially-closed and fully-closed cycles if neptunium doping is introduced earlier in the fuel cycle (e.g., in LWR fuel).

However, a key issue which should be noted for each of these recommendations is that these strategies, based on the promotion of physical barriers to proliferation, are generally most effective only for states with limited industrial and indigenous nuclear fuel cycle capacities (e.g., unsophisticated states). For sophisticated states with fully developed advanced fuel cycles, physical measures such as actinide coextraction and increasing burnup provide only a very limited proliferation resistance benefit against a nationally-directed diversion attempt (i.e., mostly through increasing the likelihood of detection by increasing the total mass of material required for diversion). Likewise, if subsequent reprocessing for plutonium extraction is assumed for fuel among even unadvanced states (e.g., through the use of an undeclared reprocessing facility: the "plutonium-only" pathway), the benefits of particular strategies such as coextraction are largely mooted. However, other benefits, such as the diminished attractiveness of the plutonium vector due to higher burnup or heat spiking, are still retained.

In light of this, the need for extrinsic safeguards measures for any cycle involving actinide separation is quite clear. While the technical measures outlined above can help to augment intrinsic proliferation resistance, no fuel cycle feature studied in this cycle indicates a par-

ticular area where such measures obviate the need for safeguards or provide increases in intrinsic proliferation resistance beyond that of the reference once-through case.

Finally, despite the overall limitations of physical barriers (particularly for sophisticated states), strategies such as "fully closed" fuel cycles employed advanced UREX-series aqueous processes or pyroprocessing for full actinide recovery and destruction in fast-spectrum reactors appears to show somewhat higher overall proliferation resistance then partial recycle cases, even for relatively sophisticated states. Thus, it is recommended that decisions to close the nuclear fuel cycle should emphasize "fully closed" options which involve the deployment of fast-spectrum reactors for full actinide consumption. Beyond the relative proliferation benefit of such cycles compared to "partially" closed cycles, the full consumption of actinides provides tangible benefits for the long-term management of nuclear waste, largely eliminating the need for engineering on million-year timescales. (While other long-lived fission products such as ^{99}Tc and ^{129}I still remain, managing these isotopes separately may prove to be an lesser challenge than the management of intact fuel, which involves both the limitation of heat loading in a repository as well as potential public dose exposure from radionuclide transport.)

7.6 Recommendations for future work

While every reasonable effort was made to explore a robust and objective set of criteria for barrier effectiveness, the effectiveness evaluation for particular barriers (such as material detectability) remain as qualitative assessments only. It is recommended that further developments of the Fuzzy Logic Barrier method focus upon means of characterizing barriers which may possibly be better characterized by physical signals information currently available due to the direct coupling with nuclear materials characterization analysis.

Further, the framework considered for this model considers only the impact of intrinsic barriers to proliferation, neglecting extrinsic measures such as institutional controls, international agreements (such as the NPT and the Additional Protocol) and other proliferation safeguards. Therefore, a logical direction for future evolution in this analysis would be to consider the impact and effectiveness of extrinsic safeguards measures, particularly through the use of available physical signals information from ORIGEN-S (e.g., radiological, nuclear, and thermal data), which may allow for the direct simulation of safeguards performance (e.g., non-destructive analysis, material assay, etc.).

Finally, given that the methodology for coupled isotopic characterization is not limited to the use of the Fuzzy Logic Barrier model alone, future studies could be conducted to directly compare different approaches to proliferation resistance evaluation, such as that proposed by Charlton [9], thus affording the ability to benchmark a suite of models based upon identical fuel cycle configurations. Such an approach thus enables a better calibration and analysis of different approaches to nuclear fuel cycle proliferation resistance assessment. Additionally, the coupling approach could be conceivably employed to fuel cycle mass loading models such as that outlined in [34], thus enabling the pursuit of multi-objective optimization, such as optimization both on intrinsic system PR as well as factors such as economics and repository capacity.

7.7 Final remarks

In addition to the application demonstrated in this work of coupling isotopic analysis to models for proliferation resistance, the coupling approach developed in this work has numerous other potential applications. For example, given the physical signals information present in the ORIGEN-S output (whose extraction is facilitated in this process), it would be a relatively trivial undertaking to directly couple isotopic characterization with models for safeguards (and in particular, NDA systems) in fuel cycle facilities, as is proposed in [18]. Such a technique has obvious applications to evaluating safeguards response and the adequacy of proposed safeguards designs for given detection targets, particularly in response to changing fuel conditions such as burnup or chemical separation efficiency.

Further, as outlined above, this technique can be applied to the task both of coupling isotopic characterization with other models for proliferation resistance, as well as enabling simultaneous benchmarking of multiple models. Given the continued interest in proliferation resistance evaluation, such a process would be a logical advance in PR modeling research.

An additional task for further analysis would be in an expansion of the fuel cycle configurations explored through this PR study. Examples of such would be in features such as neptunium doping for "protected plutonium production" in LWR fuel [29, 39, 49], alternative reactor technologies such as the Molten Salt Reactor and its variants, as well as a more detailed characterization of advanced reactor concepts such as the variety of fast spectrum reactor proposals.

Finally, again as proposed prior, the coupling of isotopic characterization can have

numerous benefits to broader fuel cycle models in general, particularly those concerned with multi-attribute optimization, such as the repository capacity and mass loading model proposed in [34] as well as fuel cycle modeling and optimization codes such as VISION [61], namely by introducing a method for on-the-fly calculation of the evolving physical character of fuel.

In as much, the coupling process proposed allows for a very detailed evaluation of nuclear material properties throughout the fuel cycle system in response to changes in fuel cycle configurations such as reactor type, enrichment, cooling time, reprocessing strategies, and so forth.

REFERENCES

[1] Vladimir Artisyuk, Masaki Saito, Alan Takibayev, and Hiroshi Sagara. Radiation Dose as a Barrier against Proliferation for Advanced Fuel Compositions. *Journal of Nuclear Science and Technology*, 45(10):1009–1015, 2008.

[2] ASTM Committee C26.02 – Fuel and Fertile Material Specifications. Standard Specification for Sintered (Uranium-Plutonium) Dioxide Pellets. West Conshohocken, PA, 2008. ASTM C833-01, DOI: 10.1520/C0833-01R08.

[3] R. Bari, L-Y Cheng, J. Phillips, J. Pilat, G. Rochau, I. Therios, R. Wigeland, E. Wonder, and M. Zentner. Proliferation Risk Reduction Study of Alternative Spent Fuel Processing. Technical report, Brookhaven National Laboratory, July 2009. BNL-90264-2009-CP.

[4] Robert Bari, 2011. Private communication.

[5] C.G. Bathke and E.A. Schneider. Report of the COSI and NFCSim Benchmark. Technical report, Los Alamos National Laboratory, 2003. LA-UR-03-8051.

[6] Charles G. Bathke et al. An Assessment of the Attractiveness of Material Associated with a MOX Fuel Cycle from a Safeguards Perspective. In *Proceedings of the Institute of Nuclear Materials Management, 50th Annual Meeting*, July 2009.

[7] Ulrich Bodenhofer. A General Framework for Ordering Fuzzy Numbers with Respect to Fuzzy Orderings. In *Proceedings of the 8th International Conference on Information Processing and Management of Uncertainty in Knowledge-Based Systems (IPMU 2000)*, volume II, pages 1071–1077, July 2000.

[8] BOOST C++ libraries. `http://www.boost.org`, 2011.

[9] William S. Charlton, Ryan F. LeBouf, Carl Beard, Sheldon Landsberger, and Michael Whitaker. Proliferation Resistance Assessment Methodology for Nuclear Fuel Cycles. *Nuclear Technology*, 157:143–145, February 2007.

[10] C. W. Coates, B. L. Broadhead, A. M. Krichinsky, R. W. Leggett, M. B. Emmett, and J. B. Hines. Radiation Effects on Personnel Performance Capability and a Summary of Dose Levels for Spent Research Reactor Fuels. Technical report, Oak Ridge National Laboratory, December 2005. ORNL/TM-2005/261.

[11] E. D. Collins, G. D. Del Cul, J. E. Rushton, and K. A. Williams. A Practical Solution to Used Nuclear Fuel Treatment to Enable Sustained Nuclear Energy and Recovery of Vital Materials. In *Proceedings of the Institute of Nuclear Materials Management, 51st Annual Meeting*, July 2010.

[12] E.D. Collins, D.E. Benker, W.D. Bond, D.O. Campbell, and B.B. Spencer. Development of the UREX+ Co-Decontamination Solvent Extraction Process. In *GLOBAL 2003*, 2003.

[13] E.D. Collins, D.E. Benker, L.L. Felker, R.D. Taylor, G.D. Del Cul, B.B. Spencer, W.D. Bond, and D.O. Campbell. Development of the UREX+2 Flowsheet–An Advanced Separations Process for Spent Fuel Processing. *Transactions of the American Nuclear Society*, 93(1):739–740, November 2005.

[14] Didier Dubois and Henri Prade. Ranking Fuzzy Numbers in the Setting of Possibility Theory. *Information Sciences*, 30:183–224, 1983.

[15] P.C. Durst, R. Wallace, I. Therios, M.H. Ehinger, R. Bean, D.N. Kovacic, A. Dougan, K. Tolk, and B. Boyer. Advanced Safeguards Approaches for New Reprocessing Facilities. Technical report, Pacific Northwestern National Laboratory (PNNL), June 2007. PNNL-16674.

[16] Gisella Facchinetti, Roberto Ghiselli Ricci, and Sivlia Muzzioli. Note on Ranking Fuzzy Triangular Numbers. *International Journal of Intelligent Systems*, 13:613–122, 1998.

[17] I.C. Gauld. MOX Cross-Section Libraries for ORIGEN-ARP. Technical Report ORNL/TM-2003/2, Oak Ridge National Laboratory, July 2003. `http://www.ornl.gov/sci/scale/pubs/116015.pdf`.

[18] I.C. Gauld, S.M. Bowman, and B.D. Murphy. Application of ORIGEN to Spent Fuel Safeguards and Non-Proliferation. In *Proceedings of the INMM 47th Annual Meeting*, July 2006.

[19] I.C. Gauld, G. Illas, B.D. Murphy, and C.F. Weber. Validation of SCALE 5 Decay Heat Predictions for LWR Spent Nuclear Fuel. Technical Report NUREG/CR-6972 / ORNL/TM-2008/072, U.S. NRC, February 2010. `http://www.nrc.gov/reading-rm/doc-collections/nuregs/contract/cr6972/cr6972.pdf`.

[20] Dominique Grenèche. A Practical Tool to Assess the Proliferation Resistance of Nuclear Systems: the SAPRA Methodology. *ESARDA BULLETIN*, 39:41–49, October 2008.

[21] W.H. Hannum, D.C. Wade, H.F. McFarlane, and R.N. Hill. Nonproliferation and Safeguards Aspects of the IFR. *Progress in Nuclear Energy*, 31(1/2):203–217, 1997.

[22] J.A. Hassberger. Application of Proliferation Resistance Barriers to Various Existing and Proposed Nuclear Fuel Cycles. Technical report, Lawrence Livermore National Laboratory, 2001. Report UCRL-IS-147001.

[23] Robert N. Hill. Comparison of Fast Reactor Transmutation Potential. Technical report, Argonne National Laboratory, September 2003. ANL-AFCI-115.

[24] E. A. Hoffman. Mixed-Oxide with Enriched Uranium Fuels In LWRs. Technical report, Argonne National Laboratory, March 2006. ANL-AFCI-164.

[25] IAEA Department of Safeguards. Proliferation Resistance Fundamentals for Future Nuclear Energy Systems. Technical report, International Atomic Energy Agency (IAEA), December 2002. IAEA STR-322.

[26] G. Ilas, I.C. Gauld, F.C. Difilippo, and M.B. Emmett. Analysis of Experimental Data for High Burnup PWR Spent Fuel Isotopic Validation–Calvert Cliffs, Takahama, and Three Mile Island Reactors. Technical Report NUREG/CR-6968 / ORNL/TM-2008/071, U.S. NRC, Office of Nuclear Regulatory Research, February 2010. `http://www.nrc.gov/reading-rm/doc-collections/nuregs/contract/cr6968/cr6968.pdf`.

[27] G. Ilas, I.C. Gauld, and B.D. Murphy. Analysis of Experimental Data for High Burnup PWR Spent Fuel Isotopic Validation–ARIANE and REBUS Programs (UO_2 Fuel). Technical Report NUREG/CR-6969 / ORNL/TM-2008/072, U.S. NRC, Office of Nuclear Regulatory Research, February 2010. `http://www.nrc.gov/reading-rm/doc-collections/nuregs/contract/cr6969/cr6969.pdf`.

[28] Jacob J. Jacobson, Gretchen E. Matthern, Steven J. Piet, and David E. Shropshire. VISION: Verifiable Fuel Cycle Simulation Model. In *Advances in Nuclear Fuel Management IV (ANFM 2009)*, April 2009.

[29] Yoshiki Kimura, Masaki Saito, and Hiroshi Sagara. Development of Methodology of Plutonium Categorization (III) – Effect of Radiation. *Transactions of the American Nuclear Society*, 103:145–145, November 2010.

[30] Wong Il Ko and Ho Dong Kim. Analysis of Nuclear Proliferation Resistance of DUPIC Fuel Cycle. *Jounal of Nuclear Science and Technology*, 38(9):757–765, September 2001.

[31] J. J. Laidler, J. E. Battles, W. E. Miller, J. P. Ackerman, and E. L. Carls. Development of Pyroprocessing Technology. *Progress in Nuclear Energy*, 31(1/2):131–140, 1997.

[32] LANL. *MCNP User's Manual*. Los Alamos National Laboratory, Los Alamos, New Mexico, LA-CP-05-0369 edition, April 2005. Available from Radiation Safety Information Computational Center at Oak Ridge National Laboratory as CCC-74.

[33] Jun Li. *A Methodology to Evaluate Nuclear Waste Transmutation/Fuel Cycle Systems*. PhD thesis, North Carolina State University, 2006.

[34] Jun Li, Anthony Scopatz, Man-Sung Yim, and Erich Schneider. The Sensitivity of Fuel Cycle Performance to Separation Efficiency. *Nuclear Engineering and Design*, 240(3):511 – 523, 2010. DOI: 10.1016/j.nucengdes.2009.02.004.

[35] Jun Li, Man-Sung Yim, and David McNelis. Assessing Proliferation Resistance of Nuclear Fuel Cycle Systems Using a Fuzzy-Logic Barrier Method. *Nuclear Technology*, 3(162):292–307, 2008.

[36] Tian-Shy Liou and Mao-Jiun J. Wang. Ranking Fuzzy Numbers with Integral Value. *Fuzzy Sets and Systems*, 50:247–255, 1992.

[37] Allison Macfarlane, Frank von Hippel, Jungmin Kang, and Robert Nelson. Plutonium Disposal, the Third Way. *Bulletin of the Atomic Scientists*, 57(3):53–57, May/June 2001.

[38] matplotlib Python libraries. `http://matplotlib.sourceforge.net`, 2011. v1.0.0.

[39] Selena Ng, Bernard Guesdon Dominique Grenèche, Richard Vinoche, Marc Delpech, Florence Dolci, Hervé Golfier, and Christine Poinot-Salanon. Neptunium in the Fuel Cycle: Nonproliferation Benefits Versus Drawbacks. *Nuclear Technology*, 164:13–19, October 2008.

[40] Nuclear Energy Agency (NEA). *Advanced Nuclear Fuel Cycles and Radioactive Waste Management*. Organization for Economic Cooperation and Development (OECD), 2006. NEA no. 5990.

[41] Office of Civilian Radioactive Waste Management. *Yucca Mountain Science and Engineering Report, Revision 1*. United States Department of Energy, Washington, D.C., February 2002. DOE/RW-0549-1, `http://www.energy.gov/media/SER.PDF`.

[42] Office of Nonproliferation and International Security (NNSA). Nonproliferation Impact Assessment for the Global Nuclear Energy Partnership Programmatic Alternatives (Draft), 2008. `http://brc.gov/library/docs/GNEP_NPIA.pdf` (Accessed: January 2011).

[43] ORNL. *SCALE: A Modular Code System for Performing Standardized Computer Analyses for Licensing Evaluations*. Oak Ridge National Laboratory, Oak Ridge, Tennessee, ORNL/TM-2005/39, Version 6.0, Vols. I-III edition, January 2009. Available from Radiation Safety Information Computational Center at Oak Ridge National Laboratory as CCC-75.

[44] Jan Jin Park, Myung Seung Yang, Ki Kwang Bae, Hang Bok Choi, Ho Dong Kim, Jong Ho Kim, and Hyung Soo Park. Technology and Implementation of the DUPIC Concept for Nuclear Spent Fuel in the ROK. Technical report, Korea Atomic Energy Research Institute, 2000.

[45] C.V. Parks. Overview of ORIGEN2 and ORIGEN-S: Capabilities and Limitations. In *International High-Level Radioactive Waste Management Conference*, April 1992.

[46] PRPPWG. Evaluation Methodology for Proliferation Resistance and Physical Protection of Generation IV Nuclear Energy Systems, Revision 5. Technical report, Brookhaven National Laboratory, 2006. Brookhaven National Laboratory Report, BNL-75546-2006-CP.

[47] PRPPWG. PR&PP Evaluation: ESFR Full System Case Study Final Report. Technical report, Gen IV International Forum (GIF), 2009. GIF/PRPPWG/2009/002.

[48] Thomas Saaty. A Scaling Method for Priorities in Hierarchical Structures. *Journal of Mathematical Psychology*, 15:234–281, 1977.

[49] Masaki Saito. Protected Plutonium Production by Transmutation of Minor Actinides for Peace and Sustainable Prosperity. In *GLOBAL 2009*, 2009. Paper 9397.

[50] William Siler and James J. Buckley. *Fuzzy Expert Systems and Fuzzy Reasoning*. Wiley and Sons, 2005.

[51] Mike Simpson, 2011. Private communication.

[52] S.E. Skutnik and I.C. Gauld. OASIS: A Simplified User Interface for Advanced Fuel Cycle Analysis in SCALE. *Transactions of the American Nuclear Society*, 101:243–244, 2009.

[53] S.E. Skutnik and M.-S. Yim. Evaluation of Fuel Cycle Proliferation Resistance Dynamics Using Coupled Isotopic Analysis. *Transactions of the American Nuclear Society*, 103:187–188, 2010.

[54] S.E. Skutnik, M.-S. Yim, and J. Li. Reevaluating Barrier Attribute Analysis for Non-Proliferation Applications Using Fuzzy Logic. *Transactions of the American Nuclear Society*, 99:205–207, November 2008.

[55] Steve Skutnik, Jun Li, Man-Sung Yim, and David McNelis. Evaluating Proliferation Resistance and Security Needs of Nuclear Fuel Cycle Technologies through a Fuzzy-Logic Barrier Model. In *Proceedings of the Institute of Nuclear Materials Management, 50th Annual Meeting*, July 2009.

[56] Tracy E. Stover. Quantification of Back-End Fuel Cycle Metrics Uncertainties Due to Cross Sections. Master's thesis, North Carolina State University, 2007.

[57] TOPS Task Force. Technological Opportunities to Increase the Proliferation Resistance of Global Civillian Nuclear Power Systems (TOPS). Technical report, Nuclear Energy Research Advisory Committee (NERAC), 2001.

[58] United States Department of Energy. *Nuclear Proliferation and Civilian Nuclear Power, Report of the Nonproliferation Alternative Systems Assessment Program*, volume II. DOE, 1980. `http://www.osti.gov/bridge/purl.cover.jsp?purl=/5352094-2m8dQu/` (Accessed January 2011).

[59] George F. Vandegrift, Monica C. Regalbuto, Scott Aase, Allen Bakel, Terry J. Battisti, Delbert Bowers, James P. Byrnes, Mark A. Clark, Jeff W. Emery, John R. Falkenberg, Artem V. Gelis, Candido Pereira, Lohman Hafenrichter, Yifen Tsai, Kevin J. Quigley, and Mark H. Vander Pol. Designing and Demonstration of the UREX+ Process Using Spent Nuclear Fuel. In *Advances for Future Nuclear Fuel Cycles (ATATLANTE 2004)*, 2004.

[60] A. M. Yacout and T. A. Taiwo. Isotopic Vector Estimation Methods for System Dynamics Fuel Cycle Models. Technical report, Argonne National Laboratory, August 2008. ANL-AFCI-240.

[61] A.M. Yacout, J.J. Jacobson, G.E. Matthern, S.J. Piet, D.E. Shropshire, and C. Laws. Vision–Verifiable Fuel Cycle Simulation of Nuclear Fuel Cycle Dynamics. In *Nuclear Waste Management Symposium*, February 2006.

[62] R.R. Yager. Ranking Fuzzy Subsets Over the Unit Interval. In *Proceedings of the 1978 CDC*, pages 1435–1437, 1978.

[63] R.R. Yager. A Procedure for Ordering Fuzzy Subsets on the Unit Interval. *Information Sciences*, 24:143–161, 1981.

[64] Myung Seung Yang, Joo Hwan Park, Won Il Ko, Kee Chan Song, Kun Mo Choi, and Jin Kyoung Kim. Evaluation of Proliferation Resistance Using the INPRO Methodology. *Nuclear Engineering and Technology*, 39(2):149–160, April 2007.

[65] Meng Yue, Lap-Yan Cheng, and Robert A. Bari. Relative Proliferation Risks for Different Fuel Cycle Arrangements. *Nuclear Technology*, 165:1–17, January 2009.

APPENDICES

APPENDIX A

Care and Feeding of the Fuzzy Logic Barrier Model

In this appendix, aspects of the operation and maintenance of the Fuzzy Logic Barrier model with coupled isotopic characterization are discussed, including analysis options present in the FLB framework and construction of fuel cycle case input files.

A.1 Requirements

The Fuzzy Logic Barrier model requires the following software/dependencies for proper compilation and execution:

- SCALE 6.1 or later, with the OASIS module present [43, 52]
- The BOOST C++ libraries [8]
- A C++ compiler
- The "matplotlib" package for Python (optional; used for graph output scripts) [38]

To compile the Fuzzy Logic Barrier model, the compiler flag for the "include" directory should include the BOOST main directory and the linker flag should point to the BOOST pre-compiled libraries (e.g., `$BOOST_MAIN\lib`).

The following directories must also be created in the directory where the the main executable resides:

- `.\output` (main output directory)
- `.\output\barriers_out` (symbolic barrier output)
- `.\output\centroid` (level & system centroid values for each system)
- `.\output\fuzzy_out` (fuzzy number output for each level/system)
- `.\output\ranking` (fuzzy outranking values for each system)
- `.\output\stage_weights` (calculated stage weights for each system)

Each of the above output directories contains the relevant output files for the FLB calculation. `barriers_out` gives a symbolic listing of barriers (in the order presented in [22]); `centroid` gives the stage and system centroid values for each system evaluated; `fuzzy_out` contains the values of the stage and systems fuzzy functions ($\mu(x)$) and is thus used for reconstructing the stage and system fuzzy numbers; `ranking` contains the fuzzy outranking data for each system (e.g., the assumed system rank is the highest linguistic barrier or barriers for which the ranking value is > 0.5); finally, `stage_weights` contains the stage weight data (calculated based upon the heavy metal inventory, mass flow, etc.) used for the calculation of the system fuzzy number (from the respective stage fuzzy functions).

A.2 Execution and analysis options

Several user options are available when executing the FLB model from the command line; these options are presented in the following sections.

Generally, the model is executed from the command line using the following structure (Figure A.1).

```
FLBM.exe batch_file_name [-adversary_flag] [-FOM_flag]
```

Figure A.1: Syntax for calling the FLB model from the command line.

The `-adversary_flag` and `-FOM_flag` parameters are optional; the model defaults to assumptions of an unsophisticated state, covert using FOM_1 for isotopic attractiveness assessment (e.g., yield-insensitive). The adversary flag impacts which barrier weight set is used for barrier weights, while the FOM flag selects whether FOM_1 or FOM_2 is used for material attractiveness evaluation.

Options for the adversary type flag are: `-sso` (sophisticated state, overt), `-ssc` (sophisticated state, covert) and `-usc` (unsophisticated state, covert). Options for the FOM evaluation are (as expected) `-fom1` and `-fom2`.

A.3 Case construction

In this section, the procedures for constructing batch input files (used to execute a series of individual cases) and case input files (e.g., a sequence of fuel cycle stages composing a fuel cycle system for evaluation) is presented.

A.3.1 Batch input file structure

Each batch input file is used to locate the individual case input files and assign a corresponding case ID and legend entry (for graphical output). One or more individual case files may be specified, however a case ID and legend entry (for graph output) are required for each case. Likewise, the graph title and legend title options on the first line are also required; the example syntax is shown as Figure A.2.

```
graph_title     legend_title
./path/to/case_1.txt     case1_ID     case1_legend_entry
./path/to/case_2.txt     case2_ID     case2_legend_entry
...
```

Figure A.2: Batch file construction for individual cases.

A.3.2 Individual case input structure

Individual fuel cases are constructed as a series of modular levels. The number of required "user-specified" barriers will vary based on the level type (e.g., 8 user-specified barriers for non-ORIGEN level types, and 5 user-specified barriers for ORIGEN-based levels).

The general structure of an individual fuel cycle level is shown as Figure A.3.

```
LEVEL_TYPE { ( par1 val1 ) ( par2 val2 ) ... } { bar1 bar2 ... }
```

Figure A.3: General syntax for FLB level specification.

A level type is specified (`LEVEL_TYPE`), followed by a series of parameter/value combinations (`( param value )`) in braces, followed by a series of linguistic barrier rankings (for users-specified barriers) in braces (e.g., `{ VH M- ... }`).

Linguistic rankings for barrier effectiveness can be any of the following: "I" (Ineffective), "L" (Low) "M" (Medium) "H" (High), or "VH" (Very High); corresponding hedge modifiers may also be used (e.g., "L+" or "M–", etc.).

The number and order of user-specified barrier rankings depends on whether a pre-reactor or post-reactor level is being specified. Pre-reactor stages expect 8 input barriers; the barriers and their corresponding input order is:

1. Radiological
2. Mass & bulk
3. Material detectability
4. Facility unattractiveness
5. Facility accessibility
6. Available mass
7. Facility diversion detectability
8. Skills, expertise, & knowledge

Other barriers (isotopic, chemical, and time) are inferred from the level type or user parameters (i.e., time).

For ORIGEN/OASIS based levels (e.g., irradiation and post-irradiation), 5 input barriers are expected from the user; these are:

1. Material detectability
2. Facility unattractiveness
3. Facility accessibility
4. Facility diversion detectability
5. Skills, expertise, & knowledge

All other barriers (isotopic, chemical, radiological, mass & bulk, available mass, time) are either calculated directly or inferred from the material form (e.g., chemical) based on the stage type and other factors.

General options

Options common to all level types include the specification of the level title (`(( title __ ))`), time (`(( time __ ))`), and time units (`(( tunits __ ))`), and an option to skip the level PR calculation (`(( skip __ ))`). For all "generic" level types and the LWR irradiation stages, an enrichment parameter can be used to specify the relative enrichment of ^{235}U as `enrich`. A listing of commands is given as Table A.1.

For Adversary Pathway Analysis, an additional parameter can be employed for ORIGEN-based stages: `atk_path`. The options for `atk_path` are given as Table A.2.

"Generic" level types

Several aliases for the "generic" level types (e.g., no OASIS operations) are used (Table A.3); an alias is assumed from the first several letters of an identified level type, where the rest of the level type name is ignored (e.g., any name may be used in place of the wildcard symbol *); for example, the level names `enrichment` and `enriched_storage` will each correspond to a level type assuming enriched UO_2 powder, with no OASIS operations assumed. Level names are not case sensitive, thus any combination of upper and lower-case letters may be used.

Table A.1: Generic commands for FLB level inputs

Command	Description
`title`	Level title (no spaces)
`id`	OASIS/ORIGEN level ID (no spaces)
`time`	Time (numeric)
`tunits`	Time units (`sec`, `min`, `hours`, `days`, `months`, or `years`)
`enrich`	^{235}U enrichment (%)
`mtu`	Basis of heavy metal (MTU / MTHM)
`skip`	Skip stage (i.e., do not calculate stage PR); values are `true` or `false`
`outfile`	Named output for fuel concentrations (string, no spaces); ORIGEN-related stages (irradiation, decay, reprocessing, etc.) only.
`atk_path`	Flag for adversary pathway in APA analysis; irradiation and post-irradiation stages only

Table A.2: Adversary pathway flag values

Value	Pathway
–1	Uranium-only
0	Plutonium-only
1	TRU only (Pu + minor actinides)
2	"Whole stream" (e.g., all products)
3	MA only (e.g., Np/Am/Cm)
4	Am/Cm only

Irradiation level types

Several fuel irradiation aliases exist to handle different irradiation case types; these aliases are listed as Table A.4.

Decay level types

For decay levels, the only applicable commands are the `stream`, `time`, and `tunits`, `title`, and `id` commands, as explained prior. Each decay level requires the use of the `stream` command in order to select a stream for decay.

Several aliases to the decay level type exist to facilitate additional clarity in stages related

Table A.3: Generic (non-OASIS) fuel cycle level aliases used

Alias	Description
`mine*`	Uranium mining
`mill*`	Uranium milling
`enrich*`	Uranium enrichment, storage, and transport
`conv*`	Uranium conversion, storage, and transport
`leu*`	LEU fuel fabrication, storage and transport

Table A.4: Irradiation level aliases for FLB level inputs

Alias	Description
`irradiate`	LEU fuel irradiation; requires `enrichment` parameter
`CANDU_irradiate`	CANDU HWR natural uranium fuel irradiation
`MOX_irradiate`	MOX fuel irradiation; requires `step` parameter for fuel concentrations
`FBR_irradiate`	FBR fuel irradiation; requires `step` parameter for fuel concentrations
`DUPIC_irradiate`	Re-irradiation of PWR fuel in CANDU; requires `step` parameter for fuel concentrations

to partially and fully-closed cycles; likewise, these aliases are automatically used to assign factors such as the associated chemical form of the fuel. A listing of these aliases is given as Table A.6. Wildcards are noted as before, using the asterisk (*) after a name, indicating that only the prefix is needed (e.g., any string following is ignored by the model, but can be employed by the user for clarifying input).

The `snf*`, `rm*`, and `aw*` aliases each have an associated adversary attack pathway by default (likewise, `snf*` has an associated chemical form of intact SNF), which can be overridden using the `( atk_path )` parameter.

Reprocessing levels

The commands for reprocessing level commands are given as Table A.7. Likewise, the reprocessing level has one special alias, `voloxidation`, in which volatile fission product gases are removed at fixed concentrations (see Table 4.21); thus, the only parameters used for this case are the stream number (`stream`), decay time (`decay`) and time units (`tunits`).

Table A.5: Irradiation-related commands for FLB level inputs

Command	Description
`enrich`	^{235}U enrichment (%; LWR only)
`down`	Down fraction [0,1)
`burnup`	Total fuel burnup ($\frac{\text{MWd}}{\text{MTHM}}$)
`ncyc`	Number of irradiation cycles
`spow`	Specific power ($\frac{\text{MW}}{\text{MTHM}}$)
`mtu`	Basis value (MTU / MTHM)
`mod`	Moderator density ($\frac{\text{g}}{\text{cm}^3}$)
`nlib`	Number of libraries per irradiation cycle
`arplib`	ARP cross-section library name (e.g., `w17x17`, `mox14x14`, etc. – c.f. [43])
`stream`	Fuel concentrations from a prior step (re-irradiation only; e.g., MOX, FBR, and DUPIC)
`force_mox`	"Forces" ARP interpolation of Pu vector for MOX libraries (e.g., for ^{239}Puvectors $< 50\%$); options are `true` and `false` (MOX cases only)

Table A.6: Decay level aliases for FLB level inputs

Alias	Description
`decay`	Generic decay level
`snf*`	SNF storage/decay
`rm*`	Recovered actinides storage/decay
`aw*`	Actinide waste storage/decay

MOX fuel fabrication

Two different options are available for MOX fuel fabrication; MOX fuel fabrication through fuel blending, MOXBLEND (e.g., blending of depleted uranium from the reprocessing stream with the Pu/TRU vector therein), and the direct specification of the MOX fuel plutonium vector (and associated impurities), MOXSPEC.

Commands for MOX fuel blending are given as Table A.9; this has generally been the preferred method for MOX fuel fabrication (given the relative ease of handling advanced UREX series treatments, i.e. correctly calculating the relative distribution of individual plutonium species and added impurities (e.g., minor actinides).

The commands for the MOX fuel user-specification case are given as Table A.10; this

Table A.7: Reprocessing-related commands for FLB level inputs

Command	Description
`fr_pu`	Extraction efficiency of plutonium [0,1]
`fr_np`	Extraction efficiency of neptunium [0,1]
`fr_am`	Extraction efficiency of americium [0,1]
`fr_cm`	Extraction efficiency of curium [0,1]
`fr_ln`	Extraction efficiency of all lanthanides [0,1]
`u_dilute`	Dilution ratio of uranium (e.g., total fraction of uranium in the stream) [0,1)
`time`	Time (numeric)
`tunits`	Time units (`sec`, `min`, `hours`, `days`, or `years`)
`stream`	Stream number to reprocess (numeric)

Table A.8: Reprocessing-related aliases for FLB level inputs

Alias	Description
`reprocess`	General reprocessing level (actinide recovery)
`voloxidation`	Voloxidation; only volatile fission products removed, all other elements preserved

method is generally a more “obsolete” method, used when the exact specifications of the plutonium vector and associated impurities in MOX fuel are known directly.

Table A.9: MOX fuel blending commands for FLB level inputs

Command	Description
`fr_tru`	Pu/Am fraction in MOX fuel (balance of U)
`fr_pu238`	Fraction of ^{238}Pu in Pu vector
`fr_pu239`	TRU fraction in MOX fuel (balance of U)
`fr_pu240`	Fraction of ^{240}Pu in Pu vector
`fr_pu241`	Fraction of ^{241}Pu in Pu vector
`fr_pu242`	Fraction of ^{242}Pu in Pu vector
`fr_am`	Fraction of Americium impurities in MOX fuel
`stream`	Stream to obtain TRU concentrations from (numeric)
`time`	Decay time (numeric)
`tunits`	Time units (`sec`, `min`, `hours`, `days`, or `years`)

Table A.10: User-specified MOX fuel fabrication commands for FLB level inputs

Command	Description
`fr_tru`	TRU fraction in MOX fuel (balance of U)
`stream`	Stream to obtain TRU concentrations from (numeric)
`time`	Decay time (numeric)
`tunits`	Time units (`sec`, `min`, `hours`, `days`, or `years`)

A.4 Example cases

The following cases are brief examples demonstrating the use of the Fuzzy Logic Barrier model input deck for analysis.

A.4.1 LWR-OT

An example of the FLB input for the analysis of a LWR-OT cycle for 60 $\frac{\text{GWd}}{\text{MTU}}$ is given as Figure A.4. Note that individual cycle stages should contain no line breaks (i.e., all input for a given stage should be on one line).

```
MINE { ( title Mining ) ( enrich 0.72 ) ( time 1.0E6 )
    ( tunits years ) } { I H M VH I I I VH }
MILLLING { ( title Milling ) ( enrich 0.72 ) ( time 10.0 )
    ( tunits years ) } { I H M VH I I I VH }
CONVERSION { ( title Conversion ) ( enrich 0.72 ) ( time 10.0 )
    ( tunits years ) } { I H M VH I I I VH }
ENRICH { ( title Enrichment ) ( enrich 4.9890 ) ( time 1.0 )
    ( tunits months ) } { I M M I-M M-VH I VH I }
LEU_FAB { ( title LEU_fuel_Fab ) ( enrich 4.9890 ) ( time 1.0 )
    ( tunits months ) } { I M M VH I I M M }
LEU_STORE { ( title LEU_fuel_Storage ) ( enrich 4.989 )
    ( time 1.0 ) ( tunits months ) } { I H M VH I I VH VH }
irradiate { ( title Reactor_Irradiation ) ( enrich 4.9890 )
    ( mtu 64.0 ) ( spow 40.2 ) ( burnup 60000 ) ( down_fr 0.1 )
    ( arplib w17x17 ) ( ncyc 3 ) ( mod 0.7230 ) } { VH L-H VH VH M }
SNF_store { ( title SNF_wet_storage ) ( time 5.0 ) ( tunits years )
    ( stream -1 ) } { VH VH M VH VH }
SNF_dry_store { ( title SNF_dry_storage ) ( id Dry_store )
    ( time 10.0 ) ( tunits years ) ( stream -1 ) } { VH VH M VH VH }
SNF_EMPLACE { ( title Final_emplacement ) ( id Emplace )
    ( time 100.0 ) ( tunits years ) ( stream -1 ) }
    { VH VH VH VH--VH VH }
```

Figure A.4: Example of a LWR-OT fuel cycle evaluation using the FLB model.

A.4.2 LWR + MOX, UREX+1b (TRU + 50% U)

An example of a fuel cycle analysis for a LWR + MOX cycle employing UREX+1b for actinide recovery (TRU + 50% U) is shown as Figure A.5.

A.4.3 LWR + FR, Pyroprocessing

An example of a fuel cycle analysis of the in the FLB model for a LWR + FR cycle employing pyroprocessing for actinide recovery is shown as Figure A.6. One should note that the FR case does not have an ARP library specification, as this is built in to the FR level type (only one FR library is available, therefore this variable is automated).

A.4.4 DUPIC

An example of the DUPIC fuel cycle analysis in the FLB framework is given as Figure A.7.

```
MINE { ( title Mining ) ( enrich 0.72 ) ( time 1.0E6 )
    ( tunits years ) } { I H M VH I I I VH }
MILLLING { ( title Milling ) ( enrich 0.72 ) ( time 10.0 )
    ( tunits years ) } { I H M VH I I I VH }
CONVERSION { ( title Conversion ) ( enrich 0.72 ) ( time 10.0 )
    ( tunits years ) } { I H M VH I I I VH }
ENRICH { ( title Enrichment ) ( enrich 4.9890 ) ( time 1.0 )
    ( tunits months ) } { I M M I-M M-VH I VH I }
LEU_FAB { ( title LEU_fuel_Fab ) ( enrich 4.9890 ) ( time 1.0 )
    ( tunits months ) } { I M M VH I I M M }
LEU_STORE { ( title LEU_fuel_Storage ) ( enrich 4.989 )
    ( time 1.0 ) ( tunits months ) } { I H M VH I I VH VH }
irradiate { ( title Reactor_Irradiation ) ( enrich 4.9890 )
    ( mtu 64.0 ) ( spow 40.2 ) ( burnup 60000 ) ( down_fr 0.1 )
    ( arplib w17x17 ) ( ncyc 3 ) ( mod 0.7230 ) } { VH L-H VH VH M }
SNF_store { ( title SNF_wet_storage ) ( time 5.0 ) ( tunits years )
    ( stream -1 ) } { VH VH M VH VH }
SNF_dry_store { ( title SNF_dry_storage ) ( id dry_store )
    ( time 10 ) ( tunits years ) ( stream -1 ) } { VH VH M VH VH }
REPROCESS { ( title Reprocessing ) ( id Reprocess ) ( time 50.0 )
    ( tunits days ) ( u_dilute 0.50 ) ( fr_pu 0.99 ) ( fr_np 0.99 )
    ( fr_am 0.95 ) ( fr_cm 0.95 ) ( stream -1 ) } { M I M VH I }
RM_STORE { ( title Recov_mat_storage ) ( id RM_store ) ( time 7.0 )
    ( tunits days ) ( stream -1 ) } { M I L M VH }
RM_TRANSPORT { ( title Recov_mat_transport ) ( id RM_transport )
    ( time 1.0 ) ( tunits days ) ( stream -1 ) } { M I L M VH }
AW_DISPOSAL { ( title Actinide_waste_disposal ) ( id AW_disposal )
    ( time 100 ) ( tunits years ) ( stream -5 ) } { VH VH VH VH VH }
MOXBLEND { ( title MOX_fuel_fabrication ) ( id MOXFAB ) ( stream 5 )
    ( fr_tru 0.100 ) ( time 50.0 ) ( tunits days ) } { M I L M M- }
MOX_store { ( title MOX_fuel_storage ) ( id MOX_store ) ( time 10 )
    ( tunits days ) ( stream -1 ) } { M VH I M VH }
MOX_irradiate { ( title MOX_Reactor_Irradiation ) ( mtu 64.0 )
    ( spow 40.2 ) ( burnup 60000 ) ( down_fr 0.1 )
    ( arplib mox14x14 ) ( ncyc 3 ) ( mod 0.7332 ) ( stream -1 )
    ( force_MOX true ) } { VH L-H VH VH M }
SNF_EMPLACE { ( title Final_emplacement ) ( time 100.0 )
    ( tunits years ) ( stream -1 ) } { VH VH VH VH--VH VH }
```

Figure A.5: Example of a LWR + MOX (UREX+1b) fuel cycle evaluation using the FLB model.

```
MINE { ( title Mining ) ( enrich 0.72 ) ( time 1.0E6 )
    ( tunits years ) } { I H M VH I I I VH }
MILLLING { ( title Milling ) ( enrich 0.72 ) ( time 10.0 )
    ( tunits years ) } { I H M VH I I I VH }
CONVERSION { ( title Conversion ) ( enrich 0.72 ) ( time 10.0 )
    ( tunits years ) } { I H M VH I I I VH }
ENRICH { ( title Enrichment ) ( enrich 4.9890 ) ( time 1.0 )
    ( tunits months ) } { I M M I-M M-VH I VH I }
LEU_FAB { ( title LEU_fuel_Fab ) ( enrich 4.9890 ) ( time 1.0 )
    ( tunits months ) } { I M M VH I I M M }
LEU_STORE { ( title LEU_fuel_Storage ) ( enrich 4.989 )
    ( time 1.0 ) ( tunits months ) } { I H M VH I I VH VH }
irradiate { ( title Reactor_Irradiation ) ( enrich 4.9890 )
    ( mtu 64.0 ) ( spow 40.2 ) ( burnup 60000 ) ( down_fr 0.1 )
    ( arplib w17x17 ) ( ncyc 3 ) ( mod 0.7230 ) } { VH L-H VH VH M }
SNF_store { ( title SNF_wet_storage ) ( time 5.0 ) ( tunits years )
    ( stream -1 ) } { VH VH M VH VH }
SNF_dry_store { ( title SNF_dry_storage ) ( id dry_store )
    ( time 10 ) ( tunits years ) ( stream -1 ) } { VH VH M VH VH }
REPROCESS { ( title Reprocessing ) ( id Reprocess ) ( time 50.0 )
    ( tunits days ) ( u_dilute 0.50 ) ( fr_pu 0.99 ) ( fr_am 0.95 )
    ( fr_np 0.99 ) ( fr_cm 0.95 ) ( stream -1 ) } { M I M VH I }
RM_STORE { ( title Recov_mat_storage ) ( id RM_store ) ( time 7.0 )
    ( tunits days ) ( stream -1 ) } { M I L M VH }
RM_TRANSPORT { ( title Recov_mat_transport ) ( id RM_transport )
    ( time 1.0 ) ( tunits days ) ( stream -1 ) } { M I L M VH }
AW_DISPOSAL { ( title Actinide_waste_disposal ) ( id AW_disposal )
    ( time 100 ) ( tunits years ) ( stream -5 ) } { VH VH VH VH VH }
MOXBLEND { ( title FBR_fuel_fabrication ) ( id MOXBLEND )
    ( fr_tru 0.330  ) ( time 50.0 ) ( tunits days ) } { M I L M M- }
MOX_store { ( title FBR_fuel_storage ) ( id FBR_store ) ( time 10 )
    ( tunits days ) ( stream -1 ) } { M VH I M VH }
FBR_irradiate { ( title FBR_Irradiation ) ( mtu 1.0  ) ( spow 40.2 )
    ( burnup 89750 ) ( down_fr 0.1 ) ( ncyc 3 ) ( mod 0.7332 )
    ( stream -1 ) } { VH I-M VH VH L }
SNF_FR_store { ( title FBR_SNF_storage ) ( id FBR_SNF_ST )
    ( time 10 ) ( tunits years ) ( stream -1 ) } { VH VH H VH VH }
```

Figure A.6: Example of a LWR + FBR (pyroprocessing) fuel cycle evaluation using the FLB model.

```
MINE { ( title Mining ) ( enrich 0.72 ) ( time 1.0E6 )
    ( tunits years ) } { I H M VH I I I VH }
MILLLING { ( title Milling ) ( enrich 0.72 ) ( time 10.0 )
    ( tunits years ) } { I H M VH I I I VH }
CONVERSION { ( title Conversion ) ( enrich 0.72 ) ( time 10.0 )
    ( tunits years ) } { I H M VH I I I VH }
ENRICH { ( title Enrichment ) ( enrich 4.9890 ) ( time 1.0 )
    ( tunits months ) } { I M M I-M M-VH I VH I }
LEU_FAB { ( title LEU_fuel_Fab ) ( enrich 4.9890 ) ( time 1.0 )
    ( tunits months ) } { I M M VH I I M M }
LEU_STORE { ( title LEU_fuel_Storage ) ( enrich 4.989 )
    ( time 1.0 ) ( tunits months ) } { I H M VH I I VH VH }
irradiate { ( title Reactor_Irradiation ) ( enrich 4.9890 )
    ( mtu 64.0 ) ( spow 40.2 ) ( burnup 60000 ) ( down_fr 0.1 )
    ( arplib w17x17 ) ( ncyc 3 ) ( mod 0.7230 ) } { VH L-H VH VH M }
SNF_store { ( title SNF_wet_storage ) ( time 5.0 ) ( tunits years )
    ( stream -1 ) } { VH VH M VH VH }
SNF_dry_store { ( title SNF_dry_storage ) ( id dry_store )
    ( time 10.0 ) ( tunits years ) ( stream -1 ) } { VH VH M VH VH }
VOLOXIDATION { ( title Voloxidation ) ( id Volox ) ( time 50.0 )
    ( tunits days ) } { M M L H H }
RM_STORE { ( title Recov_mat_storage ) ( id RM_store ) ( time 7.0 )
    ( tunits days ) ( stream -1 ) } { M I L M VH }
RM_TRANSPORT { ( title Recov_mat_transport ) ( id RM_transport )
    ( time 1.0 ) ( tunits days ) ( stream -1 ) } { M I L M VH }
DUPIC_fab { ( title DUPIC_fuel_fabrication ) ( id DUPIC_fab )
    ( mtu 84.7 ) ( time 30.0 ) ( tunits days ) ( stream -1 ) }
    { M I L M M- }
DUPIC_store { ( title DUPIC_fuel_storage ) ( id DUPIC_store )
    ( time 10.0 ) ( tunits days ) ( stream -1 ) } { M VH I M VH }
DUPIC_irradiate { ( title DUPIC_Reactor_Irradiation ) ( mtu 84.7 )
    ( spow 25.5 ) ( burnup 10000 ) ( down_fr 0.1 )
    ( arplib candu37 ) ( stream -1 ) } { VH L-H L VH M }
SNF_EMPLACE { ( title Final_emplacement ) ( time 100.0 )
    ( tunits years ) ( stream -1 ) } { VH VH VH VH--VH VH }
```

Figure A.7: Example of a DUPIC fuel cycle evaluation using the FLB model.

APPENDIX B

The OASIS module for SCALE

B.1 A simpler interface for fuel cycle analysis in SCALE

The OASIS module (**O**RIGEN and **A**RP **S**implified **I**nput **S**ystem) allows users to specify chained depletion, decay, partitioning, and batching analysis cases through use of high-level keywords [52]. This stands in marked contrast to the standard ORIGEN input, which requires the cryptic FIDO input array format.

OASIS circumvents this difficulty by constructing said FIDO input files for the user, based upon the case specified in the OASIS keyword input file. Chained analysis cases are constructed by individual events (such as irradiation, partitioning, batching, and decay). Each case is then saved to a running case file; users can thus reference prior cases within the file by referencing the case's save position using the step= keyword (discussed later).

OASIS runs as a module within SCALE, similar to ORIGEN and ARP; hence, one performs ORIGEN and ARP analyses similar to before, only using an OASIS input file rather than the standard ORIGEN deck.

The goal of this document is to provide a guide to the features OASIS module and how it can be used to perform chained depletion, decay, partitioning, and batching analysis in SCALE.

B.2 Using OASIS

The following sections illustrate the use of OASIS for constructing chained fuel depletion and decay analysis cases using SCALE. As a matter of convention, OASIS commands given in the text are given as boxed, fixed-width text: `such as this`.

B.2.1 General commands

The following commands apply to all cases and can be used with any analysis block, except where otherwise noted.

Table B.1: General commands for most OASIS case inputs.

Command	Description
`units=`	Sets time units for a given analysis step. Valid recognized types are seconds (sec), minutes (min), hours (hours), days (days), and years (years).
`decay=`	Inserts a decay period for the current process. Default time in days (change with units= option).
`cut=`	Specifies a minimum cutoff threshold for isotope tracking during irradiation and decay (in grams). Default value is 10^{-5} grams. Elements below the cutoff threshold will be deleted from output tables.

B.2.2 Irradiation

To perform an irradiation case, one must specify the ARP library, power, burn time, and down time. Multiple burns are supported. Note that the final down time indicates the "decay" cooling time for the fuel (i.e., a separate decay block is unnecessary).

The ARP library is specified by a `lib=` command, followed by a recognized ARP library (e.g., `ge8x8-4`).

To begin an irradiation block, use the keyword `read radhist`, followed by the irradiation history. Each irradiation cycle is followed by an end keyword. Finally, close the irradiation block with `end radhist`.

Optional parameters for the irradiation history case include the basis value `mtu=` (i.e.,

metric tons uranium; default of 1.0), a continuous removal rate of nuclide groups (where nuclides are given by their atomic symbols and removal rate constants are given as 1/s), and light elements which compose non-fuel elements of the assembly (given by atomic symbol and in units of grams).

An example is given as Figure B.1.

```
=oasis
  title= cooper bwr reactor 8x8
  lib= 8x8-4
  mtu 0.1902
  enrich= 2.5
  lightel= o 130.95 cr 3.366 mn 0.1525 fe 6.309 co 0.0242 ni 2.366
           zr 516.3 sn 8.412 gd 2.860 end
  read radhist
    power=12.76 burn=807 down=59 end
    power=24.227 burn=306 down=31 end
    power=18.212 burn=164 down=799 end
    power=5.878 burn=317 down=48 end
    power=7.992 burn=348 down=857 end
  end radhist
end
```

Figure B.1: Sample irradiation case with OASIS.

Required commands

The required commands for irradiation cases in OASIS are given as Table B.2.

Optional commands

Optional commands for irradiation cases in OASIS are given as Table B.3.

Table B.2: Required commands for irradiation-related case inputs.

Command	Description
`lib=`	ARP cross-section library
`power=`	Specific power (MW/MTU)
`burn=`	Burn time (days, unless units otherwise specified)
`down=`	Down time (days, unless units otherwise specified)
`enrich=`	Enrichment of ^{235}U (%)

Table B.3: Optional commands for irradiation-related case inputs.

Command	Description
`lightel=`	Light elements that compose non-fuel assembly components. Specified as atomic symbol followed by mass (in grams). Terminated by `end`
`mtu=`	Basis value (metric tons), default= 1.0
`title=`	Assembly/case title
`mod=`	Moderator density, in $\frac{g}{cm^3}$, default=0.74

B.2.3 Re-irradiation

Users can also specify a set of concentrations for re-irradiation using either an ARP library (e.g., MOX) or a user-provided (non-ARP) library. To do this, one provides the name of the user library to the `lib=` command as before (note that the user library must reside in `$TMPDIR` where SCALE is running, or the `/arpdata/` directory) and the stream position the concentrations are taken from (using `step=`). One then omits the `enrich=` command.

Required commands

The required commands for re-irradiation cases are given as Table B.4.

B.2.4 User library options

Frequently, for re-irradiation or other special cases, one will need to provide a user library in place of the standard ARP library. Likewise, occasionally one will desire to re-use a previous ARP library as a user library in order to perform minor extrapolations from the ranges within the ARP data library (note: this should be done with extreme care under very limited

Table B.4: Required commands for re-irradiation-related case inputs.

Command	Description
`lib=`	ARP cross-section library
`power=`	Specific power (MW/MTU)
`burn=`	Burn time (days, unless units otherwise specified)
`down=`	Down time (days, unless units otherwise specified)
`step=`	Stream number containing concentrations for re-burn

circumstances).

Unlike ARP-based libraries, OASIS will only use a single library position for user libraries, defaulting to the first position. Therefore, using the `libpos=` command, a user may specify the position of the user library for OASIS to use.

Likewise, to re-use an ARP library used in a prior data analysis step, one can use the library command `lib= last` – this will use the last cross-section library as a user library, without the corresponding ARP checks for the input data range. Using this in combination with the `libpos=` command, a user may thus specify a given position on the ARP library file for minor extrapolations beyond the library range (i.e., by using the last position on the library).

B.2.5 Axial profiles (irradiation)

An axial profile weighting can be applied to an irradiation history through the use of the `nax=` `axp=` and `wgt=` commands. One defines a series of axial power profiles (i.e., as a fraction of the specified irradiation power) and may also optionally apply a weighting factor to each axial location. OASIS then provides for an averaged concentration over the varied power profile once the irradiation cycles are completed.

An example of this feature is given below as Figure B.2; the two lines may be simply added to the above irradiation case (outside of the `radhist` block).

The expression in Figure B.2 can also be simplified using the notation `*N` to denote "N" repeated values, shown as Figure B.3.

One must also specify a moderator density for each axial profile case; to specify the same moderator density, one would simply insert the following `mod=` command (Figure B.4).

A varying moderator density may also be used as a function of axial profile (such as in

```
nax= 5
axp= 0.45 0.53 0.53 0.53 0.32 end
wgt= 1 1 1 1 1 end
```

Figure B.2: Specifying axial powers and relative weights in OASIS

```
nax= 5
axp= 0.45 3*0.53 0.32 end
wgt= 5*1 end
```

Figure B.3: Expressing repeated axial power values in OASIS

compensating for void fraction).

Taking the changes together, a new example case is given as Figure B.5.

B.2.6 Prior stream retrieval

Several OASIS operations involve invoking a prior concentration stream; this is accomplished by use of the `step=` command. This can be called in one of two ways; for a positive step number, the stream at the specified step number in the file is used. Alternatively, one may specify a negative step number (-1, -2, etc.); this counts backwards from the last position on the file, where -1 corresponds to the last position, -2 corresponds to the position before the last, etc. Given that the file is written sequentially, one can use the `step=-1` command to retrieve the last written concentration.

B.2.7 Decay-only

To decay a prior stream for a specified period, the decay block may used with no other operations (such as radhist, batch, solvent, etc.). Required parameters are the file step for the decay (step=) and the decay time (time=). Using the irradiation example, one can decay the above stream for an additional one year as the the example in Figure B.6.

One will note several things: first, the use of the field `units=` which specifies time units. This may be specified for any SCALE analysis block, but should be specified outside of

```
mod= 5*0.455
```

Figure B.4: Expressing multiple moderator density values for axial profile evaluation in OASIS

any "read" blocks.

Second, a deeper look at the process of chained analysis: first, the irradiation block is specified as one analysis block for SCALE (i.e., the `=oasis` block). The next analysis unit, for decay, is a new block. (**Note:** irradiation is the only case for which the **decay=** command cannot be coupled; any **decay=** command will be ignored. The final **down=** command for an irradiation cycle is instead used as the final decay period).

Finally, one will notice how the position is specified (`step=2`). In this case, the second position is requested, as the irradiation case writes on position 1 and the final decay from the irradiation case writes on unit 2; i.e., this case picks up concentrations from the irradiation case after the last decay period and decays them further. Of course, nothing stops one from going back and doing another decay immediately following discharge, in which case one would use `step=1`.

Required commands

The required commands for decay cases are given as Table B.5.

Table B.5: Required commands for decay-related case inputs.

Command	Description
`step=`	File position for concentrations to be decayed
`decay=`	Decay time (default in days)

```
=oasis
  title= cooper bwr reactor 8x8
  lib= 8x8-4
  mtu 0.1902
  enrich= 2.5
  mod= 5*0.455
  nax= 5
  axp= 0.45 3*0.53 0.32 end
  wgt= 5*1 end
  lightel= o 130.95 cr 3.366 mn 0.1525 fe 6.309 co 0.0242 ni 2.366
           zr 516.3 sn 8.412 gd 2.860 end
  read radhist
    power=12.76 burn=807 down=59 end
    power=24.227 burn=306 down=31 end
    power=18.212 burn=164 down=799 end
    power=5.878 burn=317 down=48 end
    power=7.992 burn=348 down=857 end
  end radhist
end
```

Figure B.5: Example of an OASIS irradiation case with axial power weighting

```
=oasis
  title= cooper bwr reactor 8x8
  lib= 8x8-4
  mtu 0.1902
  enrich= 2.5
  lightel= o 130.95 cr 3.366 mn 0.1525 fe 6.309 co 0.0242 ni 2.366
           zr 516.3 sn 8.412 gd 2.860 end
  read radhist
    power=12.76 burn=807 down=59 end
    power=24.227 burn=306 down=31 end
    power=18.212 burn=164 down=799 end
    power=5.878 burn=317 down=48 end
    power=7.992 burn=348 down=857 end
  end radhist
end
=oasis
  units=years
  decay=1.0
  step=2
end
```

Figure B.6: Example of stream retrieval and additional decay for 1 year in OASIS.

B.2.8 Element partitioning

One can specify chemical separation of elements using the OASIS keyword interface. To do so, one must pick up the concentrations from a prior point using step=, as done in the above case with the decay-only block. A decay time is optional following the separation; otherwise, a decay period of 1 second is used.

Two options are available for the separated mass stream: users may either track the separated nuclides themselves, or the remaining composition (i.e., without the separated nuclides). This is done via a + or – flag which immediately follows the `separate` field (this flag is also required). Following from the ± flag, a list of atomic symbols and separation efficiencies (given as a fraction from 0 to 1) is input, terminated by end.

Two examples are given below: the first (Figure B.7), where a mass stream from position 2 is separated and the remaining nuclides are saved, and another where the separated nuclides are saved (Figure B.8). In both cases, the concentration is then decayed for 10 years.

```
=oasis
  units=years
  step=2
  separate + I 0.99 cs 0.95 tc 0.99 sr 0.95
  decay= 10.0
end
```

Figure B.7: Example of element partitioning; 99% of iodine and technicium and 95% of cesium and strontium are removed from the stream at position 2; the remaining nuclides are saved and decayed for 10 years.

Required commands

The required commands for element partitioning cases are given as Table B.6.

```
=oasis
  units=years
  step=2
  separate + I 0.99 cs 0.95 tc 0.99 sr 0.95
  decay= 10.0
end
```

Figure B.8: Example of element partitioning; 99% of iodine and technicium and 95% of cesium and strontium are removed from the stream at position 2; only these separated nuclides (e.g., I/Tc/Cs/Sr) are saved and decayed for 10 years.

Table B.6: Required commands for element partitioning-related case inputs.

Command	Description
`step=`	File position for concentrations to be partitioned
`separate`	List of nuclides and removal efficiencies for separation [0,1]
+ or -	Precedes nuclide/separation list; + tracks the separated nuclides only, - tracks the stream the nuclides were separated from.

B.2.9 MOX Fuel Fabrication (from concentrations)

A special option available in OASIS is MOX fuel fabrication, in which a stream can be selected and uranium, plutonium, and other transuranics (americium, curium, and neptunium) and be selected out for re-fabrication into MOX fuel. The `read moxfab` command automatically produces a fuel assembly concentration using the maximum amount of available materials.

The first parameter of interest is the TRU fraction (including Pu); the remaining fraction is taken as uranium. This is specified by `fr_tru=` followed by a value from 0 to 1.

Next, the respective sub-fractions of the TRU portion of the fuel are given by `fr_np=`, `fr_pu=`, `fr_am=`, and `fr_cm=` where again the fractions are specified from 0 to 1. Note that the TRU fractions themselves also must sum to 1.0; if they do not, an error is given.

To fabricate the MOX fuel, the OASIS module calculates the required separation fractions from the selected stream for uranium and each TRU constituent (Pu, Np, Am, and Cm). To do this, OASIS calculates the final mass of the MOX assembly based upon the uranium fraction (i.e., the complement of the TRU fraction) and then checks the available masses of each TRU

material from the stream. The OASIS module then iteratively adjusts the mass of the final MOX assembly to match the maximum available mass of the most constraining TRU material (i.e., for a given calculated total assembly weight and fraction of TRU elements from a stream, OASIS tries to create an extraction fraction as close to 1.0 as possible for the TRU element whose concentration is most limiting to the total MOX assembly weight, based upon the element fractions). Thus, OASIS seeks to maximize the utilization of TRU materials while maintaining the respective fractions of TRU to U and between respective TRU constituents.

Specifically, OASIS calculates the separation fraction of each TRU material, based upon the mass of U extracted. If the extraction fraction of any TRU material is greater than unity, OASIS lowers the extraction fraction of U, re-calculates the final mass of the MOX assembly, and checks the required separation fractions of each TRU constituent once more, repeating this sequence until each material has an extraction ratio less than or equal to one. The extraction fractions of each material are then printed in the logfile. In this way, OASIS maximizes the utilization of materials to the most constraining material for a given case and stream.

Users can also specify to save the waste stream on an adjacent position; to do this, one simply gives the command `waste` inside the `read moxfab` block.

An example of a MOX fabrication command is given as Figure B.9 this assumes concentrations of interest on position 4. In this case, the TRU fraction is 5%, with 90% of the TRU materials being composed of plutonium, 5% of neptunium, 4% of americium, and the balance of curium. The waste products are then saved on the next adjacent unit on the binary output file.

Required parameters

The required parameters for the MOX fuel fabrication case are given as Table B.7

Table B.7: Required commands for MOX fuel fabrication cases (from a prior stream).

Command	Description
`step=`	File position for concentrations to be used for MOX fuel
`fr_tru=`	Fraction of TRU (Pu/Np/Am/Cm) in MOX fuel (balance of U)

```
=oasis
  step=4
  read moxfab
    fr_tru= 0.05
    fr_pu= 0.9
    fr_np= 0.05
    fr_am= 0.04
    fr_cm= 0.01
    waste
  end moxfab
end
```

Figure B.9: Example of MOX fuel fabrication from concentrations at file position 4. Waste from MOX fabrication stored on the next adjacent binary file unit from the stored MOX fuel fabrication concentrations.

Optional parameters

Optional parameters for the MOX fuel fabrication (from prior stream) are given as Table B.8.

Table B.8: Optional commands for MOX fuel fabrication cases (from a prior stream).

Command	Description

`fr_pu=`
`fr_np=`
`fr_am=`
`fr_cm=`
	Sub-fraction of Pu, Np, Am, and Cm in TRU fraction. Note that any given TRU constituent may be omitted (assumed to be zero), however all constituents must add up to 1.0

`waste`	Save waste stream concentrations for MOX fabrication to next adjacent position on the file

B.2.10 MOX fuel fabrication (user-specified)

One may also specify MOX fuel concentrations directly, rather than from prior stream concentrations. This is done with the read moxspec block. Concentrations may be specified either

in terms of the relative fractions of a specified basis (i.e., fraction of TRU and proportional fractions of U and Pu isotopes), or directly in kilograms.

OASIS automatically determines if the user input is in kilograms or the relative isotopic fractions by the use of the `fr_tru=` parameter. If the TRU fraction is specified (i.e., fraction of Pu and Am of heavy metal), all other parameters are interpreted accordingly; the respective plutonium and uranium inputs are interpreted as the relative isotopic fractions of the plutonium and uranium content, respectively. Likewise, the `am241=` input is interpreted as the fraction of americium-241 as a fraction of total TRU (i.e., Pu + Am). The total amount of material is derived from the basis MTU value (given by `mtu=`, default is 1 MTU)

If `fr_tru=` is not given, each isotopic input is interpreted in kilograms, with the basis value being determined by the total amount of heavy metal specified. (In this case, any basis given by `mtu=` is thus ignored).

Examples of MOX fuel specification are given both in kg (Figure B.10) and as a fraction of basis (Figure B.11).

```
read moxspec
  pu238= 0.700
  pu239= 26.560
  pu240= 15.280
  pu241= 3.970
  pu242= 3.490
  u234=  0.0090495
  u235=  6.91051
  u236=  4.45659
  u238=  938.624
end moxspec
```

Figure B.10: Example of MOX fuel fabrication from specified mass values (in kg).

Required parameters

Table B.9 gives the required commands for a user-specified MOX fuel fabrication case.

```
mtu= 1.0
read moxspec
  fr_tru= 0.05
  pu238= 0.014
  pu239= 0.5312
  pu240= 0.3056
  pu241= 0.0794
  pu242= 0.0698
  u234=  0.00000952579
  u235=  0.00727422
  u236=  0.00469115
  u238=  0.988025
end moxspec
```

Figure B.11: Example of MOX fuel fabrication from relative fractions of the total basis.

Table B.9: Required commands for MOX fuel fabrication cases (user-specified).

Command	Description
pu239=	If `fr_tru=` defined, fraction of ^{239}Pu as a fraction of TRU. Otherwise, total ^{239}Pu in kg.
pu241=	If `fr_tru=` defined, fraction of ^{241}Pu as a fraction of TRU. Otherwise, total ^{241}Pu in kg.

Optional commands

The optional commands for the user-specified MOX fuel fabrication cases are given as Table B.10.

B.2.11 Assembly batching

One can also batch together multiple sets of assembly concentrations saved by SCALE on a binary .f71 file. (**Note:** the .f71 extension is required). Optionally, one may include a single position from the current file stream in the batch operation as well. One may also specify the batching ratios of the assemblies (including the mass stream taken from the current file stream). (**Note:** The files must be copied over to the SCALE working directory (`$TMPDIR`) at

Table B.10: Optional commands for MOX fuel fabrication cases (user-specified).

Command	Description
`fr_tru=`	Fraction of TRU (Pu/Am) in MOX fuel (balance of U)
`am241=`	If `fr_tru=` defined, fractions of ^{241}Am as a fraction of TRU. Otherwise, total ^{241}Am in kg.
`pu240=` `pu242=`	If `fr_tru=` defined, respective fractions of ^{240}Pu and ^{242}Pu as a fraction of TRU. Otherwise, total ^{240}Pu and ^{242}Pu in kg.

`u234=`
`u235=`
`u236=`
`u238=`
	If `fr_tru=` defined, respective fractions of ^{234}U, ^{235}U, ^{236}U, and ^{238}U as a fraction of uranium content in the fuel (1-fr_tru). Otherwise, total ^{234}U, ^{235}U, ^{236}U, and ^{238}U in kg.

runtime in order to be found.)

Files and batch ratios are specified using the `id=` field; the input consists of the concentration file names (without extension) followed by the respective batch ratio.

Optional parameters include the date of the mass batch (`date=`), the batch name (`batch=`), output of the concentrations of each file (`edit=`) and the file positions to use on the input concentration files, terminated by end. To specify a concentration from the current stream, the field `stream=` is used, followed by the position and the batch ratio.

Figure B.12 demonstrates how two files and a position within the current file stream can be batched together.

The above analysis batches position 2 of the current stream (at ratio 1.0) to position 1 of the files asm1.f71 and asm2.f71, which are at ratios 0.9 and 2.0 respectively. The `edit=yes` field specifies that the individual file concentrations should be printed, and the `batch=pcp01` marks the batch with the unique identifier `pcp01`. The resulting concentration is then appended to the end of the current file stream.

Required parameters

Table B.11 gives the required commands for a fuel batching case.

Optional parameters

Table B.12 gives the optional commands for a fuel batching case.

```
=oasis
  read batch
    stream= 2 1.0
    title=reprocess batch pcp001
    id= asm1 0.9 asm2 2.0 end
    fpos 1 1 end
    batch= pcp01  edit=yes
  end batch
end
```

Figure B.12: Example of fuel batching; Fuel data in asm1.f71 is combined with data from asm2.f71 and the fuel data at stream position in a ratio of 0.9, 2.0, and 1.0, respectively.

Table B.11: Required commands for fuel batching cases.

Command	Description
`title=`	Title of the batch.
`id=`	List of binary files and batch ratios.
`edit=`	Assigns a unique identifier for batch file.

B.2.12 Solvent batching

An additional option available in OASIS is to dissolve a mass stream into an elemental composition, such as an acid. Such a process is useful for source term analysis with chemical treatments of fuel like reprocessing. One thus assumes in such a treatment that the mass flow (such as the fuel assembly) is mixed with a specified mixture of elements (whose isotopic composition is assumed to be at their respective natural abundances).

For example, consider a case in which a fuel assembly is dissolved in a composition of nitric acid (HNO_3), which a ratio of 10:1 of solvent to dissolved mass. The process is similar to batching of assemblies, but with slightly different required parameters. For example, no files are input, however the file position (`step=`) is now required. Likewise, the molar composition of the solvent is specified with the field comp= followed by a list of each atomic symbol and its molar value, terminated by end. Finally, the ratio of solvent to dissolved mass is given by the ratio= field.

Assuming the prior concentrations from the irradiation and decay cases have been written

Table B.12: Optional commands for fuel batching cases.

Command	Description
`fpos=`	Batches concentrations at specified position in the current file stream at the batch ratio specified.
`stream=`	List of file positions for each binary file. Must match total number of binary files specified.
`edit=`	Outputs nuclide concentrations of each binary/stream. `edit=yes` to turn on, `edit=no` to turn off.

to position 2, the example keyword input is given as Figure B.13.

```
=oasis
  read solvent
    comp= h 1.0 n 1.0 o 3.0 end
    step=2
    batch= SolBatch  edit=no
    ratio=10.0
  end solvent
end
```

Figure B.13: Example of solvent batching of fuel data; fuel data from step 2 on the file stream is batched with a 10:1 ratio of nitric acid (HNO_3) to fuel.

B.2.13 Specifying print options

One can specify the various printout options of ORIGEN using the read prntopts block. Particular features include output units, selecting libraries for output (`actinides`, `fission products`, `light elements`), and output type (`nuclides`, `elements`, or `total`).

The `read prntopts` block can be used for any analysis block, outside of any other read block.

Three fields are used: the `unit=` field, which specifies units and takes arguments of

gram-atoms / moles (given as `gm-atoms` or `moles`) , grams (`grams`), curies (`curies`), the sum of alpha, beta, and gamma watts (`abg-watt`), gamma watts (`gam-watt`), or hazard/dilution factors (in m^3) for air (`haz-air`) and water (`haz-wat`). Any number of units may be given in the `unit=` list, terminated by end.

The libraries are specified similarly with the `lib=` field, which can take fission products (`fp`), actinides (`act`), and light elements (`le`), terminated by `end`.

Finally, the output type is given by `type=` and takes the argument of nuclides (`nuc`), elements (`ele`), or summary (`sum`), again terminated by `end`. An example of the use of the print options is given as Figure B.14.

```
read prntopts
  unit= moles grams gam-watt end
  lib = fp end
  type = nuc end
end prntopts
```

Figure B.14: Example of OASIS print output options; output in moles (gram-atoms), mass (grams), and heat produced by gammas (in watts) is given for fission products, by nuclide.

Required parameters

The required commands for specifying printout options are given as Figure B.13.

Table B.13: Optional commands for fuel batching cases.

Command	Description
`unit=`	List of units for output.
`lib=`	Library type (actinides, fission products, or light elements).
`type=`	Output type (nuclides, elements, or summary).

B.2.14 Continuous mass removal

Continuous removal of elements (such as for reactors which have a continuous removal of elements for processing) can also be accomplished by using a read removal block. Multiple groups of isotopes may be specified with a common removal rate constant (expressed in units of 1/s). Elements are given as a list of their respective atomic symbols, starting with `elem=` and terminated by end as shown in the example given as Figure B.15.

```
read removal
  rate= 100.0 elem= cs sr end
  rate= 200 elem = i tc end
end removal
```

Figure B.15: Example of continuous mass removal block in OASIS.

The removal block may be specified in any subcase block.

Required parameters

The required commands for specifying continuous mass removal are given as Table B.14.

Table B.14: Optional commands for fuel batching cases.

Command	Description
`rate=`	Continuous removal rate constant (1/s).
`elem=`	Elements in continuous removal group.

B.2.15 Continuous mass feed

Similar to the continuous removal option, elements may be continuously fed into the system. This is done by a feed= command, followed by an element's symbol and its feed rate (in

moles/sec), terminated by end. Relative isotopic abundances are controlled by the natural abundances available in the natural abundance libraries. An example is given as Figure B.16.

```
feed= U 1.0 Th 2.0 B 0.01 end
```

Figure B.16: Example of continuous mass feed in OASIS.

B.2.16 Specifying neutron energy groups & spectra

Specifying a series of neutron energy groups can be done in one of two ways. The first is to specify the logical unit number of the pre-defined neutron energy group structure (refer to the SCALE manual for pre-defined photon and neutron energy group libraries); the second is to specify the energy groups manually in MeV.

To specify energy groups manually, one may input all of the energy boundaries (including the highest and lowest boundaries; thus there will be ngrp+1 entries for ngrp number of groups); an example of this is Figure B.17.

```
ngrp= Emax En En−1 ... E2 E1 end
```

Figure B.17: Example of neutron energy group specification in OASIS.

Alternatively, one may allow SCALE to perform an interpolation between a maximum and minimum boundary. This interpolation can be done linearly or logarithmically.

The syntax for automatic logarithmic interpolation of ngrp boundaries between the minimum and maximum energies (thus producing ngrp+1 groups) is thus:

```
ngrp= NgrpL Emax E1 end
```

Figure B.18: Neutron energy group specification using logarithmic interpolation in OASIS.

Likewise, one may replace the “L” with an “I” for linear interpolation.

To specify a logical library position for energy group structure, the position number should appear as a negative number after ngrp, i.e. Figure B.19.

```
ngrp= -libpos end
```

Figure B.19: Neutron energy group specification using a logical library position in OASIS.

B.2.17 Specifying gamma energy groups & spectra

Specifying the energy groups for gamma spectra is nearly identical to that of the case for neutrons, however several additional options exist, including specifying which element libraries (light elements, fission products, actinides) one wishes to see gamma spectra for.

Specifying a series of gamma energy groups can be done in one of two ways. The first is to specify the logical unit number of the pre-defined neutron energy group structure (refer to the SCALE manual for pre-defined photon and neutron energy group libraries); the second is to specify the energy groups manually in MeV.

To specify energy groups manually, one may input all of the energy boundaries (including the highest and lowest boundaries - thus there will be Ng+1 entries for Ng number of groups). An example is Figure B.20

```
read gammagrp
 ngrp= E_max E_n E_n-1 ... E_2 E_1  end
end gammagrp
```

Figure B.20: Example of gamma energy group specification in OASIS.

Alternatively, one may allow SCALE to perform an interpolation between a maximum and minimum boundary. This interpolation can be done linearly or logarithmically.

The syntax for automatic logarithmic interpolation of ng entries (producing ng+1 groups)

is shown as Figure B.21.

```
read gammagrp
 ngrp= NgL Emax end
end gammagrp
```

Figure B.21: Example of logarithmic gamma energy group interpolation in OASIS.

Likewise, one may replace the “L” with an “I” for linear interpolation.

To specify a logical library position for energy group structure, the position number should appear as a negative number after ngrp (Figure B.22).

```
read gammagrp
 ngrp= -libpos end
end gammagrp
```

Figure B.22: Gamma energy group specification using a logical library position in OASIS.

Bremstrahlung contributions to the photon spectra can be suppressed by using the `nobrem` command, placed inside the `read gammagrp` block.

The only required parameter is the `ngrp=` command.

B.2.18 Saving output

One can save the result of any concentration stream to a named output file (in the SCALE working directory, `$TMPDIR`) by giving the command `outfile=<filename>`. The resulting file, named “filename.f71” (where “filename” is the name given by the user) is written with the concentrations from that particular step. The example in Figure B.23 will output the concentrations at a particular step to the file “test.f71” in the SCALE working directory.

```
outfile= test
```

Figure B.23: Outfile specification in OASIS.

B.2.19 Stream renormalization

Users can renormalize the result of any stream after an operation to the basis (either specified by `mtu=` or to 1 MT if not specified). Users can normalize the concentration to the basis using one of several options - to the basis in MTU (metric tons uranium), MTHM (metric tons heavy metal, i.e., U + TRU), or MTM (metric tons material).

Arguments to renormalization take the form `renorm=` followed by one of "mtu", "mthm", "mtm", or "all", which represent normalization to metric tons uranium, metric tons heavy metal (U+TRU), and metric tons total (for "all" and "mtm"), respectively. Figure B.24 normalize to the basis value in metric tons heavy metal.

```
renorm= mthm
```

Figure B.24: Gamma energy group specification using a logical library position in OASIS.

B.3 Examples

In this section, two examples of chained analysis are given to demonstrate how OASIS can be used to construct modular, chained fuel cycle analysis cases.

B.3.1 A simple reprocessing example

Figure B.25 demonstrates a simple irradiation case, followed by a decay for 10 years. 99% of plutonium is then separated from the stream and the plutonium concentration is saved. Likewise, all heat data is printed by elements for actinides in the reprocessing stage.

```
=oasis
  title= Reactor_Irradiation
  id= irradiate
  lib= w17x17_ofa
  mtu= 1
  mod= 0.7332
  enrich= 3.965
  lightel= o 135.95 cr 5.91975 mn 0.328875 fe 12.9358
                co 0.074545 ni 9.86625 nb 0.7016 sn 3.508 end
  read radhist
    power= 40.2  burn= 331.675  down= 54.7264 end
    power= 40.2  burn= 331.675  down= 54.7264 end
    power= 40.2  burn= 331.675  down= 1 end
  end radhist
end
=oasis
  title= SNF_dry_storage
  id= dry_store
  units= years
  decay= 10
  step=-1
end
=oasis
  read prntopts
    unit= abg-watt end
    lib= act end
    type= ele end
 end prntopts
 title= Plutonium separation
 id= Reprocess
 separate - pu 0.99 end
 decay= 1
 units= days
 step= 5
end
```

Figure B.25: A simple chained example of irradiation, decay, and plutonium separation in OASIS.

B.3.2 A more complex chained analysis example

Figure B.26 is an example of how the individual analysis components can be fitted together for a more complex analysis.

The analysis above irradiates a composition (with a continuous feed of deuterium and helium and a continuous removal of cesium, strontium, iodine, and technetium), followed by a solvent batch in nitric acid (with gamma spectra activated) with a decay for one year, followed by a renormalization to 1 MT heavy metal (U+TRU).

```
=oasis
  title= cooper bwr reactor 8x8
  lib=ge8x8-4
  mtu=0.1902
  enrich=2.5
  lightel= o 130.95 cr 3.366 mn 0.1525 fe 6.309 co 0.0242
           ni 2.366 zr 516.3 sn 8.412 gd 2.860 end
  read radhist
    power=12.76  burn=807 down=59  end
    power=24.227 burn=306 down=31  end
    power=18.212 burn=164 down=799 end
    power=5.878  burn=317 down=48  end
    power=7.992  burn=348 down=857 end
  end radhist
  read removal
    rate= 1000.0 elem= cs sr end
  end removal
  feed= h-2 5.0 he-4 10.0 end
  outfile= radtest
end
=oasis
  title=Solute Test
  id=SolTest
  step=2
  read solvent
    comp= h 1.0 n 1.0 o 3.0 end
    batch= SolBatch   edit=no
    ratio=10.0
  end solvent
  read gamspec
    group= 18 end
    type= all
    nobrem
  end gamspec
  decay=1.0
  units= years
  renorm= MTHM
end
```

Figure B.26: A chained analysis example using OASIS.

APPENDIX C

Storage and retrieval of ORIGEN-S binary output data

An essential feature to the coupled analysis technique is the ability not only to produce nuclear fuel analysis from within the code in question (for this application, the PR model), but also to retrieve and process these results accordingly. This appendix will outline the process used for ORIGEN-s binary data retrieval, such that the technique can be reproduced for other applications.

C.1 Data storage on the FORTRAN binary

Nuclear fuel data (including radiological data) output from ORIGEN-S is stored as a FORTRAN binary file. The procedure for retrieving this data in FORTRAN is relatively straightforward, and even outlined in the ORIGEN-S user manual [43]. The relevant FORTRAN90 code for storing data on the ORIGEN-S binary is illustrated below (Figure C.1).

```
write (unit=n96) itxx, ilite, iact, ifp, nrflag, msub1, nstepo, &
      kasepo, jobpos, nocs, noblnd, ndset, ntype, ngrp, nelem, &
      nvert, ng, mmn, mout, index, mstar, nunit, kblend, nenle, &
      nenac, nenfp, l1, l2, l3, l4, tmo, fracpw, tconst, tunit, &
      twrite, pwrite, fwrite
write (unit=n96) (nucl(i),i=1,itot), (x(msub1,j),j=1,itot), &
      title, basis, (egamle(i1),i1=1,n1), (egamac(i2),i2=1,n2), &
      (egamfp(i3),i3=1,n3), (specle(i4,msub),i4=1,l1), &
      (specac(i5,msub),i5=1,l2), (specfp(i6,msub),i6=1,l3), &
      (ener(i7),i7=1,n4), (dsav(i8,msub),i8=1,ng), &
      (esav(i9,msub),i9=1,ng), (itsav(i10,msub),i10=1,20), &
      (spnnuc(i11,msub),i11=1,l4),(alpnuc(i12,msub),i12=1,l4), &
      (spneut(i13,msub),i13=1,ngrp), &
      (specan(i14,msub),i14=1,ngrp), &
      (specsp(i15,msub),i15=1,ngrp),(eneuts(i16),i16=1,n5)
```

Figure C.1: FORTRAN90 code for storing ORIGEN-S data on a binary output file [43].

Each case in OASIS / ORIGEN-S is stored on the end of the binary output file; i.e., cases are sequentially stored in order of execution. Thus, data can be retrieved by "skipping" the appropriate number of records until the correct record is found. (Each relevant file position is stored with the respective fuel cycle level class for ORIGEN-based levels.)

C.2 Retrieval of ORIGEN-S binary data in C++

Retrieval of data from a FORTRAN binary file in FORTRAN is a trivial task; i.e., it is simply a `read` operation in place of a `write`. The retrieval of data from the FORTRAN binary in C++ however is somewhat more complicated. Thus, for the aid of others who wish to reproduce the OASIS/ORIGEN-S coupling technique for other codes, the C++ code for ORIGEN-S retrieval is provided below, in the following pages. As much as possible, variable names have been structured to match those of the ORIGEN-S convention (c.f., the ORIGEN-S user manual [43]) to minimize confusion.

```
void get_origen_data(const string& fname, const int nskip,
   vector<int>& nucl, vector<float>& x, vector<float>& ener,
   vector<float>& esav,vector<float>& eneuts,
   vector<float>& specsp)
 {
        const int row1_size = 37;
        const int num_flt = 7;
        const int itxx2 = 1946;
        const int f_diff = row1_size-num_flt;
        const int flt_sz = sizeof(float);
        const int int_sz = sizeof(int);

        //Clear out the vectors (just in case)
        nucl.clear();
        x.clear();

        int row1[row1_size-num_flt];
        float row1_flt[num_flt];
        int itxx, nenle, nenac, nenfp, nstep;
        int l1, l2, l3, l4, ng, ngrp, len, npos;
        int total_bits;
        ifstream ifs(fname.c_str(),ios_base::binary);
        if(!ifs) error("Cannot open ORIGEN binary file", fname);

        //Read byte header
        ifs.read(as_bytes(len),sizeof(len));

        for(int i=0; i<row1_size; ++i) {
          if(i < f_diff) ifs.read(as_bytes(row1[i]), sizeof(row1[i]));
        }
        for(int i=0; i < num_flt; ++i) {
          ifs.read(as_bytes(row1_flt[i]), sizeof(row1_flt[i]));
        }

        itxx  = row1[0];
```

```
nstep = row1[6];
nenle = row1[23];
nenac = row1[24];
nenfp = row1[25];
l1    = row1[26];
l2    = row1[27];
l3    = row1[28];
l4    = row1[29];
ng    = row1[16];
ngrp  = row1[13];
npos  = 0;
//Quality control...
l1 = max(1,nenle);
l2 = max(1,nenac);
l3 = max(1,nenfp);
l4 = max(1,l4);

char  title[80];
char  basis[40];
vector<float> egamle;
vector<float> egamac;
vector<float> egamfp;
vector<float> specle;
vector<float> specac;
vector<float> specfp;
vector<float> dsav;
char  itsav[80];
vector<float> spnnuc;
vector<float> alpnuc;
vector<float> spneut; //Want SFN,  not  all neutrons!
vector<float> specan;
vector<float> dummy; //for chewing up skipped positions
while (npos < nskip) {
// Read row end word prefix (# bytes)
        ifs.read(as_bytes(len), sizeof(len));
        //Read row begin word prefix (# bytes)
```

```
ifs.read(as_bytes(len), sizeof(len));
++npos;

dummy.clear(); //Purge buffer before we read in again

//Figure out length of bits to chew up
total_bits = itxx + itxx;
read_push(ifs, dummy, total_bits);

ifs.read(as_bytes(title), sizeof(title)); //char string
ifs.read(as_bytes(basis), sizeof(basis)); //char string
//Figure out length of bits to chew up
total_bits = (nenle+1) + (nenac+1) + (nenfp+1);
total_bits += l1 + l2 + l3 + (ng+1) + ng + ng;

//i.e., no energy bounds if we have no energy  groups
if(ng == 0) -=total_bits;
read_push(ifs, dummy, total_bits);
ifs.read(as_bytes(itsav), sizeof(itsav)); //char string

//Figure out length of bits to chew up
total_bits = l4 + l4 + ngrp + ngrp + ngrp + (ngrp+1);

//Necessary if no groups present
if(ngrp == 0) ++total_bits;

read_push(ifs, dummy, total_bits);

// Read row end word prefix (# bytes)
ifs.read(as_bytes(len), sizeof(len));

// Read row begin word prefix (# bytes)
ifs.read(as_bytes(len), sizeof(len));

for(int i=0; i<row1_size-num_flt; ++i) {
  ifs.read(as_bytes(row1[i]), sizeof(row1[i]));
```

```
        }
        for(int i=0; i < num_flt; ++i) {
          ifs.read(as_bytes(row1_flt[i]), sizeof(row1_flt[i]));
        }
        itxx  = row1[0];
        nstep = row1[6];
        nenle = row1[23];
        nenac = row1[24];
        nenfp = row1[25];
        l1    = row1[26];
        l2    = row1[27];
        l3    = row1[28];
        l4    = row1[29];
        ng    = row1[16];
        ngrp  = row1[13];

        //Set L1-L4 (quality control)
        l1 = max(1,nenle);
        l2 = max(1,nenac);
        l3 = max(1,nenfp);
        l4 = max(1,l4);

        nucl.clear();
        x.clear();
}

//Now read the position we're after
if (itxx > 0) {
        // Read row end word prefix (# bytes)
        ifs.read(as_bytes(len), sizeof(len));
        //Read row begin word prefix (# bytes)
        ifs.read(as_bytes(len), sizeof(len));

        ++npos;

        nucl.clear();
```

```
x.clear();

//Now read in variables
read_push(ifs, nucl, itxx);
read_push(ifs, x, itxx);
ifs.read(as_bytes(title), sizeof(title));
ifs.read(as_bytes(basis), sizeof(basis));
read_push(ifs, egamle, nenle+1);
read_push(ifs, egamac, nenac+1);
read_push(ifs, egamfp, nenfp+1);
read_push(ifs, specle, l1);
read_push(ifs, specac, l2);
read_push(ifs, specfp, l3);
read_push(ifs, ener, ng+1);
read_push(ifs, dsav, ng);
read_push(ifs, esav, ng);
ifs.read(as_bytes(itsav), sizeof(itsav));
read_push(ifs, spnnuc, l4);
read_push(ifs, alpnuc, l4);
read_push(ifs, spneut, ngrp);
read_push(ifs, specan, ngrp);
read_push(ifs, specsp, ngrp);
read_push(ifs, eneuts, ngrp+1);

// Read row end word prefix (# bytes)
ifs.read(as_bytes(len), sizeof(len));

// Read row begin word prefix (# bytes)
ifs.read(as_bytes(len), sizeof(len));

ifs.read(as_bytes(len),sizeof(len));
for(int i=0; i<row1_size-num_flt; ++i) {
  ifs.read(as_bytes(row1[i]), sizeof(row1[i]));
}
for(int i=0; i < num_flt; ++i) {
  ifs.read(as_bytes(row1_flt[i]), sizeof(row1_flt[i]));
```

```
                }
                itxx  = row1[0];
                nstep = row1[6];
                nenle = row1[23];
                nenac = row1[24];
                nenfp = row1[25];
                l1    = row1[26];
                l2    = row1[27];
                l3    = row1[28];
                l4    = row1[29];
                ng    = row1[16];
                ngrp  = row1[13];

                //Set L1-L4 (quality control)
                l1 = max(1,nenle);
                l2 = max(1,nenac);
                l3 = max(1,nenfp);
                l4 = max(1,l4);

        }
        else {
                cout << "Reached end of file unexpectedly! npos = "
                << npos << ", title= ";
                for(int i=0; i<80; i++) cout << title[i];
                cout << endl;
        }
        ifs.close();
}

void read_push(ifstream& ifs, vector<int>& vec, const int len)
{
        int tmp;
        for(int i = 0; i < len; ++i) {
                ifs.read(as_bytes(tmp), sizeof(tmp));
                vec.push_back(tmp);
        }
```

```
}
void read_push(ifstream& ifs, vector<float>& vec, const int len)
{
        float tmp;
        for(int i = 0; i < len; ++i) {
                ifs.read(as_bytes(tmp), sizeof(tmp));
                vec.push_back(tmp);
        }
}
void read_push(ifstream& ifs, vector<double>& vec, const int len)
{
        double tmp;
        for(int i = 0; i < len; ++i) {
                ifs.read(as_bytes(tmp), sizeof(tmp));
                vec.push_back(tmp);
        }
}
```